Studies on the Metabolic Bioactivation of Haloperidol (HP) and Its Tetrahydropyridine Dehydration Product

by

Etsuko Usuki

Dissertation submitted to the Faculty of the Virginia Polytechnic Institute and State University in partial fulfillment of the requirements for the degree of

Doctor of Philosophy

in

Chemistry

APPROVED BY:

Dr. Neal Castagnoli, Jr., Chairman

Dr. David G. I. Kingston

Dr. Gary L. Long

Dr. Harold M. McNair

Dr. Robert H. White

June, 1996

Blacksburg, Virginia

Keywords: Haloperidol, Metabolism, HPP^+, MPTP, Bioactivation, Neurotoxicity, Cytochrome P450

Studies on the Metabolic Bioactivation of Haloperidol (HP) and Its Tetrahydropyridine Dehydration Product

by

Etsuko Usuki

Professor Neal Castagnoli, Jr., Chairman

Abstract

Haloperidol (HP), a member of the butyrophenone class of neuroleptics and a first choice for the treatment of schizophrenia, causes severe extrapyramidal side effects including acute dystonic reactions, akathisia, drug-induced parkinsonism and, following chronic treatment, tardive dyskinesias (TD). The persistence of TD in some patients after neuroleptic drug treatment has been discontinued suggests that this condition may be related to a drug-induced neuronal lesion.

HP and its tetrahydropyridine dehydration product {4-(4-chlorophenyl)-1-[4-(4-fluorophenyl)-4-oxobutyl]-1,2,3,6-tetrahydropyridine (HPTP) share structural features with the parkinsonian inducing neurotoxin 1-Methyl-4-phenyl-1,2,3,6-tetrahydropyridine (MPTP). Consequently, we have elected to examine the metabolic fate of HP and HPTP to determine if these compounds, like MPTP, undergo metabolic bioactivation to neurotoxic pyridinium metabolites.

In vitro metabolic studies have demonstrated that human monoamine oxidase A and cytochrome P450 3A4 are capable of catalyzing the oxidation of HPTP and/or HP to the toxic HP pyridinium metabolite {4-(4-chlorophenyl)-1-[4-(4-fluorophenyl)-4-oxobutyl]pyridinium species (HPP^+). Rodent liver and brain preparations also catalyze HPP^+ formation. In vivo studies in human and

rodents have led to the characterization of both HPP^+ and $RHPP^+$, that is the pyridinium metabolite derived from reduced haloperidol, a major circulating metabolite of HP. Quantitative estimates of $HPP^+/RHPP^+$ in several patients receiving high doses of HP have been recorded. $RHPP^+$ is the major urinary pyridinium metabolite in humans while HPP^+ is the major pyridinium metabolite in rodents. Both pyridinium species also were identified in the brains of mice treated with HPTP but not with HP. Toxicological studies in baboons have demonstrated HPP^+ and $RHPP^+$ formation in this animal model. This is an ongoing study that should lead to useful toxicological results.

Finally, [^{3}H]HPTP was synthesized and in vivo (mouse) and in vitro (brain) metabolism studies were carried out in C57BL/6 mice. We attempted to gain some insight into the very low mass balance observed in our earlier work. This issue remains unresolved. The results obtained with the tritiated compound suggested that the major radioactive metabolite of HPTP in this species is the pyridinium metabolite HPP^+. Overall these results emphasize the importance of pyridinium metabolite formation and argue for more extensive toxicological work to assess the possible contribution of HPP^+ and $RHPP^+$ to the extrapyramidal side effects caused by HP.

ACKNOWLEDGMENTS

I wish to express my gratitude and appreciation to Professor Neal Castagnoli, Jr. for his guidance and encouragement. His infinite range of ideas and positive way of life have profoundly affected my life.

Grateful acknowledgments are also made to Dr. David Kingston, Dr. Gary Long, Dr. Harold McNair and Dr. Robert White for their valuable advice and assistance.

I wish to thank the members of the Castagnoli research group for their suggestions, assistance, and friendship. A special tribute is given to Mrs. Kay Castagnoli for her help and Dr. Kazuo Igarashi for helping me to start graduate research at Virginia Tech.

I wish to express special thanks to my best friends, Mrs. Andrea H. Anderson and Dr. Robert L. Parsons. Both inside and outside of the lab, Andrea has been a great friend and provided professional and personal support that have made my graduate experience more enjoyable. Bob's patience was incredible and I hope it will continue in the future.

Finally, I would like to thank my family, especially my parents and sister. Their understanding and encouragement supported me through the years and made me feel I was never alone while studying in the U.S.

I also wish to thank the NIH and the Harvey W. Peters Research Center for Parkinson's Disease and Disorders of the Central Nervous System for supporting my research work.

Table of Contents

List of Schemes

List of Figures

List of Tables

Abbreviations

ACh	Acetylcholine
API	Atmospheric pressure ionization
ATP	Adenosine triphosphate
CID	Collision induced dissociation
COMT	Catechol-O-methyl transferase
CPHP	4-(4-Chlorophenyl)-4-hydroxypiperidine (**41**)
CPP	4-(4-Chlorophenyl)pyridine (**53**)
CPTP	4-(4-Chlorophenyl)tetrahydropyridine (**51**)
CYPs	Cytochromes P450
DA	Dopamine (**22**)
L-DOPA	3,4-Dihydroxyphenyl-L-alanine
DOPAC	3,4-Dihydroxyphenylacetic acid (**27**)
FAD	Flavin adenine dinucleotide
GABA	γ-Aminobutyric acid
GC/MS	Gas chromatography/mass spectrometry
5-HIAA	5-Hydroxyindoleacetic acid (**32**)
HP	Haloperidol {4-(4-chlorophenyl)-1-[4-(4-fluorophenyl)-4-oxobutyl]-4-piperidinol (**33**)}
HPLC	High performance liquid chromatography
HPLRC	High performance liquid radio-chromatography
HP-Glu	Haloperidol-O-glucuronide (**46**)
HPP^+	Haloperidol pyridinium {4-(4-chlorophenyl)-1-[4-(4-fluorophenyl)-4-oxobutyl]pyridinium species (**36**)}
5-HT	5-Hydroxytryptamine (serotonin, **24**)

HPTP	Haloperidol tetrahydropyridine {4-(4-chlorophenyl)-1-[4-(4-fluorophenyl)-4-oxobutyl]-1,2,3,6-tetrahydropyridine (**34**)}
i.m.	intramuscular
i.p.	intraperitoneal
LC/MS	Liquid chromatography/mass spectrometry
LC/MS/MS	Liquid chromatography tandem mass spectrometry
MAO-A	Monoamine oxidase-A
MAO-B	Monoamine oxidase-B
$MPDP^+$	1-Methyl-4-phenyl-2,3-dihydropyridinium (**3**)
MPP^+	1-Methyl-4-phenylpyridinium species (**4**)
MPPP	1-Methyl-4-phenyl-4-propionoxypiperidine (**2**)
MPTP	1-Methyl-4-phenyl-1,2,3,6-tetrahydropyridine (**1**)
m/z	Mass to charge ratio
NAD	Nicotinamide adenine dinucleotide
NAD^+	Oxidized nicotinamide adenine dinucleotide
NADP	Nicotinamide adenine dinucleotide phosphate
$NADP^+$	Oxidized nicotinamide adenine dinucleotide phosphate
NADPH	Reduced nicotinamide adenine dinucleotide phosphate
NE	Norepinephrine (**23**)
PA	3-*p*-Fluorophenylaceturic acid (**44**)
PD	Parkinson's disease
PFBPA	3-*p*-Fluorobenzoylpropionic acid (**43**)
RHP	Reduced haloperidol {4-(4-chlorophenyl)-1-[4-(fluorophenyl)-4-hydroxybutyl]-4-piperidinol (**39**)}
RHP-Glu	Reduced haloperidol glucuronide (**49**)

$RHPP^+$	Reduced haloperidol pyridinium {4-(4-chlorophenyl)-1-[4-(fluorophenyl)-4-hydroxybutyl]pyridinium species (**40**)}
RHPTP	Reduced haloperidol tetrahydropyridine {4-(4-chlorophenyl)-1-[4-(fluorophenyl)-4-hydroxybutyl]-1,2,3,6-tetrahydropyridine (**52**)}
SD	Spontaneous dyskinesia
TAO	Troleandomycin
TD	Tardive dyskinesia
UV	Ultraviolet

Structures of Compounds found in the dissertation

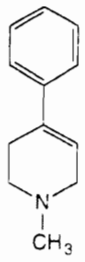

1

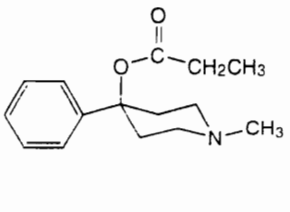

2

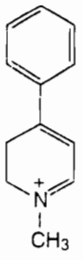

3

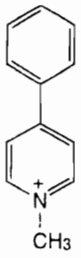

4

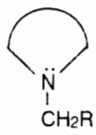

5

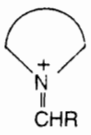

6

RCHO

7

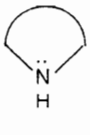

8

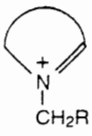

9

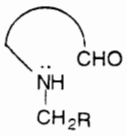

10

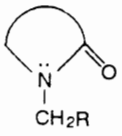

11

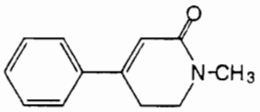

12

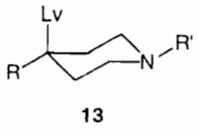

13

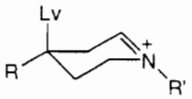

14

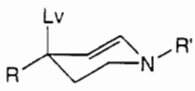

15

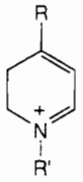

16

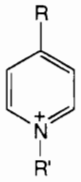

17

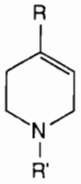

18

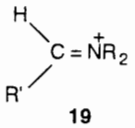

19

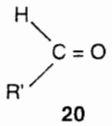

20

HNR2

21

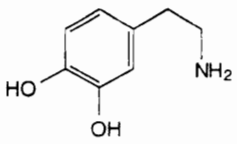

22

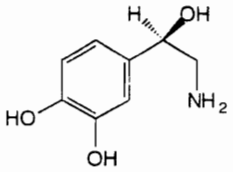

23

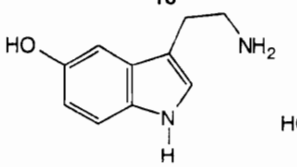

24

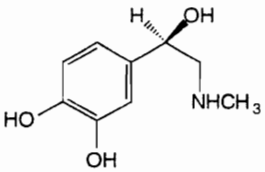

25

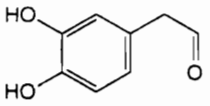

26

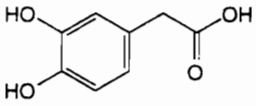

27

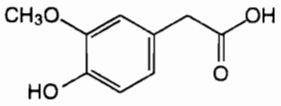

28

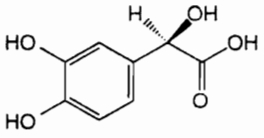

29

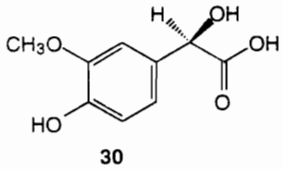

30

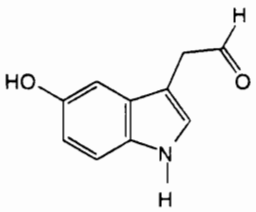

31

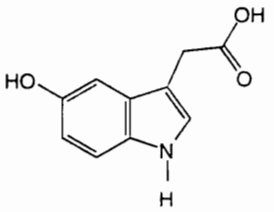

32

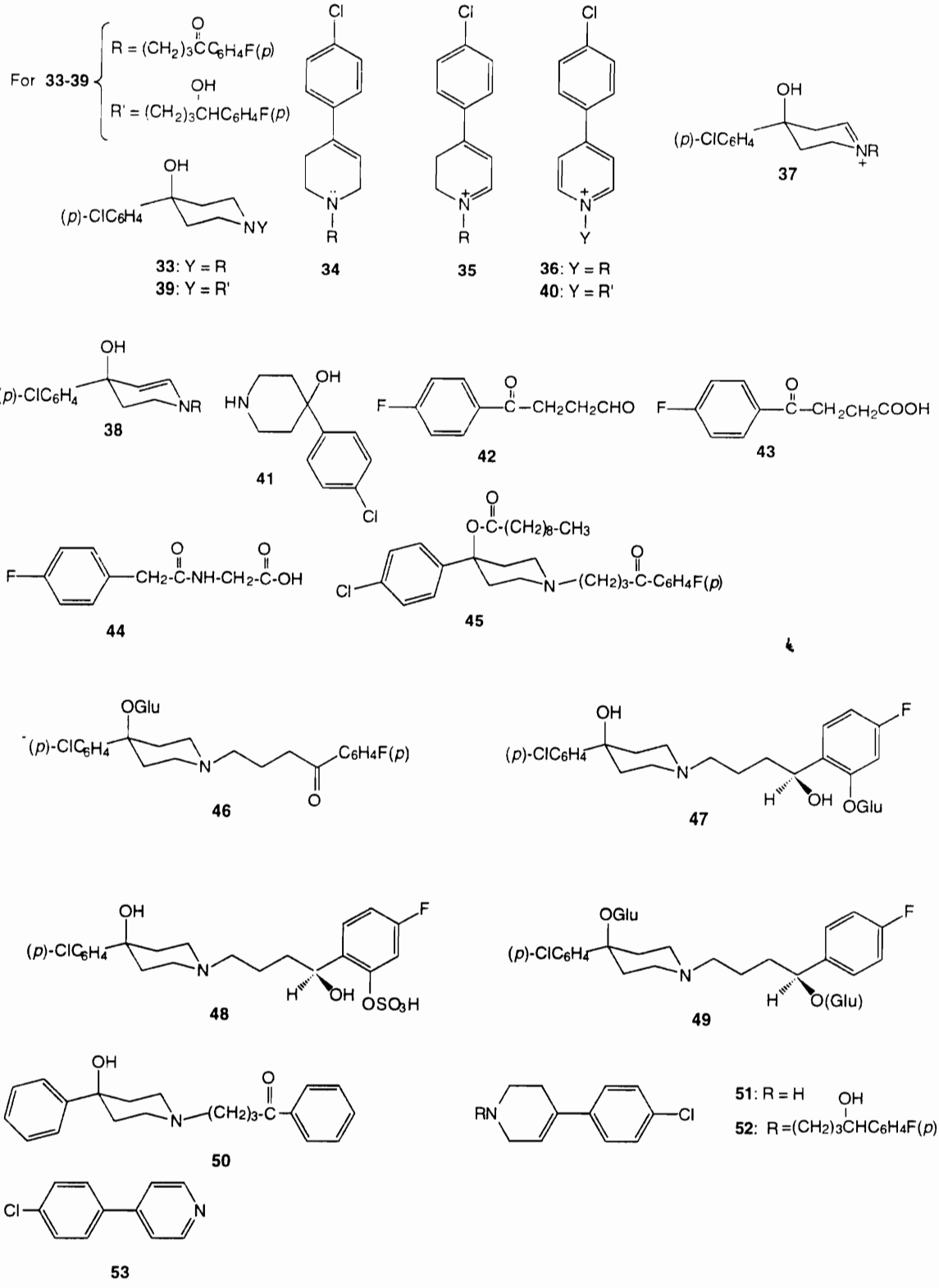
For 33-39
R = (CH2)3C(=O)C6H4F(p)
R' = (CH2)3CH(OH)C6H4F(p)
(p)-ClC6H4
OH
NY
33: Y = R
39: Y = R'
34
35
36: Y = R
40: Y = R'
37
38
41
42
43
44
45
46
47
48
49
50
51: R = H
52: R = (CH2)3CH(OH)C6H4F(p)
53

Glossary of terms used in the dissertation

Akathisia	A condition of motor restlessness, ranging from a feeling of inner disquiet to inability to sit or lie quietly or to sleep.
Choreoathetoid	Arythmic and uncoordinated, applied to foetal movements.
CYPs	Genes code for forms of cytochrome P450.
Cytochrome P450	A superfamily of hemoproteins which catalyze the biosynthesis and metabolism of numerous endogenous compounds. It also is involved in the biotransformation of foreign compounds.
Dyskinesias	Impairment of the power of voluntary movement, resulting in fragmentary or incomplete movements.
Dystonia	Disordered tonicity of muscle.
Dystonic	Pertaining to or characterized by dystonia.
Extrapyramidal	A functional, rather than anatomical, unit comprising the nuclei and fibers (excluding those of the pyramidal tract) involved in motor activities; they control and coordinate especially the postural, static, supporting, and locomotor mechanisms.
Glucuronide	Any glycosidic compound of glucuronic acid; the glucuronides, which are generally inactive, constitutes the major proportion of metabolites of many phenols, alcohols, and carboxylic acids.
Idiopathic	Of the nature of an idiopathy; self-originated; of unknown causation.

Mitochondria	Small spherical to rod-shaped components (organelles) found in the cytoplasm of cells, enclosed in a double membrane, with an internal membrane space between the two units, the inner one infolded into the interior of the organelle as a series of projections (cristae). They are the principal sites of the generation of energy (in the form of ion gradients and adenosine triphosphate [ATP] synthesis) resulting from the oxidation of food stuffs, and they contain the enzymes of the Krebs and fatty acid cycles and the respiratory pathway.
NADPH generating system	A mixture used for in vitro incubations to generate NADPH, which consists of $NADP^+$, glucose 6-phosphate, glucose 6-phosphate dehydrogenase, and $MgCl_2$.
Neuroleptic	Any drug that favorably modifies psychotic symptoms; the main categories of neuroleptics include the phenothiazines, butyrophenones, and thioxanthenes.
Nigrostriatal	Projecting from the substantia nigra to the corpus striatum.
PD	Parkinson's disease. idiopathic parkinsonism.
Parkinsonism	A group of neurological disorders characterized by hypokinesia, tremor, and muscular rigidity.
TD	Tardive dyskinesia. movement disorders marked by lateness.
Xenobiotic	A chemical foreign to the biologic system.

Chapter 1

Introduction

Schizophrenia is a chronic mental disorder that usually develops before the age of 35 years and affects about 1% of the population. The cause of this disease is unknown and patients often need to be hospitalized for long periods of time. With the introduction of neuroleptics in the 1950's,[1] out patient treatment has become more general. Although these drugs have revolutionized the treatment of schizophrenia, they also cause a wide range of extrapyramidal side effects.[2] These side effects may be categorized as drug-induced parkinsonism, akathisia, acute dystonic reactions, and chronic tardive dyskinesia.[3] The two most prevalent syndromes, parkinsonism and tardive dyskinesia, will be described in this Chapter.

1.1. Parkinson's disease

Parkinson's disease (PD) is one of the most common causes of disability among the elderly and is characterized by symptoms such as akinesia (freezing), muscular rigidity, tremor, shuffling gait, postural instability, and a mask-like face.[4] It's cause is unknown. The disease affects most pigmented brainstem nuclei, particularly the substantia nigra and locus ceruleus.[5] The primary pathology is a lesion of dopaminergic neurons in the substantia nigra pars compacta leading to dopamine depletion in the brain.[6] The symptoms of PD can often be reversed by administration of levodopa (L-DOPA), a precursor of dopamine, which restores dopamine levels in the brain. Although L-DOPA is the first choice for the symptomatic treatment of PD,[7] following some years of therapy, it loses its efficiency and often induces troublesome dyskinesias.[8] Many hypotheses have been proposed to account for this condition, however,

none has been convincing. Parkinsonism can be classified in two categories. One is idiopathic Parkinson's disease and the other is drug-induced parkinsonism. Drug-induced parkinsonism is further categorized into at least two groups, i.e. neuroleptic-induced and toxin-induced. Most neuroleptics are dopamine receptor antagonists and the blockade of extrapyramidal dopaminergic receptors, especially D_2 receptors, may be responsible for drug-induced parkinsonism. However, this hypothesis is controversial. Idiopathic PD and drug-induced parkinsonism are hard to distinguish from each other by symptoms, although it has been reported that idiopathic PD has a slow resting tremor (4-5 Hz) while drug-induced parkinsonism shows a tremor of higher frequency (7-9 Hz).[9] Idiopathic PD may include a young onset (juvenile PD) and genetic factors may contribute to some extent.[10] Most drug-induced parkinsonism occurs in patients over the age of 40 years[11] and the mean age of onset with drug-induced parkinsonism (70.6 ± 1.4 years) was significantly higher than that of idiopathic PD (60 ± 1.1 years).[12] It has been reported that neuroleptic-induced parkinsonism occurs in 50 to 75% of the patients during the first month of treatment and in 90% during the first three months.[11] The overall prevalence among schizophrenic patients is about 40%.[13] In the case of drug-induced parkinsonism, females have twice the risk as males.[14] This sex-difference has not been observed in idiopathic PD.

1.2. Tardive dyskinesia

Tardive dyskinesia (TD) is one of the extrapyramidal complications of chronic neuroleptic treatment. Since some cases of TD are irreversible, it is considered as one of the most serious side-effects. This syndrome is described as tardive because the involuntary movements generally begin at least 3

months after the first drug exposure and sometimes only after years of drug treatment.[3,15] Characteristic symptoms involve choreoathetoid movements, including chewing movements, tongue protrusions and, in advanced cases, licking and rotating tongue movements, both inside and outside the mouth.[16] Often choreoathetoid movements are seen in the limbs and trunk. Parkinsonism has been shown to coexist in up to 70% of TD patients and the coexistence increases with age.[17] Although it is rare, this syndrome can be life-threatening due to respiratory and gastrointestinal complications. The abnormal movements that characterize TD may occur naturally and be unrelated to schizophrenia and neuroleptic treatment. This is called spontaneous dyskinesia (SD). The results of 18 studies suggest a TD prevalence of 19.8% (7200 patients) and a SD prevalence of 5.9% (5900 patients).[18] Therefore, a better estimate of the prevalence of TD may be 15% of patients under neuroleptic treatment. Several risk factors associated with neuroleptic treatment have been reported. Approximately 10% of patients are under 40 years old and the prevalence increases with age to over 50% in patients 60 years or older. Also females have a higher risk of getting TD than males (1.68/1).[19] The higher the dose of neuroleptic and the longer the period of treatment, the greater the risk of TD. Patients with anxiety, agitation, and stress can temporarily aggravate the syndrome.[20] TD can be diminished by increased neuroleptic dosage and aggravated by reduced dosage or anticholinergic therapy. However, TD is usually treated by decreasing the dose of neuroleptic, if possible. The most serious aspect of TD is its irreversibility. After discontinuation of the drug, the symptoms remain in some patients. It has

been reported that TD can decline over 2-5 years after discontinuance of the drug.[18] It has been estimated that 60% of TD cases resolve within 5 years.[21]

The most widely accepted pathophysiological theory for TD is dopamine receptor supersensitivity. According to this theory, TD is based on striatal dopaminergic hyperfunction, specifically an increase in number (supersensitivity) of postsynaptic D_2 dopamine receptors in the striatum (caudate/putamen).[22,23] Neuroleptic drugs block postsynaptic dopamine receptors, leading to an increase in acetylcholine turnover. During or after chronic treatment, dopamine receptor blockade evokes a receptor hypersensitivity. This hypersensitivity is related to an increase in the number of dopamine receptors resulting from an upregulation to compensate for the initial receptor blockade by neuroleptic drugs. This theory has been supported by a number of clinical observations, including the initial onset after the long period of neuroleptic treatment, acute worsening of TD by L-DOPA, amelioration by the dopamine agonist, apomorphine, and partial and temporary suppression by dopamine antagonists including receptor blockers (neuroleptics) and dopamine storage blockers (reserpine, tetrabenazine) which inhibit the storage of dopamine in the presynaptic vesicles.[24] Clozapine (a so-called atypical neuroleptic, which exhibits antipsychotic activity in the absence of debilitating, short- or long-term extrapyramidal side-effects)[25] has a low D_2 receptor affinity and high 5-HT_2 receptor affinity. On the other hand, typical neuroleptic drugs have a high selectivity for D_2 receptors (D_2 receptor occupancy of approximately 80% and little or no D_1 receptor occupancy).[26] This fact could support D_2 receptor hypersensitivity. On the other hand, the atypical neuroleptics sulpiride and remoxipride have high affinity for the D_2 receptor. In

recent years, various observations, especially with post-mortem brains of schizophrenic patients, further weaken this theory. These observations include the following: 1. No correlation was observed between the presence of drug-induced TD and D_1 and D_2 receptor numbers in the basal ganglia, 2. No difference in D_2 receptor binding in the putamen was observed between patients with and without TD, and 3. Abnormalities have been observed in multiple neurotransmitter systems, including D_1 and γ-aminobutyric acid (GABA) receptor function.[27-29]

Observed alterations in GABA systems have led to the GABA theory of TD. There are two types of GABA neurons projecting from striatum. One type, from the anterior striatum, projects to lateral segments of the globus pallidus and is inhibited by dopamine. Another type, from the posterior striatum, projects to the reticular zone of the substantia nigra and the medial segment of the globus pallidus. This type is excited by dopamine.[30] GABA is an inhibitory neurotransmitter throughout the brain. However, when a GABA neuron inhibits another GABA neuron, the result is excitatory. Thus, in the anterior part of striatum, neuroleptics may cause a parkinsonism symptom and at the same time, in the posterior part of striatum, they may cause TD-like symptoms. Real symptoms may depend on the balance between these two functions and this may explain the coexistence of drug-induced parkinsonism and TD.

Clinical responses to several agents suggest dopamine excess and acetylcholine (ACh) and GABA deficiency in TD patients.[31,32] However, efficient treatments using ACh or GABA-enhancing agents have not been documented.

Because of the supportive observations, the dopamine hypersensitivity theory has not been excluded and currently a combination of the dopamine theory and the GABA theory appears to be most generally accepted. The debate, however, continues.

1.3. MPTP

The neurotoxic effects of 1-methyl-4-phenyl-1,2,3,6-tetrahydropyridine (MPTP, **1**) were first reported in humans.[33] These individuals were drug abusers who had used a street drug, 1-methyl-4-phenyl-4-propionoxypiperidine (MPPP, **2**), a meperidine analog. The symptoms of these patients, including movement disorders, and lesions in the dopaminergic pathways of the nigrostriatal tract, resemble those of patients with idiopathic PD. Furthermore, these individuals responded to L-DOPA therapy. GC/MS analysis of the reaction mixture designed to yield MPPP showed that the preparation was contaminated with MPTP.[34] MPTP destroys nigrostriatal dopaminergic cells in the pars compacta of the substantia nigra of human,[35] monkeys[36,37] and mice.[38-41] Rats, however, are resistant to the toxic effects of MPTP.[34] An important aspect of the pathway leading to neurodegeneration is as follows: MPTP partitions into brain where it is oxidized to the unstable dihydropyridinium intermediate 1-methyl-4-phenyl-2,3-dihydropyridinium [$MPDP^+$ (**3**)] by monoamine oxidase B (MAO-B).[42,43] $MPDP^+$ undergoes spontaneous oxidation to 1-methyl-4-phenylpyridinium MPP^+ (**4**).

The catalytic role of MAO-B was established by an inhibition experiment which showed MPP^+ formation from MPTP was blocked by selective MAO-B inhibitors (pargyline, deprenyl) but not by the selective MAO-A inhibitor clorgyline.[42,43] Animal studies demonstrated that the neurotoxicity of MPTP was prevented by blocking MPP^+ formation by MAO-B inhibitors, suggesting that the pyridinium metabolite MPP^+ is the ultimate neurotoxin.[44-46] Since MAO-B is localized in the glial cells, it is thought that MPP^+ is formed extraneuronally. Then MPP^+ leaks out of the glial cells and into the

extracellular space where it is selectively sequestered by striatal dopaminergic neurons via the DA transporter.[47] When inhibitors of dopamine uptake were administered to mice, MPTP-induced neurotoxicity was not observed.[47,48] Once localized intraneuronally, MPP^+ is concentrated further within the inner mitochondrial membrane[49] where it inhibits electron transport.[49-51] MPP^+ blocks oxidation of NAD^+-linked substrates such as pyruvate yet leaves the oxidation of succinate unaffected, demonstrating that MPP^+ inhibits electron transport in the mitochondria at the Complex I level. Inhibition of Complex I results in the depletion of ATP and cell death.[52,53]

Extensive in vitro and in vivo studies using MPP^+ and various pyridinium analogs have been conducted to assess their neurotoxicity. From in vivo microdialysis studies[54,55] and in vitro mitochondrial respiration and cell culture experiments,[56-58] these compounds turned out to be potent, selective and irreversible neurotoxins for dopaminergic neurons. It has been established that C57BL/6 mice may be a useful animal model to study MPTP-induced neurotoxicity.[59]

Scheme 1. Structure of MPPP and the MAO-B Catalyzed Oxidation of MPTP.

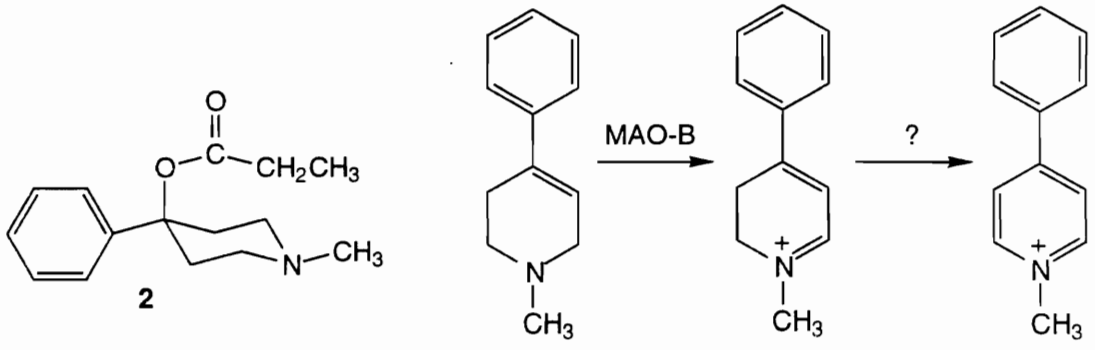

2 **1** **3** **4**

Chapter 2

2.1. Metabolism of cyclic tertiary amines

The most important catalysts for the biotransformation of tertiary amines are members of the microsomal cytochrome P450 family of hemoproteins.[60,61] However, as just mentioned, more recently the outer mitochondrial membrane bound flavoproteins monoamine oxidase A and B (MAO-A and MAO-B) have been shown to be efficient catalysts for the α-carbon oxidation of a specific class of cyclic tertiary amines, namely 4-substituted 1-methyl-1,2,3,6-tetrahydropyridines.[62,63]

Cyclic tertiary amines (**5**) can undergo oxidative N-dealkylation via hydrolysis of the enzyme generated exocyclic iminium intermediates **6** to yield aldehydes **7** and the cyclic secondary amines **8** (Scheme 2). The corresponding oxidation of a ring α-carbon atom generates the cyclic iminium intermediate **9**. Unlike the exocyclic regioisomer **6**, hydrolytic cleavage of **9** to yield the aminoaldehyde **10** is reversible and consequently the fate of **9** must be considered separately. These intermediary metabolites often are oxidized further to the corresponding lactam **11** in a reaction that is catalyzed by the liver cytosolic enzyme aldehyde oxidase.

Scheme 2. Alternative Oxidative Biotransformation Pathways for Cyclic Tertiary Amines.

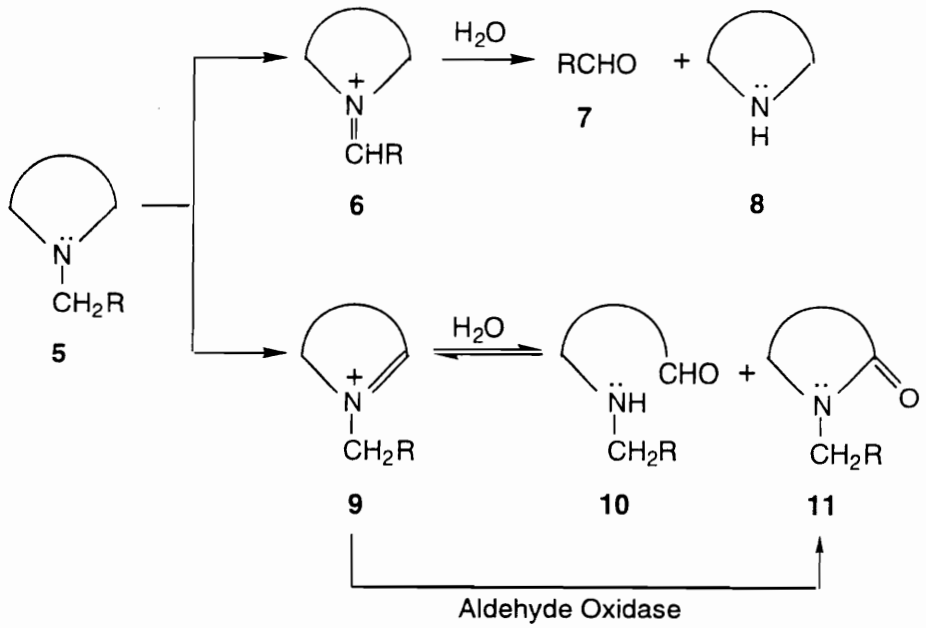

As described in section 1.3, MPTP is a cyclic tertiary amine and is metabolized by MAO-B to $MPDP^+$. Since $MPDP^+$ is an excellent substrate for aldehyde oxidase, the corresponding lactam (**12**) was observed in the whole liver tissue incubation mixtures of MPTP.[64] It has been documented that cytochrome P450 also catalyzes MPP^+ formation from MPTP.[65] The ultimate fate of a particular cyclic iminium species will depend on where it is formed and on the chemical features of the molecule itself.

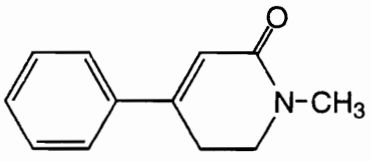

12

2.2. Metabolism of functionalized cyclic tertiary amines

The possibility that other cyclic tertiary amines may undergo enzyme catalyzed oxidation to form potentially neurotoxic pyridinium or related metabolites is worthy of consideration even though the toxic outcomes may be more subtle than those identified with MPTP. Of particular interest in this regard are piperidine derivatives bearing a potential leaving group (**Lv**), i.e. compounds (**13**), at the same oxidation state as MPTP. The ring α-carbon oxidation of **13** generates the iminium product **14** which, as the corresponding enamine free base **15**, will undergo spontaneous elimination to form the unstable dihydropyridinium product **16** that will autoxidize to the pyridinium species **17**. An alternative pathway would involve initial elimination of the leaving group to yield tetrahydropyridine **18** as the intermediate leading ultimately to the pyridinium product (Scheme 3).

Scheme 3. Proposed Bioactivation Pathway of Functionalized Piperidine Derivatives.

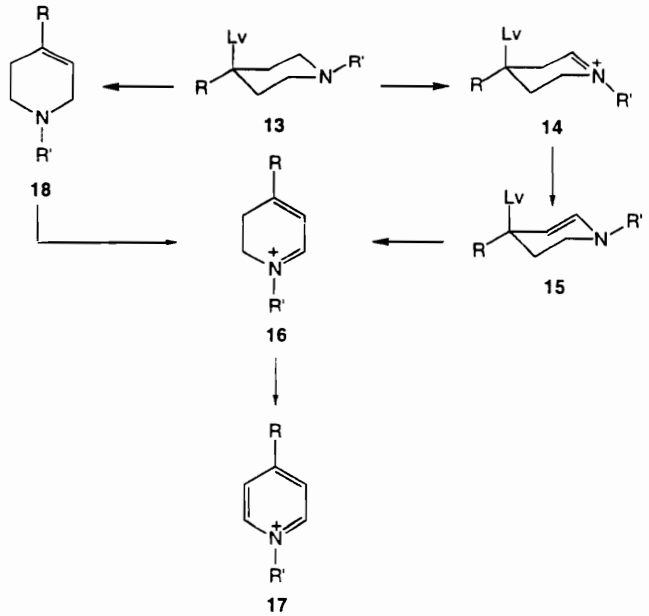

2.3. Enzymes of interest

Drugs and other xenobiotics are metabolized by a wide variety of enzymes. Most drugs are metabolized to inactive, polar compounds which can be rapidly excreted via the kidneys (detoxification). However, some drugs are biotransformed to reactive, toxic metabolites which sometimes are responsible for the adverse effects of drugs. Drug metabolism occurs primarily in the liver. However, it also occurs to some extent at other sites including brain, kidney, skin, lung and gastrointestinal tract.[66] In this Chapter, the general features of the cytochromes P450 and monoamine oxidases, the enzymes of interest in this work, are described.

2.3.1. Cytochrome P450

Cytochromes P450 (CYPs) are a superfamily of hemoproteins and the most important enzymes in the biosynthesis and metabolism of numerous endogenous compounds (e.g., fatty acids, steroids, eicosanoids, and vitamins). These enzymes also metabolize xenobiotics such as drugs, environmental pollutants, and industrial chemicals.[67] The metabolism of xenobiotics may lead to less active (toxic) compounds or could produce toxic metabolites. P450s reside in the endoplasmic reticulum and require NADPH as a co-factor. The major location of the P450s is the liver and therefore this organ plays a major role in drug metabolism.

Depending on the product formed, metabolic reactions can be classified as Phase I and Phase II. Phase I reactions include carbon hydroxylation, heteroatom oxygenation, oxidative N- and O-dealkylation, dehydrogenation, epoxidation, mechanism-based inactivation, and reduction.[67] Oxidations by

P450s can be understood in the context of abstraction of hydrogen atoms or non-bonded π electrons from the substrate by hypervalent iron (FeO^{3+}) followed by radical recombination.[68] The stoichiometry of such reactions is described as follows:

$$(P^{III}450) + NADPH + H^+ + O_2 = (P^V450)O + NADP^+ + H_2O$$

$$RH\ (drug) + (P^V450)O = ROH + (P^{III}450)$$

$$RH + NADPH + O_2 + H^+ = ROH + NADP^+ + H_2O$$

Phase II reactions include glucuronidation, sulphation, acetylation and conjugation with glutathione and amino acids such as glycine. In general, conjugates are more water soluble than the parent drugs and are thus rapidly excreted through the kidneys into the urine. Therefore, Phase II reactions are for the most part, detoxification pathways. At last count 221 P450 genes had been characterized and classified into 36 gene families with members of the same family having at least 40% amino acid sequence identity (homology) (e.g., CYP1, CYP2, etc.). Twelve of these gene families exist in all mammals examined to date. These are further subdivided into 22 subfamilies (CYP1A, CYP1B, etc.) with sequence identity ≥55%.[69] About 30 human P450s (CYP1A1, CYP1A2, etc.) have been characterized.[70,71] Members of CYP1, CYP2, and CYP3 families include those enzyme families responsible primarily for the metabolism of xenobiotics.[72] In addition to the liver, the gastrointestinal tract, kidneys, lungs, skin and brain have been identified as potential sites of drug metabolism.[66] In the brain, P450 is present at a concentration of approximately 1% of the level found in the liver.[73] In human liver, CYP2D6 and

CYP3A4 seem to be dominant in terms of the variety of drugs that are substrates.[71] Furthermore, CYP3A4 levels are as high as 60% of the total P450.[74] In recent years, methods for the characterization of P450 substrate selectivity have been developed. These methods include correlation of the activity under consideration with known marker activities for individual P450s (liver microsomal panels), selective inhibition or induction, immunoinhibition, enzyme purification and reconstitution, and heterologous expression (cloned DNA).[75,76]

2.3.2. Monoamine oxidases

Since the cytochromes P450 play a major role in drug metabolism, research in this area has focused on these monooxygenases. However, the oxidations of amines, including the biogenic amines, are catalyzed by amine oxidases, not P450 enzymes. Amine oxidases also are involved in the metabolism of a number of xenobiotics.[77] Amine oxidases can be categorized in two groups: the flavin-adenine dinucleotide (FAD)-dependent amine oxidases and the amine oxidases not containing FAD.[78] The non FAD-dependent amine oxidases include the copper containing enzymes that catalyze the oxidative conversion of primary amines only.[78] The amine oxidases we are interested in belong to the FAD dependent enzymes. The two well characterized flavin containing monoamine oxidases are MAO-A and MAO-B.

Monoamine oxidase (EC 1.4.3.4: MAO) catalyzes the oxidation of amines (**18**) to the corresponding aldehydes (**20**) and the released amines (**21**) via the iminium ion intermediates (**19**) (Scheme 4). Importantly, these enzymes

catalyze the oxidative deamination of the biogenic amines, such as dopamine (DA, **22**), norepinephrine (NE, **23**), 5-hydroxytryptamine (5-HT, also known as serotonin, **24**), and epinephrine (**25**). DA is the most abundant neurotransmitter in the central nervous system of most mammals. The highest levels of DA are found in the striatum and the nucleus accumbens.[79] Neurotransmitters maintain a dynamic balance between synthesis, storage, release, reuptake and degradation in the nerve terminals.[80] Neurotransmitters are released from the presynaptic nerve terminals and cause changes in the post-synaptic neuronal membrane potential that result in the generation of an impulse in the newly stimulated neuron.

Scheme 4. General mechanism of the oxidative deamination of substrates by MAO.

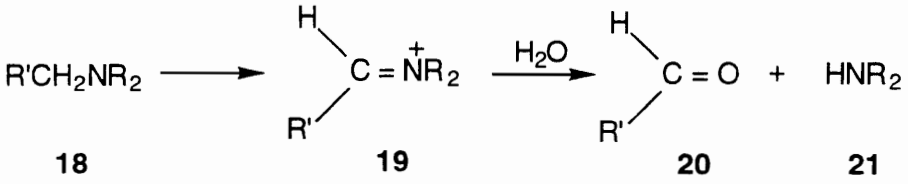

18 **19** **20** **21**

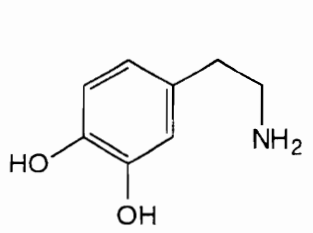

22

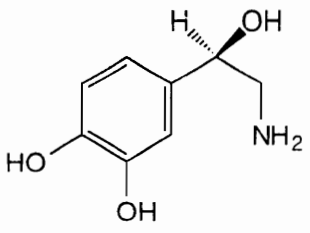

23

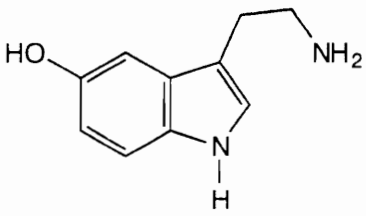

24

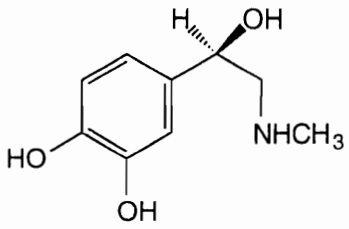

25

Since abnormalities in dopaminergic systems are the first pathophysiological features of PD and TD (see Chapter 1), the metabolism of DA is of considerable importance. DA (**22**) is metabolized by MAO to 3,4-dihydroxyphenylacetaldehyde (**26**) which is further oxidized by aldehyde dehydrogenase to form 3,4-dihydroxyphenylacetic acid (DOPAC, **27**), then via catechol-O-methyl transferase (COMT) to form homovanillic acid (**28**). DA is also metabolized by dopamine-β-hydroxylase to yield NE (**23**) which, via phenylethanolamine-N-methyl transferase, is converted to epinephrine (**25**). Both undergo oxidative deamination by MAO to give 3,4-dihydroxymandelic acid (**29**), then further metabolism via COMT yields vanillylmandelic acid (**30**) (Scheme 5).

Scheme 5. Dopamine Metabolism.

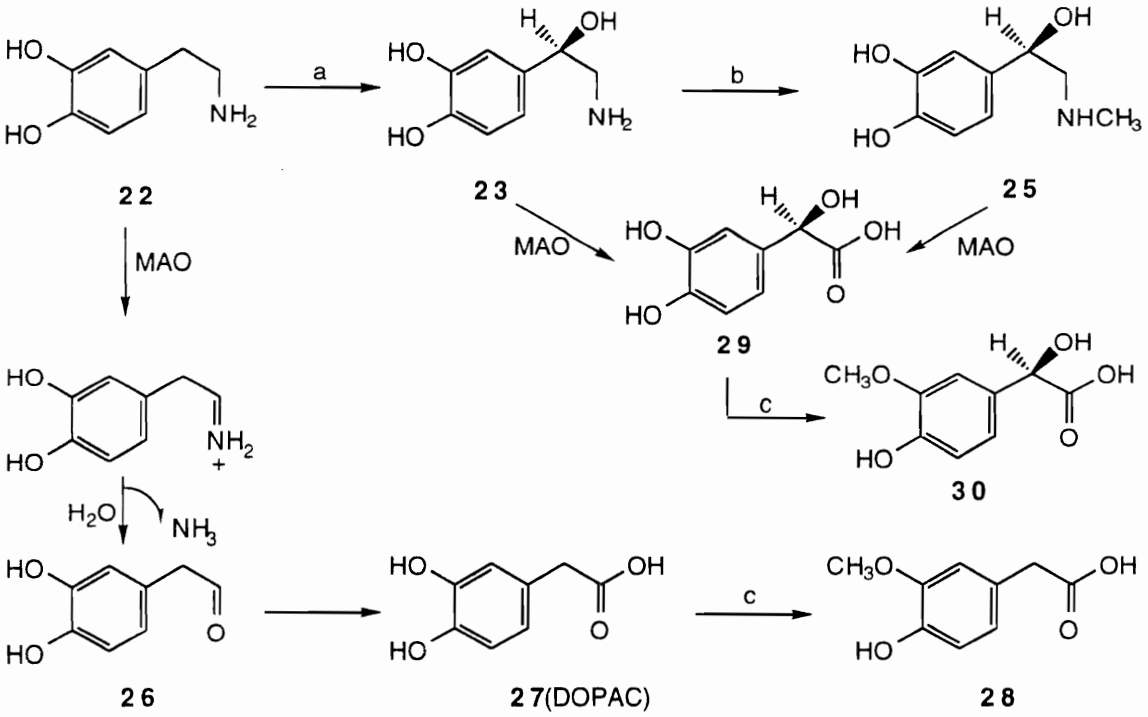

a: Dopamine β-hydroxylase, b: Phenylethanolamine-N-methyl transferase, c: Catechol-O-methyl transferase (COMT).

Serotonin (**24**) is metabolized by MAO to yield 5-hydroxyindoleacetaldehyde (**31**) which is further oxidized by aldehyde dehydrogenase to yield 5-hydroxyindoleacetic acid (5-HIAA, **32**) (Scheme 6).

Scheme 6. Serotonin Metabolism.

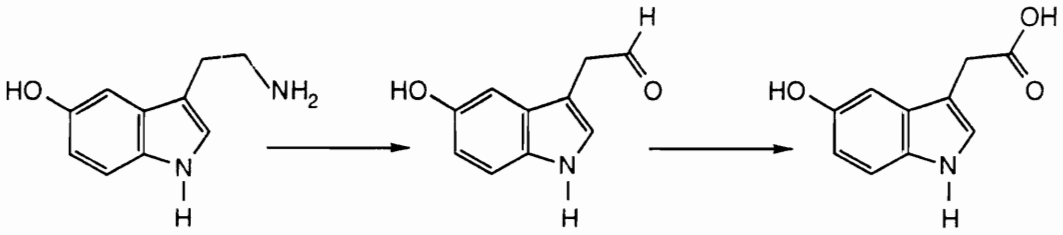

24 31 32

MAO activity is present in many mammalian tissues, including the brain, intestine, liver, muscle, and blood platelets.[81,82] Although some activity has been reported in microsomes,[83,84] MAO is primarily a mitochondrial enzyme and is tightly bound to the outer mitochondrial membranes of neuronal, glial and other cells.

MAO exists in two forms -- MAO-A and MAO-B -- which differ in their substrate specificities, sensitivity to inhibitors, and tissue localization.[85] MAO-A is selectively inhibited by low (nanomolar) concentrations of clorgyline and preferentially catalyzes the oxidative deamination of serotonin.[86] MAO-B is selectively inhibited by nanomolar concentrations of (R)-deprenyl and preferentially catalyzes the oxidative deamination of benzylamine and β-phenylethylamine.[80] Clorgyline does not inhibit MAO-B until micromolar concentrations are reached and the reverse is true of (R)-deprenyl and MAO-A.

As described in Chapter 1, the major and most consistent pathology in Parkinson's disease (PD) is a striking loss of neurons in the substantia nigra in the brain leading to dopamine depletion.[6] Primary treatment for this neurodegenerative disease is the administration of L-DOPA, a precursor of DA

which restores dopamine levels in the brain. This treatment, however, loses its efficacy following some years of therapy and often induces troublesome dyskinesias.[8] MPTP (**2**) is known to be a parkinsonian inducing agent (see Chapter 1.3) and the fact that MPTP is a substrate of MAO-B and deprenyl blocks MPTP toxicity by inhibiting its metabolism to MPP^+ (**4**), led to an interest in using the inhibition of MAO-B to protect against nerve cell loss.[87] Currently, (R)-deprenyl is used as well as L-DOPA for the treatment of PD. Both forms of MAO are present in most human tissues. However, a few tissues express exclusively one form of the enzyme; examples include the human placenta with more than 90% MAO activity being MAO-A, and blood platelets and chromaffin cells in which more than 95% of MAO activity is the B form.[87] In beef liver, MAO activity also is specifically MAO-B (more than 95%). Human placenta and beef liver are regarded as the best sources from which to obtain purified MAO-A and MAO-B, respectively.[88]

Chapter 3

3. Haloperidol

As discussed in Chapter 2.2, piperidine derivatives bearing a potential leaving group that may undergo enzyme catalyzed oxidation to form potentially neurotoxic pyridinium or related metabolites are worthy of consideration (see Scheme 3). One compound of particular interest that fits this description is the neuroleptic agent haloperidol {4-(4-chlorophenyl)-1-[4-(fluorophenyl)-4-oxobutyl]-4-piperidinol, HP (**33**)}. HP was introduced into therapy over forty years ago and is the prototypical drug of the butyrophenone class of neuroleptics and one of the most widely used drugs for the treatment of schizophrenia.[89] The mechanism of its antipsychotic effect is thought to be due to its dopamine antagonistic properties, especially its inhibitory effects on the D_2 receptor.[26] One difficulty in HP treatment is a very large inter individual variation in metabolizing capacity resulting in a wide range of steady-state plasma concentrations and varying therapeutic effects.[90] Although HP often is the first choice for antipsychotic therapy, it causes severe extrapyramidal side effects including acute dystonic reactions, akathisia, drug-induced parkinsonism and, following chronic treatment, tardive dyskinesia (TD).[19] As mentioned earlier, supersensitivity of up-regulated D_2 receptors has been considered a possible mechanism to account for these movement disorders.[68] This theory, however, remains controversial.[16,92] As mentioned earlier, the persistence of TD in some patients after neuroleptic drug treatment has been discontinued[93] suggests that this condition may be related to a drug-induced neuronal lesion.

HP is a 1,4-disubstituted 4-piperidinol and resembles MPTP in that it bears an aryl group at C-4 of the piperidinol. Furthermore, simple dehydration

of HP, a reaction which is reported to occur in microsomal incubations,[94] gives the corresponding 1,2,3,6-tetrahydropyridine derivative HPTP (**34**). Consequently, interest in the possible metabolic formation of a neurotoxic metabolite of HP has been under consideration.

As proposed in the previous section (Chapter 2.2.), functionalized piperidines may be oxidized to neurotoxic pyridinium metabolites. The conversion of HP and/or HPTP to the pyridinium product HPP^+ (**36**), presumably via the dihydropyridinium intermediate **35**, could be catalyzed by MAO. An alternative metabolic pathway that may lead to **35** involves initial conversion of HP to the corresponding cyclic iminium species **37** which, via the enaminol free base **38**, would be expected to undergo rapid conversion to the dihydropyridinium intermediate **35**. Subsequent autoxidation of **35** results in pyridinium **36** formation (Scheme 7). The proposed reaction sequence **34** –> **36** is a typical example of the ring α-carbon oxidation pathway outlined in Scheme 2 for cyclic tertiary amines, i.e. **5** –> **9**. Oxidative N-dealkylation (pathway **5** –> **6** –> **7** + **8**, Scheme 2) is a major metabolic pathway for HP[95] and therefore ring α-carbon oxidation might be expected to be a competing pathway. In addition to the sequence with haloperidol, we also will consider the corresponding metabolism of reduced haloperidol {4-(4-chlorophenyl)-1-[4-(4-fluorophenyl)-4-hydroxybutyl]-4-piperidinol (RHP, **39**), the major circulating metabolite of HP, to the pyridinium product $RHPP^+$ (**40**).

Scheme 7. Proposed Metabolic Pathway Leading to the Pyridinium Metabolite HPP+ (36) of Haloperidol (33).

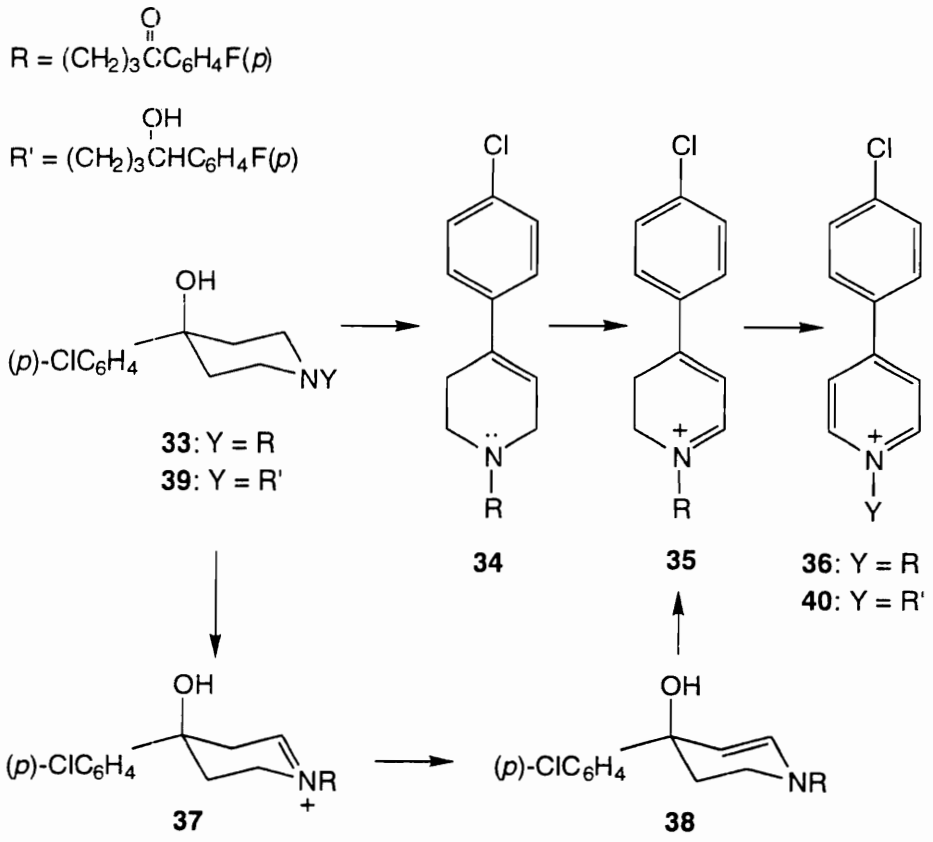

Our investigation on the metabolic fate of HP and HPTP has focused on the formation of potential neurotoxic metabolites (pyridinium species). In this section, the literature describing the metabolism of HP is summarized.

The principal metabolic pathways reported for HP are (1) N-dealkylation, (2) ketone reduction, and (3) O-conjugation. These are considered individually below. Special consideration will be given to the human and the rodent. HP metabolism has been studied most extensively in these two species.

3.1. N-dealkylation

In the human, cleavage of HP by oxidative N-dealkylation leads to the piperidine metabolite 4-(4-chlorophenyl)-4-hydroxypiperidine (CPHP, **41**) and initially the 3-*p*-fluorobenzoylpropional (**42**). This aldehyde undergoes further oxidation to yield the corresponding 3-*p*-fluorobenzoylpropionic acid (**43**). This acid undergoes a complex sequence of reactions to give, eventually, *p*-fluorophenylaceturic acid (PA, **44**) (Scheme 5).[95]

Scheme 8. N-Dealkylation Pathway.

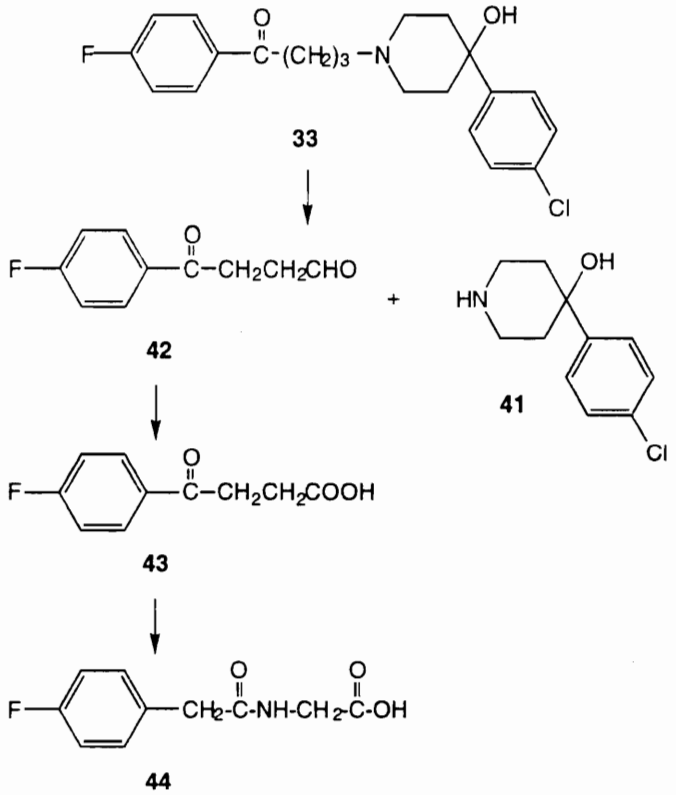

Forsman et al. had first isolated **43** and **44** from the urine of patients. Metabolite characterization was by GC/MS.[95] Their study was conducted on

three HP-treated patients dosed with 3-15 mg HP/day. Roughly 1% of HP was excreted unchanged in the 24-hour urine sample. However, no quantitative data for the N-dealkylated metabolites were reported.

Radiolabeled HP also has been used to study HP-metabolism. Miyazaki et al. examined the metabolism of intramuscularly administered [^{14}C]HP (^{14}C on carbonyl carbon) in rats. [^{14}C]HP was suitably diluted with unlabeled HP and dissolved in 10% lactic acid and a dose of 5 mg/Kg was administered to rats. Within 96 hours after intramuscular administration, a total of 99% of the dose was excreted in the urine (46%) and feces (53%).[96] The extracts obtained from urine and bile were analyzed by analytical TLC for the identification of metabolites. Radioactive spots on the developed plates were scraped off and suspended in ethyl acetate or methanol for extraction of radioactive metabolites. This extract was then subjected to gas chromatography/mass spectrometry (GC/MS). The major urinary and biliary metabolites were PA (**44**) and O-conjugates (glucuronide and sulfate) of HP. PA was about 34% of the dose in the initial 24-hour urine sample and the conjugates were 26% of the dose in a corresponding 24-hour bile sample. These conjugates will be described in a later section. The recovery of radioactivity in the 24-hour urine was 44% of the dose, therefore, 77% of the radioactivity in the 24-hour urine was due to PA. The authors did not observe the glucuronide conjugate in urine. No statement was made regarding the remaining 60% in urine and 70% in bile. In another study, [^{14}C]HP decanoate (**45**), which is the 4-O-decanoyl derivative of HP, was administered to rats intravenously and intramuscularly and urinary and fecal excretion of ^{14}C activity was measured in order to determine the biological half-life of the radioactive material.[97]

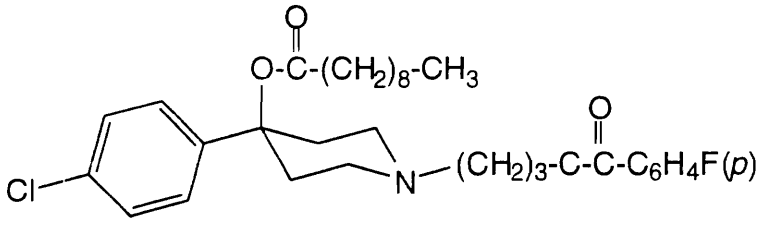

45

This ester is administered in a sesame oil vehicle. After intravenous administration (50 mg /Kg), the half-life was 1.5 days (average of urinary and fecal excretion data) and about 95% of the dose was excreted within 10 days. After intramuscular administration of 5 mg/Kg and 50 mg/Kg, half-lives were 16.4 and 11.2 days, respectively. About 90% of the dose was excreted within 42 days. In contrast to their previous study in which the free base was used,[96] the amount of PA in urine was low in this study. Comparing the results of intramuscular administration of 5 mg/Kg dose, PA was 7.1% in the 42 hour-urine and slow excretion (42 days to excrete 90% of the dose in urine and bile) was observed.[97] Even though 90% of the radioactivity was excreted into urine and feces, over 80% of the radioactive material was not characterized.

In another study, [^{3}H]HP was administered to rats subcutaneously and urinary and fecal metabolites were identified using TLC and paper electrophoresis.[98] This study reported the major metabolites to be PA (60-70%) and 3-*p*-fluorophenylacetic acid (**43**) (20-30%). In that study, the recovery of radioactivity in urine was 23% in 24 hours (28% in 4 days), therefore, the % conversion of HP to PA was about 13% in 24 hour urine. Except for the administration of [^{14}C]HP decanoate, a major portion of radioactive material appeared to be excreted in urine or bile within 24 hours after the administration. Even though these reports documented that PA is the major metabolite of HP,

since their quantitation depended on the radioactivity of ^{14}C on the carbonyl carbon, or ^{3}H in the fluorophenyl ring, no data were available regarding the other half of the molecule containing the piperidine moiety **41**. No other quantitative information regarding this metabolite is available. This N-dealkylation pathway is still considered as a major metabolic pathway of HP.

3.2. Reduced Haloperidol

Reduced haloperidol (RHP, **39** in scheme 7) as a urinary metabolite of HP in humans was first identified by mass spectrometry in 1978.[99] Initial estimates of RHP plasma concentrations were equal to those of the parent compound, HP. RHP also has been identified in human serum, urine and liver homogenates by GC/MS analysis.[100]

The enzymatic reduction of HP in human liver is catalyzed by a ketone reductase which is present in cytosolic fractions.[101] This reductase also appears to be present in human red blood cells. The reduction of HP to RHP was blocked by menadione, daunorubicin, ethacrynic acid and, to a lesser extent, naloxone and methyrapone; all are known ketone reductase inhibitors or substrates.[102] On the other hand, the reduction was not inhibited by phenobarbital, an aldehyde reductase inhibitor.[102] Ketone reductase is found ubiquitously in mammalian tissues. HP is reduced to RHP in guinea pig liver cytosolic and microsomal fractions. However, since rats do not have ketone reductase,[103] the reduction does not occur in rat liver microsomal fractions.[104] The reduction is NADPH dependent and is inhibited by carbon monoxide.[101,103,104] The stereoselectivity of HP reductase in the cytosolic fractions of human brain and liver and in whole blood has been examined.[105]

The reaction was stereospecific in that only the S(-) enantiomer was detected in brain and blood. Of the RHP formed in the liver, 99.2 ± 0.1% was the S(-) enantiomer.

The physiological importance of RHP is not clear, although it has been reported that the plasma levels of RHP accounted for about 23% of the HP administered after a one 10 mg dose when given to Chinese patients.[106] The authors focused on the quantitative measurement of RHP level in plasma and therefore, mass balance of HP metabolism was not reported. The effect of RHP (1 mg/Kg, i.p. rat) is almost as great as HP on dopamine turnover (dopamine turnover is expressed as the efficiency of the conversion of dopamine to 3,4-dihydroxyphenylacetic acid or homovanillic acid). On the other hand, RHP was only 1/400 as effective as HP in displacing ^{3}H-spiperone from rat striatal membranes.[107] RHP itself is oxidized back to HP,[108] and therefore may serve as a delayed source of HP in vivo.

According to an in vivo study using guinea pigs, the formation of RHP from HP occurs rapidly.[108] HP and RHP (0.1 mg/Kg) were administered i.p. to guinea pigs and one hour later the concentrations of HP and RHP were measured by HPLC with an electrochemical detector. The highest concentration of RHP was observed in the liver which suggests the liver as the major site of reduction. However, since RHP was observed in other tissues including cerebellum, striatum and prefrontal cortex, these tissues also may be active. The concentrations of RHP and HP reported in this study are shown in Table 1.

TABLE 1

Mean (± S.D.) concentrations of HP and RHP in guinea pigs 1 hour after i.p. injection of HP or RHP.[108]

Drug administered	HP (0.1 mg/kg)		RHP (0.1 mg/kg)	
Compound quantitated	HP (μg/L)	RHP (μg/L)	HP (μg/L)	RHP (μg/L)
Cerebellum	104 ± 16	197 ± 16	4.5 ± 1.9	253 ± 56
Liver	165 ± 19	1690 ± 112	66 ± 13	2085 ± 223
Plasma	*[b]	7.3 ± 1.5	*	8.6 ± 2.3
P-cortex[a]	81 ± 24	158 ± 40	10.1 ± 4.9	221 ±120
Striatum	90	1165	17	186

[a]: Prefrontal cortex.

[b]: Below the sensitivity of the assay.

If RHP is administered to rats, the oxidation of RHP to HP appears to be rapid.[103] Two hours after RHP administration (1 mg/Kg, i.p.), the concentrations of HP and RHP were equal in the striatum. The concentrations of HP and RHP were 0.56 ± 0.06 (μmol/Kg tissue) and 0.61 ± 0.19 (μmol/Kg tissue), respectively (values are mean ± SEM, n = 4). This oxidation occurs much faster in liver than in plasma or brain and it is suggested that the primary site of oxidation is in the liver.

It has been proposed that the oxidation of RHP to HP is catalyzed by CYP2D6.[109-111] This enzyme is a member of the cytochrome P450 family of enzymes and is characterized by its ability to catalyze the oxidation of

debrisoquine to 4-hydroxydebrisoquine.[112] Quinidine, a selective CYP2D6 inhibitor and sparteine (inhibitor and also substrate) blocked HP formation from RHP in human liver microsomal incubations.[88] The expression of CYP2D6 in human is polymorphic. The metabolic rate (MR) of the CYP2D6 catalyzed oxidation of debrisoquine is defined as below.

$$MR = \frac{\%\text{ dose excreted as unchanged debrisoquine}}{\%\text{ dose excreted as 4-hydroxydebrisoquine}}$$

The poor (deficient in the CYP2D6 isozyme) metabolizers are defined as those individuals have MR value of 12.6 or greater.[112] In contrast to the in vitro results, in vivo human studies showed no correlation between oxidation of RHP to HP and CYP2D6 activity.[113] HP (5 mg) or RHP (5 mg) was administered orally to 13 healthy male volunteers with and without a prior (1 hour) oral dose of quinidine (250 mg bisulfate). Poor metabolizers produced substantial levels of HP after the administration of RHP and the amount of HP was even higher with quinidine than without. These in vivo results indicate that the interconversion of HP and RHP (Scheme 9) is not linked to CYP2D6.

Scheme 9. Interconversion between HP and RHP.

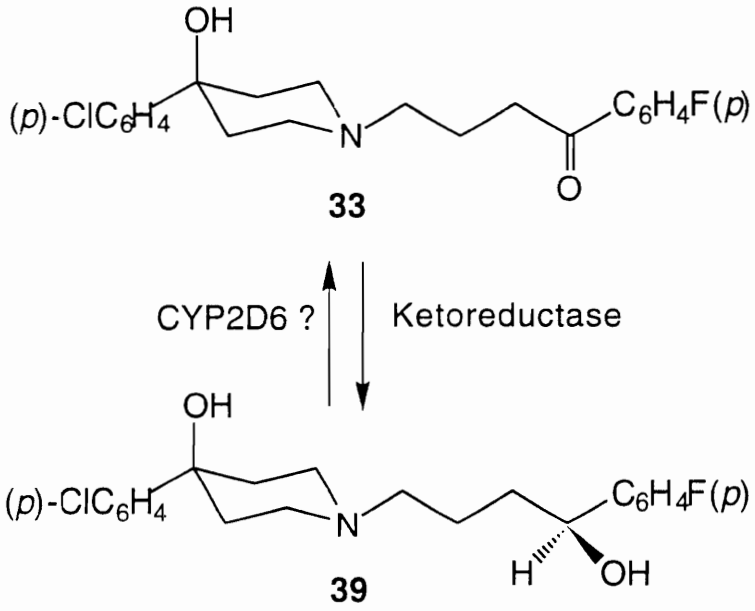

3.3. Conjugation

HP is also metabolized via conjugation. Three conjugated metabolites of HP have been isolated from the urine obtained from HP-treated patients and healthy volunteers.[114] Patients were dosed with 30-40 mg/day and volunteers with 1 mg/day. The metabolites were purified by HPLC with immunological detection using three types of anti-HP antisera. These conjugated metabolites have been identified by UV spectrometry, ^{1}H-NMR and field desorption mass spectrometry. HP-O-glucuronide (HP-Glu, **46** in Chart 1) turned out to be a major urinary metabolite. About 18% of the dose was excreted as HP-Glu in the 24 hour urine collection. Two other conjugates were a glucuronide conjugated at the 2-hydroylated 4-fluorophenyl ring of RHP (**47**) and a sulphate conjugated at the 2-hydroylated 4-fluorophenyl ring of RHP (**48**). The amount of these two conjugates was less than 1% of the dose.

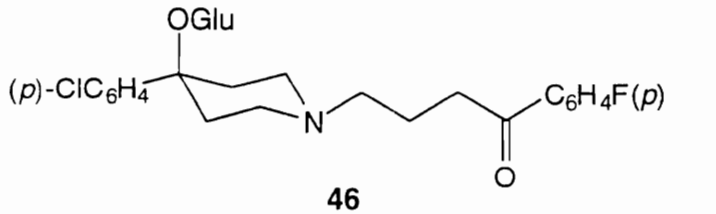

46

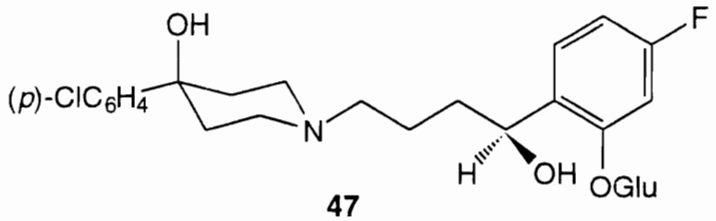

47

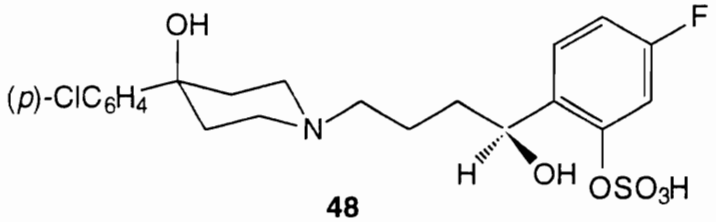

48

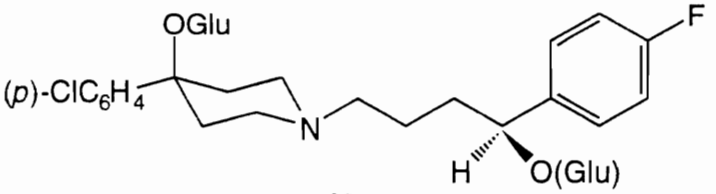

49

Chart 1. Structures of conjugated metabolites of HP.

As mentioned earlier, it was reported that HP-Glu was 26% of the dose in the 24 hour-bile of rat after [^{14}C]HP treatment.[96] The authors obtained this number by measuring the change in the amount of HP in urine and bile before and after the incubation with β-glucuronidase. In contrast to the result of the study described above,[114] they did not observe conjugates in the urine sample. However, others reported that de-glucuronidation by β-glucuronidase failed due to its steric hindrance.[95,114] Human plasma concentrations of HP-Glu, RHP-

Glu (**49**), HP and RHP were measured using HPLC with UV detection.[115] HP was administered to 39 patients orally three times a day for at least two weeks at a constant dosage (2.25-50 mg/day) until the time of blood sampling. Blood samples were collected 12 hours after the evening dose. Plasma concentrations of glucuronides were determined by incubating plasma with β-glucuronidase and measuring the amount of HP and RHP before and after the reaction. According to these observations, the ratio of mean plasma concentration of HP-Glu to RHP was 2.5/1. Since the reduction pathway has been shown to account for 23% of HP metabolism by measuring RHP levels in plasma,[106] simple combination of these data indicate that about 50-60% of the HP metabolism could involve HP-Glu formation. The authors also referred to two studies previously reported. One study documented that 18% of the dose was excreted as HP-Glu into human urine.[114] Another study reported that only 30% of the radioactivity was recovered in human urine after [^{14}C]HP oral administration,[116] suggesting HP-Glu could account for about 60% of all urinary metabolites. The authors did not report conjugates (**47**, **48**) which have been documented in urine.[114] At the same time, the previous report did not mention the observation of **49** in urine.[114] These differences might be due to the sampling of different matrices, i.e. urine and plasma. However, it has been reported that de-glucuronidation by β-glucuronidase failed due to its steric hindrance[95,114] and thus the differences in these reports remains unclear.

3.4. Pyridinium metabolites derived from HP

The 4-(4-chlorophenyl)-1-[4-(4-fluorophenyl-4-oxobutyl]pyridinium species HPP^+ (**36**) was first isolated and identified in urine and brain tissues of HP-treated rats.[117] HPP^+ was characterized by HPLC/diode array analysis and HPLC/thermospray mass spectrometry. With a highly sensitive atmospheric pressure ionspray HPLC/MS/MS, HPP^+ was also identified in the urine extracts of HP-treated patients and extracts of NADPH-supplemented human liver microsomal incubation mixtures containing HP.[118] The neurotoxic properties of HPP^+ have been examined and compared with those of MPP^+ in vivo in the rat by intracerebral microdialysis. It was demonstrated that the perfusion of the striatum with HPP^+ leads to the irreversible depletion of striatal dopamine in a manner similar to that observed with MPP^+.[119,120] HPP^+ was a less potent dopaminergic neurotoxin than MPP^+ (ED_{90} values were 500 min and 60 min). However, the two compounds showed comparable toxicity on the serotonergic system (ED_{90} values were 165 min and 120 min for HPP^+ and MPP^+, respectively).[120] Similar to MPP^+, HPP^+ is reported to be a substrate for the brain synaptosomal dopamine transporter,[121,122] and to be toxic to rat embryonic mesencephalic neurons in culture[121] and to cultured neuroblastoma cells.[123] HPP^+ proved to be a weaker inhibitor of mitochondrial respiration than MPP^+ in vivo as measured by increases in intracerebral extracellular lactate levels.[119] On the other hand, HPP^+ is more potent than MPP^+ as an inhibitor of mitochondrial respiration in vitro with IC_{50} values of 12 μM for HPP^+ and 160 μM for MPP^+.[119] Thus HPP^+ was established as an MPP^+-type neurotoxin and therefore HP as a potential MPTP-type protoxin.

The critical question concerns the neurotoxic potential of HP in the human. Since the development of drug induced tardive dyskinesias often requires months or even years of drug exposure,[3,15] the demonstration of a drug induced lesion in experimental animals may be difficult. Furthermore, due to the dramatic species selectivity of MPTP[34] with the subhuman primate being by far the most sensitive model, the absence of a detectable anatomical lesion in HP or HPTP treated rodents may not provide a definitive answer to the question of the neurotoxic potential of HP.

These previous studies have documented HPP^+ formation from HP and HPTP and also its toxicity. However, quantitative information has not been available.

Overall, it appears that previous studies focused on the identification of metabolites and when analysis is quantitative, measurement of metabolites only dealt with one specific metabolic pathway. The systematic studies for the mass balance of HP metabolism had not been conducted.

Our principal interest was to examine the metabolic fate of HP and HPTP, especially in terms of the formation of a neurotoxic pyridinium metabolite. However, since previous studies[96,114-116] could not account for the major part of the metabolism of the parent drug HP, we wanted to obtain quantitative information regarding the pyridinium formation as well as confirm previously reported metabolites and identify possible additional metabolites. First, we focused our attempts on the development of an assay for the quantitative analysis for HPP^+.

Chapter 4

4.1. Assay development

HPP^+ has been characterized in both in vivo and in vitro studies with rats and HP-treated patients with the aid of HPLC/thermospray mass spectrometry and API-HPLC/MS/MS.[117,118,124] Although HPLC/MS has the advantage of adding mass characterization of analytes, we needed to develop a flexible technique in order to analyze metabolites on a routine basis. Since we were particularly interested in the formation of HPP^+, a possible neurotoxic metabolite of HP and HPTP, we attempted to develop a method that was sensitive and selective for pyridinium species. As described in Chapter 3, HPP^+ is structurally similar to the neurotoxin MPP^+, a metabolite of the parkinsonian inducing agent MPTP. Previously, the quantitative determination of MPP^+ by HPLC with UV detection was of limited utility because of lack of sensitivity and selectivity. In most cases, the sample matrices are complex, i.e., biological matrices like urine and tissue homogenates. These samples require extractions or other purification steps prior to analysis. For example, for one reported MPP^+ analysis in MPTP incubation mixtures, after extraction of unreacted MPTP with an organic solvent, MPP^+ was converted into MPTP by reduction with sodium borohydride and then the MPTP generated was measured by HPLC/UV analysis.[42,125] The possibility of an improved assay was realized when the fluorescent properties of MPP^+ were identified. HPLC with fluorescence detection was found to be able to measure 10 fmol of MPP^+.[126]

Although HPP^+ is more lipophilic than MPP^+, both are pyridinium species and therefore we considered the possibility of developing an HPLC/fluorescence assay for the analysis of HPP^+ in biological samples. In

work carried out in collaboration with Dr. Kazuo Igarashi, a synthetic standard of $HPP^+ I^-$ (prepared in our laboratory)[117] was scanned on a Perkin Elmer LS-240 HPLC fluorescence system in the stopped flow mode. HPP^+ was found to be fluorescent and, based on excitation and emission spectral characteristics, optimal wavelengths for excitation and emission were determined to be 304 and 374 nm, respectively (Figure 1).

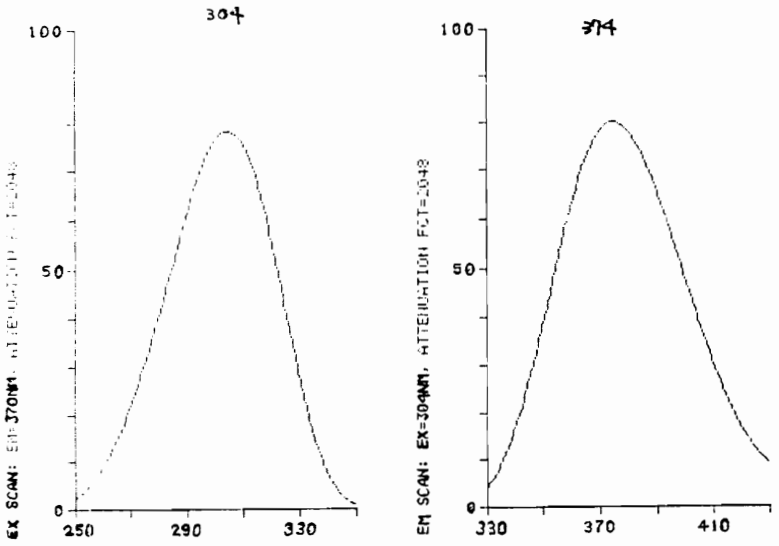

Figure 1. Excitation and emission spectra of HPP^+.

With these wavelength settings, the HPP^+ standard was analyzed on an HPLC system composed of a μBondapak C18 column (10 μm particle size, 150 mm x 3.9 mm, Waters, Assoc., Milford, MA), a Perkin Elmer LS-240 fluorescence detector (Perkin Elmer, UK), LCI-100 integrator (Perkin Elmer), and a model 110A constant-flow pump (Beckman Instruments, Fullerton, CA) set at a flow rate of 1 mL/min. The mobile phase was filtered and degassed prior to use. The mobile phase used for the MPP^+ assay consisted of 30 mM ammonium

acetate buffer-acetonitrile (80:20, v/v) containing 0.5% triethylamine, and 10 mM 1-heptanesulfonic acid. The pH was adjusted to 7.5 with acetic acid. However, due to its lipophilic character, HPP^+ was not eluted by this mobile phase. In order to achieve a reasonable retention time for HPP^+, the ratio of 30 mM ammonium acetate buffer-acetonitrile was changed to 60/40 (v/v) and triethylamine content was lowered to 0.2%. Using trifluoroacetic acid, the effects of pH (2-7) on the retention time of the analyte was investigated. As shown in Figure 2, the retention time was minimal at pH 3.5. In contrast to the properties observed for MPP^+,[126] the fluorescence intensity of HPP^+ proved to be essentially independent of pH.

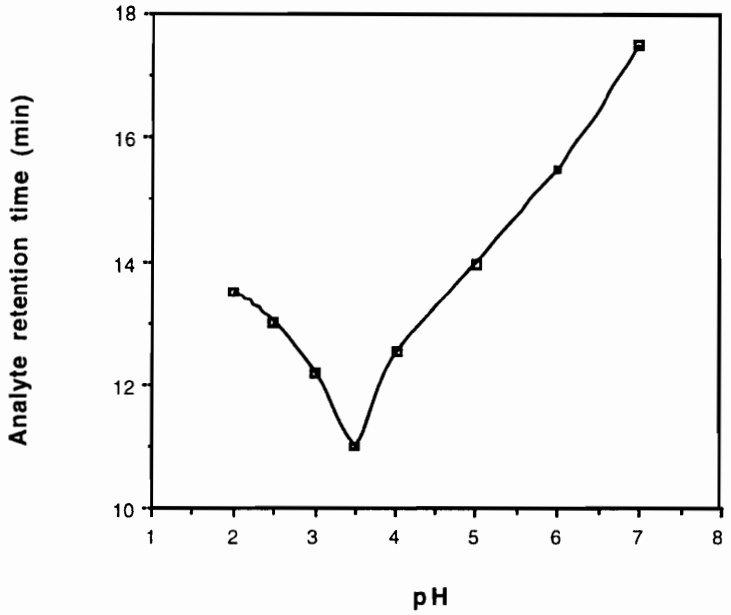

Figure 2. Variations in retention time of HPP^+ versus pH.

Based on these results, the initial assay development employed a mobile phase consisting of 30 mM ammonium acetate buffer-acetonitrile (60:40, v/v) modified with 0.2% triethylamine and adjusted to pH 3 with trifluoroacetic acid. Later, the mobile phase was changed to 10 mM ammonium acetate buffer-acetonitrile (60:40, v/v) containing 0.2% triethylamine and 0.1% acetic acid. Since the difference in concentration of buffer between 10 mM and 30 mM did not affect the fluorescence intensity, the buffer concentration was reduced to 10 mM in order to extend the column life and maintain system stability. The pH, which occurred at 6.2 as a result of mixing all components, also was satisfactory. This made the process of preparing the mobile phase much easier. The retention time of HPP^+, HP and HPTP were 12.5, 8.0, and 21.0 min, respectively.

Our aim was to develop a quantitative HPLC assay for HPP^+ which we could run easily on a daily basis. For the analysis of real samples (i.e., incubation mixtures, tissue homogenates, urine, feces, plasma), we also wanted to be able to measure simultaneously non-fluorescent compounds such as HP, HPTP and other possible metabolites. Therefore, a Model D variable-wavelength UV detector (LDC Analytical, Riviera Beach, FL) was placed in-line after the fluorescence detector. HPP^+ also was UV sensitive (λ_{max} 305 nm, ε 24,000 and 245 nm, ε13,500 in 0.1 M sodium phosphate buffer). The limit of detection of HPP^+ by fluorescence detection was 1.3 pmol on column with a signal-to-noise ratio of 4:1. As shown in the HPLC/fluorescence and UV tracings of 240 nM (12 pmol on column) HPP^+ standard (Figure 3), the fluorescence assay is at least 20 times more sensitive than the UV assay. Therefore the quantitative measurement of HPP^+ was conducted by

fluorescence detection while the UV detector was set at 245 nm to measure non-fluorescent compounds.

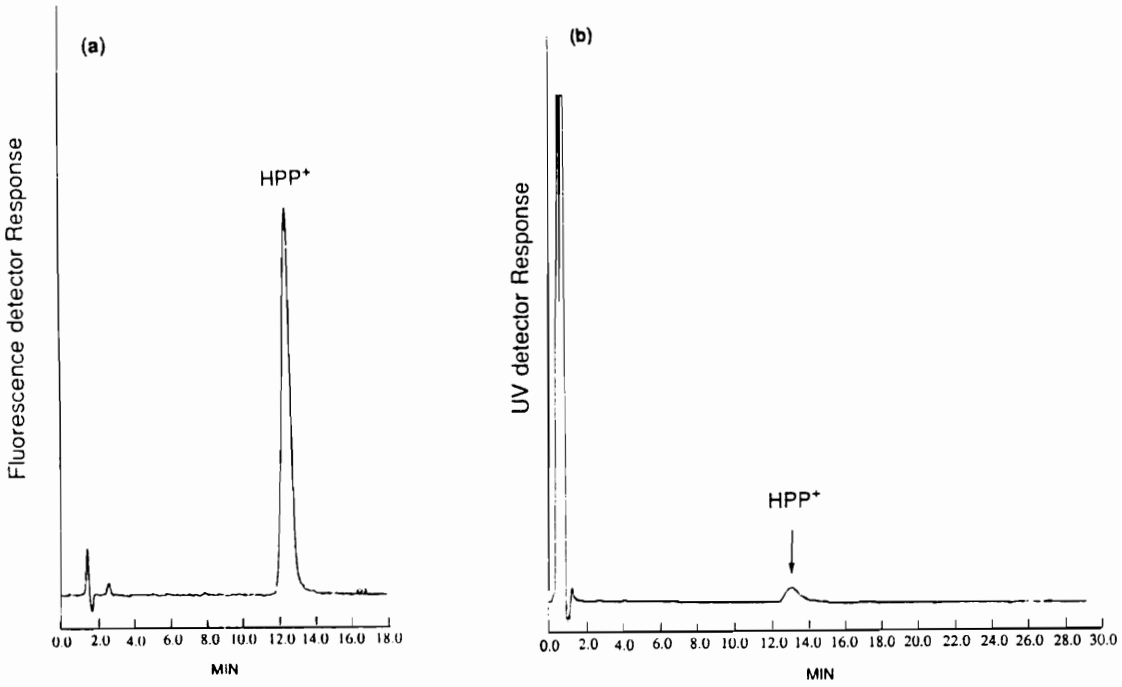

Figure 3. HPLC tracings of HPP^+ standard (12 pmol on column) with fluorescence and UV detection. For the fluorescence detection, the excitation wavelength was 304 nm and the emission wavelength was 374 nm. For UV, the wavelength was 305 nm.

Originally, attempts to use the perchlorate salt of the 4-phenyl-1-(4-phenyl-4-oxobutyl)pyridinium species (**50**) as an internal standard were pursued. However, the excitation and emission λ_{max} values of this compound were 275 and 330 nm, respectively, and its fluorescence intensity under the assay conditions was only about 1/15th that of HPP^+. We were not able to find an appropriate internal standard. Since (as will be discussed later) we could obtain reproducible linear external calibration curves with a small coefficient of

variation (C.V.) from biological samples, we decided to use these external calibration curves.

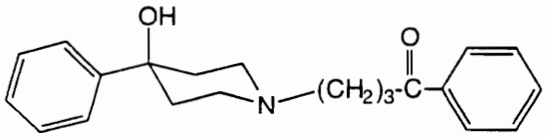

50

Previously HPP^+ had been identified in urine samples and brain tissues of HP-treated rats by HPLC-diode array analysis and HPLC/thermospray mass spectrometry.[117] In that study, HPP^+ was extracted from urine into chloroform as an ion pair as $HPP^+{\cdot}I^-$. An independent study established that $HPP^+{\cdot}I^-$ recovery from aqueous solutions buffered to pH 4-10 was achieved with low overall recoveries of 36-45% using ethyl acetate and 53-55% using chloroform. In addition to these rather low recoveries, the corresponding extracts from biological samples (urine, brain tissues obtained from untreated rats) spiked with HPP^+ showed many background peaks (Figure 4).

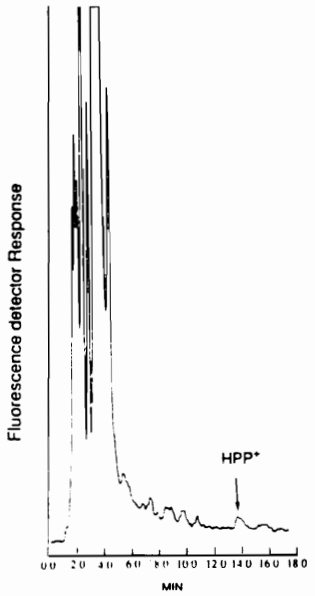

Figure 4. HPLC/fluorescence tracing of $HPP^+{\cdot}I^-$ spiked urine extracted with ethyl acetate.

An alternative liquid-solid clean-up and extraction method using C18 cartridges was investigated. First, Sep-pak classic C18 cartridges (Waters, Assoc.) were used. Initially, luer-lock glass syringes were used for the sample processing and all steps were done manually. Cartridges were preconditioned by washing with 10 mL of methanol followed by 10 mL of 30 mM ammonium acetate. A 0.1-mL aliquot of the standard solution of $HPP^+ \cdot I^-$ (52 nM in water) was mixed with 1.0 mL of 30 mM ammonium acetate and the resulting mixture was loaded onto a preconditioned cartridge. After a 1-minute equilibration period, the solvent was gently purged from cartridge. Then the cartridge was washed with 10 mL of 30 mM ammonium acetate followed by 5 mL of methanol-water (50:50, v/v). Then HPP^+ was eluted with 3 mL of methanol or a solution of 0.5% glacial acetic acid in methanol. The use of acidic methanol improved the recovery of HPP^+ from Sep-paks compared to the elution with methanol. The % recoveries of HPP^+ from the Sep-Pak when eluted with methanol and acidic methanol were 55 ± 4% and 94 ± 5%, respectively (n = 3). The eluent was evaporated to dryness under a nitrogen stream at room temperature. The residue was dissolved in 0.1 mL of the mobile phase and a 50 µL-aliquot was injected onto the HPLC system. The recovery of HPP^+ was above 80% (85 ± 7%, n = 6). A more extensive recovery experiment was performed. $HPP^+ \cdot I^-$ (1.3-52.0 pmol) was spiked into urine and plasma (Table 2) obtained from rats and the % recovery was examined under these conditions. In order to prepare plasma samples, blood samples were obtained by cardiac puncture using heparinized syringes from animals anaesthetized with diethyl ether. After a centrifugation at 1000 g for 5 minutes, the plasma fraction was obtained. The plasma was spiked in the same way as urine. Each fraction, including washes

(ammonium acetate, water, 50% methanol), were collected and dried, then redissolved in the mobile phase and analyzed by HPLC. Many endogenous components from the biological samples were removed by 30 mM ammonium acetate and 50% methanol wash fractions. A small amount of HPP^+ was lost in the 50% methanol wash. As summarized in Table 2, the % recoveries from both urine and plasma are acceptable. Since inter-day variability was observed, calibration curves with spiked HPP^+ were constructed each time when biological samples were processed for HPLC analysis.

TABLE 2

HPP^+ recovery from classic Sep-pak™ (C18) extraction

Sample	Spike HPP^+ (pmol)	Intra-day (n = 5)		Inter-day (n = 5)	
		% recovery	% C.V.	% recovery	% C.V.
Plasma	2.6	96.0	6.3	94.0	6.8
	5.2	98.5	5.7	97.5	5.9
Urine	13	99.4	4.3	100.2	4.6
	52	99.7	4.1	99.9	5.0

Recoveries of HPP^+ from urine and plasma were calculated by comparing the peak height of the extracted HPP^+ versus the peak height obtained with a standard aqueous solution of $HPP^+ \cdot I^-$ analyzed by the same procedure.

After these procedures had been established, urine and brain tissues obtained from HP- or HPTP-treated C57BL/6 mice were processed and analyzed. The HPLC/fluorescence tracing of urine obtained from HPTP-treated mice is shown in Figure 5. The major fluorescent peak (t_R = 12.0 min), coeluted with the synthetic HPP^+. In order to confirm the structure of the metabolites, pooled urine from HP or HPTP treated mice was analyzed by API LC/MS and LC/MS/MS (by Dr. Fouda at Pfizer, Inc.) The details of these experiments will be discussed in Chapter 6.1. The fluorescent peak that eluted at 7.3 minutes was identified as reduced HPP^+ ($RHPP^+$). This peak coeluted with a synthetic standard of $RHPP^+$ which was synthesized as its chloride salt.[148] The structure also was confirmed by API LC/MS and LC/MS/MS (see Chapter 6.1.). We have been able to employ this assay also with brain tissues. In this case we found that Sep-pak purification and extraction were not necessary. The method is described in a later section in this Chapter. Urine samples obtained from HPTP-treated baboons and HP-treated psychiatric patients also were analyzed by these procedures (see Chapter 6.2, 6.3). Both synthetic standards, $RHPP^+$ and HPP^+, were spiked into control human urine and calibration curves were constructed each time when samples were processed. Human control urine was used to for spiked calibration curves in order to construct calibration curves as close to the matrices of real biological samples as possible.

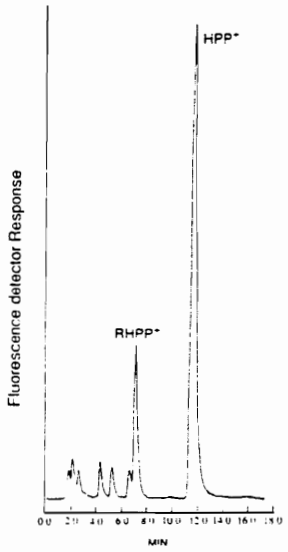

Figure 5. HPLC/fluorescence tracing of urine extracts obtained from an HPTP-treated C57BL/6 mouse.

During the early phase of this assay development using Sep-paks, several problems were encountered. We detected an artifact peak in HPLC/fluorescence tracings. This peak coeluted with the synthetic standard HPP^+ and was observed in control plasmas from untreated patients. This peak turned out to be due to a component that was extracted from the Sep-paks. At that time, we were using Waters C18 classic Sep-paks made of polyethylene. Therefore, we sought more solvent resistant solid-liquid extraction cartridges. Waters Sep-pak Vac (syringe type cartridge) 1 cc, 3 cc-size cartridges and Supelco Spelclean (syringe type) 1 cc-size cartridges were used for the spiked HPP^+ recovery check. These cartridges were made of polypropylene (and did not contain the substance present in the polyethylene that was causing the problem). Optimization of the assay conditions included purging solvents gently with a nitrogen stream instead of the use of luer lock glass syringes in order to

avoid solvent-surface contact. Also solvent volumes for the preconditioning and washing were reduced in order to reduce the risk of extracting any substance from Sep-paks. The concentration of ammonium acetate buffer was reduced from 30 mM to 10 mM (the same as the modified mobile phase) and water was used between the ammonium acetate buffer and methanol in order to avoid any salt precipitate that clogged the cartridge. Out of three syringe type cartridges tested, both Waters and Supelco 1 cc-size cartridge showed low % recovery (63 to 70%). Using Waters Sep-pak Vac 3 cc^{TM}, the % recovery of spiked HPP^+ remained as high as that obtained by the previous method but employed less solvent. Most importantly, no artifact peak was observed in control samples.

Another problem was found as we analyzed more urine samples obtained from HP- or HPTP-treated mice. Analysis of some urine samples did not show the pyridinium peaks as expected. This absence of the analytes appeared to be a problem with the extraction procedure. The pH of these mouse urine samples was measured and turned out to be in the range of 6 to 8 for those samples showing pyridinium metabolites in the assay. On the other hand, urine samples that showed no pyridinium peaks were acidic (pH ~4). The effects of pH of the samples were examined at three pH levels. $HPP^+ \cdot Cl^-$ was spiked into human control urine (pH 5.5) to make a final concentration of 20 μM and the pH was adjusted to 2, 5, and 7 with aqueous HCl or NaOH. As shown in Table 3, in all 3 cases, HPP^+ was lost in the 50% methanol wash. The more basic the samples are, the higher % recovery in the 0.5% acetic acid/methanol fraction. Even at pH 7, the % recovery in the 0.5% acetic acid/methanol fraction is lower than the result obtained from our preliminary recovery check (shown in Table 2). We do not have a clear answer for this result. However, the urine

samples used for that experiment might have had the higher pH. Since HPP^+ was lost in the 50% methanol solution at all pH values studied, this washing step prior to the elution was skipped after the water wash. Unfortunately, this increased some biological background peaks. However, those peaks did not interfere with the analysis of $RHPP^+$ or HPP^+. Although by skipping this wash, the pH effect could be ignored, in order to keep sample conditions consistent, the pH of the samples was adjusted to 8.5 with 0.5 M K_2HPO_4.

TABLE 3

Effect of pH on the recoveries of HPP^+ spiked urine utilizing Sep-paks extraction

	50% methanol wash		0.5% acetic acid/methanol	
	% recovery	% C.V.	% recovery	% C.V.
pH 2	71	3.1	33	3.2
pH 5	33	2.4	59	1.9
pH 7	14	5.7	79	1.0

Current procedures (see below) was used for the study.

The final procedure which emerged from these studies is as follows: Waters Sep-pak Vac 3 cc was preconditioned with 1.5 mL methanol followed by 1.5 mL of Milli-Q water and 1.5 mL of 10 mM ammonium acetate buffer. Then urine samples (in general 400 µL) treated with 0.5 M K_2HPO_4 to adjusted pH to 8.5 were loaded onto the Sep-paks. The loaded Sep-paks were washed with 2 mL of Milli-Q water, following which the analytes were eluted using 3 mL of 0.5% acetic acid/methanol. The procedure after the Sep-pak elution step is the

as same as the original method. With this procedure, the % recovery of $RHPP^+$ and HPP^+ from urine was reproducible and acceptable (Table 4).

TABLE 4

Recoveries of pyridinium analytes spiked in control urine using Sep-pak Vac 3 cc™

	% recovery	% C.V.
$RHPP^+$ (n = 6)	87 ± 6	7.1
HPP^+ (n = 6)	89 ± 3	3.4

% Recovery was calculated using slopes of the calibration curves obtained from spiked urine samples compared to that of standard solutions of corresponding pyridinium derivatives injected directly onto HPLC without Sep-pak process.

As mentioned earlier, since an appropriate internal standard was not available, external calibration curves were constructed by spiking $HPP^+ \cdot Cl^-$ and $RHPP^+ \cdot Cl^-$ into control urine. The amounts of pyridinium standards used for the spiked calibration curves were chosen to give concentrations of those points that would produce peak heights within the recording range of the integrator following injection of a 50-µL aliquot. These calibration plots (four concentrations, Figure 6) were linear over the concentration range of 0-542 nM HPP^+ (0-27 pmols on column) and 0-88 nM $RHPP^+$ (0-4.4 pmols on column). The detector response of $RHPP^+$ was approximately 4 times greater than that of HPP^+. The lower limits of detection were approximately 1.3 pmol of HPP^+ and 0.4 pmol of $RHPP^+$.

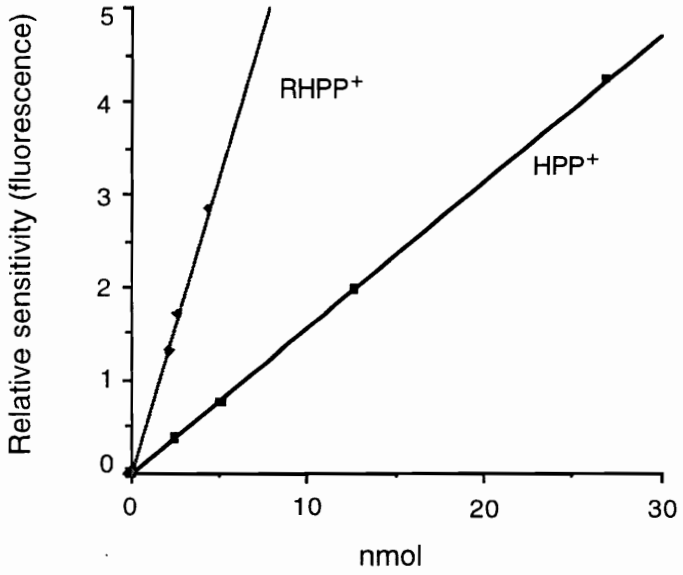

Figure 6. Typical calibration curves for the HPLC/fluorescence assay of HPP^+ and $RHPP^+$.

In addition to the urine analysis, we attempted to analyze the metabolites excreted into feces utilizing this Sep-pak extraction procedure. Since the samples were normally dry at the time of collection (24 hours after administration), samples were first soaked in methanol for a few hours and then were ground in Eppendorf tubes. These samples were centrifuged and the supernatant was applied to the Sep-pak. After the samples were loaded onto the Sep-paks, all procedures were the same as for urine samples. In order to be consistent, 0.1 g of dried feces was soaked in 1 mL methanol for 1 hour and the centrifugation was at 14,000 rpm for 6 minutes. A 400 μL-aliquot of supernatant was applied to Sep-pak. Feces from HP and HPTP-treated mouse were examined to see if HPP^+ was present in the fecal extracts. HPP^+ was observed in the HPLC/fluorescence tracings. However, this measurement of HPP^+ in fecal extracts was established in the later period of in vivo work.

Therefore, this method was mainly used in the studies concerned with the fate of HPP^+ administered to the animals (see Chapter 6.1.). In order to construct calibration curves, methanolic $HPP^+ \cdot Cl^-$ was spiked into methanol-feces sample tubes (final concentration 0-271 nM, 0-14 pmol on column) and processed as same as the samples. The % recovery of the spiked HPP^+ was 60-65%, which was lower than that of the urine samples. However, the curve was linear in this concentration range. As with the urine analysis, the calibration curve was constructed each time the samples were processed.

The next step was to investigate which enzyme system(s) is(are) contributing to the formation of these pyridinium metabolites from HP and HPTP in the in vitro incubation studies. Therefore we also wanted to be able to apply this assay to incubation mixtures derived from various tissue. HP and HPTP incubations were to be conducted with C57BL/6 mouse liver microsomes, whole brain homogenates, human placental MAO-A, beef liver MAO-B and human liver microsomes. These incubation mixtures contained protein (tissue homogenates, or further purified fractions, such as microsomal, mitochondrial preparations) and buffer, substrate (i.e., HP or HPTP) and sometimes cofactors. This type of matrix is essentially the same as that encountered in the in vivo studies involving brain tissue homogenates. When the tissue homogenates from the in vivo studies were purified and extracted by Sep-paks, it was noticed that these samples were much cleaner than the urine samples. Consequently, we attempted to extract the pyridinium metabolites without Sep-pak processing. It appeared that protein was the only contaminant that would interfere with the HPLC assay. Therefore, an acidified organic solvent was used to precipitate protein. The control brain homogenates were prepared by homogenizing three

C57BL/6 mouse brains with 4 volumes of 1.15% aqueous KCl using a glass Potter-Elvehjem homogenizer. The homogenates were mixed together and homogenized again. Then 100 μL of 1 mM HPTP·HCl solution (10% methanol/water) was spiked into 300 μL of the mouse brain homogenate in 600 μL of 0.1 M potassium phosphate buffer to make a final concentration of 100 μM (total sample volume 1 mL). As soon as the HPTP was spiked and the samples were vortexed, 600 μL of this mixture was removed and 600 μL of 0.1% (or 2%) acetic acid in acetonitrile was added. This sample was vortexed and centrifuged at 14,000 rpm for 6 minutes to precipitate the protein. The supernatant was removed and dried under nitrogen. Then this sample was redissolved into the mobile phase and analyzed by HPLC/UV at 254 nm to examine the % recovery of HPTP from the tissue homogenates. As summarized in Table 5, good recovery was observed in both 0.2% and 2% acetic acid/acetonitrile elution.

TABLE 5

HPTP recovery from brain homogenates spiked with HPTP·HCl

Elution	% recovery	% C.V.
0.2% acetic acid/CH_3CN	102 ± 2.1	2.1
2% acetic acid/CH_3CN	110 ± 1.5	1.4

Numbers are the mean ± S.D. of triplicate determinations.

HPP^+ also was spiked into the mouse brain homogenates to examine its recovery. A 600 μL-aliquot was removed from the homogenate and transferred to an Eppendorf centrifuge tube. $HPP^+ \cdot Cl^-$ solution (in acetonitrile) was added

to make final concentrations of 0 (no spiking), 164, 264, and 328 nM. A 480 μL-aliquot of 2% glacial acetic acid/98% acetonitrile was added and acetonitrile was added to make the total volume of the sample always 1200 μL. The homogenates were vortexed and allowed to stand at room temperature for 5 minutes. The samples were vortexed again and then centrifuged in an Eppendorf microcentrifuge at 14,000 rpm for 6 minutes. All the supernatant was removed from centrifuge tube and evaporated under a nitrogen stream. The residue in 240 μL of the mobile phase was vortexed and again centrifuged at 14,000 rpm for 6 minutes. A 50 μL-aliquot of the supernatant was analyzed by HPLC/fluorescence. The amount of HPP^+ was compared with the external HPP^+ calibration curve. As summarized in Table 6, good recovery from the brain tissue homogenates with acceptable C.V. was observed. The HPLC tracings did not have any interfering biological background peak (Figure 7). This process is much faster and easier than when the Sep-pak extraction was required. For the tissue analysis (brain, liver, kidney, etc.) for in vivo studies (Chapter 6), the samples were homogenized and the supernatant fractions were analyzed as described above. The limit of detection for HPP^+ was 1.3 pmol on column which corresponds to 25 pmol/g wet tissue.

TABLE 6

HPP^+ recovery from brain homogenates spiked with HPP^+

Spiked $HPP^+ \cdot Cl^-$ (nM)	% recovery	% C.V.
0	0	0
164	98.2 ± 2.6	2.6
264	91.0 ± 4.5	5.0
328	101.4 ± 1.2	1.2

All numbers were the mean ± S.D. of three measurements.

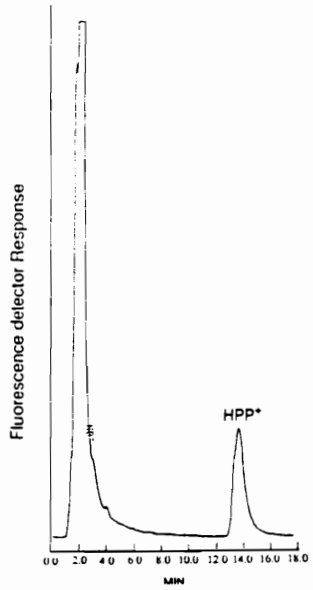

Figure 7. HPLC/fluorescence tracing of HPP^+ spiked in the mouse brain homogenate processed by protein precipitation method.

We also attempted to identify possible metabolites including 3-*p*-fluorobenzoylpropionic acid (**43**) and HP-O-Glu (**46**), reported metabolites in the in vivo studies. Also CPHP (**41**), an N-dealkylated metabolite only reported in in vitro studies, was of interest. These attempts are discussed in later Chapters.

Chapter 5

In Vitro Studies on HP and HPTP Metabolism

5.1. Incubation studies with MAO.

A major impetus for considering the possible bioactivation of cyclic tertiary amines is based on results from studies on the parkinsonian inducing nigrostriatal neurotoxin MPTP. It has been documented that the outer mitochondrial membrane bound flavoproteins MAO-A and MAO-B are efficient catalysts for the α-carbon oxidation of a specific class of cyclic tertiary amines, namely 4-substituted 1-methyl-1,2,3,6-tetrahydropyridines including MPTP.[62,63] Extensive investigations have documented that the neurodegenerative properties of MPTP ultimately result from the inhibition of mitochondrial electron transport by its MAO-B generated pyridinium metabolite MPP^+. MPTP is oxidized to the dihydropyridinium species $MPDP^+$ by MAO-B and $MPDP^+$ is further oxidized to MPP^+.

As mentioned earlier, HP resembles MPTP in that it bears an aryl group at C-4 of the piperidinol moiety. Furthermore, simple dehydration of HP, a reaction which is reported to occur in microsomal incubations,[94] gives the corresponding 1,2,3,6-tetrahydropyridine derivative HPTP. The in vivo formation of HPP^+ in rodents and humans has been reported.[117,118] Both compounds are biotransformed to HPP^+ by rat liver microsomal preparations, presumably via cytochrome P450 catalysis since the conversion is NADPH dependent.[124] These studies were conducted by HPLC/UV analysis with a much lower sensitivity than that of the HPLC/fluorescence assay (see Chapter 4),. Consequently we attempted to gain additional insights into the metabolic

fate of HP and HPTP using this assay. In this Chapter, we report the results of our studies on the MAO-A and MAO-B substrate properties of HP and HPTP.

Results and Discussion

A previous report concerns the substrate properties of HP and HPTP with MAO-B and P450 and utilized an HPLC/UV assay which has a low sensitivity (reported detection limit, 3 μM).[124] We wanted to use the more sensitive assay to examine the possible contribution of MAO to the oxidation of HP and HPTP. HP and HPTP (substrate concentrations 1 μM to 20 μM) were incubated with MAO-A (purified from human placenta) to see if HPP^+ was formed from these substrates. After 15 minutes at 37 °C, the incubation mixtures were analyzed by the HPLC/fluorescence assay described in the previous Chapter. The substrate was incubated in the absence of enzyme to provide a control sample. As shown in Figure 8, HPP^+ formation was observed with HPTP as substrate (panel c) but not HP (panel b). Even at the highest concentration of HP (40 μM), the HPLC tracings obtained from the HP incubation mixture (b) were not different from that of the control (a) which has no protein in the incubation mixture.

HPP^+ formation from HPTP was completely blocked by the selective MAO-A inhibitor clorgyline (9 μM). In order to establish more rigorously that the HPP^+ formation from HPTP is MAO-A catalyzed, nanomolar levels of clorgyline should have been used to block the HPP^+ formation. Since we did not examine this inhibition systematically, this result should be considered as preliminary. However, since HPTP is likely to be a substrate for MAO-A, we attempted to

obtain the kinetic parameters for this transformation. HPTP was incubated over a substrate concentration of 1 μM to 40 μM and analyses were performed during the 0 to 15 minute time period. By knowing the amount of MAO-A used for the incubation (0.3μM), HPP^+ formation was plotted as pmols of HPP^+ formed/nmol of MAO-A against time for each substrate concentration (Figure 9).

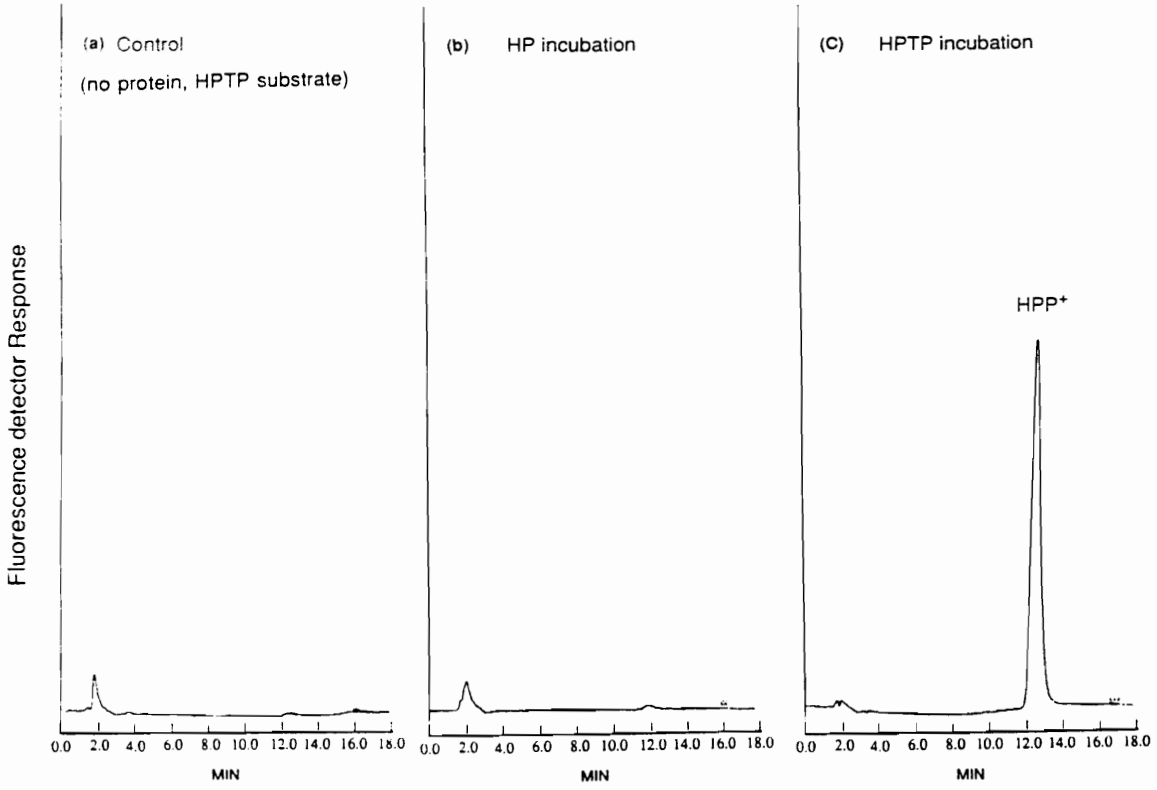

Figure 8. HPLC/fluorescence tracings of obtained from MAO-A incubation mixtures of (a) control; no protein, HPTP substrate, (b) HP substrate and (c) HPTP substrate.

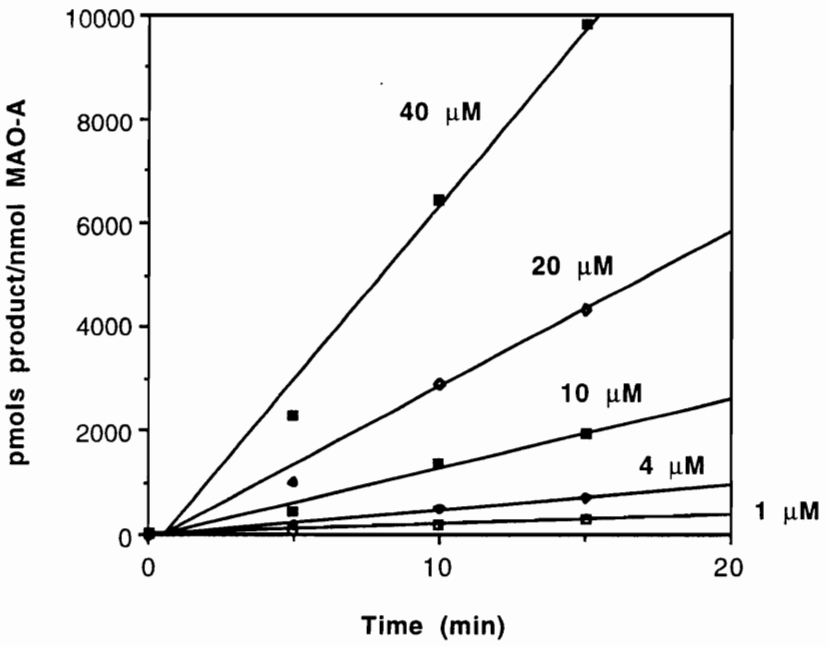

Figure 9. Kinetic plots of the MAO-A catalyzed oxidation of HPTP.

HPP^+ formation from HPTP was time and substrate concentration dependent. The rates of HPP^+ formation from HPTP were obtained from Figure 9 for each substrate concentration (the slopes of the curves give the rates of HPP^+ formation in pmol/nmol of enzyme-min). Then a double reciprocal plot of the rate of HPP^+ formation against substrate concentration (Lineweaver-Burke plot) was constructed (Figure 10). The k_{cat} and K_M values were calculated to be 0.45 min^{-1} and 25 μM, respectively. Although this experiment should be repeated with a more homogeneous MAO-A preparation, the k_{cat}/K_M ratio of 18 $min^{-1}mM^{-1}$ suggests that this compound is a relatively poor MAO-A substrate (for example, the k_{cat}/K_M value for the MAO-B catalyzed oxidation of MPTP at 37 °C is about 1400 $min^{-1}mM^{-1}$).[127]

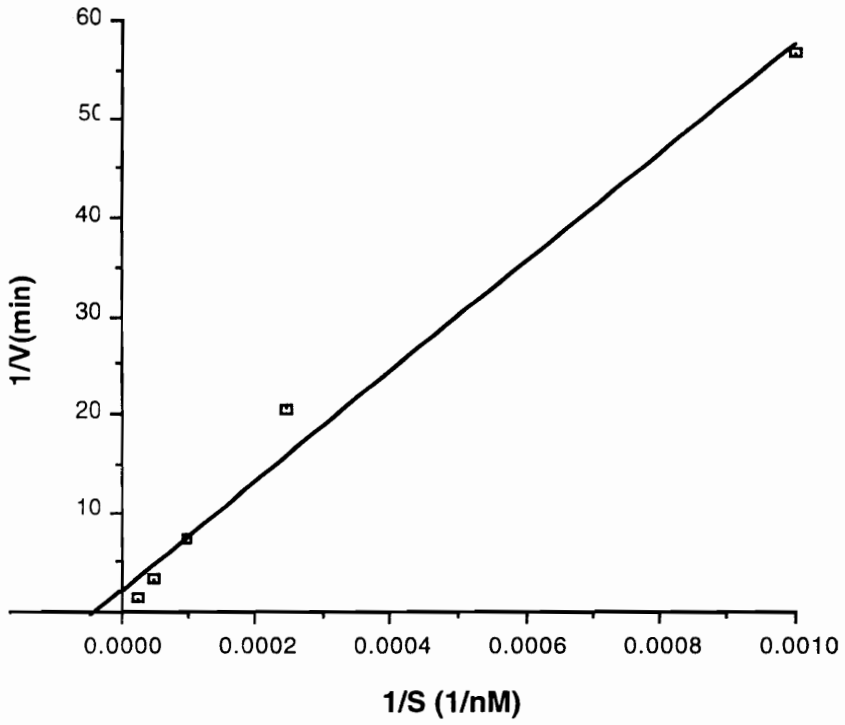

Figure 10. Double reciprocal plot of the MAO-A catalyzed oxidation of HPTP.

HPTP was incubated with MAO-B (purified from beef liver) under the same conditions used in the MAO-A experiment. HPP^+ formation was observed (Figure 11a) and was found to be substrate concentration and time dependent. Values for k_{cat} and K_M were estimated to be 1.31 min^{-1} and 260 μM, respectively; k_{cat}/K_M = 5.1 $min^{-1}mM^{-1}$. However, HPP^+ formation from HPTP was not blocked by deprenyl, a selective MAO-B inhibitor, even at 30 μM (20% inhibition only). HPP^+ was not observed in control samples (in the absence of substrate or MAO-B, or at 0 time, as shown in Figure 11b) which suggested that the HPP^+ formation was not an artifact. We concluded, however, that HPP^+ formation from HPTP in this experiment was not purely MAO-B catalyzed. It has been shown that the production of MPP^+ from MPTP was reduced to 11% but was not completely blocked by deprenyl in the primary cultures of mouse

astrocytes.[128] The authors demonstrated that this MPP+ formation is iron-dependent, suggesting the oxidation via MAO is the primary but not the only pathway of MPTP bioactivation and that transition metals may contribute to the generation of MPP+ in biological systems. We did not examine the possible effects of transition metals on HPP+ formation, an experiment that should be pursued.

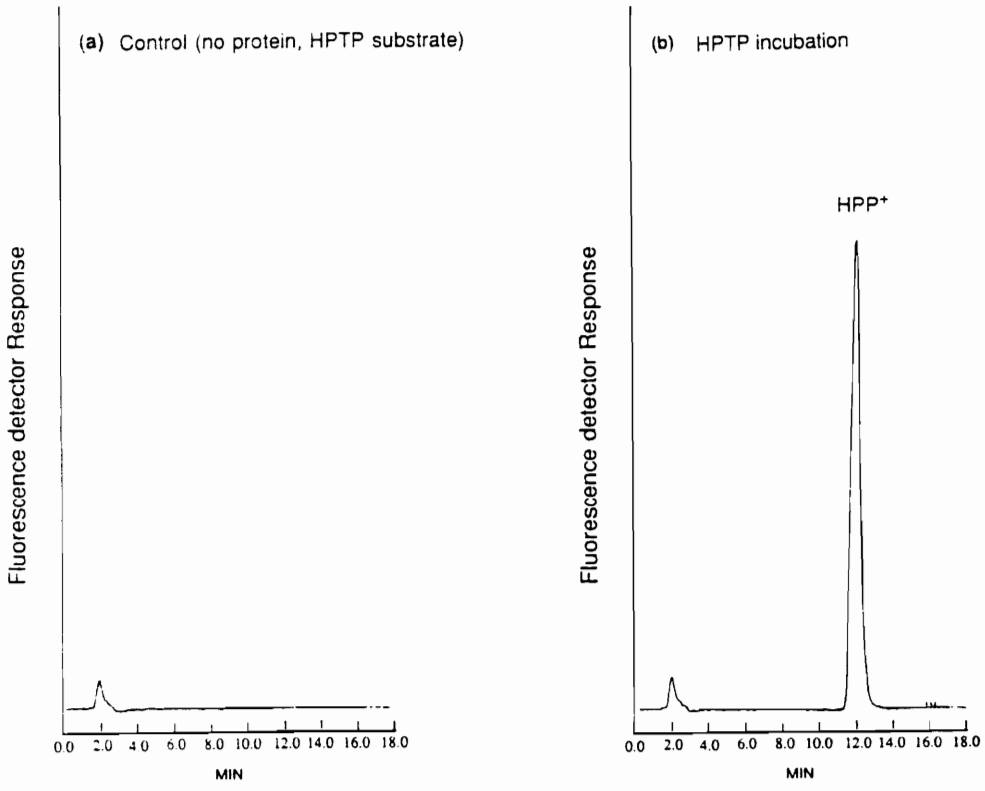

Figure 11. HPLC/fluorescence tracings obtained from incubation mixtures of (a) control; no protein, HPTP substrate and (b) MAO-B, HPTP substrate.

Experimental

Materials. MAO-A and MAO-B were purified from human placenta and beef liver, respectively.[88] HP (Sigma Chemical Co., St. Louis, MO), HPLC-grade solvents (Fisher Scientific Co., Springfield, NJ), clorgyline hydrochloride and L (-) deprenyl hydrochloride (Research Biochemicals, Natick, MA) were obtained from commercial sources. HPTP·HCl was prepared in this laboratory.[124]

HP and HPTP metabolism by MAO-A and MAO-B. Incubation mixtures containing 100 μL of HP or HPTP (final concentration 1~ 40 μM), 0.31 nmol of MAO-A (180 μL-aliquot of a 1.7 nmol/mL enzyme solution in 20 mM sodium phosphate/20% glycerol buffer, pH 7.2) or 0.26 nmol of MAO-B (30 μL-aliquot of an 8.7 nmol/mL enzyme stock solution in 50 mM sodium phosphate/50% glycerol buffer, pH 7.2) and 100 mM Tris-HCl buffer (Tris hydroxyaminomethane buffer, pH 7.4) in a final volume 1 mL were incubated for 0 to 15 minutes at 37 °C. Since the MAO-A stock solution was viscous, this 17.0 nmol/mL enzyme stock solution was diluted in 1/10 to Tris-HCl buffer and 180 μL-aliquot of this solution was used for the incubations. The reaction was initiated by the addition of the substrate solution. After a 0, 5, 10, 15 minutes incubation period, a 0.2 mL-aliquot of the incubation mixture was added to 0.2 mL of ice-cold 2 % acetic acid/acetonitrile (v/v) to terminate the reaction. This mixture was vortexed and centrifuged at 14,000 rpm for 4 minutes to precipitate protein. The supernatant was transferred to an Eppendorf tube and stored at -70 °C until HPLC analysis. The HPLC/fluorescence assay is that described in Chapter 4.

Inhibition study. Clorgyline hydrochloride was dissolved in Milli-Q water to make a 90 μM solution and a 100 μL-aliquot of this solution was added to the incubation mixtures containing MAO-A and the resulting mixtures were preincubated for 5 minutes at 37 °C. Then HPTP (final concentration 20 μM) was added and the incubation continued for 10 minutes. The total volume of the incubation sample was 1 mL. Therefore the final concentration of clorgyline was 9 μM. The (L)-deprenyl study with MAO-B was conducted in the same way except that the final concentration of deprenyl was 30 μM. After a 10 minute incubation period, the samples were processed in the same way as the other incubation samples.

5.2. The conversion of HP, HPTP and RHP to neurotoxic pyridinium metabolites by C57BL/6 mice and human liver microsomes.

The in vivo oxidative biotransformation of HP and HPTP to HPP^+ and $RHPP^+$ in rats and HP to HPP^+ and $RHPP^+$ in humans has been documented (see Chapter 6 for detail).[117,118,129,130] Our interest was to elucidate which enzyme system(s) contribute to these oxidations. In order to obtain more quantitative data on these biotransformations, in vitro studies (liver microsomal incubations) were conducted.[118,124,131,132]

The liver microsomal catalyzed oxidations of HP and HPTP are dependent on NADPH and are inhibited by SKF-525A[124] suggesting that they are mediated by one or more members of the cytochrome P450 family of enzymes. The identification of the forms of P450 involved should prove useful in assessing the possible participation of brain enzymes that could catalyze these oxidations and also could provide an opportunity to carry out inhibition studies in vivo. This information also should be of value when attempting to assess the potential role of these metabolic pathways in drug induced toxicities. In collaboration with Dr. Andrew Parkinson and Dr. Robin Pearce of the University of Kansas, Medical Center, a series of human liver microsomal incubation studies was conducted. In parallel with these experiments, C57BL/6 mouse liver microsomal incubation studies also were conducted on a smaller scale. In this Chapter, the results of these liver microsomal incubation studies are described.

5.2.1. C57BL/6 mice liver microsomal incubations.

The C57BL/6 mouse was chosen to be the species for this experiment for the following reasons: (1) HPP^+ formation from HP and HPTP has been documented in rodents. However, it is known that the rat does not reduce HP to RHP. RHP is a major circulating metabolite of HP in the human.[107] (2) The C57BL/6 mouse is susceptible to the neurotoxicity of MPP^+ derived from MPTP. (3) Characterization of the in vitro metabolic fate of HP and HPTP in this species will complement our in vivo studies (see Chapter 6.1.).

Results and Discussion

HP (**33**), HPTP (**34**) and RHP (**39**) were incubated with C57BL/6 mouse liver microsomal preparations to see if these compounds are metabolized to pyridinium products. All compounds (final concentration 100 μM) were incubated for 30 minutes at 37 °C as a preliminary test. Incubation mixtures were analyzed by the HPLC/fluorescence and HPLC/UV assay as described in Chapter 4. In HPLC/fluorescence tracings (Figure 12), HPP^+ (**36**) and $RHPP^+$ (**40**) were observed in incubation mixtures of HP (Fig. 12c) and HPTP (Fig. 12d). Only $RHPP^+$ was observed in incubation mixtures of RHP (Fig. 12e). Control samples (containing no microsomal protein) showed no pyridinium formation (Fig. 12b). HPLC/UV tracings (Fig. 13, the wavelength was set at 245 nm) were obtained in order to detect non-fluorescent compounds, such as unchanged parent and possible metabolites. An HPLC/UV tracing from the control samples (Fig. 13a) shows only one peak assigned to the unchanged substrate (HP). Analysis of control samples for HPTP and RHP also showed only the parent compound demonstrating that these compounds are chemically

stable under these conditions. In the HPLC/UV tracing of the HP microsomal incubation mixture (Fig. 13b), unchanged HP (t_R = 8.1 minutes) was the major peak. The small HPP^+ peak (t_R = 14.4 minutes) also was observed. No other significant UV absorbing peak was present. The HPLC/UV tracing of the HPTP (Fig. 13c) incubation mixtures showed four peaks (M1-M4, t_R = 3.5, 4.3, 8.1, and 12.0 minutes) in addition to the peak for unchanged HPTP (t_R = 21.4 minutes) and HPP^+. The identity of these peaks was not considered in these preliminary experiments (see later section for the attempt to identify these compounds). Since both RHP and $RHPP^+$ do not have a chromophore at 245 nm, which is the wavelength chosen for UV detection, the HPLC/UV tracing of the RHP incubation mixture (Fig. 13d) showed no peak. In all HPLC/UV tracings, a large peak for early eluting material was observed (t_R = 2 minutes). This peak also was observed in control samples. We do not know the source of this material, however, it is most likely to be biological background signals. As a part of these preliminary experiments, these three compounds were incubated in the absence of the NADPH generating system or in the presence of denatured protein (boiling water for 10 minutes). No peak other than the parent compounds was observed in either case.

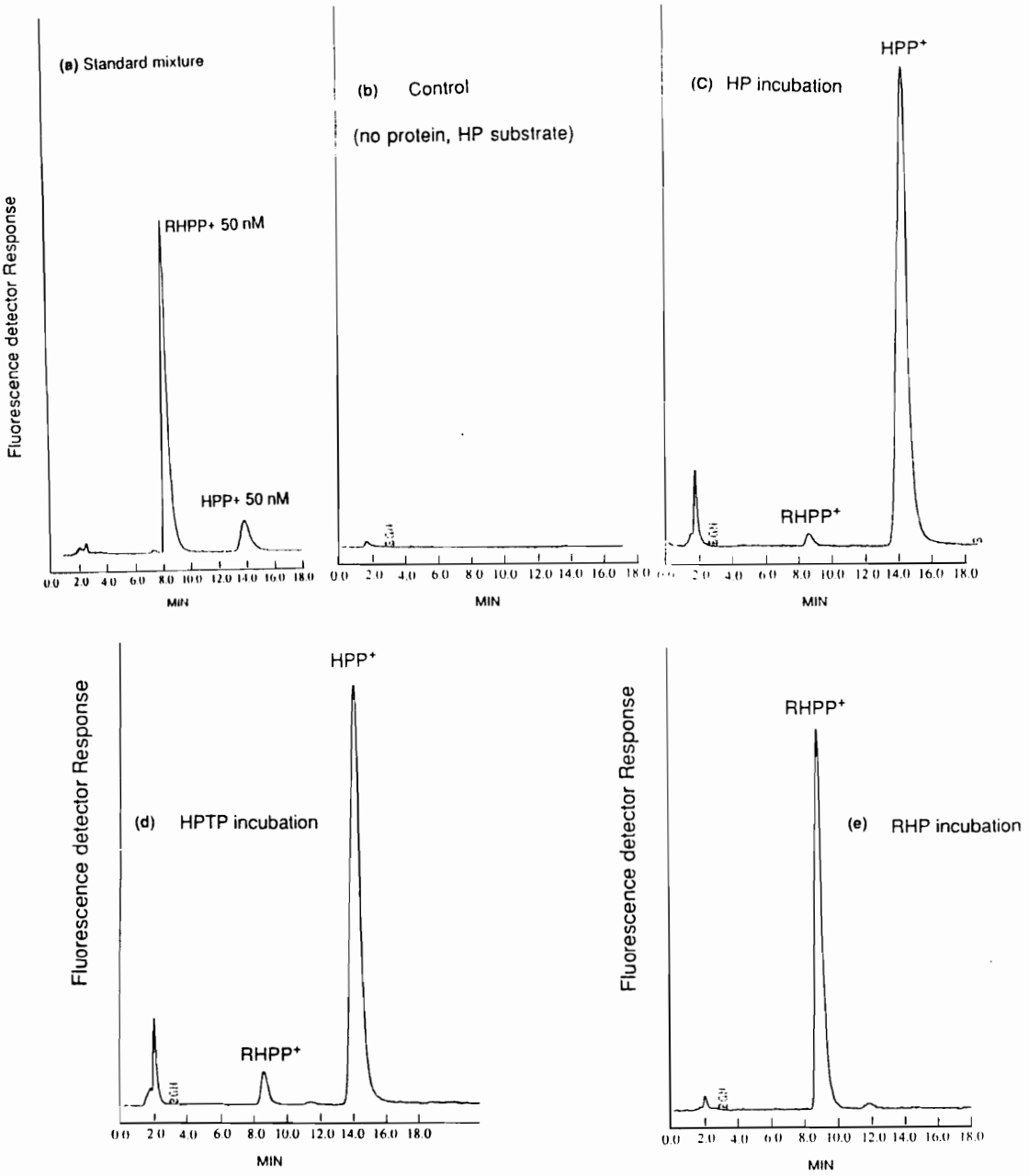

Figure 12. HPLC/fluorescence tracing of (**a**) synthetic RHPP+/HPP+ and obtained from C57BL/6 mouse liver microsomal incubation mixtures of (**b**) control; no protein, HP substrate, (**c**) HP, (**d**) HPTP and (**e**) RHP. The retention time for RHPP+ and HPP+ are 8.3 min and 14.4 min, respectively.

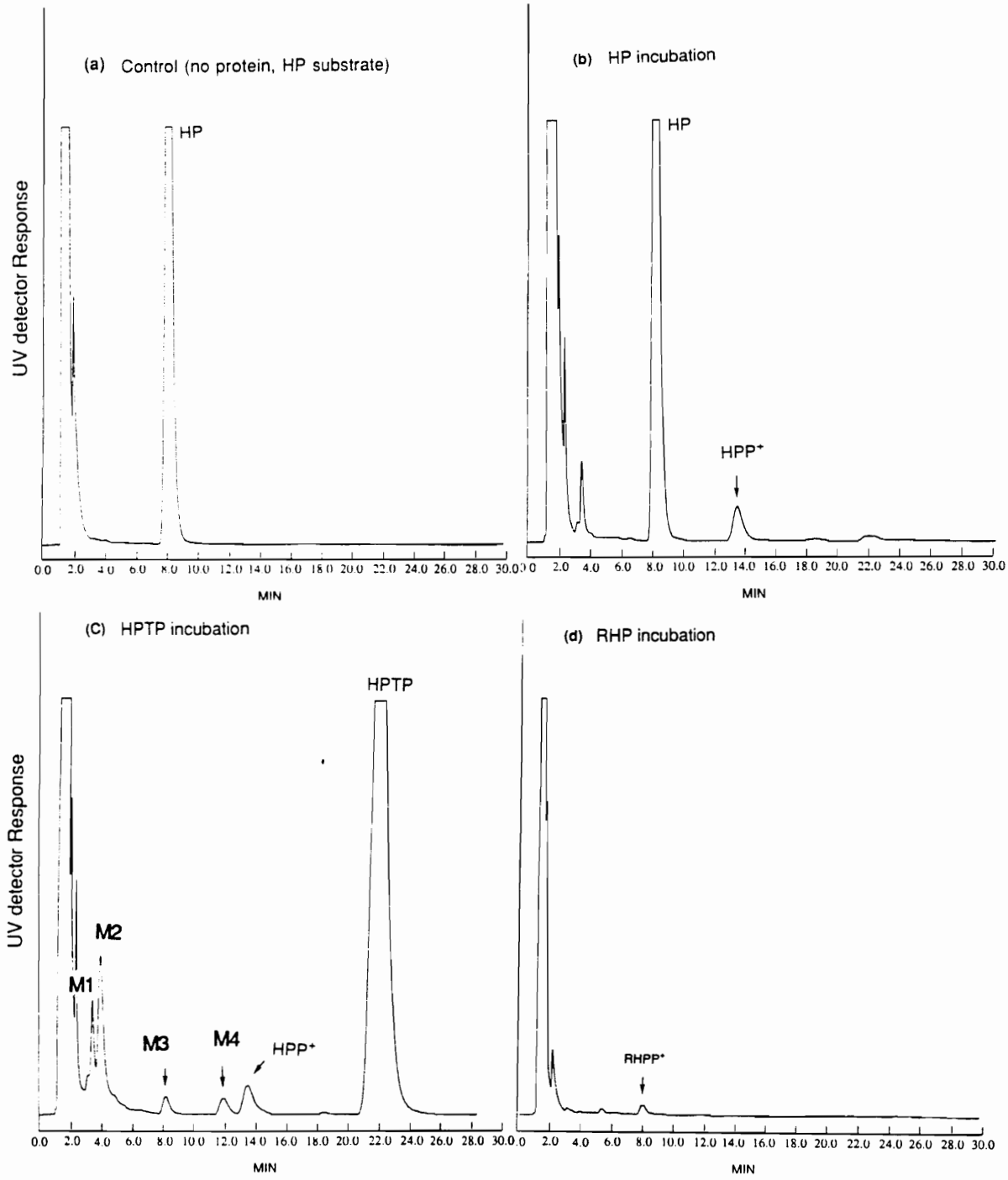

Figure 13. HPLC/UV tracings obtained from liver microsomal incubation mixtures of (**a**) control; no protein, HP substrate, (**b**) HP, (**c**) HPTP and (**d**) RHP.

Following these preliminary experiments, we attempted to obtain kinetic parameters on the formation of HPP^+ and $RHPP^+$ from HP, HPTP and RHP. Although the solubility of HP·HCl was sufficient for these studies, the low solubility of HPTP·HCl and RHP free base in 0.1 M potassium phosphate buffer (about 0.4 mM) required the use of methanol. We examined the influence of methanol content on the formation of pyridinium metabolites from HP. In this experiment, time dependency was also examined. HP·HCl was dissolved to make a final concentration of 100 μM in the incubation mixture. The % of methanol was adjusted to be 0%, 2.5%, and 10% of the total incubation volume. The mixtures were incubated for 0, 10, 20, and 30 minutes at 37 °C. Although HPP^+ formation was incubation-time dependent (at least up to 30 minutes) in all incubations, the 10% methanol containing incubation group lost 46% of the enzyme activity (Figure 14). The 2.5% methanol containing group lost only 6% compared to the 0% methanol group. Therefore, the final % of methanol was kept at 2.5% in incubation samples throughout all mouse liver microsomal incubations.

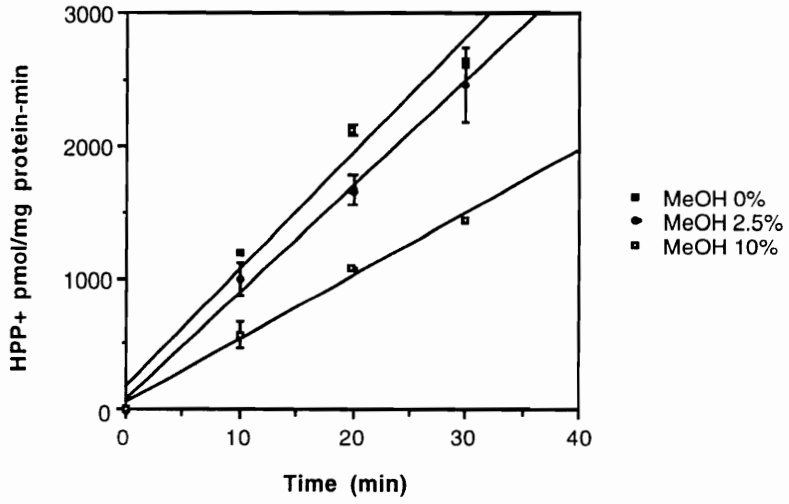

Figure 14. Effect of methanol content and incubation time on HPP^+ formation from HP·HCl. Substrate (final concentration of 100 μM) was incubated with 1 mg/mL liver microsomal protein for 0 to 30 minutes. Numbers are the mean ± S.D. of triplicate determinations.

HP, HPTP and RHP were incubated with the mouse liver microsomal preparation (1 mg protein/mL) for 0 to 30 minutes in the final concentration range of 25 μM to 250 μM. Pyridinium formation appeared to be saturable at higher substrate concentrations. When the substrate concentration was higher than 250 μM (500 μM and 1 mM), pyridinium formation was no longer substrate concentration dependent (Figure 15).

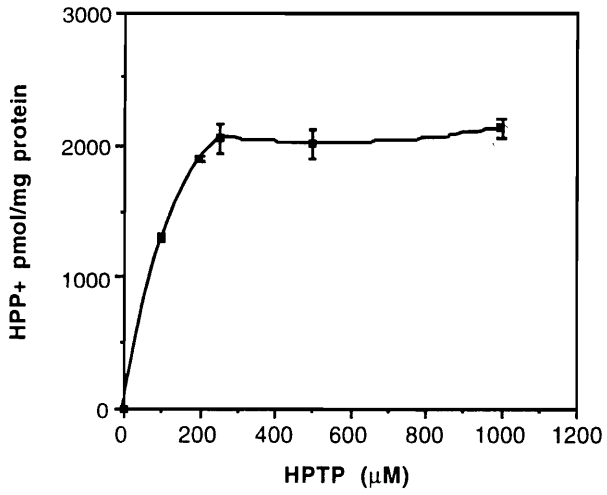

Figure 15. Effect of substrate concentration on HPP^+ formation from HPTP. HPTP (100 μM to 1 mM) was incubated with 1 mg protein/mL for 30 minutes. Numbers are the mean ± S.D. of 4 determinations.

Before studying the quantitative estimations on the % conversion of HP and HPTP to HPP^+ and RHP to $RHPP^+$, the effects of the amount of protein on HPP^+ formation were examined. HPTP 100 μM (final concentration) was incubated with 1 mg and 2 mg of the mouse liver microsomal protein per incubation (total volume 1 mL) for 30 minutes. As shown in Figure 14, HPP^+ formation from HPTP was linear for 30 minutes. The only difference was the amount of the protein in the samples. The amounts of HPP^+ formed from HPTP with 1 mg protein/mL and 2 mg protein/mL were 2043 ± 138 pmol/mg protein and 1780 ± 28 pmol/mg protein, respectively (both numbers are the mean ± S.D. of triplicate determinations). The effects of protein concentration were not thoroughly examined in these mouse microsomal incubation studies. However, it was examined more extensively in the human liver microsomal studies (see

Chapter 5.2.2.). In that study, HPP^+ formation from both HP and HPTP were protein concentration dependent in the range of 0.5 mg/mL to 2.0 mg/mL (0.05 mg to 0.2 mg per incubation mixture).

Quantitative estimations of HPP^+ and $RHPP^+$ from HP, HPTP and RHP were obtained by the HPLC/fluorescence assay. HPP^+ was the major metabolite observed by HPLC/fluorescence in both the HP and HPTP incubation mixtures. $RHPP^+$ also was detected in both HP and HPTP incubation mixtures (Figure 12c,d). However, the ratio of HPP^+ to $RHPP^+$ ranged from 60 to 130 (higher $RHPP^+$ formation was observed with HPTP as substrate). These low amounts of $RHPP^+$ formation were not surprising because of the limited ketone reductase activity present in the mouse liver microsomal preparations. On the other hand, RHP showed only $RHPP^+$ suggesting that the oxidation from RHP to $RHPP^+$ is preferred over the oxidation of RHP to HP.

By measuring the concentrations of HPP^+ and $RHPP^+$ in the samples and by comparing those to the substrate concentrations of the corresponding incubation mixtures, the % conversions of HP and HPTP to HPP^+ and RHP to $RHPP^+$ were estimated. For example, if the concentration of HPP^+ measured in a 100 μM HPTP incubation mixture (1 mg protein/incubation, 30 minutes) was 2 μM (after taking the dilution factor for the HPLC assay into account), then the % conversion will be 2%. Table 7 summarizes the % conversion to the pyridinium metabolites from HP, HPTP and RHP with the starting concentrations ranging 25 μM to 250 μM.

TABLE 7

Summary of the quantitative estimates for the % conversion to the pyridinium metabolites from HP, HPTP and RHP.

[S][a]	HP		HPTP		RHP	
	HPP^+ (nM)	%	HPP^+ (nM)	%	$RHPP^+$ (nM)	%
25 μM	896 ± 89	3.6	713 ± 36	2.9	1028 ± 129	4.1
50 μM	1429 ± 188	2.9	1045 ± 67	2.1	1261 ± 198	2.5
100 μM	2095 ± 238	2.1	2077 ± 134	2.1	1715 ± 226	1.7
200 μM	2436 ± 543	1.2	1973 ± 236	1.0	2299 ± 197	1.1
250 μM	2556 ± 477	1.0	2036 ± 257	0.8	2644 ± 208	1.1

[a]: Substrate concentration. All samples were incubated for 30 minutes. Numbers are the mean ± S.D. of triplicate determinations.

As shown in Table 7, in the substrate concentration range of 25 μM to 250 μM, the % of conversion HP and HPTP to HPP^+ and RHP to $RHPP^+$ was about 1-4%. As mentioned earlier, HPLC/UV analysis was conducted for the analysis of non-fluorescent compounds in parallel with the quantitative estimation of the pyridinium metabolites by HPLC/fluorescence analysis. By HPLC/UV analyses, the amount of unchanged substrates was approximately 70 to 90% for all three compounds. Consequently, these pyridinium metabolites represent a significant fractions of the substrate consumed. The nature of the unaccounted for consumed substrate remains unknown.

Using the range of 25 μM to 250 μM substrate, apparent K_M and V_{max} values were obtained. For HP, V_{max} = 111 pmol/mg-min, K_M = 68 μM and

V_{max}/K_M = 1.63 pmol/mg protein-min-μM. For HPTP, V_{max} = 96 pmol/mg-min, K_M = 78 μM, V_{max}/K_M = 1.23 pmol/mg protein-min-μM. For RHP, V_{max} = 87 pmol/mg-min, K_M = 42 μM, V_{max}/K_M = 2.07 pmol/mg protein-min-μM (Table 8; see Figure 16 for Lineweaver-Burke plots). All three compounds were biotransformed to pyridinium metabolites with similar K_M and V_{max} values. This may suggest that the oxidation of HP, HPTP and RHP may be catalyzed by same form(s) of P450 in the mouse liver.

TABLE 8

C57BL/6 mouse pooled liver microsomal incubations (Apparent kinetic data).

Substrate	Metabolite	V_{max} (pmol/mg-min)	K_M (μM)	V_{max}/K_M[a]
HP	HPP^+	96	78	1.23
HPTP	HPP^+	111	68	1.63
RHP	$RHPP^+$	87	42	2.07

[a]: pmol/mg protein-min-μM.

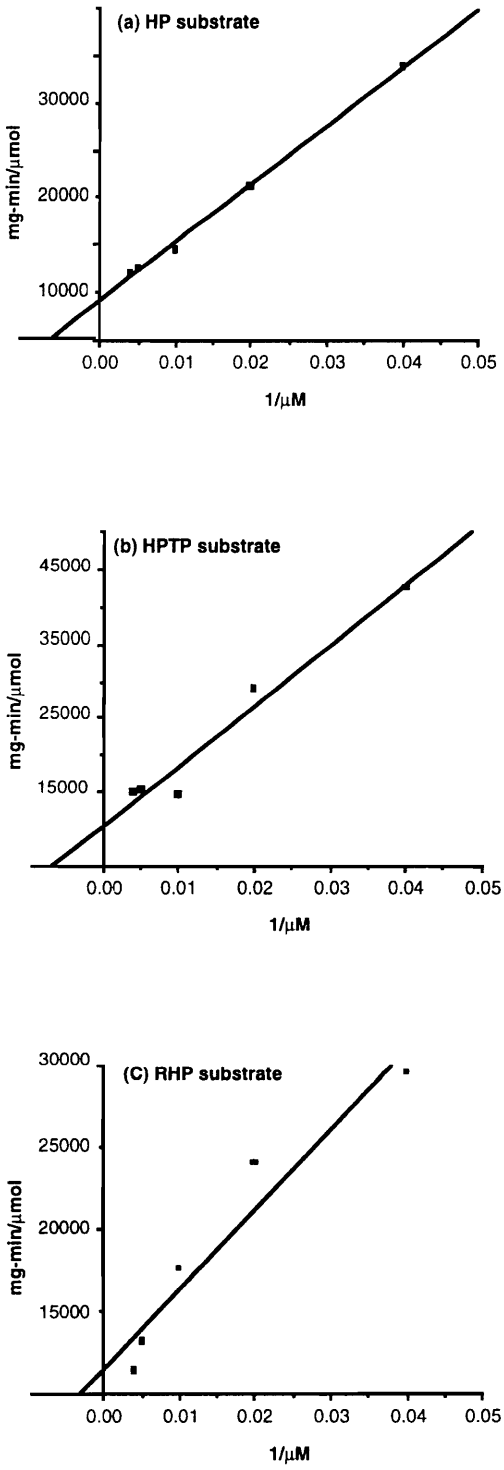

Figure 16. Lineweaver-Burke plots for HPP^+ and $RHPP^+$ formation from (a) HP, (b) HPTP and (c) RHP.

HPLC/UV analysis for the identification of unknown peaks.

As mentioned earlier, 4 peaks were observed in addition to HPP^+ and unchanged HPTP in the HPLC/UV tracings with HPTP as substrate (Figure 13c, M1-M4). We attempted to identify these peaks by comparing these retention times and UV spectra with those of possible metabolites. As described in Chapter 3, from in vivo studies, 3-*p*-fluorobenzoylpropionic acid (**43**), PA (**44**) and 4-(4-chlorophenyl)-4-hydroxypiperidine (CPHP, **41**) are the oxidative N-dealkylation products of HP. This pathway has been reported as one of the major metabolic pathway of HP.[95] The quantitative measurement of **44** has been documented and the authors stated **44** to be a major metabolite in rats.[96-98] However, the other half of the molecule CPHP (**41**) has not been extensively studied. Although available references are limited, Fang and Gorrod have reported the formation of **43** in rat hepatic microsomal incubations.[131] They also reported that CPHP is the major metabolite of HP in mouse hepatic microsomal incubations.[132] Since this piperidine molecule may be further oxidized to pyridinium metabolites, we were particularly interested in this half of the molecule.

In our HPLC/UV tracings of HPTP incubation mixtures (Figure 13c), M1 (t_R = 3.5 minutes) and M2 (t_R = 4.3 minutes) were not observed in control samples (no protein or no substrate), suggesting that these compounds are drug related metabolites. M1 was observed in both HP and HPTP substrates incubation mixtures. Since **43** and **44** could be formed from both HP and HPTP, compound **43** (standard solution) was analyzed by HPLC/UV under the same assay conditions used in the incubation experiments. The retention time of **43** was 2.5 minutes which overlapped with the biological background signals

and did not match with the retention time of the peaks under consideration. M1 has not been characterized.

M2 (t_R = 4.3 minutes) was always observed with HPTP as substrate (except tracings obtained from t =0 min or in the absence of protein). Formation of this peak was HPTP concentration and incubation time dependent. One possible assignment is 4-(4-chlorophenyl)-1,2,3,6-tetrahydropyridine (CPTP, **51**), an N-dealkylation product of HPTP which corresponds to **41** derived from HP. It also may be formed from **41** via dehydration. Although characterization of this compound has not been extensively described, there is a report stating that **51** is present in incubation mixtures of HPTP with mouse liver microsomal preparation.[132] In our attempts to identify the unknown peaks, we obtained the λ_{max} and ε values of **41**, **43** and **51** of synthetic standards. These values are λ_{max}: 219 nm, 242 nm, 248 nm and ε : 11100 M^{-1}, 9700 M^{-1} and 15500 M^{-1} for **41**, **43** and **51**, respectively. Compound **41** would not be detected at 245 nm, the wavelength used in our HPLC/UV assay. Also it was not likely for HPTP to be metabolized to **41**. It is more likely to observe the formation of **41** from HP. Compound **51** was analyzed by HPLC/UV under the same assay conditions used in the incubation experiments. Compound **51** coeluted with the unknown peak M2 (t_R = 4.3 minutes). Additionally, the diode array UV spectra of the metabolite peak M2 was the same as that of CPTP (**51**) (Figure 17).

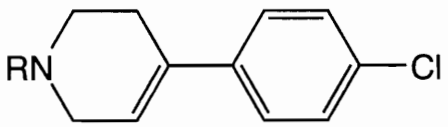

51: R = H

52: R = $(CH_2)_3CH(OH)C_6H_4F(p)$

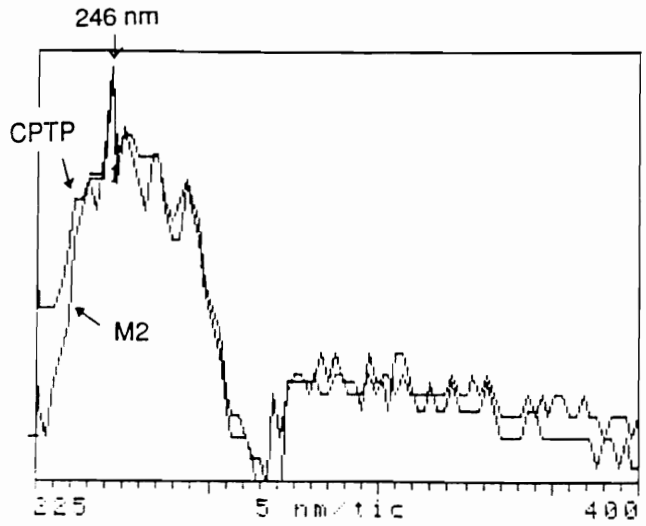

Figure 17. UV spectra of the metabolite M2 and CPTP (**51**).

The peak M3 (t_R = 8.0 minutes) turned out to be HP (a contaminant from the HPTP·HCl synthesis). The amount of HP was about 3%. This problem was solved by recrystallization (see Chapter 6.2. for detail).

Based on its coelution with the synthetic standard (prepared in our laboratory) and its UV characteristics, the peak M4 (t_R = 12.0 minutes) was assigned to be {4-(4-chlorophenyl)-1-[4-(4-fluorophenyl)-4-hydroxybutyl]-1,2,3,6-tetrahydropyridine (RHPTP, **52**). Compound **52** has not been studied extensively. However, recently the presence of **52** in the urine obtained from baboons treated with HPTP has been reported (see Chapter 6.2.).

Kinetic data for the formation of CPTP (**51**) and RHPTP (**52**) from HPTP were not obtained because of an occasional interfering peak in the HPLC/UV tracings. The retention time of **51** was 4.3 minutes and sometimes early eluting biological background peaks interfered with the CPTP peak. Also, the RHPTP (**52**) peak sometimes was not resolved from the HPP^+ peak. However, the %

conversion of HPTP to CPTP and RHPTP appeared to be about 5-7% and 1-2%, respectively.

By HPLC/UV analyses, the amount of unchanged substrates was approximately 70 to 90% for both HP and HPTP. Since RHP does not absorb at 245 nm, we were not able to estimate unchanged RHP in the incubation mixtures. For incubation mixtures with HPTP as substrate, if we attempt to explain the mass balance of the in vitro metabolism with mouse liver microsomes, the % accountable is approximately 90%. For HP incubation mixture, since only uncharacterized peak M1 was observed other than the unchanged HP substrate and HPP^+, about 20% is not accountable.

Inhibition study.

These studies with C57BL/6 mouse liver microsomal preparations were conducted in parallel with studies with human liver microsomal preparations (Chapter 5.2.2.). We have demonstrated that the major catalyst for HPP^+ formation from HP and HPTP is CYP3A in human liver. According to this information, inhibition studies using the CYP3A specific inhibitors ketoconazole (1 μM) and troleandomycin (100 μM) were conducted with mouse liver microsomal preparations. Ketoconazole (1μM) blocked HPP^+ formation from HP (83%), HPTP (28%) and $RHPP^+$ formation from RHP (85%). With troleandomycin (100 μM), pyridinium formation was inhibited 23% (HP), 45% (HPTP) and 42% (RHP) (Figure 18).

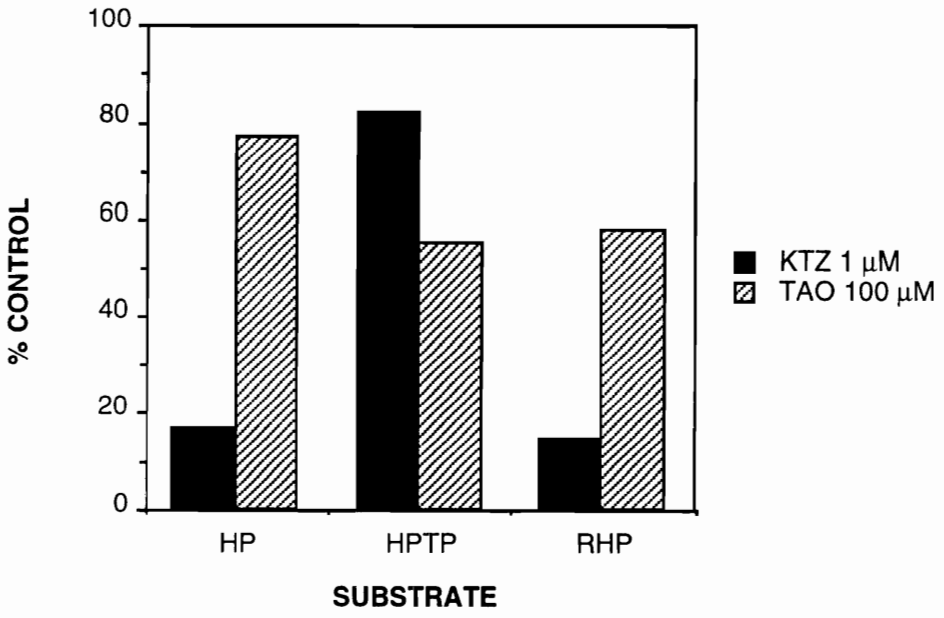

Figure 18. Effect of ketoconazole and troleandomycin on the conversion of HP and HPTP to HPP^+ and RHP to $RHPP^+$.

Although 1 μM ketoconazole effectively inhibited HPP^+ formation from HP and $RHPP^+$ formation from RHP, inhibition by 100 μM troleandomycin was marginal. Furthermore, HPP^+ formation from HPTP was not effectively inhibited by ketoconazole or troleandomycin. Therefore CYP3A is not likely to be the major catalyst for these reactions. No further experiments were conducted to characterize specific form(s) of cytochrome P450 which contribute to these reactions.

It has been reported that HPP^+ is a selective MAO-B inhibitor (a Ki of 0.83 μM studied with human platelet MAO-B).[133] The inhibition effect of HPP^+ on P450 has not been studied. The results from our incubation study shows that HPP^+ formation from HP and HPTP are time-dependent up to 30 minutes.

Therefore at least during that time period, the presence of HPP^+ in the incubation mixture does not seem to be suppressing further HPP^+ formation from HP and HPTP.

Possibility of the further metabolism of HPP^+.

In order to examine the possibility of the further metabolism of HPP^+, $HPP^+ \cdot Cl^-$ (50 μM) was incubated with C57BL/6 mouse liver microsomal preparations according to the procedure used for the HP, HPTP, and RHP incubations. Samples were incubated up to 6 hours. We were particularly interested in the possibility of HPP^+ undergoing oxidative N-dealkylation to form 4-(4-chlorophenyl)pyridine (CPP, **53**). The λ_{max} and ε values of **53** were found to be 260 nm and 22,500, respectively. The limit of detection of this compound by HPLC/UV analysis at 245 nm was about 40 pmol on column (800 nM). Therefore, if the % conversion of HPP^+ to **53** was above 3%, we should be able to detect the peak on UV. We did not observe any trace of CPP. The wavelength of the UV detector was changed to 260 nm, the λ_{max} of CPP. The synthetic standard CPP and HPP^+ were resolved on the HPLC system under the conditions routinely used (t_R = 15.4 minutes and 14.4 minutes, respectively). Therefore, the overlapping of two peaks was not possible. In these experiments, we did not observe any peak other than HPP^+ itself in the HPLC/fluorescence and HPLC/UV tracings. The % recovery of CPP from the incubation mixture averaged 80 ± 6% (n = 4) using HPLC/UV tracings. Thus, HPP^+ in these incubation mixtures is stable.

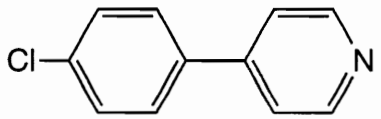

53

In summary, in these in vitro studies with mouse liver microsomes, we attempted to evaluate the reported in vivo metabolic pathways of HP. We expected to see PA and CPHP. We were not able to confirm the formation of these compounds. However, we observed CPTP and RHPTP formation from HPTP. In our in vivo C57BL/6 mice studies with HP and HPTP (see Chapter 6.1.), we also found that the % conversion of these compounds to HPP^+ was low (maximum 1-4% in the 48 hours urine). We do not have a clear understanding of what the mass balance of these compounds will be. As mentioned earlier, even though it has been reported that N-dealkylation is a major pathway of HP as well as reduction and conjugation pathways (see Chapter 3), the metabolism of HP remains unclear. The % conversion to HPP^+ from HP and HPTP was about 3% in the in vitro studies. Since 70-90% of the substrate remains unchanged, the oxidation pathway to form pyridinium metabolites appears to be a significant pathway. As mentioned in the section on inhibition studies, HPP^+ itself did not inhibit HPP^+ formation. However, we do not know how HPP^+ will affect the other metabolic pathways of HP and HPTP. It might be an interest.

Experimental

Chemicals. HP, NADP, glucose-6-phosphate, $MgCl_2$ and glucose-6-phosphate dehydrogenase were purchased from Sigma Chemical Co. (St.

Louis, MO). HPLC-grade solvents were purchased from Fisher Scientific Co. (Springfield, NJ). HP·HCl, HPTP·HCl, RHP and RHPTP were synthesized in this laboratory.[124,134,135] Troleandomycin was a gift from Dr. F. P. Guengerich and ketoconazole was a gift from Dr. A. Parkinson. Other chemicals were obtained from commercial sources.

Preparation of microsomal fractions from C57BL/6 mouse liver. Retired breeder male C57BL/6 mice (Harlan-Sprague Dawley, Dublin, VA) were used for the liver microsomal preparations. Livers (from 3 to 4 mice) were used to prepare pooled microsomes for each experiment. The livers were dissected and homogenized in 4 volumes of ice-cold 0.25 M sucrose-10 mM Tris-HCl buffer. Microsomal fractions were obtained as a pellet after a series of centrifugation steps according to an established procedure.[64] This pellet was resuspended with two volumes of 0.1 M phosphate buffer, pH 7.4, containing 20% (v/v) glycerol and the resulting suspension was rehomogenized. Protein concentrations were determined by the Bradford method using bovine serum albumin as a standard[135] and the liver microsomes were used immediately.

General protocol for determining the metabolism of haloperidol and its derivatives by C57BL/6 mouse liver microsomes. Mouse liver microsomal incubations contained HP, HPTP or RHP (various concentrations), 50 to 300 μL of microsomal enzyme (1 or 2 mg/mL), 0.1 M phosphate buffer (pH 7.4 at 37 °C), 5 mM $MgCl_2$, 5 mM glucose-6-phosphate, 0.5 mM NADP, and 1 unit/mL glucose-6-phosphate dehydrogenase in 1.0 mL. Reactions were initiated by addition of substrate. After 0 ~ 30 minutes incubation periods, reactions were terminated by adding a 0.6 mL-aliquot of the incubation mixture to an equal volume of acetonitrile

containing 2% acetic acid. The precipitated protein was separated by centrifugation at 14,000 rpm for 6 minutes and supernatant fractions were stored at - 70 °C until HPLC analysis.

Inhibition experiments. Ketoconazole (1 μM) and troleandomycin (100 μM) were incubated with 100 μM HP, HPTP and RHP under the same conditions as described above. Troleandomycin was preincubated for 5 minutes prior to the addition of the substrate.

Kinetic studies. In order to obtain apparent K_M and V_{max} data, mouse liver microcosms were incubated with substrates at a range of 25-250 μM for 30 minutes. The time-dependency of the formation of the pyridinium metabolites was examined in separate experiments. K_M and V_{max} values were estimated from Lineweaver-Burke plots.

HPLC analysis. The HPLC assay is described in Chapter 4.

5.2.3. Human liver microsomal incubations.

The results from the rodent studies established that HP, HPTP were metabolized to HPP^+ in the liver microsomal incubations.[124,131,132] It was suggested that these oxidations may be catalyzed by one or more forms of liver microsomal P450 in the rat.[124] In our C57BL/6 mice liver incubation studies, the formation of HPP^+ and $RHPP^+$ (to much lesser extent) was confirmed and apparent kinetic data were obtained (Chapter 5.2.2.). In contrast to the incubation study with MAO which appears to be catalyzing only HPTP oxidation (Chapter 5.1.), HP and HPTP were both metabolized to HPP^+ by the microsomal preparations and approximately at the same level. All data suggested that these oxidations are catalyzed by P450 in the mouse liver. However, the specific form(s) of P450 were not further investigated. In the in vivo rodent studies, we demonstrated that HP and HPTP were also converted to HPP^+[117,129] and $RHPP^+$ (Chapter 6.1.).

Our principal interest is human exposure. It has been documented that HPP^+ is present in the plasma and post mortem brain tissue[137] and HPP^+ and $RHPP^+$ in the urine obtained from HP-treated schizophrenic patients.[118,130] In order to characterize more fully the pathway leading to the formation of the pyridinium metabolites, we have examined the metabolism of HP and HPTP with human liver microsomal preparations. The studies reported here were designed to identify the specific form(s) of human cytochrome P450 that catalyze(s) the oxidation of HP and HPTP to HPP^+. The experiments include: kinetic studies, correlation studies with specific marker substrates of CYPs, chemical, immunochemical inhibition studies, and incubations with microsomes prepared from a human lymphoblastoid cell line co-expressing cloned DNA.

The identification of the enzymes catalyzing the biotransformation of HP, HPTP in human liver microsomes should prove useful in assessing the possible participation of brain enzymes that could catalyze these oxidations and also will be of value when attempting to assess the potential role of these metabolic pathways in drug induced toxicities.

Results

HPLC/Fluorescence assay. The HPLC/fluorescence assay used in the studies is the same as described in Chapter 4. The HPLC system with fluorescence detection employed satisfactorily resolved $RHPP^+$ (t_R 7.5 min) and HPP^+ (t_R 12.5 min) (Fig. 19a). Calibration plots (4 concentrations, Fig. 20) prepared with synthetic standards were linear over the concentration range of 0-250 nM HPP^+ (0-12.5 pmol on column) and 0-88 nM $RHPP^+$ (0-4.4 pmol on column). The lower limits of detection were approximately 1.3 pmol of HPP^+ and 0.4 pmol of $RHPP^+$. The fluorescence response from $RHPP^+$ under the conditions of this assay was approximately 4 times greater than that of HPP^+ (see Chapter 4). Similar calibration plots were constructed in all assays before, during and following sample analyses. The slopes of these plots remained unchanged during the course of the study. The extent and reproducibility of the recovery of the pyridinium metabolites from the incubation mixtures were estimated by analyzing control liver homogenates that had been spiked with concentrations of HPP^+ and $RHPP^+$ that were comparable to those observed in the incubation studies. The percent recoveries of both pyridinium species ranged from 92 to 100% (4 concentrations run in triplicate). Consequently, the

concentrations of metabolites estimated in these studies are likely to be accurate to within 10% of the reported values.

Approximately 40 samples were analyzed sequentially in each assay over a period of about 16 hours. The entire study involved the analysis of approximately 2000 samples. "Control" samples in which either the microsomal preparation or the NADPH-generating system was absent also were included. No metabolite formation was observed in these control samples; no carry over of analytes was observed (control samples and zero concentration calibration samples). Typical HPLC fluorescence tracings obtained from pooled liver microsomal incubation mixtures with HP as substrate (19b) and HPTP as substrate (19c) together with the tracing from one of the calibration sets (19a) are shown in Figure 19.

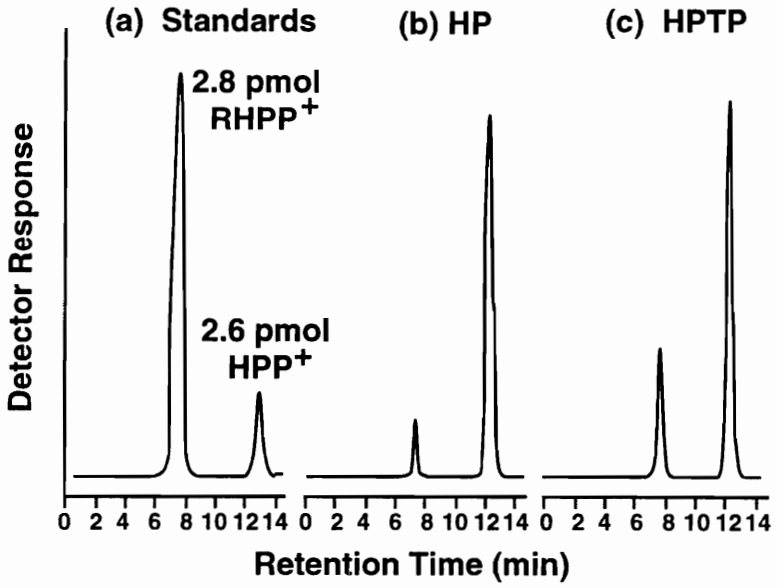

Figure 19. HPLC/fluorescence tracings (a) of a mixture of synthetic standards used to construct the calibration plot shown in Figure 20, (b) of a typical incubation mixture extract with HP as substrate and (c) with HPTP as substrate.

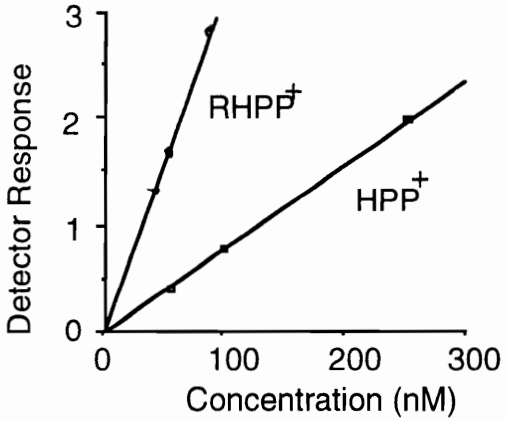

Figure 20. Typical calibration curves for the HPLC/fluorescence assay of HPP^+ and $RHPP^+$.

Metabolism of HP and HPTP by human liver microsomes. Kinetic analysis. Preliminary experiments established that both 100 μM HP and HPTP were converted in a time, NADPH and protein concentration dependent manner to HPP^+. HP and HPTP were incubated from time 0 to 60 minutes and protein concentration was varied from 0 to 2 mg/mL (0-0.2 mg per incubation) to examine the time and protein concentration dependency. The substrate concentration (2.5 to 250 μM) dependent rates for these conversions were estimated following 30 minute incubations with microsomes (1.0 mg/mL) prepared from a pool of five livers (460 nmol P450/mg protein) and from a single (#16), highly active liver sample (680 nmol/mg protein). The double-reciprocal plots of the rates of HPP^+ formation as a function of HP and HPTP concentration were prepared from the linear plots of metabolite formation vs time and were analyzed by an enzyme kinetic program from Trinity Software. Table 9 summarizes the apparent k_{cat}, K_M and k_{cat}/K_M values obtained from these studies. The corresponding values for the formation of $RHPP^+$ from HPTP

also were determined but levels of $RHPP^+$ from HP were too low to estimate accurately.

TABLE 9

Kinetic values for the conversion of HP to HPP^+ and of HPTP to HPP^+ and $RHPP^+$ by human liver microsomes[a]

		Pooled Liver Microsomes		
Substrate	Metabolite	k_{cat}[b]	K_M[c]	k_{cat}/K_M[d]
HP	HPP^+	0.53	0.080	6.60
HPTP	HPP^+	0.96	0.164	5.85
HPTP	$RHPP^+$	0.02	0.026	0.77
		Sample #16 Liver Microsomes		
HP	HPP^+	0.45	0.066	6.81
HPTP	HPP^+	0.67	0.088	7.61
HPTP	$RHPP^+$	0.06	0.035	1.71

[a]: All values were calculated from double reciprocal plots obtained from oxidation rates run in triplicate (S.D. < ± 5% except at very low substrate concentrations in which case the S.D. < ±10%). [b]Pmol metabolite formed/pmol total P450-min (i.e. min^{-1}). [c]mM. [d]$min^{-1}mM^{-1}$.

Correlation analysis. In an effort to identify the specific form(s) of cytochrome P450 responsible for these oxidative transformations, we examined the rates of HPP^+ formation catalyzed by 14 samples of human liver microsomes using a final concentration of HP and HPTP of 100 μM, which is close to their K_M values (Table 9). The results (Figure 21, left panel) were

analyzed in terms of sample-to-sample variations in the rates of HPP^+ formation from HP vs HPTP (Fig. 21, right panel). We also compared the rates of HPP^+ formation from HP and HPTP with the sample-to-sample variations in the rates of oxidation of various cytochrome P450 marker substrates. These included ethoxyresorufin O-dealkylation[138] (P450 1A), coumarin 7-hydroxylation[139] (P450 2A6), tolbutamide 4-hydroxylation[140] and S-mephenytoin 4'-hydroxylation[141] (P450 2C), dextromethorphan O-demethylation[142] (P450 2D6), chlorzoxazone 6-hydroxylation[143] (P450 2E), testosterone 6β-hydroxylation[144,145] (P450 3A) and lauric acid 11- and 12-hydroxylation[146] (P450 4A). Good correlations were observed only with testosterone 6β-hydroxylase activity (Fig. 22). $RHPP^+$ was detected in all of these microsomal incubations but the maximum levels reached were 10% or less of the corresponding HPP^+ levels. Consequently, reliable quantitative data were not obtained.

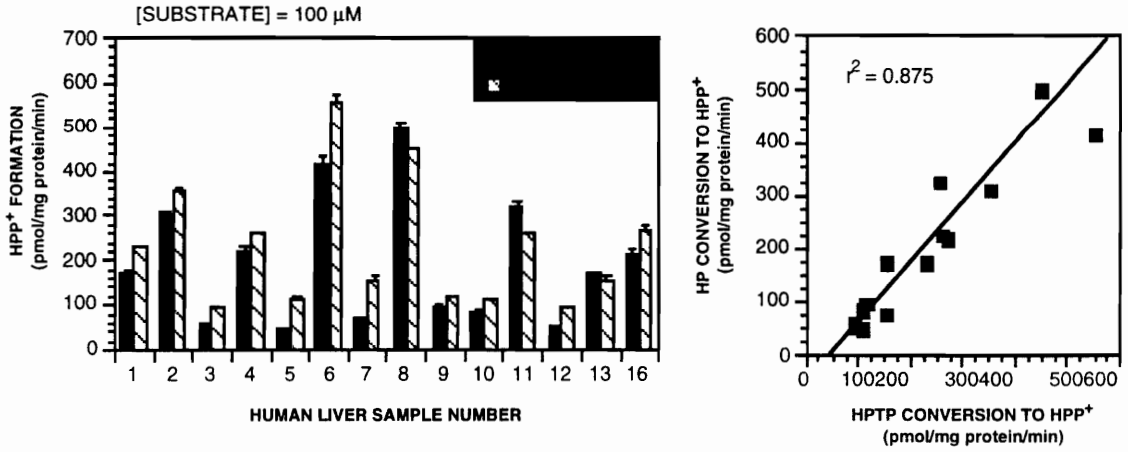

Figure 21. Rates of conversion of HP (solid bars) and HPTP (striped bars) to HPP^+ by various human liver microsomal preparations (left) and correlation of these rates with HP and HPTP serving as substrates (right).

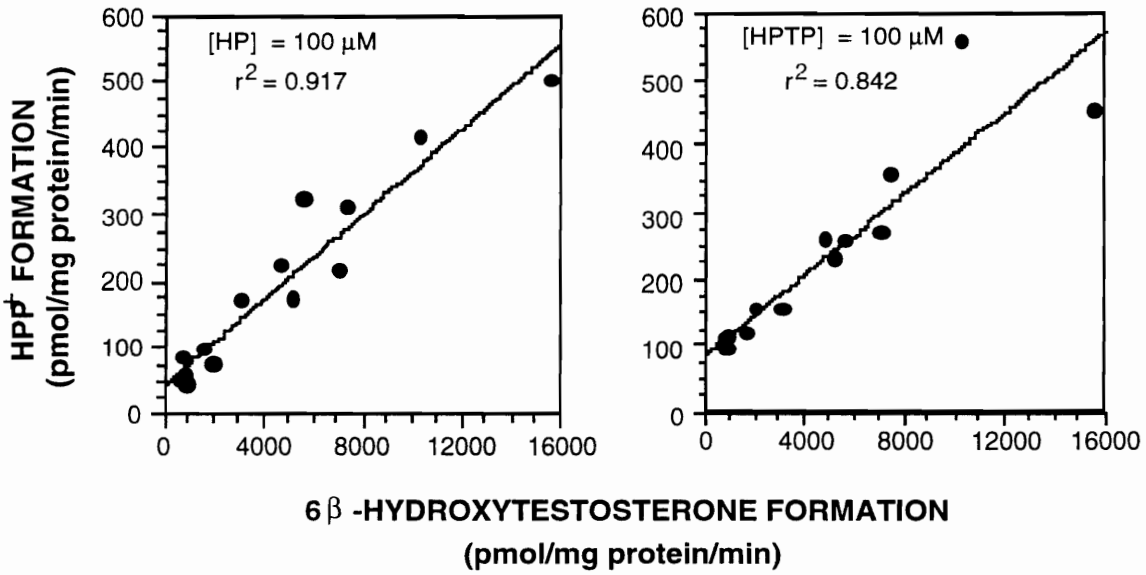

Figure 22. Correlation between the rates of HPP^+ formation from HP (left) and HPTP (right) and testosterone 6β-hydroxylation activity (P450 3A activity).

Metabolism by cDNA-expressed P450 enzymes. Eight cDNA-expressed human P450 enzymes (P450 1A1, 1A2, 2A6, 2B6, 2C9, 2D6, 2E1 and 3A4) were examined for their ability to metabolize 100 μM HP and HPTP. In these experiments only trace amounts of HPP^+ were detected. However, the commercially available P450 3A4 co-expressed with NADPH-cytochrome P450 reductase (P450 3A4 + OR) catalyzed the conversion of HP (41 pmol/mg protein-min) and HPTP (31 pmol/mg protein-min) to HPP^+.

Chemical inhibition. Fourteen P450 substrates and inhibitors (100 μM) were evaluated for their effects on the conversion of HP and HPTP (also 100 μM) to HPP^+ and $RHPP^+$. The results (Fig. 23, left panel) show a range of responses with ketoconazole being the most effective inhibitor and α-naphthoflavone being a stimulator of metabolism. We attempted to measure the

effects of these inhibitors on the rates of formation of RHPP+ from HP but the quantities of RHPP+ from HP were too low for accurate quantification (<4 pmol RHPP+ formed/mg protein-min). We also examined the concentration dependence of the inhibition of these reactions by ketoconazole (Fig. 23, right panel). This compound at 1 μM inhibited by more than 50% the formation of HPP+ from HP and HPTP.

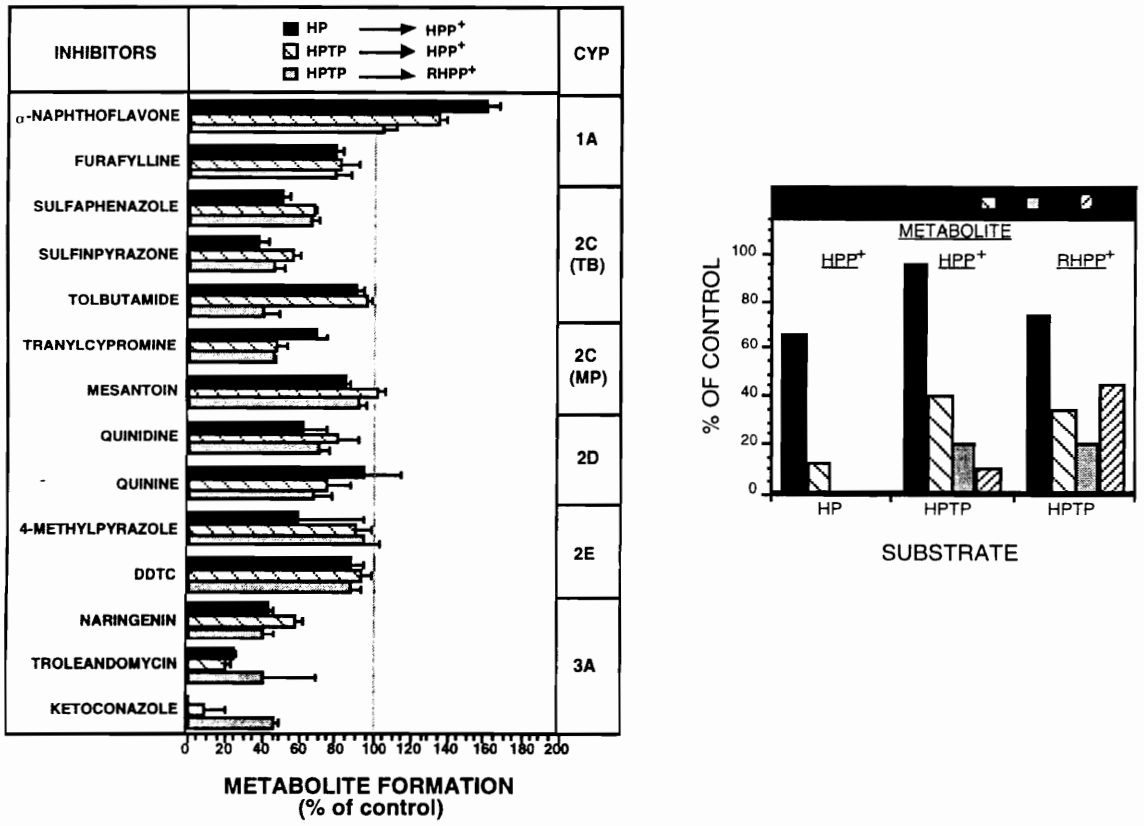

Figure 23. Effects of various selective cytochrome P450 inhibitors on the rates of conversion of HP and HPTP to HPP+ and HPTP to RHPP+ by a pooled human liver microsomal preparation (left panel) and the effect of ketoconazole concentration on the inhibition of these reactions (right panel).

Antibody inhibition. Various antibodies were examined for their ability to inhibit the conversion of HP and HPTP to HPP^+ by human liver microsomes. These antibodies were raised against rat P450 enzymes (P450 1A, 2B, 2C and 3A) although they also inhibit the corresponding P450 enzymes in human liver microsomes.[139, 147] As shown in Figure 24, the rates of HPP^+ formation from both HP and HPTP were strongly inhibited by the antibody against P450 3A under conditions that resulted in little or no inhibition by pre-immune IgG or the other antibodies tested.

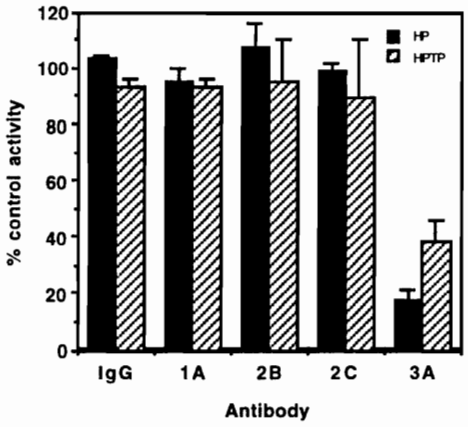

Figure 24. Effects of antibodies against rat P450 enzymes on HP and HPTP metabolism by human liver microsomes. Uninhibited rates of HPP^+ formation were, 360 and 323 pmol/mg protein/min from HP and HPTP, respectively. All assessments were analyzed as the mean ± S.D. of triplicate determinations.

Discussion

The potential contribution of HPP^+ and $RHPP^+$ to the mediation of the extrapyramidal side effects observed in patients treated with HP has prompted

studies that resulted in the characterization of these pyridinium metabolites in the urine of patients treated with HP[118, 130] and the urine of rodents treated with HP and HPTP.[129,148] Studies with rodent[124] and human[118] liver microsomal preparations suggest that the oxidations of HP and HPTP to these pyridinium metabolites are catalyzed by one or more forms of cytochrome P450. The principal goal of the present study was to characterize the form(s) of cytochrome P450 present in human liver microsomes that catalyze these reactions.

The HPLC-fluorescence tracings shown in Figure 19 confirm that HP and HPTP are biotransformed to HPP^+ and $RHPP^+$ by human liver microsomal enzymes. Metabolite formation was fully dependent on the presence of an NADPH generating system. Michaelis-Menton kinetic analyses performed with two liver preparations show that the k_{cat}/K_M values for HPP^+ formation from HP and HPTP (5.85 to 7.61 min^1mM^{-1}, Table 9) are comparable to each other and also to values commonly reported for moderately good P450 substrates.[149,150] The k_{cat} values reported here are minimal since they are expressed in terms of total P450 content and not in terms of the specific P450 form(s) that actually catalyze the reactions. The k_{cat}/K_M values for $RHPP^+$ formation from HPTP (0.77 to 1.7 $min^{-1}mM^{-1}$) in general are no more than 20% of the corresponding values for HPP^+ even though the ratio of $RHPP^+$ to HPP^+ in the urine of HP treated patients is about 6 to 1.[130] These low rates of $RHPP^+$ are not unexpected because of the limited ketone reductase activity present in human liver microsomal preparations. In any event, since only low levels of $RHPP^+$ were observed in these studies, these in vitro studies will focus on the HPP^+ results.

HPTP has been reported to be only a minor microsomal metabolite of HP.[94] Therefore, we speculate that the biotransformation of HP to HPP^+ proceeds directly through ring α-carbon oxidation to generate initially the iminium intermediate **37** which, via the corresponding enamine free base **38**, will undergo spontaneous elimination of OH^- to yield the dihydropyridinium intermediate **35**[151] as shown in Figure 25. Compound **35** was not detected in these incubation mixtures presumably because it undergoes spontaneous oxidation to HPP^+.[124] The conversion of HP to the iminium intermediate **37** is analogous to the initial step in metabolic oxidative N-dealkylation reactions, such as reported for HP,[95] except that attack at the ring α-carbon atom leads to an endocyclic iminium species which cannot undergo hydrolytic carbon-nitrogen bond cleavage.

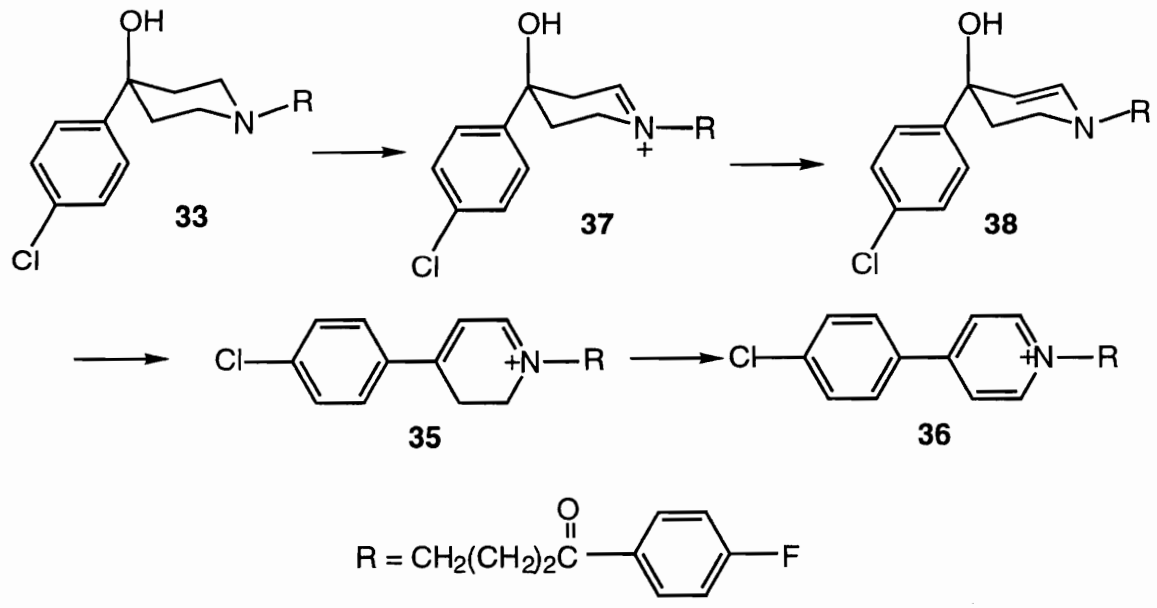

Figure 25. Proposed catalytic pathway for the cytochrome P450 catalyzed oxidation of HP to HPP^+.

Several approaches were taken to identify the cytochrome P450 enzyme(s) responsible for the conversion of HP and HPTP to the pyridinium species HPP^+. The first involved estimating the rates of formation of HPP^+ by a bank of human liver microsomes at 100 μM HP and HPTP. The results of these studies (Fig. 21, left panel) establish that the rates of conversion of HP and HPTP to HPP^+ are highly correlated ($r^2 = 0.875$) with each other (Fig. 21, right panel), suggesting that both conversions are catalyzed by the same enzyme(s). Furthermore, the sample-to-sample variations are highly correlated ($r^2 = 0.917$ and 0.842 for HP and HPTP, respectively) with the rates at which testosterone undergoes 6β-hydroxylation (Fig. 22). This reaction is considered to be a good marker of P450 3A activity[144, 145] suggesting that this form of cytochrome P450 contributes to the conversion of HP and HPTP to HPP^+. Similar results have recently been reported for oxidation of HP and HPTP to HPP^+ catalyzed by rat liver microsomal preparations.[152] No other P450 enzyme activity correlated well with the sample-to-sample variations in HPP^+ formation. Results consistent with these correlation data were obtained with cDNA expressed human P450 enzymes. Of the 9 enzyme preparations studied, only P450 3A4 co-expressed with NADPH cytochrome P450 reductase showed significant catalytic activity. Unfortunately, P450 3A4 was the only enzyme preparation with the co-expressed reductase available and therefore this is an incomplete evaluation of the potential activities of the other forms of cytochrome P450 examined in this experiment.

Further support for the catalytic activity of P450 3A4 was obtained with studies on a variety of selective enzyme inhibitors and antibodies directed against specific forms of cytochrome P450 . As shown in the left panel of Figure

23, the extents of formation of HPP^+ from both HP and HPTP are most effectively inhibited by ketoconazole and troleandomycin, known selective inhibitors of P450 3A.[75] A more detailed study showed that the inhibition of these reactions by ketoconazole is concentration dependent (Fig. 23, right panel). At 1 μM ketoconazole, a concentration which is reported to be selective for P450 3A,[153] both reactions are inhibited by more than 50%. Furthermore, the selective stimulator of P450 3A activity, α-naphthoflavone,[154] enhanced the formation of HPP^+ from HP and HPTP. Finally, of those preparations tested, only antibodies directed against P450 3A were effective in inhibiting these oxidations (Fig. 24).

Taken together, it is evident that human liver P450 3A4 is capable of catalyzing the oxidation of HP and HPTP to HPP^+. The evidence summarized above indicate that only P450 3A4 displays significant catalytic activity for HP and HPTP. We conclude, therefore, that P450 3A4 is the principal form of P450 that catalyzes the oxidation of HP to HPP^+ in vivo. This is the same enzyme that has been shown to catalyze the oxidative deamination of a variety of cyclic tertiary amines[155-157] and we speculate that it may also catalyze the oxidative deamination of HP, a major metabolic pathway for this compound. Since rat P450 3A1 also catalyzes the oxidation of HP and HPTP to HPP^+, studies on metabolic drug-drug interactions and on the effects of P450 3A inhibitors on HPP^+ formation and drug induced toxicities performed in this species should be relevant to humans.

Experimental

Materials. The HCl salts of HP,[134] HPTP,[124] HPP^+[121] and $RHPP^+$[148] were prepared as described previously. HP free base, α-naphthoflavone,

naringenin, naringin, diethyl dithiocarbamate, tranylcypromine, sulfinpyrazone, tolbutamide, quinidine, quinine, 4-methylpyrazole, ketoconazole, papaverine, $NADP^+$, glucose 6-phosphate and glucose 6-phosphate dehydrogenase were purchased from Sigma Chemical Co. (St. Louis, MO). Furafylline was purchased from Research Biochemicals Inc. (Natick, MA). Other drugs were obtained from the following sources: sulfaphenazole from Ciba-Geigy (Basel, Switzerland), mesantoin from Sandoz Ltd. (Basel, Switzerland), and troleandomycin from Pfizer, Inc, (Groton, CT). HPLC-grade solvents were purchased from Fisher Scientific Co. (Springfield, NJ). Other chemicals were obtained from commercial sources.

Human liver microsomes (HepatoSome Test Kit) were obtained from Human Biologics, Inc. (Phoenix, AZ) along with data on the sample-to-sample variations in the activities of specific forms of P450. Microsomes from a human lymphoblastoid cell line expressing human P450 1A1, 1A2, 2A6, 2C9, 2D6, 2E1, 3A4 or 3A4 co-expressed with NADPH-cytochrome P450 reductase (P450 3A4 + OR) were purchased from Gentest Corp. (Woburn, MA).

HPLC Analyses. All samples were coded and were analyzed blinded. HPLC analyses for $RHPP^+$ and HPP^+ were performed with a HPLC system (including conditions, mobile phase) described in Chapter 4. Because appropriate internal standards were not available, calibration curves with synthetic HPP^+ and $RHPP^+$ were established to estimate metabolite concentrations in incubation mixtures. The percent recoveries from tissue samples were determined by assaying control liver homogenates that had been spiked with the analytes at appropriate concentrations.

HP and HPTP metabolism. Microsomal cytochrome P450 levels were determined by the method of Omura and Sato.[158] Human liver microsomes or lymphoblastoid microsomes containing cDNA-expressed P450 enzymes were incubated at 37 ± 1 °C. The incubation mixtures were prepared from the appropriate stock solutions to give the final concentrations indicated in a final volume of 0.4 mL: 100 μL enzyme preparation (0.1-2.0 mg protein/mL); 180 μL of a solution containing potassium phosphate buffer (50 mM, pH 7.4), $MgCl_2$ (3 mM) and EDTA (1 mM); 100 μL of an aqueous solution containing substrate (2.5-250 μM) and 20 μL of an NADPH generating system [$NADP^+$ (1 mM), glucose 6-phosphate (5 mM) and glucose 6-phosphate dehydrogenase (1 Unit/mL)] which was added to initiate the reaction. The reactions were terminated at various times (0 to 60 minutes) by the addition of 0.8 mL of ice-cold acetonitrile containing 0.1% acetic acid. The resulting mixtures were agitated vigorously on a batch vortexer (3 x 1 min) and the resulting protein precipitate was removed by centrifugation (2000 *g* x 10 min). An aliquot (50 μL) of the clear supernatant fraction was analyzed by HPLC.

Chemical-inhibition experiments. The following P450 enzyme substrates/inhibitors were examined for their effects on HP and HPTP metabolism by human liver microsomes: α-naphthoflavone and furafylline (P450 1A2 inhibitors), diethyl dithiocarbamate (P450 2A6 and P450 2E1 inhibitors), sulfaphenazole, sulfinpyrazone and tolbutamide (P450 2C9/10 inhibitors), mesantoin (R,S-mephenytoin) and tranylcypromine (P450 2C19 inhibitors), quinidine and quinine (strong and weak P450 2D6 inhibitors), 4-methylpyrazole (P450 2E1 inhibitor) and troleandomycin, ketoconazole and papaverine (P450 3A inhibitors). With the exception of diethyl dithiocarbamate

and tranylcypromine, which were dissolved in water, the inhibitors were added to 0.4 mL-incubations in 4 μL of methanol at a final concentration of 0.1 to 100 μM. Control incubations contained 4 μL of methanol or water. The mechanism-based inhibitors, troleandomycin and furafylline, were preincubated with the microsomes containing the NADPH-generating system for 10 minutes before starting the reaction by the addition of substrate. All other reactions were initiated with the NADPH-generating system, as described above.

Antibodies and immunochemical inhibition experiments. Antibodies against purified rat P450 1A1, 2B1, 2C7 and 3A1 were raised in rabbits as described previously.[159] All antibodies, except the antibody against P450 2C7, were subjected to immunoabsorption chromatography to remove antibodies that cross-reacted with P450 enzymes in other gene subfamilies. Some of the immunoabsorbed antibodies were not monospecific in that they recognized two or more distinct proteins belonging to the same P450 subfamily, as described previously. For antibody-inhibition experiments, two panels of liver microsomes (0.04 mg protein/incubation) were mixed with 0.04-0.40 mg of antibody. The final concentration of antibody was adjusted to 0.4 mg/mL with the IgG fraction purified from rabbit pre-immune serum. After incubating for 20 minutes at room temperature, HP or HPTP metabolism was measured as described above.

5.3. Brain metabolism of HP and HPTP in C57BL/6 mice.

It has been documented that the total P450 levels in male rat brain are approximately 100 pmol/mg protein which is about one-tenth the corresponding hepatic levels.[160] The female brain levels are 60% of those in the males. The brain P450s are located both in the mitochondrial and microsomal fractions with higher levels in the mitochondria. Despite the low levels, brain P450s have been identified as functional enzyme systems which metabolize xenobiotics as well as a wide variety of endogeneously occurring substances.[161,162]

Because of the neurotoxic properties of pyridinium species,[119-123] we have been interested in the possible metabolic oxidation of HP and HPTP by brain enzymes. As will be discussed later (Chapter 6.1.), HPP^+ and related pyridinium species have been identified in the brains of mice treated with HPTP, but not HP. HPP^+ also has been observed in brains of HP-treated rats and humans.[137,152] We therefore attempted to examine the in vitro brain metabolism of HP and HPTP. In all experiments, whole brain homogenates (1 mg protein/mL) were used. The following set of 5 experiments was conducted;

1. Preliminary HP and HPTP incubations with brain homogenates.
2. Time dependent studies.
3. Protein concentration dependent studies.
4. Inhibition studies.
5. Cumene hydroperoxide supplemented incubations.

Results and Discussion

Preliminary metabolic studies were conducted with HP and HPTP in an effort to determine if any oxidase activity could be detected in the mouse brain homogenates. Since previous incubation studies with C57BL/6 mouse liver microsomes documented that the K_M values of HPP^+ formation from HP, HPTP and RHP were 78, 68, 42 μM, respectively (Chapter 5.2.1.), we conducted this preliminary experiment with a substrate concentration of 50 μM HP and HPTP. Substrates were incubated for 0 to 30 minutes. Control experiments were conducted in the absence of NADPH or protein.

In addition to the HPLC/fluorescence assay for the pyridinium metabolites, HP and HPTP were also detected by HPLC/UV analysis as unchanged substrates. Although it has been documented that HPTP can be detected in the incubation mixture of HP with mouse hepatic microsomes,[131,132] HPTP was not observed as a metabolite in the HP substrate incubation mixtures.

As summarized in Table 10, HPP^+ formation was observed in both HP and HPTP incubations. $RHPP^+$ was observed in HPTP incubations but not in HP incubations. However, the amounts of $RHPP^+$ formed were lower than the limits required for quantitative analysis (0.4 pmol on column). No HPP^+ was detected in the absence of the brain homogenate or substrate or in the presence of denatured enzyme (protein was heated in boiling water for 10 minutes) or at t =0. Consequently, we conclude that the pyridinium species detected in these incubation mixtures are not artifacts and are formed enzymatically.

TABLE 10

HPP^+ formations from HP and HPTP catalyzed by C57BL/6 whole brain homogenates (preliminary experiment).

	HP (50 μM)		HPTP (46 μM)	
	pmol/mg protein	pmol/mg protein/min	pmol/mg protein	pmol/mg protein/min
No enzyme[a]	0 ± 0	0 ± 0	0 ± 0	0 ± 0
No NADPH	38.4 ± 4.8	1.3 ± 0.2	1453 ± 115	48.4 ± 3.8
t = 0 min	0 ± 0	0 ± 0	0 ± 0	0 ± 0
t = 10 min	2.4 ± 1.2	0.2 ± 0.1	732 ± 74	73.2 ± 7.4
t = 20 min	20.4 ± 6.0	1.0 ± 0.3	868 ± 187	43.4 ± 9.4
t = 30 min	56.4 ± 9.6	1.9 ± 0.3	1072 ± 222	35.8 ± 7.4

[a]: No enzyme and No NADPH samples were incubated for 30 minutes. All values were the mean ± S.D. of three determinations.

As shown in Table 10, HPP^+ formation from HP and HPTP was dependent on the presence of the homogenates. The HPP^+ formation from HPTP was roughly (average of 10 to 30 minutes) 40 pmol/mg protein/min and from HP was much lower (1 to 2 pmol/mg protein/min). HPP^+ formation from HP showed partial NADPH dependency (68%). Although HPTP appeared to be a better substrate than HP in the mouse brain, its conversion to HPP^+ was not NADPH dependent. HPP^+ formation (pmol/mg protein) was not linear during the course of the incubation for either compound. With HPTP, the rate of HPP^+ formation started to decrease already after 15 minutes. These features are very different from what was observed in the liver microsomal study (see Chapter

5.1.). In the mouse liver homogenates, the rates of HPP^+ formation from HP and HPTP were comparable and its formation from both substrates was completely NADPH-dependent. Also, the rates of HPP^+ formation were linear for HP and HPTP up to 30 minutes.

More detailed time dependent studies were conducted in an effort to estimate more quantitatively the rates of HPP^+ formation. During the course of the study, it was found that incubation samples needed to be preincubated at least for 10 minutes in the 37 °C water bath in order to reach temperature equilibrium (brain homogenates were kept on ice during preparing homogenates). Since the length of preincubation time did not affect HPP^+ formation between 10 to 30 minutes, all samples were preincubated for 10 minutes throughout these studies. The reactions were terminated at incubation times t = 0, 2, 4, 6, 8, 10, 20, 30, 60 and 120 minutes for both substrate incubations. Control incubations were conducted in the absence of the NADPH-generating system or substrate. Substrate concentrations were kept at 50 μM, the same as in the preliminary experiment. Table 11 summarizes the data on HPP^+ formation from HP and HPTP as catalyzed by mouse brain homogenates. Rate estimates were obtained by calculating only the peaks which provided values above the limits of detection.

TABLE 11

HPP^+ formation from HP and HPTP catalyzed by C57BL/6 mice whole brain homogenates.

	HP (50 μM)		HPTP (50 μM)	
Incubation time (minutes)	pmol/mg protein	% conversion[a]	pmol/mg protein	% conversion[a]
No protein (t = 30)	0 ± 0	0	0 ± 0	0
No NADPH (t = 30)	33.3 ± 7.6	0.06	2851 ± 57	5.7 ± 0.1
0	0 ± 0	0	0 ± 0	0
2	~ 0 ± 0	~ 0	580 ± 41	1.1 ± 0.1
4	~ 0 ± 0	~ 0	886 ± 93	1.8 ± 0.2
6	3.3 ± 0	0.01	1040 ± 89	2.1 ± 0.2
8	14.6 ± 3.2	0.03	1341 ± 69	2.7 ± 0.1
10	14.8 ± 0.1	0.03	1573 ± 26	3.1 ± 0.1
20	42.7 ± 1.3	0.08	2136 ± 134	4.3 ± 0.3
30	61.0 ± 3.0	0.08	2558 ± 140	5.1 ± 0.3
60	129.2 ± 11.0	0.23	2883 ± 264	5.8 ± 0.5
120	196.7 ± 30.4	0.39	3198 ± 158	6.4 ± 0.3

[a]: % conversion was calculated using the amount of HPP^+ formed from 50 μM substrates. No HPP^+ formation was observed in the absence of substrate at 30 minutes incubation time. All samples were preincubated for 10 minutes prior to the addition of substrate. All values were the mean ± S.D. of three determinations.

Figure 26 shows the plot of HPP^+ formation (pmol/mg protein) against incubation time for HP and HPTP incubations. By obtaining more time points and using longer incubation times, we were able to observe in more detail the behavior of these two compounds in the brain homogenates. HPP^+ formation from HP was very slow but the rate appears to be linear. The rate of HPP^+ formation from HPTP is linear only for the first 10 to 15 minutes and then starts to decrease. By taking the data of the first 10 minutes, the initial rate of HPP^+ formation from HPTP was estimated to be 160 pmol/mg protein-min.

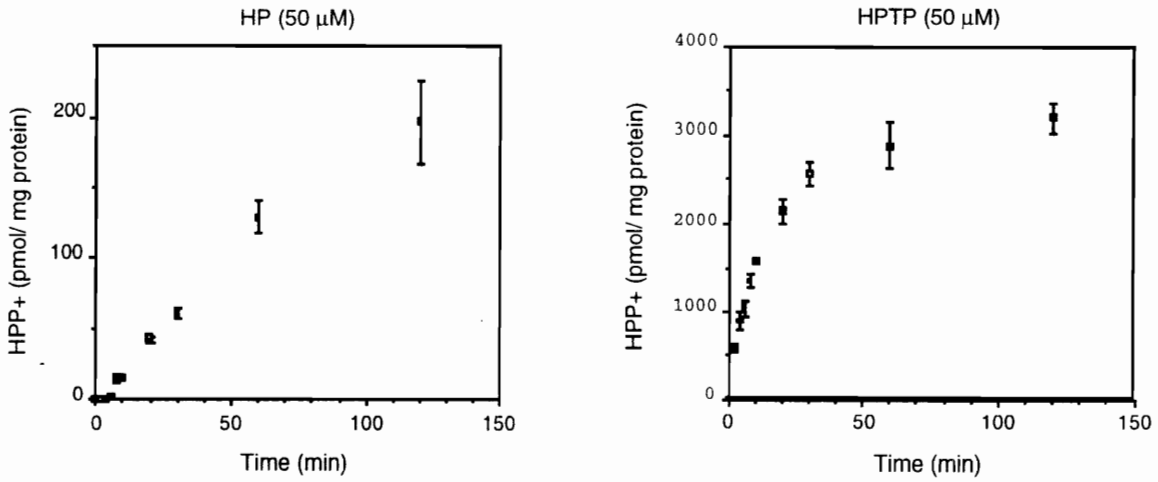

Figure 26. HPP^+ formation (pmol/mg protein) against incubation time for HP and HPTP incubations. All values are the mean ± S.D. of three determinations.

Possible reasons for loss of enzyme activity include (1) time dependent enzyme inhibition and (2) substrate depletion. Since large amounts of unchanged HPTP were observed in the HPLC/UV tracings throughout the study, substrate depletion can not contribute to loss of enzyme activity. Possible relationships between protein concentration, incubation time and rates of oxidation therefore were examined. The experiment was conducted as follows:

(1) The initial incubation was conducted in the presence of 1 mg protein/mL. After 30 minutes an additional amount of protein was added to make a final total of 2 mg protein/2 mL and the mixture was incubated for an additional 30 minutes. (2) In separate sample tubes, HPTP also was incubated with 2 mg protein/mL for 30 minutes. (3) The same experiment was performed with 2 mg protein/mL for 60 minutes and (4) with 1 mg protein/mL for 30 minutes. In this way, we hoped to determine if the preparation was undergoing a time dependent loss of enzyme activity.

The results are summarized in Table 12 and Figure 27. HPP^+ formation from HPTP was incubation time and protein concentration dependent. Combining these facts and the result from control experiments (no protein, t = 0) which showed no HPP^+ formation, we confirmed that the oxidation of HPTP to HPP^+ was enzyme catalyzed. The first experiment (1) showed about the same amount of HPP^+ formation as found in the second experiment (2). This suggests that as far as enzyme is available in the incubation mixture, there is enough HPTP to be metabolized to HPP^+. By comparing (2) and (4), we find that HPP^+ shows a dependence on protein concentration. However, the amount of HPP^+ formed was not doubled when the protein concentration was doubled. If one compares (2) and (3), HPP^+ formation was incubation time dependent at the same protein concentration (2 mg/mL). However, HPP^+ formation also was not doubled when the time was doubled. These results suggest that enzyme depletion is not likely to be the reason for the decrease in the rate of HPP^+ formation. The cause for the non-linear behavior of HPTP to HPP^+ conversion in mouse brain homogenates remains to be determined.

TABLE 12

Protein concentration and incubation time dependency on HPP^+ formation from HPTP.

Sample set	Protein concentration (mg/mL)	Incubation time (minutes)	HPP^+ pmol/total time
(1)	1 + 1	30 + 30 (total 60)	3673 ± 270
(2)	2	30	3275 ± 39
(3)	2	60	4038 ± 98
(4)	1	30	1990 ± 40

All results are the mean ± S.D. of three determinations. All samples were incubated at 37 °C and contained NADPH generation system.

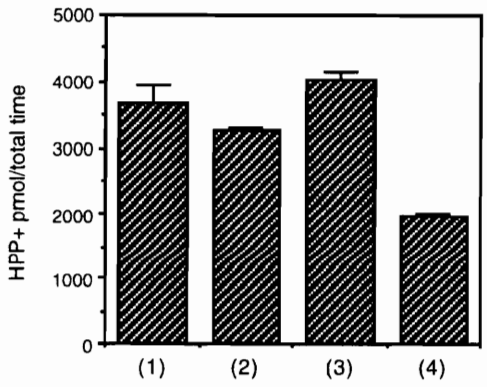

Figure 27. Protein concentration and incubation time dependency of HPP^+ formation from HPTP (50 μM). See text for the description of the experimental protocol followed. All values are the mean ± S.D. of triplicate determinations.

The dependency of the formation of HPP^+ on NADPH was considered once more in this experiment by comparing the amount of HPP^+ formed in the

presence and absence of the NADPH-generating system following a 30 minutes incubation period. Similar to what was observed in the preliminary experiment, in the case of HP as the substrate, the rate of HPP^+ formation decreased to 60% of the maximum observed in the absence of NADPH. However, the results with HPTP as substrate again showed no NADPH dependency.

Although HPP^+ formation from HPTP is considered to be enzymatic, these two experiments suggest that this reaction may not be P450 catalyzed. Consequently, enzyme(s) other than P450 may contribute to this oxidation. In our previous in vitro studies, it was found that MAO-A catalyzes the oxidation of HPTP to HPP^+ but not HP (Chapter 5.1.). Therefore, we attempted inhibition experiments using clorgyline (an MAO-A selective inhibitor) and deprenyl (an MAO-B selective inhibitor) to examine the possibility of the participation of MAO(s) in the formation of HPP^+.

The brain homogenates were preincubated with 10 μM, 25 μM and 50 μM clorgyline or deprenyl for 10 minutes, then the reaction was initiated by addition of substrate (50 μM HP or HPTP). Again, HPP^+ was not detected in control experiments (no substrate, no protein, t = 0 incubation after 10 minutes preincubation). By setting the amount of HPP^+ formed from HP and HPTP without inhibitors as 100%, the amounts of HPP^+ from HP and HPTP in the presence of the inhibitors were calculated as % remaining activity. Summarized in Table 13 and Figure 28 are the results of these experiments. No inhibition was observed with deprenyl. Weak inhibition on HPP^+ formation from HP and moderate, concentration dependent inhibition from HPTP were observed with clorgyline.

TABLE 13

Summary of inhibition study.

	HP (50 μM)		HPTP (50 μM)	
	pmol/mg protein[a]	% remaining activity	pmol/mg protein	% remaining activity
No inhibitor, preincubation 10 min	204.6 ± 2.9	100[b]	3087 ± 424	100
clorgyline 10 μM	186.7 ± 2.9	91.3	2451 ± 201	79.4
clorgyline 25 μM	169.9 ± 7.1	83.0	2142 ± 84	69.4
clorgyline 50 μM	148.6 ± 4.7	72.6	1671 ± 75	54.1
deprenyl 10 μM	205.4 ± 0.4	100.4	3259 ± 517	105.6
deprenyl 25 μM	201.9 ± 1.3	98.7	3185 ± 387	103.2
deprenyl 50 μM	182.6 ± 0.6	89.3	2605 ± 296	84.4

[a]: HPP^+ formed from 50 μM HP or HPTP incubated for 30 minutes incubations.

[b]: The amount of HPP^+ formed from HP or HPTP incubated for 30 minutes in the absence of inhibitor was set as 100% activity. All inhibition incubations were preincubated for 10 minutes before the addition of substrate which was followed by a 30 minutes incubation. All values are the mean ± S.D. of two determinations.

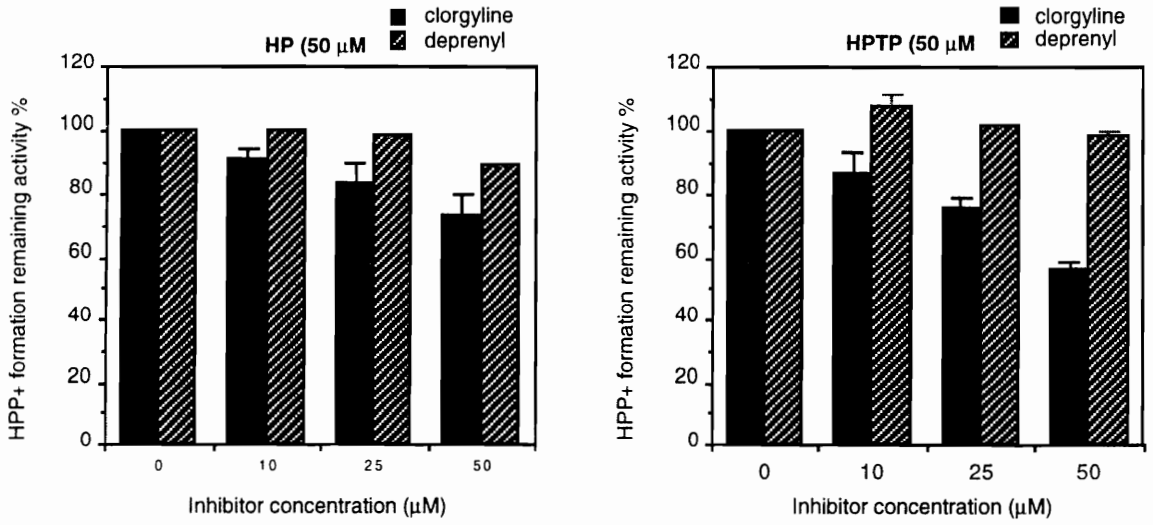

Figure 28. Effect of clorgyline and deprenyl on HPP^+ formation from HP and HPTP.

These results suggest that HPP^+ formation from HPTP may be catalyzed by MAO-A but not by MAO-B in the mouse brain. This is consistent with the evidence that HPTP is converted to HPP^+ in the presence of partially purified MAO-A (Chapter 5.1.). However, MAO-A is known to be sensitive to inhibition by nanomolar concentrations of clorgyline.[87] Therefore, this inhibition of HPP^+ formation suggests that MAO-A may contribute only partially to this oxidation. It should be noted that other work in our laboratory suggests that the 10 minutes preincubation used in these studies may not be adequate to fully inhibit brain MAO-A.

In the previous inhibition experiment, clorgyline was found to inhibit HPP^+ formation from HP and HPTP, but only at high concentrations. Since these experiments were conducted in the presence of an NADPH-generating system, the inhibition experiment was repeated in the absence of the NADPH-generating system. Samples were preincubated with clorgyline for 10 minutes and then incubated for 30 minutes. This preincubation time (10 minutes) was

chosen according to the result obtained from MAO-A inhibition study with HPTP (see Chapter 5.1.). In that study, MAO-A was preincubated with 9 μM of clorgyline for 10 minutes and under that condition, HPP^+ formation from HPTP was completely blocked However, as just mentioned, this time may not be adequate when working with brain homogenates.

As summarized in Table 14, again only partial inhibition of HPP^+ formation was observed. By incubating samples in the absence of NADPH, we expected to exclude all contributions of P450 and to see stronger inhibition. These results suggest oxidase activity other than that derived from MAO and P450 may contribute to the conversion of HPTP to HPP^+.

TABLE 14

Effect of clorgyline on HPP^+ formation from HPTP.

Clorgyline (μM)	HPP^+ pmol/mg protein	RA %[a]
0	1925 ± 66	100 ± 3
10	1795 ± 346	93.3 ± 17
100	718 ± 85	37.3 ± 4

[a]: Relative activity (% of HPP^+ formation from HPTP). All samples contained 1 mg protein/incubation. Samples were incubated in the absence of an NADPH-generating system for 30 minutes at 37 °C. All values were HPP^+ formed pmol/ mg protein, average ± S.D. of three determinations.

As shown in Figure 29, it is known that peroxides have the ability to substitute for O_2 and NADPH (electron donor) in the P450 catalytic cycle (peroxide shunt).[61,163] Cumene hydroperoxide (CuOOH), which is stable and

readily available, is most often used in mechanistic studies of P450.[163] In order to examine the possibility of peroxide-supported P450 catalysis of HP, HPTP metabolism to HPP^+, we conducted incubations using CuOOH.

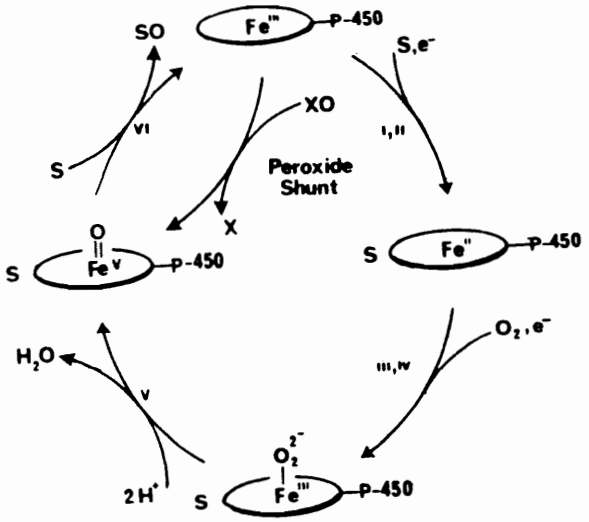

Figure 29. Catalytic cycle of P450 with Peroxide shunt. S represents the drug substrate and SO the corresponding oxidized metabolite. [Adapted from reference 61.]

For these incubations, CuOOH (110 μM and 220 μM) replaced the NADPH-generating system. The samples were preincubated for 10 minutes and the reaction was initiated by the addition of substrate. Then samples were incubated for 10 minutes at 37 °C. As control experiments, CuOOH was incubated in the absence of brain homogenates or substrate. If one takes the amount of HPP^+ formed in the absence of CuOOH as 100%, 110 μM CuOOH enhanced HPP^+ formation from HP and HPTP to 330% and 137%, respectively. Also 220 μM CuOOH enhanced HPP^+ formation from HP and HPTP to 535%

and 188%, respectively. Table 15 and Figure 30 summarize the effects of CuOOH on HPP^+ formation from HP and HPTP. CuOOH itself did not convert HP or HPTP to detectable levels of HPP^+.

TABLE 15

Activation effect of CuOOH on HPP^+ formation from HP and HPTP.

	HP (50 μM)		HPTP (50 μM)	
CuOOH (μM)	HPP^+ [a]	RA %[b]	HPP^+	RA %
110 (no protein)	0 ± 0	0	0 ± 0	0
110 (no substrate)	0 ± 0	0	0 ± 0	0
0	40 ± 4.6	100 ± 12	2041 ± 59	100 ± 3
110	132 ±13.2	330 ± 33	2796 ± 192	137 ± 9
220	214 ± 20.5	535 ± 51	3843 ± 185	188 ± 9

[a]: HPP^+ formation (pmol/mg protein). b: % relative activity for the rate of formation of HPP^+. All values were the mean ± S.D. of two determinations. Incubation conditions are described in the text.

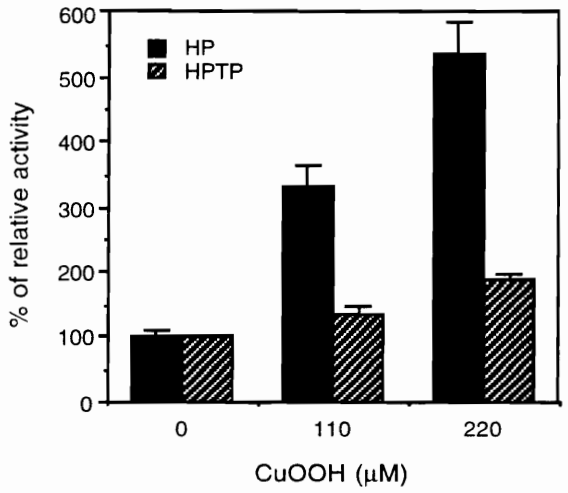

Figure 30. Activation effect of CuOOH on HPP^+ formation from HP and HPTP.

These results demonstrate the activation effect of CuOOH on HPP^+ formation to be more significant with HP as substrate. As described earlier, HPP^+ formation from HP was approximately 60% NADPH dependent. This result is consistent with the activation by CuOOH, which can replace the NADPH-generating system as an oxygen donor for the P450 catalysis. We also showed that HP and HPTP are not chemically oxidized to HPP^+ in the absence of brain homogenates. HPP^+ formation from HPTP also was enhanced. However, the relative increase in % activity was not as significant as with HP.

Subsequently, we obtained a reference[164] describing the optimal conditions for CuOOH-mediated oxidation. We attempted to examine the effect of CuOOH on HPP^+ formation from HPTP by following the conditions which were established with bufuralol 1'-hydroxylation. The authors reported that the rate of formation of 1'-hydroxybufuralol was maximal at around 150 μM CuOOH and was linear with time for at least 10 minutes at 25 °C. When microsomes

were incubated at 37 °C, product formation was linear for less than 2 minutes. In our study, brain homogenates were preincubated with CuOOH at 25 °C for 5 minutes and HPTP (final concentration 50 μM) was added to the sample; then the mixtures were further incubated with CuOOH (55 and 110 μM) for 10 minutes. Also, in order to examine the possibility that CuOOH may oxidize HPTP to HPP^+ (i.e., without the involvement of enzyme catalysis), HPTP was incubated with 1.1 mM CuOOH for 10 minutes in the absence of the mouse brain homogenate.

As shown in Table 16, at 25 °C, HPP^+ formation was low compared to the values observed at 37 °C (see Table 15). However, HPP^+ formation was enhanced to 145 % with 55 μM CuOOH and 154% with 110 μM CuOOH. The conversion of HPTP to HPP^+ was fully dependent on the brain homogenates. Even at 1.1 mM CuOOH in the absence of brain homogenate, HPP^+ could not be detected. Consequently, it appears that the CuOOH supported oxidation of HPTP to HPP^+ is not a simple chemical process but one that requires the participation of an enzyme or some comparable biological system. The increased activity, however, is only 4 fold.

TABLE 16

Effect of CuOOH on HPP^+ formation from HPTP at 25 °C.

CuOOH (μM)	Protein (mg)[a]	HPP^+ pmol/mg protein	RA %[b]
0	1	236 ± 5	100 ± 2
55	1	343 ± 7	145 ± 3
110	1	364 ± 16	154 ± 7
1100	0	0 ± 0	-
1100	1	973 ± 71	410 ± 30

[a]: The amount of protein (mg/incubation). b: Relative activity % of the formation of HPP^+. All numbers are the mean ± S.D. of two determinations of HPP^+ formed in the absence of NADPH-generation system for 10 minutes incubations.

In summary, HP and HPTP are oxidized to HPP^+ in mouse brain homogenates. HPP^+ formation is incubation time and protein concentration dependent, which suggests the oxidations of both HP and HPTP are enzyme catalyzed. However, in contrast to the results obtained with mouse liver, HPP^+ formation appears to be not completely P450 catalyzed. In fact, HPP^+ formation from HPTP in the brain did not show any NADPH-dependency. The study with CuOOH suggested the possibility of a peroxide-supported mechanism for catalysis. Also, inhibition studies with MAO inhibitors suggest the possibility of MAO-A catalysis in the mouse brain. These effects of CuOOH and the MAO-A inhibitor (clorgyline) were more significant for HP oxidation to HPP^+ than for HPTP. The results obtained in these studies may suggest that HPTP and HP

behave somewhat differently in the mouse brain. As mentioned earlier and as will be described in detail in Chapter 6.1., in vivo studies with C57BL/6 mouse, HPP^+ (and $RHPP^+$) were observed in the mouse brain treated with HPTP but not HP. This might be due to the low % conversion of HP to HPP^+. Even if HPP^+ were present in the brains of mice treated with HP, the amount might below the detection limit. This consistency in the difference in behavior between HP and HPTP in vivo and brain needs to be noticed.

Experimental

Materials. Cumene hydroperoxide were purchased from Sigma Chemical Co. (St. Louis, MO). See the experimental section in Chapter 5.1. for other chemicals.

Preparation of mouse brain homogenates. Male C57BL/6 mice (n =2) weighing 25-30 g were decapitated and the brains were rapidly removed. Brain homogenates were prepared by following the established method[152] Protein concentrations were determined by the method of Bradford using bovine serum albumin as a standard.

HPLC Analyses. HPLC analyses for $RHPP^+$ and HPP^+ were same as described in Chapter 4.

HP and HPTP metabolism (general). The incubation mixtures were prepared from the appropriate stock solutions to give the final concentrations indicated in a final volume of 1.0 mL: 70 to 90 μL enzyme preparation (1.0 mg protein/mL); 50 μL of an aqueous solution containing substrate (50 μM) and 100 μL of an NADPH generating system [$NADP^+$ (1 mM),

glucose 6-phosphate (5 mM) and glucose 6-phosphate dehydrogenase (1 Unit/mL)], and 760 to 780 μL of a solution containing potassium phosphate buffer (50 mM, pH 7.4), $MgCl_2$ (3 mM). The reactions were initiated by the addition of substrate solution and terminated at various times (0 to 120 minutes) by the addition of 600 μL of ice-cold acetonitrile containing 2 % acetic acid to 600 μL-aliquot of incubation mixtures. Control experiments were conducted in the absence of protein or substrate. The resulting mixtures were agitated vigorously on a batch vortexer and the resulting protein precipitate was removed by centrifugation (14000 rpm x 6 minutes). An aliquot (50 μL) of the clear supernatant fraction was analyzed by HPLC. HP incubation samples were not diluted and HPTP samples were diluted 2 fold with the mobile phase.

Chemical inhibition experiments. Clorgyline hydrochloride and L (-) deprenyl hydrochloride were dissolved in Milli-Q water (1 mM) and added to incubation mixtures to make final concentrations of 10, 25 and 50 μM. These mixtures containing 1 mg/mL of brain homogenate, 1 mM NADPH generating system (+ or -) and 50 mM phosphate buffer were preincubated for 10 minutes and reactions were initiated by addition of 50 μM-substrate solution (HP and HPTP) and further incubated at 37 °C for 30 minutes.

Cumene hydroperoxide (CuOOH) incubations. Incubation experiments were conducted at 25 °C or 37 °C. CuOOH (80 % in cumenol) was insoluble in water. Therefore methanol was used to dissolve the CuOOH. The methanol content was kept to 1% in all final incubation mixtures. Incubation samples were preincubated with CuOOH for 5 minutes (for 25 °C set) according the literature[164] and 10 min (for 37 °C set) and reaction was initiated by the addition of substrate.

Experiment with varying protein concentrations in the incubation mixture. All samples were preincubated for 10 minutes and the reaction was started by the addition of HPTP. The final concentration of HPTP was 50 μM in all incubations. The experiment was conducted as follows: (1) The initial incubation was conducted in the presence of 1 mg protein/mL. After 30 minutes an additional amount of protein was added to make a final total of 2 mg protein/2 mL and the mixture was incubated for an additional 30 minutes. (2) In separate sample tubes, HPTP also was incubated with 2 mg protein/mL for 30 minutes. (3) The same experiment was performed with 2 mg protein/mL for 60 minutes and (4) with 1 mg protein/mL for 30 minutes.

Chapter 6

In Vivo Studies on HP and HPTP Metabolism

6.1. In vivo C57BL/6 mouse study.

As described earlier, recent studies have documented the in vivo oxidative biotransformation of HP to HPP^+ in both rodents[117,129] and humans.[118,130] HPP^+ has been identified in both urine and brain tissues isolated from HP treated rats using HPLC with diode array detection and HPLC-thermospray mass spectrometry.[117] With a highly sensitive atmospheric pressure ionspray HPLC/MS/MS, HPP^+ was identified in urine extracts from HP-treated patients and in extracts of NADPH-supplemented human liver microsomal incubation mixtures containing HP.[118] As discussed in Chapter 5, it has been reported that HPP^+ also is formed in rat liver microsomal incubation mixtures from both HP and HPTP. These conversions were NADPH dependent and were inhibited by SKF-525A.[124] In an effort to characterize further the conversion of HP to potential neurotoxic pyridinium metabolites, we have examined the in vivo metabolic fate of HP and HPTP in C57BL/6 mice, a species known to be susceptible to the neurotoxic properties of MPTP.

The studies summarized below describe our efforts to obtain qualitative and quantitative information on the biodisposition and metabolic fate of HP and HPTP in this species. In some studies, RHP also was examined. A major interest focused on the enzymes systems that catalyze the formation of HPP^+ and $RHPP^+$ from HP and HPTP. As will be discussed later in this Chapter, $RHPP^+$ was first identified in the C57BL/6 mouse urine obtained from HP, HPTP and RHP.

Results and Discussion

Urine and brain analysis after HP, HPTP and RHP administrations. Our initial efforts were concerned with the detection of HPP^+ and $RHPP^+$ in urine and brain tissues isolated from animals treated with HP, HPTP and RHP. This was the first experiment to examine the possibility of HPP^+ formation from HP and its derivatives in C57BL/6 mice. The HPLC/fluorescence tracings of the urine extracts obtained from HP and HPTP treated animals (Figure 31 b, c) show a number of fluorescent peaks, designated as M1-M5, which are not present in the tracings of the corresponding vehicle treated (control) mouse urine extracts (Figure 31a). Consistent with pyridinium type structures,[125] treatment of the urine extracts from drug injected animals with $NaBH_4$ caused these peaks to disappear (Figure 31d), presumably due to conversion to the corresponding tetrahydropyridine derivatives (Figure 31e).

(a)
(b)
(C)
M1
M2
M3
M4
M5
Fluorescence detector Response
MIN
0.0
2.0
4.0
6.0
8.0
10.0
12.0
14.0
16.0
18.0

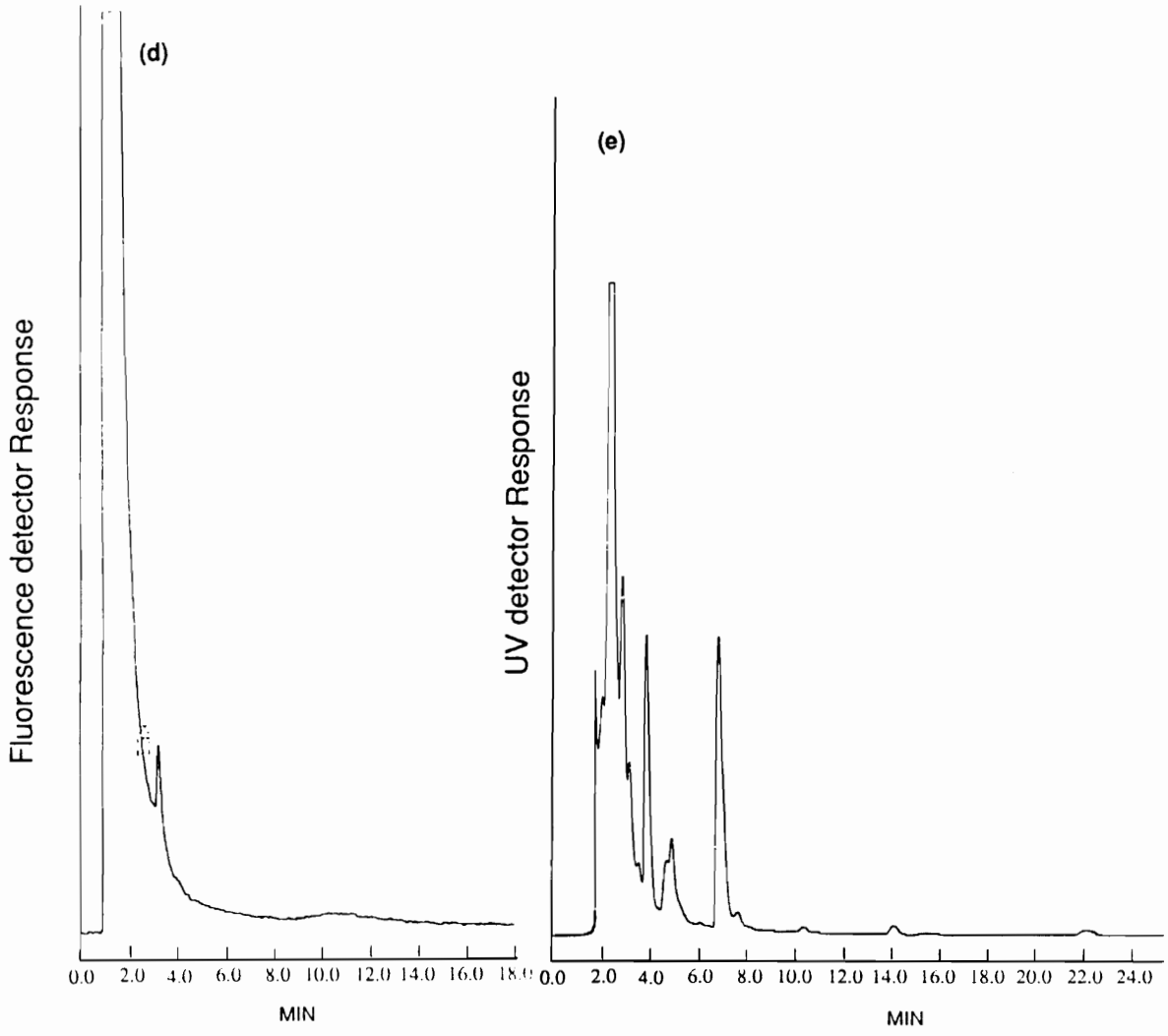

Figure 31. HPLC/fluorescence tracings of urine extracts obtained from C57BL/6 mice treated with (a) vehicle, (b) HP, (c) HPTP, (d) HPTP followed by $NaBH_4$. Fig. 31(e) is the corresponding HPLC/UV tracing of (d).

As shown in the tracings in Figure 30, the size of the solvent front peaks (t_R = ~2 minutes) vary even though all urine samples are 48 hour collections and samples analyzed after Sep-pak extraction and diluted with 240 volumes of mobile phase for the HPLC analysis. We have analyzed urine samples obtained from over 100 different mice and the size of this peak did not appear to be related to the drug treatment (control, HP or HPTP). This problem remains unsolved.

Based on its coelution with the synthetic standard, the major peak eluting at 12.2 minutes, M5, was identified as HPP^+. Confirmation of this assignment was obtained by API-LC/MS and LC/MS/MS analysis of pooled urine extracts from animals receiving HP by Dr. Fouda at Pfizer Inc.[148] Total ion and reconstructed ion chromatograms of several possible metabolites obtained from API-LS/MS analysis of pooled urine from HP-treated mice are shown in Figure 32 (see Table 17 for mass spectral data). The peak numbers in the chromatograms correspond to those of in Figure 31. The peak corresponding to M5 displayed a pair of ions at m/z 354 and 356, the ^{35}Cl-and ^{37}Cl-containing parent ions, respectively, expected for HPP^+. The CID daughter ion spectrum of the m/z 356 ion contained a weak fragment ion at m/z 192 (5%), assigned to the ^{37}chlorophenylpyridinium species **i**, and strong fragment ions at m/z 165 (100%) and 123 (45%) which previously had been assigned to structures **ii** and **iii** (Figure 33a and Table 17).[118] The possibility that the HPP^+ detected in these urine samples was due to autoxidation of HP or HPTP was ruled out by chemical stability studies using human urine samples spiked with 1 mM HP or 1 mM HPTP (both contained 10% methanol) which were stored in air for 72 hours. The peak heights corresponding to that due to HPP^+ observed in the

HPLC/fluorescence tracings were less than 1% of those observed in the tracings obtained with the experimental urine samples.

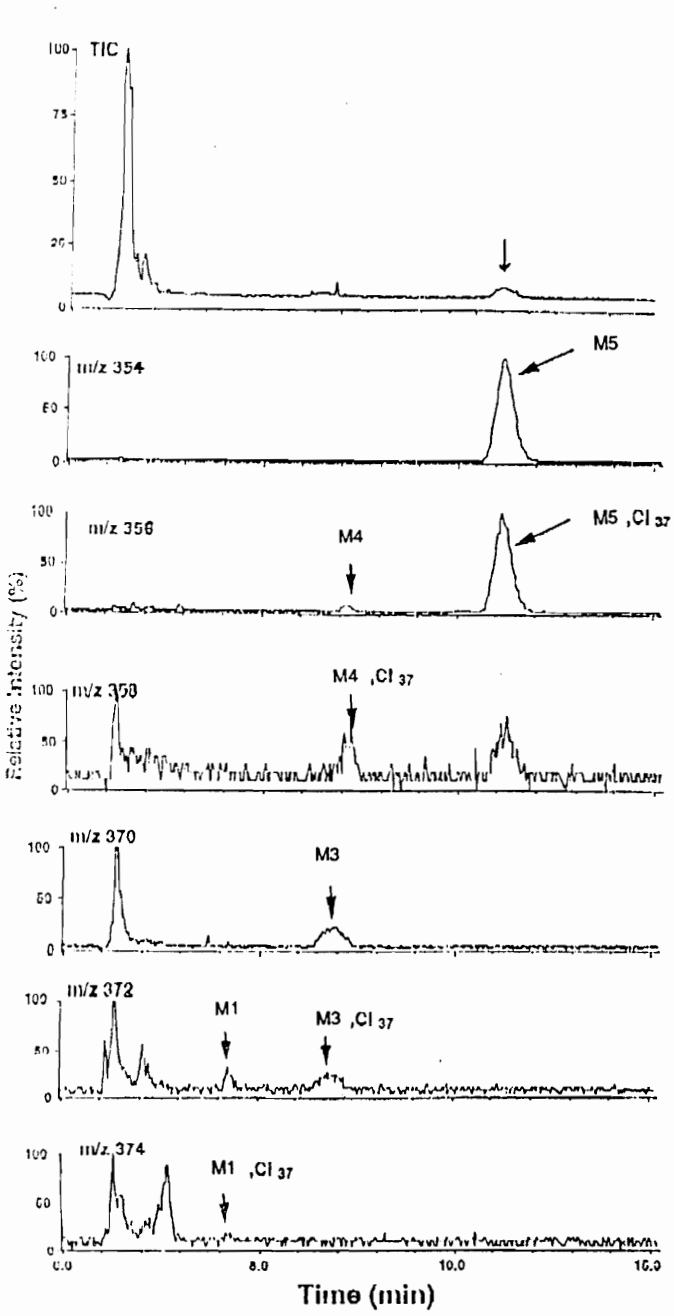

Figure 32. API-LC/MS spectrometric analysis of urine from HP-treated mice. Total (top) and reconstructed ion chromatograms of several pyridinium metabolites.

TABLE 17

API LC/MS/MS CID Fragmentation Data for HP and HPTP Metabolites present in C57BL/6 Brain and Urine.

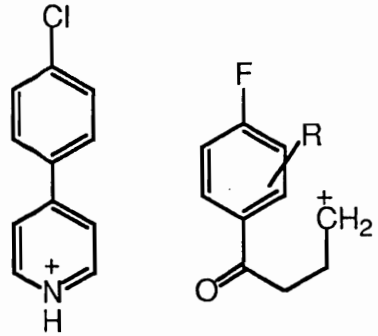

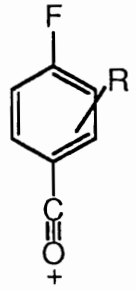

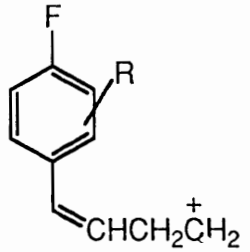

Metabolite	M^+				
M1/2	372/374	190/192 **(i)**	NP	NP	165 (R = OH: **vii**)
M3	370/372	190/192 **(i)**	181 (R = OH: **v**)	139 (R = OH: **vi**)	NP
M4 ($RHPP^+$, **40**)	356/358	190/192 **(i)**	NP	NP	149 (R = H: **iv**)
M5 (HPP^+,**36**)	354/356	190/192 **(i)**	165 (R = H: **ii**)	123 (R = H: **iii**)	NP

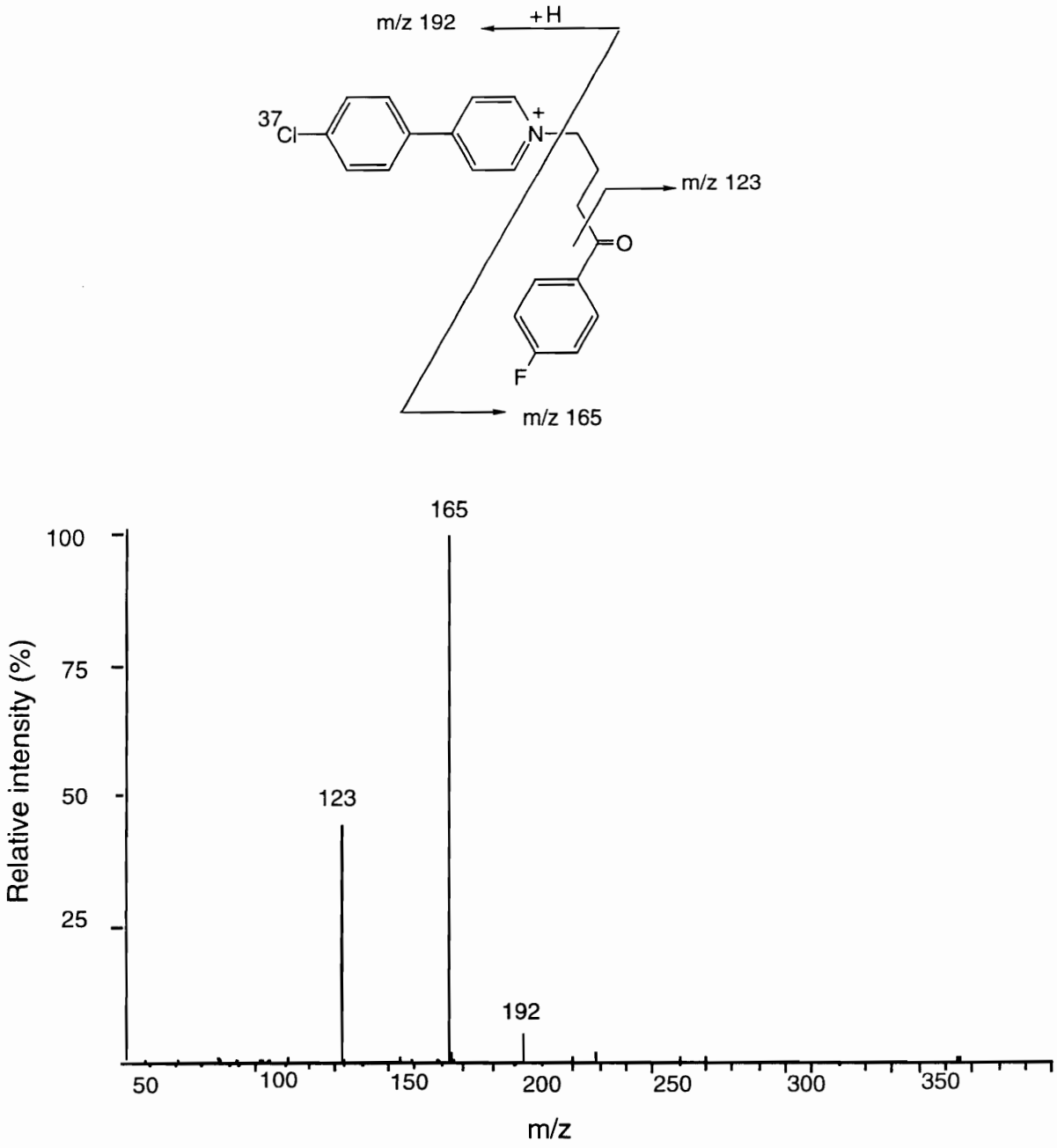

Figure 33 (a). HPLC/MS spectrometric analysis of urine of HP-treated mice. CID product ion spectrum of m/z 356 from the major pyridinium metabolite M5.

Figure 32 (top) shows the HPLC total ion current chromatogram obtained by scanning the first quadrupole over the range m/z 190 to m/z 600. Only the major pyridinium metabolite HPP^+ was noted. Addition to peak M5, three unknown peaks were observed in the HPLC/fluorescence tracings obtained from urine of HP-treated mice and four peaks from urine of HPTP-treated mice (see Figure 31). Since the same column and mobile phase were used for the HPLC/fluorescence and API LC/MS analyses, the retention times of the new metabolites, relative to HPP^+, should be similar to those observed in HPLC/fluorescence tracings (Figure 31).

Characterization of these minor metabolites was sought by examining reconstructed ion current chromatograms which monitored specific parent ions. The tracing of the m/z 356 ion chromatogram obtained from the urine of HP-and HPTP-treated mice showed in addition to the peak for M5 (HPP^+) another peak with t_R = 7.3 minutes. This peak corresponds to M4 in Figure 31. The CID daughter ion spectrum of this ion displayed fragment ions at m/z 190 (75%) and 149 (100%) (Figure 33b). The m/z 190 fragment ion may be assigned to the ^{35}chlorophenylpyridinium species **i** (Table 17) while the fragment ion at m/z 149 is likely to be derived from the fluorophenyl containing portion of the molecule. One plausible structure (**iv**) for this fragment ion would result from cleavage of the chlorophenylpyridyl moiety with dehydration of the carbinol group formed from metabolic reduction of the carbonyl group present in HP. These considerations lead us to the possibility that the peak at t_R = 7.3 minutes (M4) is the pyridinium species $RHPP^+$ (^{35}Cl-M^+ = 356) which could be formed by metabolic oxidation of RHP. Since this peak is much more significant in the HPTP-treated animal compared to HP-treated animal (Figure 31 b,c), the

pathway probably involves the reduction of HPTP to RHPTP and then oxidation of RHPTP to $RHPP^+$.

Further clarification of the structure of M4 was sought by synthesis of $RHPP^+$.[148] $RHPP^+ \cdot Cl^-$ was synthesized by Dr. J. Rimoldi in this group. The HPLC t_R of synthetic $RHPP^+$ was identical to that of the peak observed in the tracing from analysis of the urine extract (t_R = 7.3 min). Full confirmation of the structure of this peak was obtained by API-LC/MS which displayed the expected parent ions for the $^{35}Cl/^{37}Cl$ isotopes at masses 356/358. The CID spectra of these parent ions displayed fragment ions at m/z 190/192 and 149 which we assign to structures **i** and **iv**, respectively.

Since the parent ions of both HPP^+ and $RHPP^+$ fragment under API LC/MS/MS conditions to generate the 4-(4-chlorophenyl)pyridinium fragment ion **i** at m/z 190, an m/z 190 selected ion chromatogram was reconstructed from the spectra of the pooled urine extracts obtained from HP and HPTP treated mice to search for additional pyridinium metabolites. The tracing (identical to that shown in Figure 31b) from the HP urine sample showed a peak (t_R = 7.0 min) corresponding to M3 which eluted at the leading edge of the M4 peak, and an earlier eluting peak (t_R = 4.0 min) corresponding to M1. The API-LC/MS spectrum of M3 (Figure 33c) displayed parent ions at m/z 370/372 ($^{35}Cl/^{37}Cl$), i.e. 16 mass units higher than those observed for HPP^+, and 372/374 for M1 (Figure 33d), i.e. 16 mass units higher than those observed for $RHPP^+$. Analysis of these results led us to propose hydroxylated derivatives of HPP^+ and $RHPP^+$ for these new metabolites of HP and HPTP. In addition to the weak ion at m/z 190 (5%), the CID spectrum of m/z 370 from metabolite M3 showed fragment ions at m/z 181 (100%) and 139 (75%), i.e. 16 mass units higher than

the fragment ions **ii** and **iii** observed in the corresponding CID spectrum of the ^{35}Cl-HPP$^+$ parent ion. These data suggested that M3 is a fluorophenyl hydroxylated derivative of HPP$^+$ in which case the CID fragment ions at m/z 181 and 139 may be assigned to structures **v** and **vi** (Table 17). Similar analysis of the m/z 372 ions for M1 showed, in addition to the strong fragment ion at m/z 190 (70%, **i**), a fragment ion at m/z 165 (100%), i.e. 16 mass units higher than the RHPP$^+$ derived base peak fragment ion **iv**. Based on this analysis, we suggest the structure of M1 is a fluorophenyl hydroxylated derivative of RHPP$^+$. The reconstructed m/z 190 ion chromatogram observed in the HPTP experiment also showed peaks for M1 and M3. An additional peak was observed in this tracing which corresponded to M2 (t_R = 5.9 min). The CID spectrum of the ion at m/z 372 displayed fragment ions at m/z 190 (70%) and 165 (100%; **vii**) consistent with a regioisomer of M1.

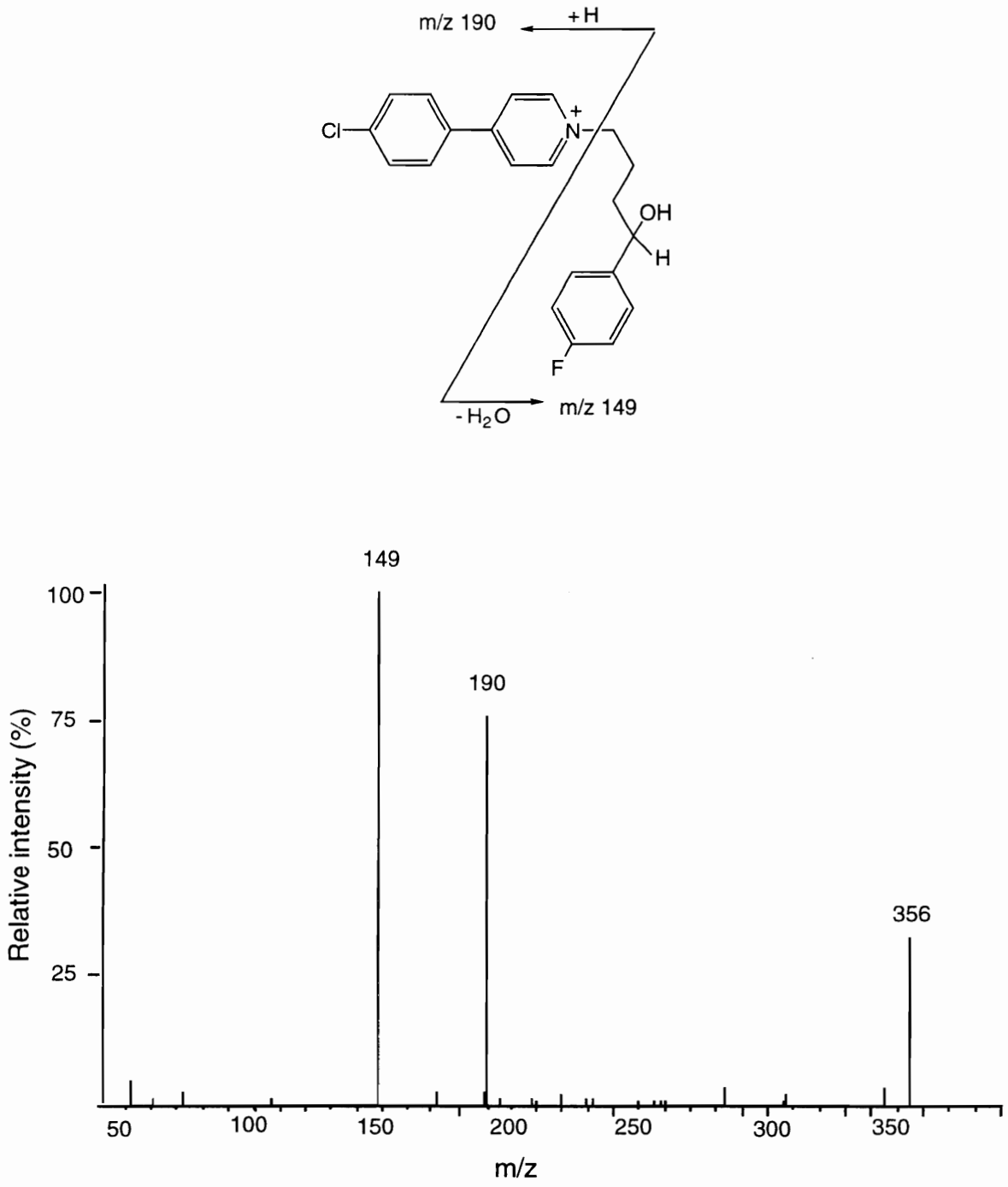

Figure 33 (b). HPLC/MS spectrometric analysis of urine of HP-treated mice. CID product ion spectrum of m/z 356 from the pyridinium metabolite M4.

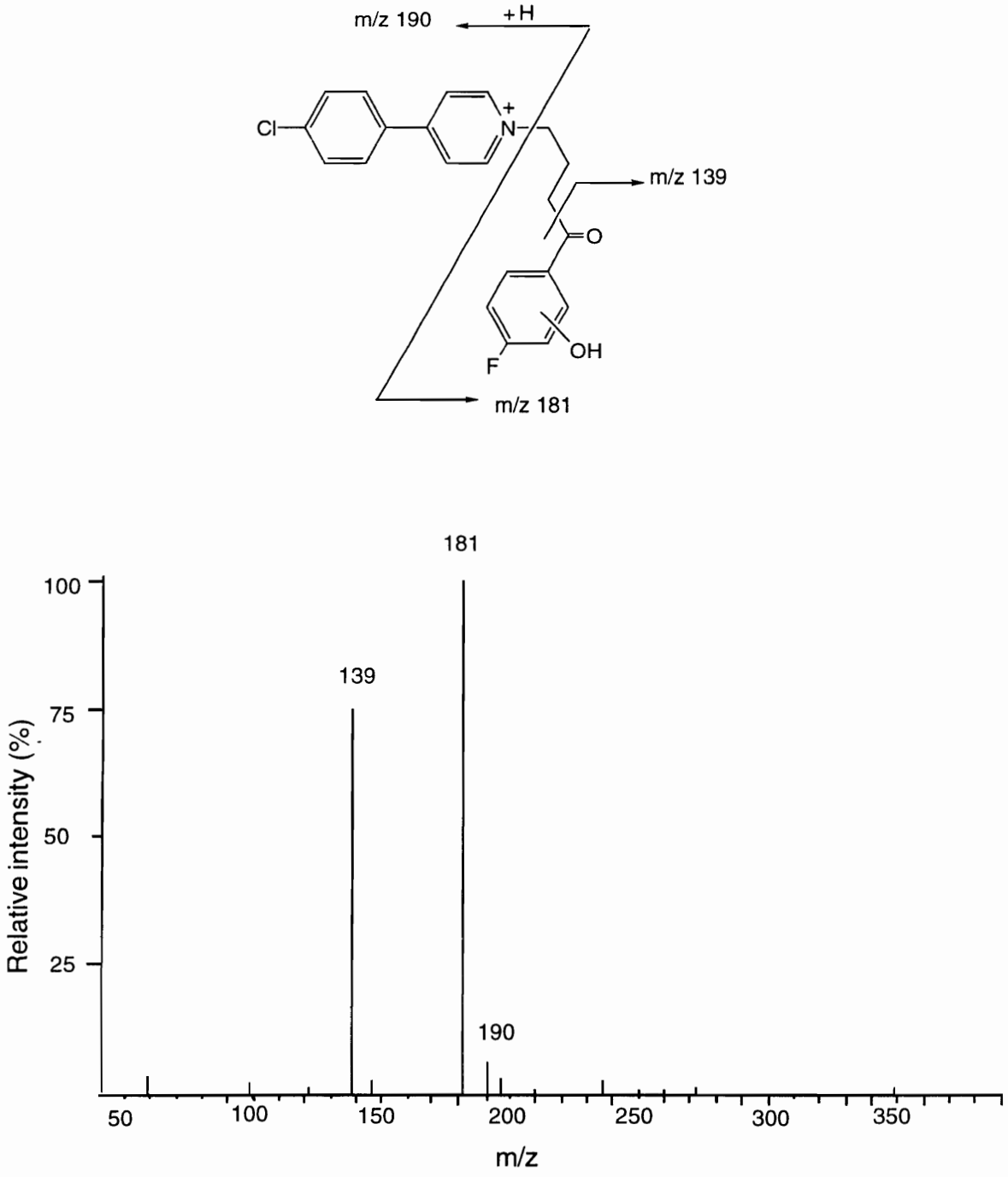

Figure 33 (c). HPLC/MS spectrometric analysis of urine of HP-treated mice. CID product ion spectrum of m/z 370 from the pyridinium metabolite M3.

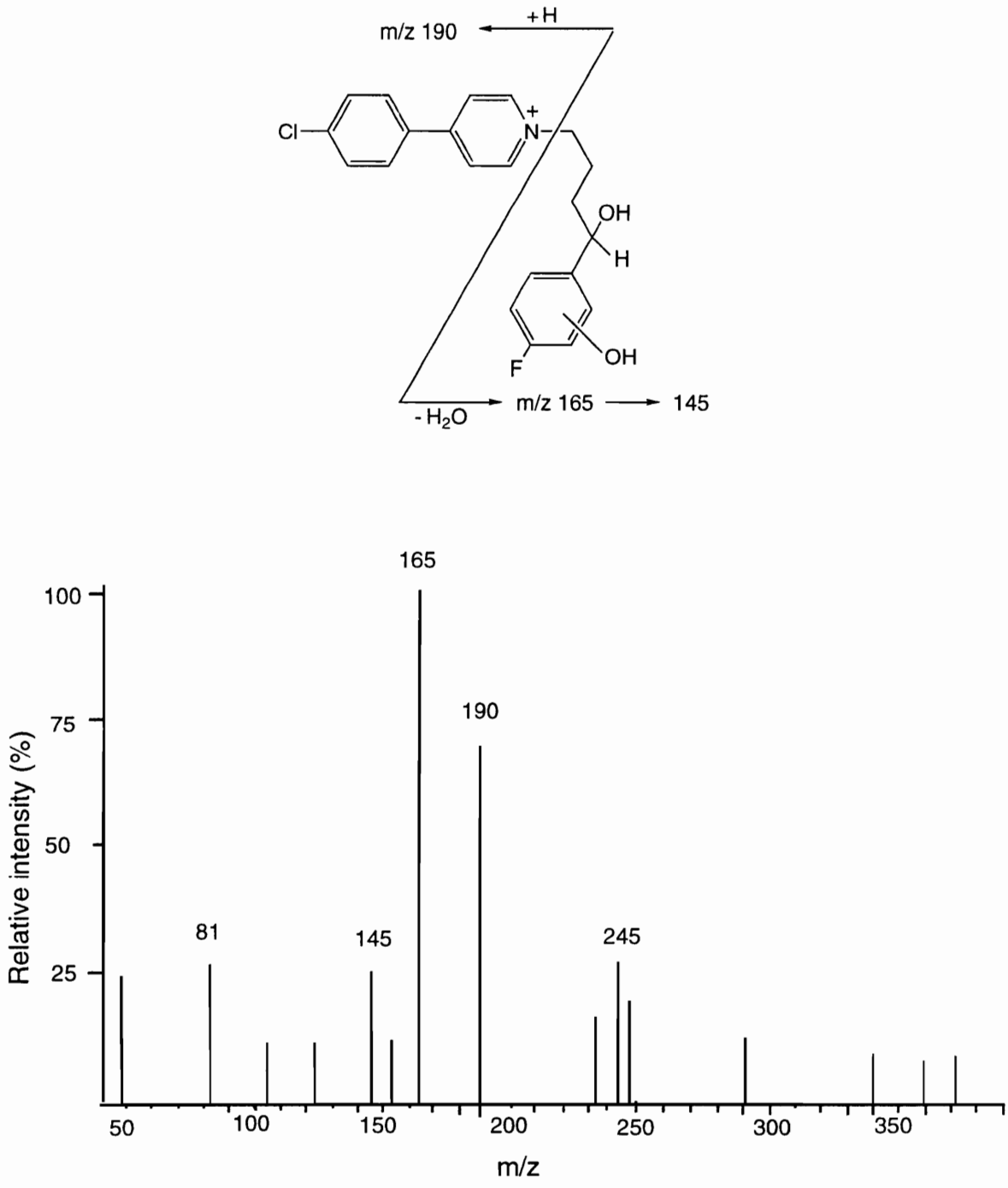

Figure 33 (d). HPLC/MS spectrometric analysis of urine of HP-treated mice. CID product ion spectrum of m/z 372 from the major pyridinium metabolite M1.

Although, as summarized in Chapter 4, we were able to obtain good quantitative estimates for the formation of pyridinium metabolites from HP and HPTP, similar studies with RHP are less useful because in the early stage of the development of the urine assay, we did not recognize the need for the pH adjustment of urine samples prior to Sep-pak extraction. Consequently, our data on the metabolism of RHP were not reliable.

The HP and HPTP (but not the RHP) studies were repeated with appropriate pH adjustment prior to the Sep-pak extraction step and we were able to establish an accurate quantitative assay for urinary metabolites. Even though no quantitative data were obtained for the RHP-treated mouse urine samples, it still is possible to compare the ratios of $HPP^+/RHPP^+$ in these samples. The ratios of $HPP^+/RHPP^+$ in the urine samples obtained from HP and HPTP-treated mice were approximately 60 and 12, respectively. When RHP was administered to the mouse, the urinary $HPP^+/RHPP^+$ ratio was found to be approximately 2 (Figure 34). The values differ from results obtained in the liver microsomal incubation studies for all three compounds. From HP and HPTP, more $RHPP^+$ was formed compared to that formed in liver microsomal incubations. This difference between in vitro and in vivo results may be due to the lack of ketone reductase in the liver microsomes as discussed in Chapter 5. For RHP, no detectable amount of HPP^+ was formed in the incubation mixtures but HPP^+ was formed in vivo. Possible pathways are (1) oxidation of RHP to HP and then HP to HPP^+ or (2) oxidation of RHP to $RHPP^+$ then $RHPP^+$ to HPP^+.

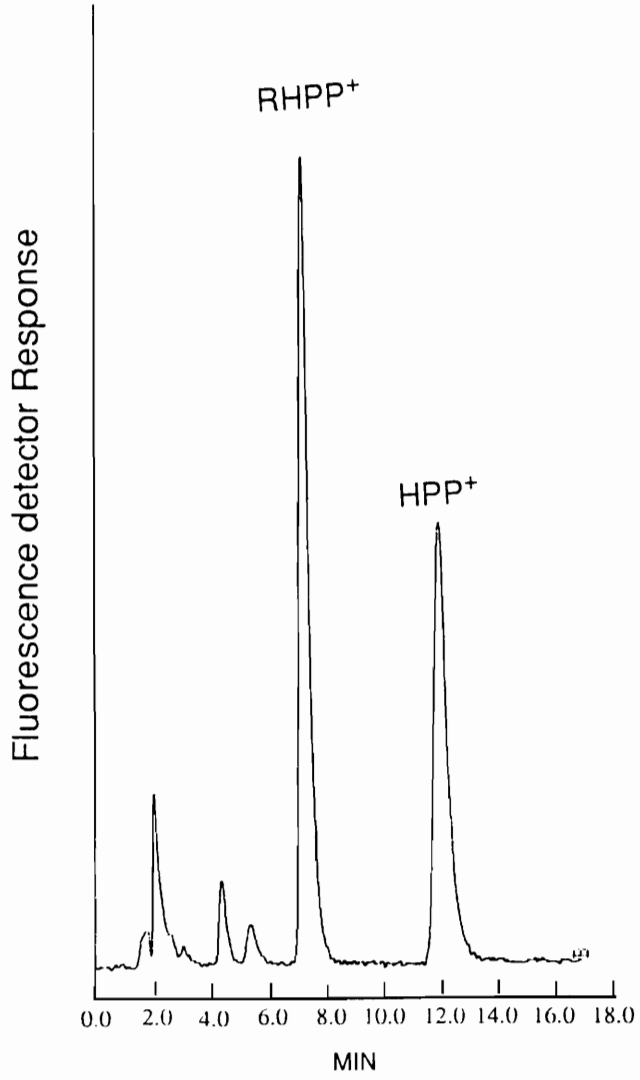

Figure 34. HPLC/fluorescence tracing of urine extract obtained from C57BL/6 mice treated with RHP.

We also have attempted to determine if any of these pyridinium metabolites may be present in brain tissues of HP or HPTP treated mice. The HPLC/fluorescence tracings of mouse brain homogenate extracts from HP treated mice were essentially identical to those from control mice. On the other

hand, all of the corresponding tracings of the HPTP treated mouse brain extracts showed peaks eluting at the retention times of HPP^+, $RHPP^+$, M1 and M2 (Figure 35). Quantitative estimations (see Chapter 4) indicate that the amount of HPP^+ in the brain of mice treated with HPTP is 231 $\pm$ 81 pmol/g tissue (n = 24). Although the brains of HP-treated mice also showed a small peak at the same retention time as synthetic HPP^+, control brain extracts also showed such a small peak at this region. Unlike the HPTP-treated animals, the brains of the HP-treated mice did not have any other peaks but HPP^+. The "HPP^+-type" peak in the control samples was less than the limit we set for unambiguous detection (LOD = 25 pmol/g, see Chapter 4). However, the levels of this peak in HP-treated brains also corresponded to 30 pmol HPP^+/g. On the other hand, HPTP-treated brains always showed significant amounts (200-400 pmol/g) and a characteristic profile of 4 pyridinium related peaks. Furthermore, the HPLC chromatographic pattern was observed in every analysis.

The relative peak heights of these metabolites in the brain are different from those seen in the chromatograms of the HPTP treated mouse urine extracts. This raises the possibility that these pyridinium metabolites may accumulate selectively in the brain or may be formed in the brain. The significance of these results is difficult to interpret. Furthermore, the absence of pyridinium metabolites in the HP-treated mice need not reflect the situation in humans. In any event, the source of potentially neurotoxic pyridinium metabolites in the brains of these animals need to be identified and the unusual profile illustrated in Figure 35 needs to be understood.

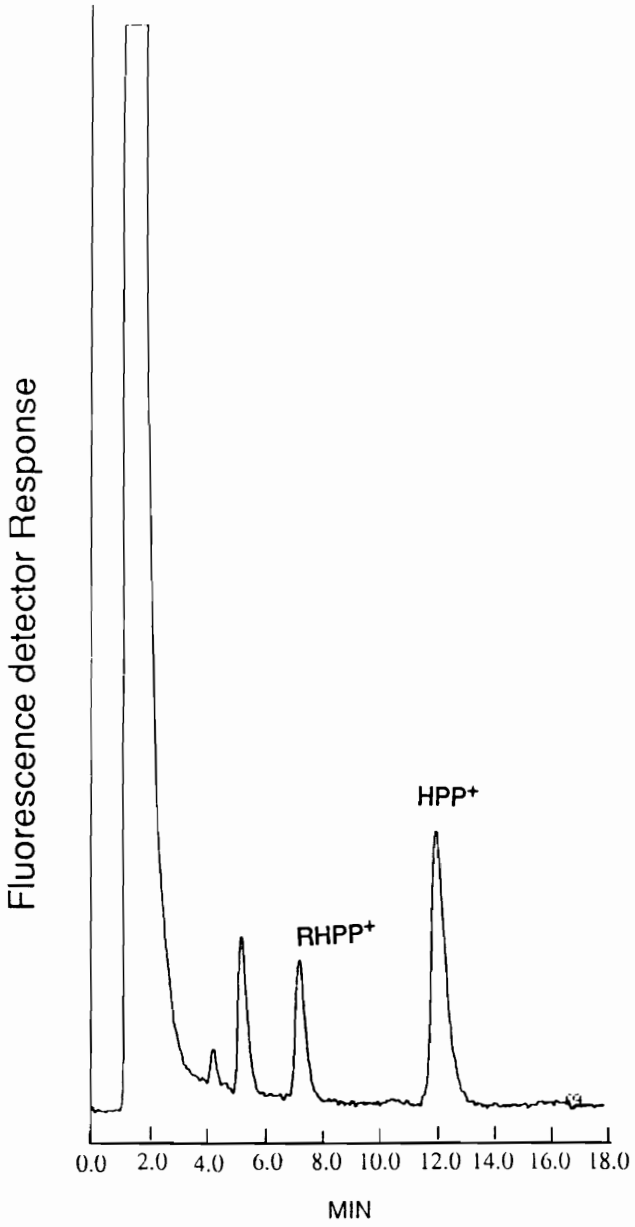

Figure 35. HPLC/fluorescence tracing obtained from HPTP-treated C57BL/6 *mice* brain extracts.

Another difference in the HP versus HPTP experiments is the dose of the compounds. Our regular protocol was to inject 50 mg/Kg of HPTP·HCl once a day (total dose 1500 μg, 3.81 μmol) while we used 10 mg/Kg x 3 of HP (total dose 900 μg, 2.36 μmol) to minimize the catalepsy caused by the drug. Consequently, the failure to detect HPP^+ in the brains of mice treated with HP may have been a consequence of the lower dose. Therefore, we decided to examine the brains of HPTP treated mice following the same dosage and protocol as used for HP. HPTP was administered intraperitoneally at a dose of 10 mg/Kg x 3 (once a day, 900 μg, 2.28 μmol). Then, 48 hours later the brains were analyzed. HPP^+ formation was very small in brain [32 ± 5 pmol/g (n = 3)], which is just above the detection limit (25 pmol/g). However, the HPLC chromatographic pattern (Figure 36) was essentially the same as that observed following a 50 mg/Kg HPTP dose (Figure 35, peak pattern not observed in the HP experiments). In this experiment, HPTP recovery also was studied using an HPLC/UV detector. HPTP was not observed in the urine samples, but was detected in the kidney, liver and brain. The total amount, however, less than 0.2% of the administered dose. Consequently, much is unclear with respect to the fate of HPTP in the mouse.

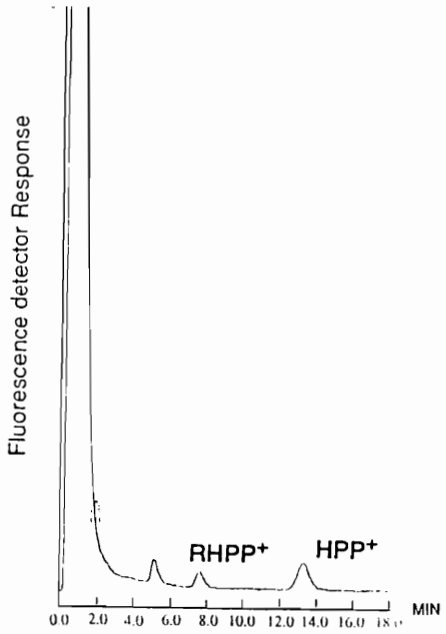

Figure 36. HPLC/fluorescence tracing of brain extract obtained from a C57BL/6 mouse treated with a 10 mg/Kg (x 3) dose of HPTP.

In summary, the results obtained here demonstrate that C57BL/6 mice metabolize HP and HPTP to HPP^+, $RHPP^+$ and what appear to be phenolic pyridinium species. Furthermore, HPLC/fluorescence analysis provides evidence for the presence of HPP^+, $RHPP^+$ and two phenolic pyridinium metabolites in the brain tissues of HPTP treated animals.

We next attempted to determine the source of these pyridinium species. Will the pyridinium metabolites be formed in the periphery and then partition into the central nervous system? Or, similar to MPP^+ formation (MPTP is oxidized to MPP^+ in the brain[165]), are HPP^+ and $RHPP^+$ formed in the brain after HPTP has partitioned into brain? In order to answer this question, the brains of two animals treated twice with HPP^+ (50 mg/Kg x 2, total dose 7.7 μmol) were examined 48 hours after the second injection to determine the

amount of HPP^+ in the brain. The HPLC/fluorescence tracings showed only HPP^+ and the average values of the 2 mice was 50 ± 35 pmol/g tissue. This value is much lower than that observed in the brains of mice examined 48 hours after a 50 mg/Kg i.p. dose of HPTP (243 ± 71 pmol/g). These results suggest that HPP^+ does not pass the blood brain barrier to any significant extent, which is not surprising since it is a quaternary pyridinium species. Therefore, it appears that HPP^+ is formed in the brain from HPTP.

The presence of these metabolites in the HPTP but not HP treated mouse brain homogenates might argue that the tetrahydropyridines are intermediates in the formation of the corresponding pyridinium metabolites, at least in the brain. Although more detailed information regarding the metabolic pathways leading to these compounds is required, these preliminary results suggest that oxidative aromatization of partially oxidized piperidine ring systems such as HP and HPTP may represent a more common metabolic route than previously recognized.

Quantitative estimates of urinary and fecal HPP^+ excretion and washout profile after HPP^+ administration. As described above, both HPP^+ and $RHPP^+$ are excreted in the urine of C57BL/6 mice after HP and HPTP administration. Quantitative estimates show that of the 30 mg/Kg (10 mg/Kg x 3) of HP or 50 mg/Kg (50 mg/Kg x 1) of HPTP administered i.p., only 1-3% can be accounted for in the 48 hour urine collection. HPLC/UV (245 nm) was used on-line together with HPLC/fluorescence to measure unchanged HP, HPTP and also to detect possible non-fluorescent products. As shown in Figure 37, HPLC/UV tracings of HP and HPTP-treated mouse urine extracts are complicated with big biological background peaks. In most cases, unchanged

HP and HPTP were not observed in the tracings and even when peaks were observed, the percent of these against the dose administered was less than 2% for the both compounds.

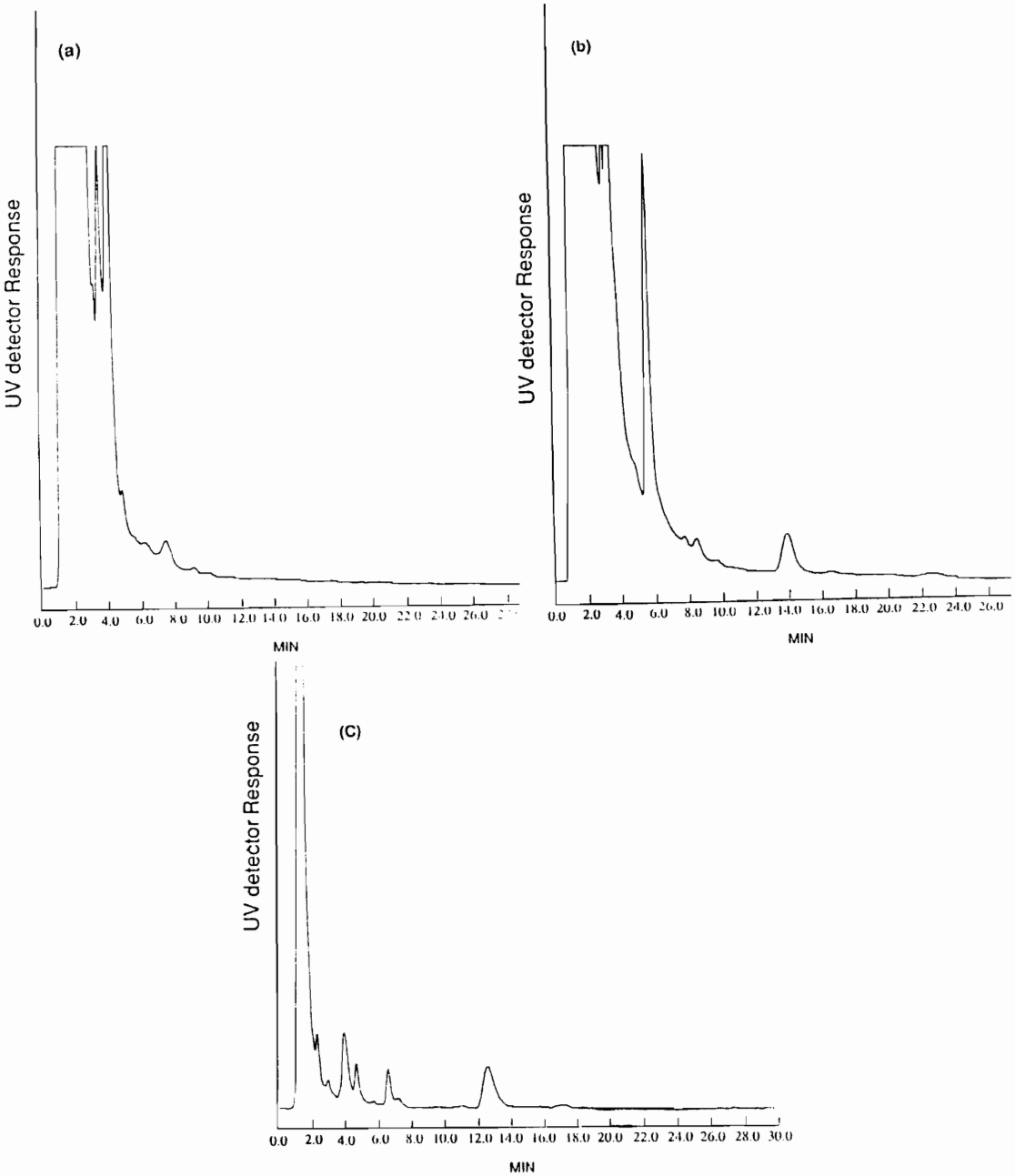

Figure 37. HPLC/UV tracings of urine extracts obtained from (a) vehicle, (b) HP and (c) HPTP-treated mice.

The results were the same when several urine samples were analyzed without the Sep-pak extraction step in order to confirm that none of material in the samples was lost by the extraction. If HPP^+ is about 3% of the drug administered and 2% remains as unchanged drug, the fate of 95% of the parent drug is missing. As summarized in Chapter 3, it has been reported that N-dealkylation, reduction and O-conjugation are the major in vivo metabolic pathways of HP in rodents and humans. Those reports show that unchanged HP is only 1% of the dose in the 24-hour urine collections of patients.[95] The metabolic conversion of HP to PA (**44**), an acidic metabolite generated via oxidative N-dealkylation, has been reported to represent 34% of the dose in the 24-hour urine of rats treated with [^{14}C]HP free base intramuscularly.[96] The recovery of radioactivity in the 24-hour urine was 44% of the dose, therefore, 77% of the radioactivity in the 24-hour urine should be found in this metabolite. The authors observed HP-O-Glu in the 24-hour bile but not in the urine. This is reported to represent 26% of the dose. When [^{14}C]HP decanoate was administered intramuscularly, the % conversion of HP to PA decreased to 7% (observed in the 42-hour urine) and slow excretion (42 days to excrete 90% of the dose in urine and bile) was observed.[97] Even though 90% of the radioactivity was excreted into urine and feces, over 90% of the radioactivity was unaccounted for. Also with [^{3}H]HP, when administered subcutaneously, PA was identified as a major urinary metabolite (60-70% of the urinary metabolites).[98] In that study, the recovery of radioactivity in urine was 23% in 24 hours (28% in 4 days). Therefore, the % conversion of HP to PA is about 13% in the 24 hour urine. Except for the administration of [^{14}C]HP decanoate, the major portion of radioactive material appeared to be excreted in urine or bile

within 24 hours after the administration. These reports document PA to be a major metabolite of HP. Since the analysis depended on the radioactivity of ^{14}C on the carbonyl carbon or ^{3}H in the fluorophenyl ring, no data were available to account for the other half of the molecule containing piperidine moiety. This analysis suggests that in all experiment conducted to date, the fate of the majority of HP administered to humans and rodents remains unaccounted.

In our in vitro and in vivo studies, we attempted to assess the N-dealkylation pathway of HP and HPTP. We observed CPTP (**51**), the N-dealkylation product of HPTP, in C57BL/6 mice liver microsomal incubation mixtures (see Chapter 5). However, we were not able to identify other products. Compound **41** (from HP) is non-fluorescent and UV absorbing only at very low wavelength. Therefore it would not be detected in our HPLC assays. The 3-*p*-fluorobenzoylpropionic acid (**43**) product is a precursor of PA (**44**). This is also a reported N-dealkylation product of HP[132] and is commercially available. The retention time of standard **43** was 2.5 minutes on our HPLC system. Thus, even if **43** were present in the incubation samples, the peak would overlap with early eluting biological background peaks. Therefore, we attempted to modify the mobile phase to obtain better elution characteristics for this compound. By lowering the pH of the mobile phase from 6.2 to 4.5, the retention time was changed to 8.0 minutes. The mouse liver microsomal incubation mixture with HPTP as substrate was analyzed with this mobile phase and a small peak was observed at 8.0 minutes. However, this peak was very small and does not represent a significant in vitro metabolite. For the confirmation of **43** and **44**, urine samples should be analyzed with a modified mobile phase, however,

HPLC/UV tracings of urine extracts obtained from C57BL/6 mice (Figure 37) showed an even higher early eluting background peak than in the in vitro studies and therefore, more extensive assay development will be needed.

Conjugation pathways also have been reported as major metabolic routes of HP. It has been documented that after an oral dose of 1 mg/Kg, the % conversion of HP to HP-O-Glu (**46**) was 18% in the 24-hour urine of human volunteers.[114] As just mentioned, HP-O-Glu was measured in the rat 24-hour bile after [^{14}C]HP was administered intramuscularly and 26% conversion was observed.[96] The authors obtained this number by measuring the change in the amount of HP in urine and bile before and after the incubation with β-glucuronidase. They did not observe conjugates in the urine sample. However, others have reported that de-glucuronidation by β-glucuronidase fails in this case due to its steric hindrance.[95,114]

We attempted to see if there is any difference in the HPLC/UV tracing obtained from HP-treated mouse feces (bile sample was not available) before and after the incubation with β-glucuronidase following the reported conditions.[96] The fecal extract was obtained as described in Chapter 4 and was incubated with β-glucuronidase for 17 hours. HPLC/UV tracings before and after the incubation did not show any difference. This experiment was conducted just once and should be noted as a preliminary result.

The last major metabolic pathway reported for HP is the formation of RHP via reduction by ketone reductase.[101] Even though it is known that RHP is oxidized back to HP, from the study of RHP blood levels in humans, it was found that about 23% of the biotransformation of HP involves this reduction pathway.[107] The authors focused on the quantitative analysis for RHP and no

information regarding the mass balance of metabolism was reported. Overall, it appears that each literature focuses on one specific metabolic pathway and that systematic studies on the mass balance of HP has not been conducted.

Our interest is to estimate the importance of oxidative pathways, i.e., HPP^+ and $RHPP^+$ formation from HP and HPTP. However, since we were not able to account for about 95% of the metabolic fate of HP and HPTP, it was difficult to interpret the meaning of the 1-4% conversion to pyridinium metabolites. As discussed above, the available literature focused only on specific metabolites. For example, when RHP was reported to be 23% of the metabolism of HP, remaining 77% was not considered. That is the same for the other studies, 60-70% of the administered HP is never accounted for. Consequently, the 4% conversion to pyridinium metabolites might be more significant than it appears to be.

The missing 95% might be due in part to the behavior of HPP^+ and $RHPP^+$. It has been documented that following a single infusion of MPTP or MPP^+ to sheep, only MPP^+ was detected in serum. MPP^+ had a very long half life in this animal.[165] The approximate half life of MPP^+ following the administration of 1 mg/Kg of MPP^+ is about six days. The half life of MPP^+ following the administration of 3 mg/Kg was considerably longer. After 11 days its concentration was still over half of the peak concentration observed after two days. The quick disappearance of MPTP and the presence of MPP^+ in the serum already at the first time point (30 minutes after the infusion) were observed. This demonstrated that this extraordinarily long half life was not due to the slow production of MPP^+ from MPTP. Generally, one anticipates that positively charged compounds, such as the quaternary pyridinium species

MPP^+, would be cleared readily by the kidneys. The authors suggested that factors such as protein binding or an active reuptake system in the kidneys could be considered as explanations of the long half life.

Since no information was available on the biodisposition of HPP^+ and $RHPP^+$ (i.e. the possibility of being further metabolized or excreted in urine or feces very slowly, etc.), we decided to examine the in vivo metabolic fate of HPP^+ in mice. In order to document the excretion profile of HPP^+, urine samples were collected 24 hour to 7 days after 50 mg/Kg (i.p., 1500 μg, 3.85 μmol) of $HPP^+ \cdot Cl^-$ administration. However, due to animal regulations (we are not allowed to keep mice in metabolic cages over 72 hours), urine data were obtained at 24 hours, 48 hours, and 6 days and 7 days only. HPLC/UV also was used on-line with HPLC/fluorescence to see if there was any UV active but non-fluorescent products.

From the results of the HPP^+ washout study over a period of 7 days (Table 18, Figure 38), the total % of HPP^+ recovered from urine and feces were only about 15% and 5%, respectively. It appears that HPP^+ excretion into urine was maximal during the first 24 hours and decreased gradually. HPP^+ excretion into feces was about the same in the first 24 hours and second 24 hours (24-48 hours). However, after 6 days, HPP^+ was no longer detectable.

TABLE 18

HPP^+ excretion (nmoles) and % recovery of the dose after HPP^+ (3.85 μmoles) i.p. administration at 24 hours, 48 hours, 6 days and 7 days in urine and feces samples.

	Urine		Feces	
	HPP^+ (nmoles)	% recovery	HPP^+ (nmoles)	% recovery
24 hours	377 ± 62	9.8 ± 1.5	82 ± 87	2.1 ± 2.2
48 hours	130 ± 18	3.4 ± 0.5	91 ± 94	2.1 ± 1.1
6 days	0.7 ± 0.6	0.02 ± 0.03	ND*	-
7 days	1.0 ± 1.0	0.03 ± 0.03	ND	-

*ND: Not Detected. Samples were collected over 24 hours at each time point. All values were the mean ± S.D. of three animals.

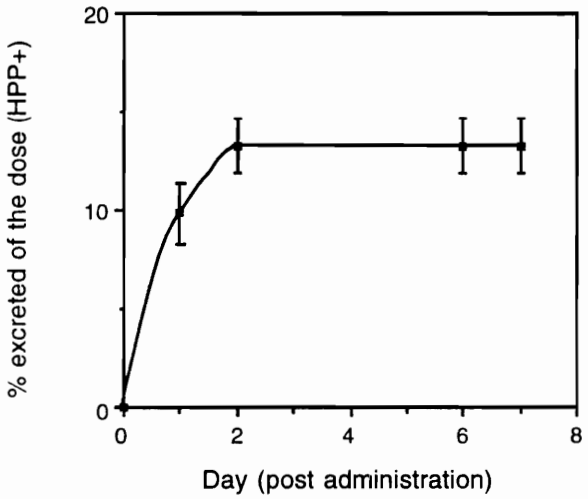

Figure 38. HPP^+ excretion profile in urine over 7 day period after HPP^+ (50 mg/Kg, 3.85 μmoles) administration.

The values from the 6 day and 7 day urine samples appear to be very small and, as shown in Figure 38, after 2-3 days of administration, excretion appears to have reached a plateau. However, control (untreated) mouse urine showed no HPLC/fluorescence peak. Therefore, these values are significantly different from zero, suggesting that small amounts of HPP^+ are still being excreted. It was not clear why HPP^+ excretion plateaud after only 20% (15% in urine and 5% in feces) had been excreted from the body. HPLC/fluorescence and HPLC/UV tracings obtained from urine treated with HPP^+ are shown in Figure 39 (a) and (b), respectively.

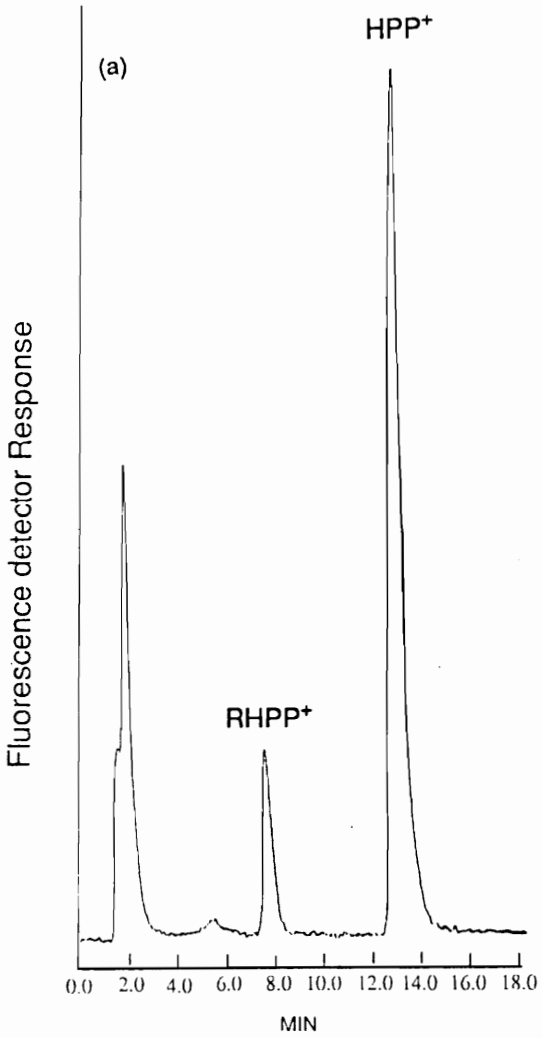

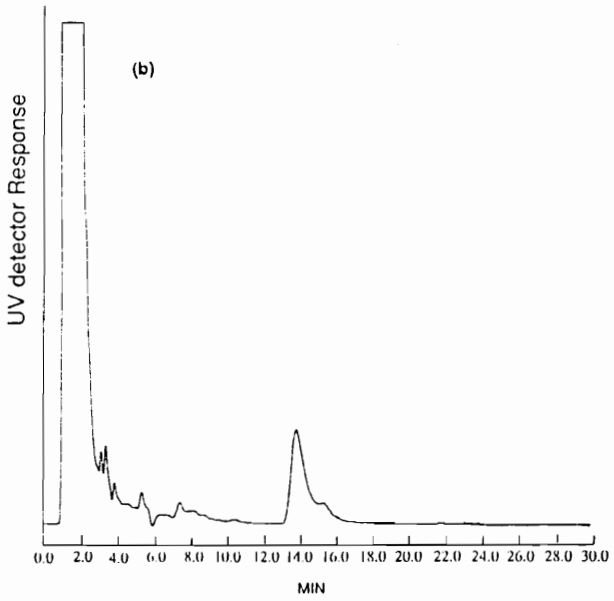

Figure 39. HPLC tracings of urine extracts obtained from a C57BL/6 mouse treated with HPP^+ (a) fluorescence and (b) UV tracings.

$RHPP^+$ was observed in the HPLC/fluorescence tracings obtained from both urine (Figure 39a) and feces extracts (not shown) after the HPP^+ administration. Even though $RHPP^+$ was observed, the amount was only 5% of that of HPP^+. In the case of HPP^+ incubations with mouse liver microsomes, only HPP^+ was observed. This difference in in vivo versus in vitro results may be attributed to the lack of ketone reductase in microsomes. This applies to both HP and HPTP. $RHPP^+$ was formed more from HPTP than HP in vitro and especially in vivo. We observed only a small peak at the retention time corresponding to RHPTP in urine extracts of mice treated with HPTP. This value was lower than the detection limit for RHPTP (12 pmol on column) and therefore we are not able to confirm the in vivo formation of RHPTP from HPTP in the mouse.

Other than the 5% reduction to $RHPP^+$, no peak other than HPP^+ was observed in the HPLC/fluorescence tracings of the urine extracts from mice treated with HPP^+. Also, we did not observe any other major metabolites in the HPLC/UV tracings. In the urine analysis, samples were diluted in the mobile phase (up to 1 in 1200) to give concentrations of analytes that would produce peak heights within the recording range of the integrator following injection of a 50 μL-aliquot. Since the UV detector is not as sensitive as the fluorescence detector, a very concentrated sample was injected (1 in 5 dilution) to check for the possibility of other metabolites. One peak which might be 4-(4-chlorophenyl)pyridine (CPP, **53**), a possible N-dealkylated product of HPP^+, was observed in the UV tracing. This compound, with t_R = 15.4 minutes, coelutes with synthetic CPP. When estimated as CPP, the % conversion from HPP^+ was less than 0.3%.

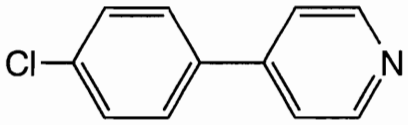

53

These results suggest that HPP^+ is stable in vivo and thus once HPP^+ (and most likely $RHPP^+$, too) is formed from HP and HPTP, no further metabolism occurs. However, since only 20% of the administered HPP^+ was excreted in the urine and feces, the need to account for the remaining 80% must still be addressed. One possibility might be the accumulation of HPP^+ in tissue deposits. Consequently, the in vivo metabolic fate of HPP^+ in the mouse was examined following serial injections.

In the previous experiment, we could not account for 80% of HPP^+ in the mouse. We thought that it should be possible to displace the HPP^+ in the mouse by injecting a second dose of HPP^+ following the first excretion period. Therefore, HPP^+ 50 mg/Kg was administered on day 1 and urine, and feces were collected for 24 and 48 hours and then at 6 days the second 50 mg/Kg dose of HPP^+ was administered and the urine and feces were collected at 24 and 48 hours.

Surprisingly, the amount of HPP^+ excreted was lower in days 6 and 7 than days 1 and 2 (Table 19). One explanation could be that the first HPP^+ administered accumulates in a deep body pool that does not equilibrate readily. Also urine output may be compromised in the drug treated animals. Typically, we obtain 1-3 mL urine from control mice. As shown in Table 19, urine volumes appear to be low, especially over the 24 hour period after the second injection. Maybe the HPP^+ causes the kidneys to shut down. The results from both the previous and this experiment indicated that HPP^+ accumulates in the body. Therefore we examined tissues that might have retained HPP^+.

TABLE 19

Summary table of HPP+ (50 mg/Kg x 2, i.p.) wash out study.

		Mouse #1		Mouse #2	
		urine	feces	urine	feces
Control[a]	volume	1400 µL	0.23 g	2350 µL	0.75
	HPP+ (nmoles)[b]	0	0	0	0
	% of dose	0	0	0	0
first i.p. 24h	volume	600 µL	0	1450 µL	0.08 g
	nmoles	413	0	161	5.2
	% of dose	10.7	N/A[c]	4.2	0.1
48h	volume	1100 µL	0.16 g	3500 µL	0.65 g
	nmoles	70.4	130	151	12.4
	% of dose	1.8	3.4	3.9	0.3
second i.p. 24h	volume	600 µL	0.22 g	50 µL	0.01 g
	nmoles	51	22.7	45.3	N.D.[d]
	% of dose	1.3	0.6	1.2	N.D.
48h	volume	1500 µL	0.73 g	1800 µL	0
	nmoles	97.5	182	106	0
	% of dose	2.5	4.7	2.8	N/A

[a]: Control, Mice were housed in metabolic cages 24 hours prior to the HPP+ administration and urine feces were collected as control samples. [b]: The amount of HPP+ in the sample (nmoles). [c]: N/A, Not available. [d]: N.D., Not detected.

The very poor recovery of HPP^+ in the urine and feces prompted additional mass balance studies. $HPP^+ \cdot Cl^-$ (50 mg/Kg, 3.85 μmol) was administered i.p. once and 48 hours later the brains, kidneys, livers, and abdominal tissues (the area into which HPP^+ had been injected) were dissected and analyzed. The amounts of HPP^+ in the brains were less than the detection limit while the kidneys and liver accounted for 4058 ± 4171 pmol/g and 2957 ± 1759 pmol/g (average of 3 mice), respectively. HPP^+ was not detected in the abdominal tissue. These amounts correspond to 0.07% (kidney) and 0.1% (liver) of the dose. Combining with results from previous experiments, all data suggest that we can account for only about 20% of a 50 mg/Kg dose of HPP^+ when given i.p. No evidence for further metabolism or accumulation could be obtained. Supporting the results of a previous experiment, the fact that HPP^+ was not observed in the brain after HPP^+ was administered peripherally, suggests that HPP^+ does not penetrate the blood brain barrier to any significant extent. Since we clearly observe pyridinium metabolites in the brains of HPTP -treated mice, we conclude that these metabolites are formed by brain enzymes

Previously, all drug administrations were by the i.p. route. Since 80% of the administered HPP^+ could not be accounted for, we attempted a similar mass balance study following i.v. dosing. $HPP^+ \cdot Cl^-$ (50 mg/Kg, 3.85 μmol) was administered i.v. via the mouse tail vein (n = 3) by Mr. Dave Gemmel of the Animal Care Facility and samples were collected as before. The total HPP^+ excreted into urine following two days was 308 ± 87 nmoles. This is 8.1 ± 3.2 % of the dose. The brain level was once again less than the detection limit. These results confirmed that HPP^+ does not penetrate the blood brain barrier. The low

recovery of HPP^+ after i.v. administration in this experiments is consistent with the results from the i.p. studies.

Inhibition studies. Previously, we examined the in vitro metabolic fate of HP and HPTP using MAOs, human and mouse liver microsomal preparations, and mouse brain homogenates (see Chapter 5). From these results, it was found that HPTP but not HP, was a MAO-A substrate, although a poor one. HP and HPTP were both metabolized to HPP^+ in the human liver microsomal incubations at comparable rates and we demonstrated that these oxidations were catalyzed by P450. Specifically CYP3A is the major contributor for these reactions.[166] It has been reported that CYP3A is also the major form of P450 catalyzing the oxidation of HP to HPP^+ in the rat liver microsomal preparations.[152] In the mouse brain, we have observed enzymatic oxidation of HP and HPTP to HPP^+. However, the rate of HPP^+ formation was about 10 times faster from HPTP than HP. HPP^+ formation from HP appeared to be caused by a mixture of P450 and MAO-A. HPP^+ formation from HPTP was not NADPH-dependent and our attempt to characterize the enzyme systems catalyzing HPP^+ formation in the mouse brain has not been successful.

Consequently, an important question concerns the enzyme system(s) that are responsible for the conversions of HP and HPTP to HPP^+ and $RHPP^+$, both in terms of peripheral and brain metabolism. With all of the available information from the in vitro studies, we have designed in vivo inhibition and induction studies. Although the in vivo studies primarily address peripheral metabolism, we also analyzed brains to see if there is any change in the formation of the pyridinium metabolites in the brain. We started with the inhibition study with clorgyline, a selective MAO-A inactivator.

As mentioned above, previous in vitro studies with MAO-A purified from human placenta documented that the conversion of HPTP, but not HP, to HPP^+ (K_M = 25 μM, k_{cat} = 0.45 min^{-1}, k_{cat}/K_M = 18 $mM^{-1}min^{-1}$). HPP^+ formation was completely blocked by 9 μM clorgyline, an established and selective inactivator of MAO-A. Therefore, we have examined the effects of clorgyline on the in vivo metabolism of HPTP in C57BL/6 mice. The animals were pretreated with 2.5 mg/Kg of clorgyline 24 hours prior to receiving 50 mg/Kg of HPTP (both i.p.). After two days, the total amount of HPP^+ excreted in urine was 101 ± 66 nmoles (2.7 ± 1.8% of the dose). The brain level was 166 ± 48 pmols/g (n = 3). If one takes the average of the control values (50 mg/Kg i.p. HPTP only), the amounts of HPP^+ excreted in urine were 2.3 ± 0.3% of the dose and 231 ± 81 pmols/g in the brain (n = 24). Thus, clorgyline did not effect the urinary excretion of HPP^+ formed from HPTP but did appear to reduce brain levels of HPP^+ somewhat.

Since it has been demonstrated that CYP3A is the major catalyst for HPP^+ formation from HP and HPTP in human liver microsomal preparations,[165] we have examined the effect of ketoconazole, a selective inhibitor of CYP3A,[153] on HPP^+ formation in mice. Pretreatment with 20 mg/Kg of ketoconazole was 24 hours prior to the 50 mg/Kg dose of HPTP. Unfortunately, no urine was obtained. The dose used was well tolerated in animal not treated with HPTP. Therefore it is likely that the poor condition of these animals was due to the combination of a high dose of ketoconazole and HPTP. In fact, this dose of ketoconazole appeared to make the animals quite sick. We did, however, analyze the brain. HPP^+ formation was 270 ± 55 pmol/g in brain (average of 3 mice). Comparing this value with the control value of 247 ± 120 pmol/g, we concluded that ketoconazole did not inhibit the in vivo brain conversion of HPTP

to HPP^+ in C57BL/6 mice. Clearly, additional studies will have to be performed before any conclusion can be reached with respect to inhibition of CYP3A and HPTP metabolism.

Induction studies. As described above, we were not able to obtain any evidence to support the involvement of these enzymes in the systemic metabolism of HPTP to form HPP^+. One problem is the lack of a well established in vivo inhibition protocol for CYP3A. Therefore, we attempted to explore a different approach for the characterization of these enzyme systems by examining the effects of inducers on HPTP metabolism, compounds such as dexamethasone (DEX), a synthetic glucocorticosteroid reported to induce CYP3A activity in vivo.[167,168] DEX induces transcriptional activation of CYP3A genes in vivo in rodents. This effect results in increased accumulation of the specific mRNA levels. DEX (one i.p. 100 mg/Kg dose) treatment increases the level of CYP3A mRNA in male C57BL/6 mice by 15-fold.[167] Since the optimized protocol for the CYP3A in vivo induction was described clearly, we decided to attempt an induction study with DEX treatment prior to the HPTP administration.

Following the protocol of Corcos,[167] DEX (83 mg/Kg, i.p.) was administered once 24 hours prior to a 50 mg/Kg dose of HPTP. Brains (n = 3) were dissected 24 hour post HPTP administration. The control group was treated with vehicle instead of DEX prior to HPTP. The amount of HPP^+ in the brain of control group (n = 3) and DEX-treated group (n = 3) were 267 ± 159 pmol/g, 216 ± 32 pmol/g, respectively. Thus, no induction was observed. However, one might not expect to see brain induction. The most significant induction effect would be observed in the urine. Unfortunately, metabolic cages

were not available and therefore, only brain tissues were analyzed. The induction studies need to be repeated on the effects of DEX on HPTP metabolism including urine collection before reaching any conclusions.

It has been suggested that HP induces cytochrome P450 in rat brain (Dr. M. Warner, personal communication). Although a well established protocol was not available, we attempted to examine the effects of HP on HPP^+ formation from HPTP in C57BL/6 mouse brain. HP (10 mg/Kg) was administered once a day for 2 days followed by 5 mg/Kg on the third day. Then, 24 hours later, HPTP (50 mg/Kg) was administered and brains were dissected 24 hour post HPTP administration. The control group was treated with vehicle instead of HP. The amount of HPP^+ in the brain of the control group (n = 3) and HP-pretreated group (n = 3) were 364 ± 121 pmol/g, 381 ± 71 pmol/g, respectively. No difference was observed between the control and HP treated groups.

The experiments described in this section failed to provide any insight into the enzyme systems that are responsible for the formation of HPP^+ and $RHPP^+$ from HP and HPTP. Neither inducers nor inhibitors had any significant effect on the parameters we examined and we are not able to reach any definite conclusion. Especially, since urine samples were not collected (or, in some cases, no urine was produced), some experiments need to be repeated. Also, HPTP recovery from urine samples was always very low (at most 2%). The major part of the fate of HPTP remains unclear. It has been reported that when [^{14}C] HP decanoate is administered i.m. and i.v. to rats, neither HP nor HP-decanoate was detected in the urine.[97] Also in humans, unchanged HP in urine was found to be only about 1% of the dose.[95] Our results are consistent with these reports. Miyazaki et al. have documented that after 5 mg/Kg i.m.

[^{14}C] HP free base treatment in rats that unchanged HP was detected in several tissues, especially in lung, liver, kidneys, and brain.[96] However, unchanged HP in the lung, which showed the highest concentration, was only about 2% of the dose one hour after the administration, and decreased to 0.25% at 6 hours. They reported that the major urinary metabolite was PA, however, the amount of PA was 15% of the dose in 24 hours urine. It appears that nobody has solved the mass balance problem.

The brain related data are summarized in Table 20. In these 9 experiments, the limit of detection was 25 pmol/g. As described above, the amount of HPP^+ in the brain after HPTP administration does not change significantly following treatment with the various inducers and inhibitors we examined. Only clorgyline may inhibit brain metabolism. The reproducible HPLC/fluorescence pattern observed in the tracings obtained from HPTP-treated brain extracts demonstrated that the pyridinium species are actually formed from HPTP and most likely are formed in the brain.

TABLE 20

Summary table of HPP^+ formation in C57BL/6 mice brain after HP (10 mg/Kg x 3, 2.39 μmol), HPTP (50 mg/Kg x 1, 3.81 μmol) treatment.

Experiment	pretreatment	Substrate	HPP^+ (pmol/g)
1	none	vehicle	ND[a] (n = 4)[b]
	none	HP	ND (n = 3)
	none	HPTP	221 ± 17 (4)
2	none	HP	ND (3)
	none	HPTP	185 ± 13 (5)
3	none	vehicle	ND (6)
	none	HPTP	247 ± 120 (6)
4	none	vehicle	ND (2)
	none	HP	ND (3)
	none	HPTP	121 ± 59 (3)
5	clorgyline	HPTP	166 ± 48 (3)
6	ketoconazole	HPTP	270 ± 55 (3)
7	none	HPTP 10 mg/Kg x 3	32 ± 5 (3)
8	none	HPTP	267 ± 159 (3)
	DEX	HPTP	216 ± 32 (3)
9	none	HPTP	364 ± 121 (3)
	HP	HPTP	381 ± 71 (2)

[a]: below the detection limit (25 pmol/g tissue). b: number of animals.

Compared to the results with the 50 mg/Kg dose, after 10 mg HPTP/Kg x 3, the amount of HPP^+ in brain was borderline background. However, as shown earlier in Figure 36, the typical pyridinium peak pattern was observed in the HPLC/fluorescence tracings as well. Whether these low levels of HPP^+ can have any relevance to the human situation is difficult to address. Recently, it has been reported that HPP^+ is present in the substantia nigra of the brain obtained from a schizophrenic patient who died during continuous administration of HP (i.m., 15 mg/day for 7 days). The level detected was about 10 ng/g wet tissue.[137] This is about 30 pmol/g of HPP^+. Because of its neurotoxic properties (see Chapter 3), the chronic presence of HPP^+ in the human brain still may be significant, despite the low levels.

Experimental

Chemicals. HP, Tween 80, Dexamethasone (Sigma Chemical Co., St. Louis, Mo), trioctanoin (Pfaltz & Bauer Inc., Waterbury, CT) were obtained from commercial sources. Ketoconazole was a gift from Dr. A. Parkinson. The HCl salts of HP,[134] HPTP,[124] HPP^+[121] and $RHPP^+$[148] were prepared as described previously.

Animal studies.

Urine and brain analysis after HP, HPTP administrations. HP (10 mg/Kg x 3) and HPTP (50 mg/Kg x 1) were administered intraperitoneally in 0.2 mL of sterile 0.9 % sodium chloride solution containing 20 % Tween 80 to groups of 12 retired breeder male C57BL/6 mice (Harlan-Sprague Dawley, Dublin, VA) weighing approximately 30 g each. A control group of 12 vehicle-treated mice was included in the study. For urine and feces collections, animals were housed in individual metabolic cages designed to separate urine and

feces. Food and drinking water were supplied *ad libitum*. Urine samples were collected during the 48 hour period following the injection of drug or vehicle. For the LC/MS/MS analyses, urine collections from three HP or HPTP treated mice were pooled. At the termination of the urine collections, mice were sacrificed by cervical dislocation and the whole brains were isolated and weighed. The samples were stored at -70 °C prior to analysis.

HPP+ administrations. $HPP^+ \cdot Cl^-$ (50 mg/Kg) was administered intraperitoneally in 0.2 mL of sterile 0.9% sodium chloride solution containing 20% Tween 80 to 3 retired breeder male C57BL/6 mice. Samples collection and animal handling were same as described above. Mice were housed the day before the HPP^+ administration and urine and feces samples were collected over 24 hour period as control samples. After the HPP^+ injection, urine and feces samples were collected 0 to 24 and 24 to 48 hours period. After three days break, mice were housed in the metabolic cages again to collect 6 and 7 days samples. Samples were stored at -70 °C prior to HPLC analysis. For the second experiment, $HPP^+ \cdot HCl$ (50 mg/Kg, i.p.) was administered to C57BL/6 mice (n = 3) and urine and feces were collected over a 48 hour period. Prior to the injection, control samples were collected. After six days from the first injection, the second $HPP^+ \cdot HCl$ (50 mg/Kg) was administered. Urine and feces samples were collected over a 48 hours period. For the tissue analysis, two sets of experiments were performed. For the first set, $HPP^+ \cdot HCl$ (50 mg/Kg) was administered to C57BL/6 mice (n = 3) and 48 hours later, brains, kidneys, livers were dissected. Samples were stored at -70 °C prior to HPLC analysis. For the second set, two mice were treated with $HPP^+ \cdot HCl$ (50 mg/Kg) and 48 hour later, brains and abdominal fat tissues were dissected.

HPP^+ administration (i.v.) experiment. HPP^+·HCl (50 mg/Kg) was administered the tail vein of C57BL/6 (n = 3) and urine and feces samples were collected over 48 hours. Brains were dissected and samples were analyzed by HPLC/fluorescence and HPLC/UV.

Tissue analysis after HPTP administration. HPTP·HCl (10 mg/Kg x 3) was administered to mice (n = 3) and 48 hours later brains, kidneys, and livers were dissected. Tracings of brain extracts were compared to those of previous HP (10 mg/Kg x 3)-treated mouse brain extracts.

Inhibition studies.

Clorgyline·HCl (2.5 mg/Kg) was injected 24 hour prior to the 50 mg/Kg of HPTP·HCl. Urine and feces were collected prior to the HPTP administration as controls and over 48 hour period after HPTP administration. Brains were dissected 48 hour after the HPTP administration.

Ketoconazole (20 mg/Kg) was administered 24 hour prior to the 50 mg/Kg of HPTP·HCl to the mice (n = 3) and urine and feces sample collection was attempted. Brain, kidney, liver were dissected 48 hours after the HPTP administration.

Induction studies.

The mice (3 mice each for control and experimental groups) received one i.p. injection containing DEX (83 mg/Kg) or vehicle (trioctanoin). After 20 hours, they received HPTP·HCl (50 mg/Kg). After 24 hours, they were sacrificed by cervical dislocation and brains were dissected and stored at -70 °C until HPLC analysis.

HP was administered for 3 days (10 mg/Kg x 2, then 5 mg/Kg) and on the 4th day, HPTP·HCl (50 mg/Kg) was administered (n = 3). Control mice (n = 3)

were treated with vehicle only for the first 3 days prior to HPTP administration. After 24 hours, brains were dissected for the HPLC analysis.

Sample analysis. Sample preparations and HPLC/fluorescence analysis are described in Chapter 4. The pooled urine extracts were analyzed by API LC/MS/MS on a SCIEX API III triquadrupole mass spectrometer as described previously.[148] The samples obtained from the Sep-paks were dissolved in 500 μL of the mobile phase and 50 μL aliquots were introduced via a Rheodyne 7413 injection valve onto the same HPLC column using essentially the same HPLC conditions as described above. The ionspray interface was set at 4000 V and the nebulizer pressure at 40 psi air. The collision energy was -30 V for collision induced dissociation (CID) experiments.

6.2. Metabolic studies on HPTP in Baboons.

The purpose of the studies described in this Chapter was to establish an animal model and, in particular, a primate model to investigate the metabolic fate and neurotoxicity of HP and HPTP. It has been reported that HP is metabolized in rodents[117,129] and humans[118,130] to the pyridinium species $RHPP^+$ and HPP^+, compounds which are structurally similar to the neurotoxin MPP^+. Initially, HP was selected as the test compound. However, the study was discontinued due to the severe cataleptic effects of HP in Baboons. Since HPTP is likely to be metabolized to the same pyridinium species,[148,166] this compound was used in the majority of these experiments. HPTP administration was started using four drug-treated baboons and four control baboons in March, 1994 using a dose of 7 mg/Kg i.m. three times a week over 6 months. Five sets of urine collection were made with this group of baboons and additional urine, plasma and cerebrospinal fluid (CSF) samples were obtained from new 2 baboons from a 1 to 5 week period post initiation of HPTP dosing. The following summarizes the experimental protocols for these 6 studies.

1. Urine collection over a 24-hour period after 7 mg/Kg dose in June, 1994 (3 months post initiation of HPTP administration).
2. Washout study: Urine collections (each 24 hours) at 24, 48, 72, and 96 hours after the last injection of 7 mg/Kg dose in July, 1994 (4 month data).
3. A 1 week washout study: Urine collection over a 24-hour period after the last 7 mg/Kg dose in August, 1994 (6 month data).
4. Urine collection over a 24-hour period after 7 mg/Kg dose in November, 1994 (8 month data).

5. A 2 and 4 week washout study: Urine collection over a 24-hour period at 2 and 4 weeks after the last 8 mg/Kg dose in March, 1995 (1 year data).
6. Using new 2 baboons, urine collection over a 24-hour period at week 1, 2, 3, 4 and 5 post initiation of 8 mg/Kg. The 1, 3 and 5 week plasma samples and 5 week CSF sample also were obtained.

During the early phases of these studies, it was found that HPTP was contaminated with up to 3% HP and, therefore, the recrystallization procedure was modified and the purity of HPTP was monitored thoroughly by HPLC/UV and HPLC/fluorescence.

This Chapter summarizes (1) HPTP·HCl synthesis and purification, (2) HPLC analyses of HPTP-treated baboon urine samples, and (3) attempts to identify an unknown peak formed in HPLC/fluorescence tracings of urine samples.

Results and Discussion

(1) HPTP·HCl synthesis and purification. The standard procedure for synthesizing the hydrochloride salt of HPTP involves heating HP under reflux in 6 N HCl for 6 hours. The product was characterized by GC/MS, ^{1}H NMR, and elemental analysis. By the HPLC/fluorescence analysis, the absence of pyridinium contaminants in the sample was confirmed (Fig. 40a). However, during the course of the study, HP was detected in HPTP·HCl (Fig. 40b). This problem would lead to complications in assigning metabolic pathways and pharmacological effects including movement disorders of interest as a model for human TD. Therefore, HPTP·HCl needed to be purified in order

for us to state that the all results can be linked to HPTP. HPLC/UV analysis was added to the purity check.

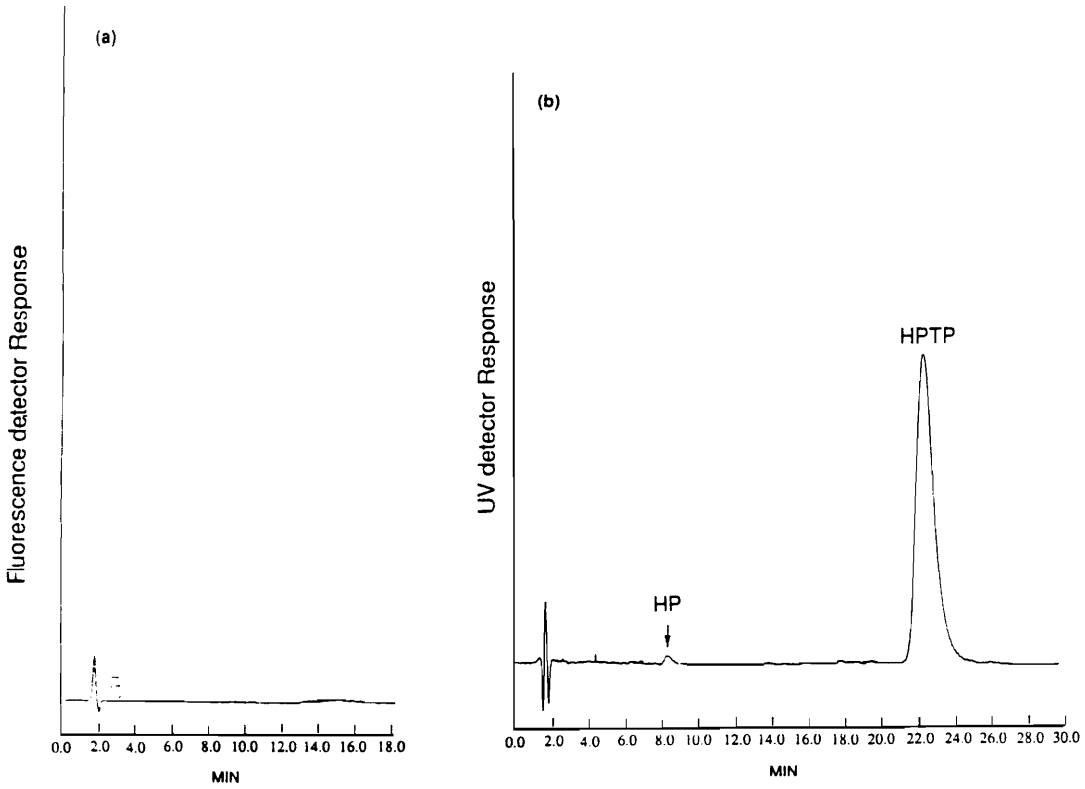

Figure 40. HPLC tracings of HPTP·HCl (a) fluorescence (b) UV detection. The amount injected was 5 nmol on column.

The reaction mixture was cooled to room temperature after heating HP (24.4 g, 64.9 mmol) under reflux for 6 hours. The crude product obtained weighed 25.0 g (63.7 mmol, 98% yield) after drying in a vacuum oven (no heat) overnight. The product was estimated to contain 1.4% of HP (Fig. 40b). The crude product was recrystallized from water/ethanol. Recrystallization was repeated and the product was monitored by HPLC. After the first and second recrystallizations, the % HP was 0.3 and 0.2%, respectively. After the third recrystallization, HP was not detected (Fig. 41). At the same time, HPLC/fluorescence confirmed the absence of pyridinium contaminants. HPTP·HCl is a white crystalline solid (13.0 g, 33.1 mmol, 51%) melting with decomposition at 182-183 °C.

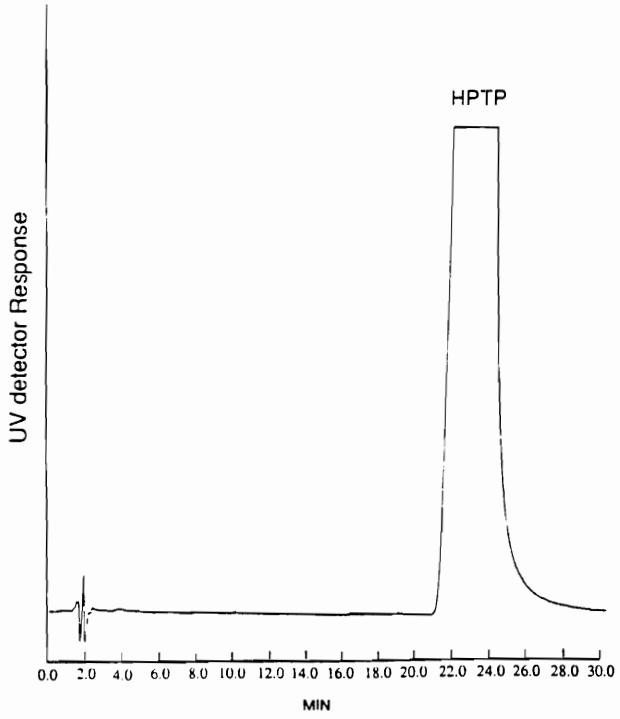

Figure 41. HPLC/UV tracing of HPTP·HCl after the third recrystallization.

(2) Urine analysis. The HPLC/UV tracings of HPTP-treated baboon urine extracts (Fig. 42b) are not significantly different from that observed with control urine samples (Fig. 42a). The HPLC/fluorescence tracings of the urine extracts obtained from HPTP-treated baboons (Fig. 43b) showed two fluorescent peaks which were not present in the tracings of the corresponding vehicle-treated control baboon urine extracts (Fig. 43a). These two compounds were identified as $RHPP^+$ (t_R 8.6 min) and HPP^+ (t_R 14.0 min) by comparison of chromatographic features with synthetic standards and reference to earlier LC/MS/MS work. This HPLC pattern ($RHPP^+/HPP^+$ ratio) was similar to that observed with HP-treated human patients (see Chapter 6.2.) and very different from that of the HPTP-treated mouse (Chapter 6.1.). The amounts of both pyridinium metabolites were measured using external calibration curves which were prepared as follows: Human control urine was spiked with $RHPP^+$ and HPP^+ at 4 concentrations and processed in the same way as the baboon urine samples were processed. The recoveries of the pyridinium species from the C18 Sep-pak cartridges (Vac 3 cc^{TM}) were 80-90% and the linearity of these curves (r^2) was always above 0.998.

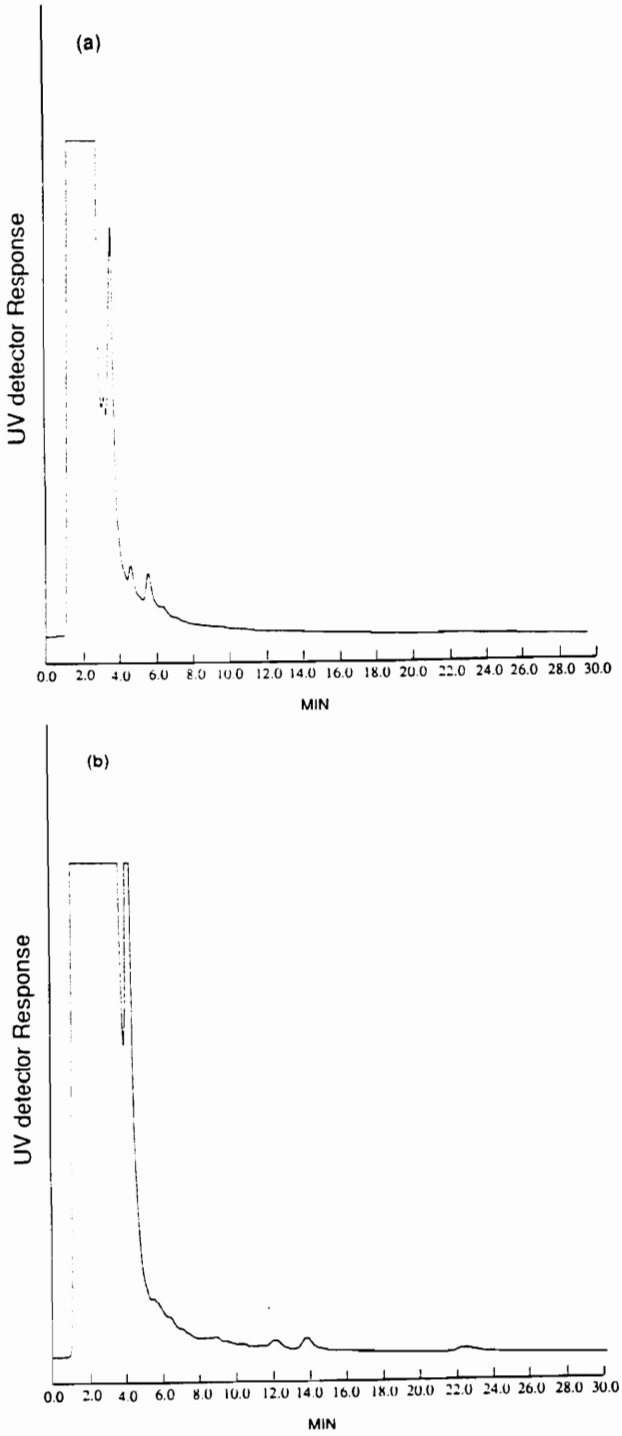

Figure 42. HPLC/UV tracings of urine extracts obtained from (a) control baboon and (b) an HPTP-treated baboon.

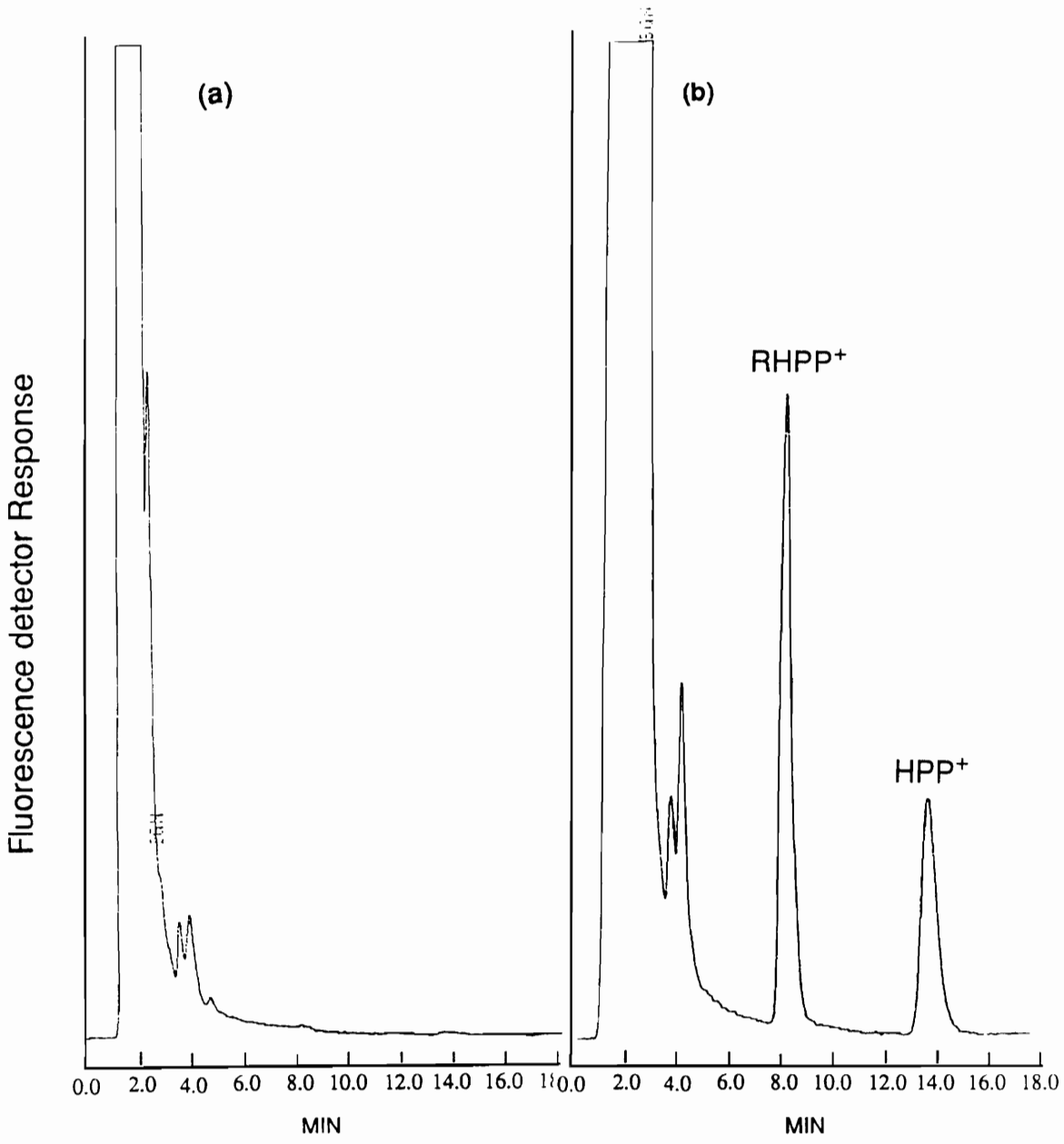

Figure 43. HPLC/fluorescence tracings of urine extracts obtained from (a) control baboon and (b) an HPTP-treated baboon.

1.1. Data following 3 months on drug. Urine samples were collected over a 24-hour period from 4 control and 4 HPTP-treated baboons 3 months post initiation of the 7 mg/Kg dose and the amounts of pyridinium metabolites were measured and the % conversions were calculated (Table 21). The ratios of $RHPP^+$ to HPP^+ ranged from 0.75 to 2.0. These values are much higher than the corresponding ratios observed in the HPTP-treated mouse urine extracts (0.08).

TABLE 21

Summary table of $RHPP^+/HPP^+$ formation and % of the administered dose from first 24 hour urine samples

Control group	Baboon 1	Baboon 2	Baboon 3	Baboon 4
$RHPP^+/HPP^+$ nmols	0/0	0/0	0/0	0/0
% of the dose administered	0/0	0/0	0/0	0/0
HPTP-treated group	Baboon 5	Baboon 6	Baboon 7	Baboon 8
$RHPP^+/HPP^+$ nmols	157/263	170/344	136/156	110/169
% of the dose administered	0.04/0.06	0.04/0.08	0.03/0.04	0.02/0.04

1.2. and 1.3. Washout study at 4 months. The results from 24 hours to 1 week washout studies are summarized in Table 22. In these studies, control urine was not collected and baboon 7 did not participate for the 24 to 96 hour collection period. This study was designed to observe the urinary excretion profile of HPP^+ ad $RHPP^+$. Once the urine collection was started no drug was administered and "the % of the dose administered" was calculated from the amount of pyridinium metabolites excreted in the 24 hour period against the amount of the last dosing of HPTP·HCl before the urine collection was started (7 mg/Kg, 444 μmols) as 100%.

TABLE 22

Summary table of $RHPP^+/HPP^+$, HPTP measured in 24-h to 1 week washout urine samples from HPTP-treated baboons

	Baboon 5	Baboon 6	Baboon 8	Average (R^+/H^+)
24-h				
conc. of $RHPP^+/HPP^+$(nM)	333/590	408/709	387/602	
volume of urine	360 mL	460 mL	300 mL	
amount (nmols)	120/212	188/326	116/181	141 ± 40/240 ± 76
% of the dose administered	0.03/0.05	0.04/0.07	0.03/0.04	

continue to the next page

48-h				
conc. of RHPP+/HPP+(nM)	1089/754	534/1009	948/1479	
volume of urine	270 mL	270 mL	170 mL	
amount (nmols)	294/204	144/272	161/251	200 ± 82/242 ± 35
% of the dose	0.07/0.05	0.03/0.06	0.04/0.06	
72-h				
conc. of RHPP+/HPP+(nM)	1178/719	1418/978	958/1512	
volume of urine	150 mL	170 mL	130 mL	
amount (nmols)	177/108	241/166	125/197	181 ± 58/157 ± 45
% of the dose	0.04/0.02	0.05/0.04	0.03/0.04	
96-h				
conc. of RHPP+/HPP+(nM)	521/672	732/1525	935/1720	
volume of urine	190 mL	180 mL	130 mL	
amount (nmols)	99/128	132/275	122/224	118 ± 17/209 ± 75
% of the dose	0.02/0.03	0.03/0.06	0.03/0.05	
1 week				
conc. of RHPP+/HPP+(nM)	180/357	115/285	241/370	
volume of urine	330 mL	300 mL	430 mL	
amount (nmols)	59/118	35/86	104/159	66 ± 35/121 ± 37
% of the dose	0.01/0.03	0.01/0.02	0.02/0.04	

The amounts of RHPP+ and HPP+ excreted in each 24 hour period (average of 3 animals) are plotted in Figure 44.

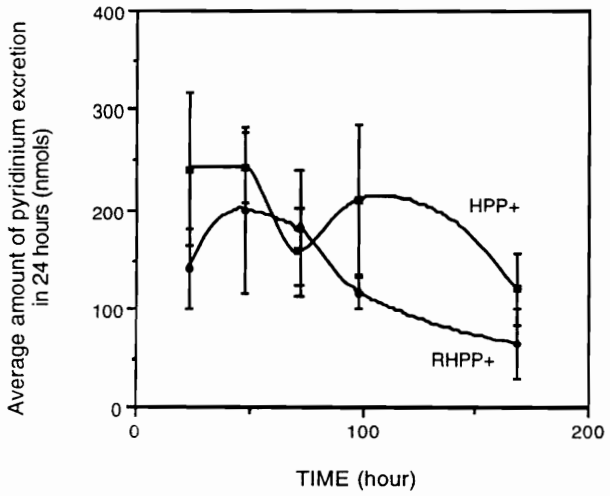

Figure 44. The average amount of pyridinium metabolites excreted in urine over 24 hour period (washout study).

It appears that both pyridinium metabolites are excreted slowly into the urine. HPTP was observed in only two cases (both at the 96 hour collection) and the amounts were very low (0.3 and 2.4% of the dose, measured by HPLC/UV). This low amount of unchanged drug is consistent with the results obtained from mouse in vivo studies.

1.4. Data following 8 months on drug. The urine samples were collected over a 24 hour period after the 7 mg/Kg dose (0.175 g/baboon). Control baboon 2 was injected 0.126 g of HPTP once by mistake. No detectable amount of unchanged HPTP was observed in the HPLC/UV tracings. The amounts of pyridinium metabolites are summarized in Table 23.

TABLE 23

Summary table of RHPP+/HPP+ measured in urine collection over 24-h of 8 months post initiation.

Controls	Control 1	Control 2	Control 3	Control 4
RHPP+/H+ (nM)	0/0	770/~0	0/0	0/0
volume of urine	330 mL	530 mL	760 mL	530 mL
amount (nmols)	0/0	408/~0	0/0	0/0
% of the dose	0/0	0.13/~0	0/0	0/0
Treated	**Baboon 5**	**Baboon 6**	**Baboon 7**	**Baboon 8**
RHPP+/H+ (nM)	812/636	779/402	892/408	1386/483
volume of urine	360 mL	330 mL	490 mL	410 mL
amount (nmols)	292/229	257/133	437/200	568/198
% of the dose	0.07/0.05	0.06/0.03	0.10/0.05	0.13/0.04

Compared to the results from earlier samples (1.1. 24-hour collection following 3 months on drug), the ratio of RHPP+/HPP+ was greater. The range of the ratio at this time point (8 months) is 1.4/1 to 4.3/1. As will be discussed in

Chapter 6.2, this observation was same for the patients treated with HP. The $RHPP^+/HPP^+$ ratio in the urine increased as the drug therapy continued. This may suggest that the induction of the ketone reductase that catalyzes the reduction of HPTP to RHPTP.

1.5. Data obtained with 2 weeks and 4 weeks washout at 1 year. Urine samples were collected from the HPTP-treated group (Table 24). The % of the dose excreted was not different from that obtained from the earlier washout study.

TABLE 24

Summary table of $RHPP^+/HPP^+$ measured in 2 and 4 weeks washout urine samples at 1 year.

	Baboon 5	Baboon 6	Baboon 7	Baboon 8
2 weeks				
conc. $RHPP^+/HPP^+$ (nM)	162/210	509/220	261/289	464/206
volume of urine (mL)	430	760	550	390
amount (nmols)	70/90	234/167	144/159	181/80
% of the dose	0.01/0.02	0.05/0.03	0.03/0.03	0.04/0.02
4 weeks				
conc. $RHPP^+/HPP^+$ (nM)	196/204	112/201	54/-	29/-
volume of urine (mL)	470	760	840	420
amount (nmols)	92/96	85/153	45/-	12/-
% of the dose	0.02/0.02	0.02/0.03	0.01	0.002

1.6. Urine sample analysis of 1, 2, 3, 4 and 5 weeks post initiation of HPTP administration. The studies were carried out in two new animals which were not part of the earlier experiments. The baboons were treated three times a week during the period of this study. The amount of pyridinium metabolites are summarized (Table 25) and also the average of these amounts was plotted against time (Fig. 45).

TABLE 25

Summary table of $RHPP^+/HPP^+$ measured in 1 through 5 weeks post initiation of 8 mg/Kg HPTP dose.

	Baboon 9	Baboon 10
	$RHPP^+/HPP^+$	$RHPP^+/HPP^+$
8/17/95	Total urine volume	Total urine volume
(1 week)	500 mL	335 mL
conc.	1359/1336 nM	1286/570 nM
amount	770/668 nmol	431/191 nmol
% of the dose	0.15/0.13	0.09/0.04
8/24/95	195 mL	115 mL
(2 week)		
conc.	621/1741 nM	2012/2926 nM
amount	121/339 nmol	231/336 nM
% of the dose	0.02/0.07	0.05/0.07
8/31/95	190 mL	215 mL
(3 week)		
conc.	1896/764 nM	1106/1424 nM

amount	360/145 nmol	238/306 nmol
% of the dose	0.07/0.03	0.05/0.06
9/7/95 (4 week)	260 mL	180 mL
conc.	581/1328 nM	572/1312 nM
amount	151/345 nmol	103/236 nmol
% of the dose	0.03/0.07	0.02/0.05
9/14/95 (5 week)	510 mL	750 mL
conc.	1486/1190 nM	1182/657
amount	758/607 nmol	887/493
% of the dose	0.15/0.12	0.18/0.1

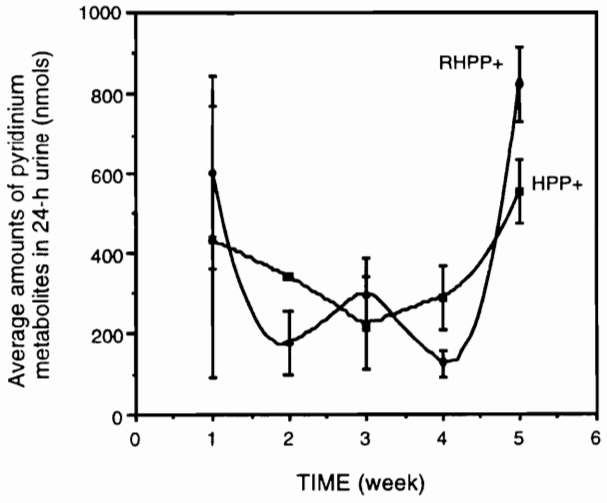

Figure 45. The average amount of pyridinium metabolites excreted in urine over 24 hour period (data following 5 weeks on drug).

The excretion of pyridinium metabolites was about the same as observed previously (amount, % conversion of the dose). The amount of $RHPP^+$ again was in the same level or higher than the amount of HPP^+. Although we do not have a good explanation, the amounts of both pyridinium metabolites increased at 5 week. Some problem was encountered with some urine samples at 1 week (Aug. 17, 95). Lyophillization might not have been complete and therefore the values reported in these animal may not be accurate. Other than the sample at 1 week, samples were well lyophilized and the slope of the calibration curves prepared with synthetic $RHPP^+$ and HPP^+ spiked in control urine (made every time when urine samples were processed) did not change. Hence, we consider these values to be reliable.

Unchanged HPTP was observed in 8 out of 10 of the HPLC/UV traces. However, in all 8 cases the amount was very small (less than 1% of the dose administered) Previously, we had occasionally observed RHPTP (identified based on its coelution with synthetic RHPTP) in the HPLC/UV tracings. We attempted to measure the amount of RHPTP using an external calibration curve prepared with synthetic RHPTP. However, the values varied from 0 to 14% of the dose and we are not certain the presence of RHPTP. We were not certain this variation is due to the overlapping peak or extraction problem, or actually the amount of RHPTP varies between sample to sample. Although we did not attempt to develop the quantitative assay for RHPTP, it should be investigated.

Plasma samples (1, 3 and 5 week samples from baboon 9 and 10) were also analyzed. However, neither $RHPP^+$ nor HPP^+ was detected in these samples. CSF samples from Baboon 9 and 10 (5 weeks) also were analyzed

(HPLC/fluorescence, HPLC/UV). Again, we did observed neither metabolites nor unchanged HPTP.

Overall, these urine analyses have demonstrated that HPTP is metabolized to $RHPP^+$, HPP^+ and (RHPTP?) in baboons and that the ratio of $RHPP^+/HPP^+$ in urine is similar to that of human patient urine samples. Therefore, we consider the baboon to be a good model to study toxicity of HP in humans as it may relate to the formation of toxic pyridinium metabolites.

(3) Attempts to identify an unknown peak observed in HPLC/fluorescence tracings. As shown in Figure 44(b), the peaks detected on the HPLC/fluorescence tracings using our standard mobile phase (pH 6.2) were $RHPP^+$ and HPP^+. Other early eluting peaks (t_R 3 to 4 min) were observed in the control urine extracts and therefore may not derived from HPTP. It has been proposed by others that by using a mobile phase at pH 3, 4-(4-chlorophenyl)pyridine (CPP, **53**) can be detected in HPLC/fluorescence tracings obtained from HPTP-treated baboon urine extracts (Dr. D. Eyles personal communication).

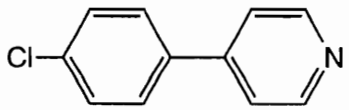

53

The retention time of synthetic CPP, which can be detected both by fluorescence and UV detection, was 15.0 minutes on our system. We found no evidence for the presence of CPP. We attempted to confirm this observation using a pH 3 mobile phase. Synthetic CPP eluted at 6.9 minutes with this mobile phase. Again, no peak was observed in this region in the tracings of HPTP-treated baboon urine extracts (Fig. 46b). The recovery of synthetic CPP when spiked in human control urine using the Sep-pak assay was 70 to 80%.

The procedure used by others (Dr. S. Pond's group, described in the experimental section) gave a 90% recovery of CPP. Therefore, we tried both procedures for extracting urine samples isolated from HPTP-treated baboons. CPP was not observed in either tracing. This HPLC/fluorescence assay with pH 3 mobile phase was started in order to examine the possible presence of CPP in HPTP-treated baboon urine. However, interestingly, instead of CPP, a major fluorescent peak was observed at 14.1 minutes in tracings processed by both procedures and analyzed with the pH 3 mobile phase system (Fig. 46b). This peak was observed in all HPTP-treated baboon urine extracts but not in the control baboon urine extracts (Fig. 46a) suggesting this material is derived form HPTP. HPTP-treated C57BL/6 mice urine extracts were also analyzed on this system and the corresponding peak was not observed. Therefore this metabolite seems to be specific for baboons. This sample was sent to Dr. H. Fouda (Pfizer Inc., CT) for HPLC/MS analysis. However, he was not successful in characterizing this material. This subject warrants additional work.

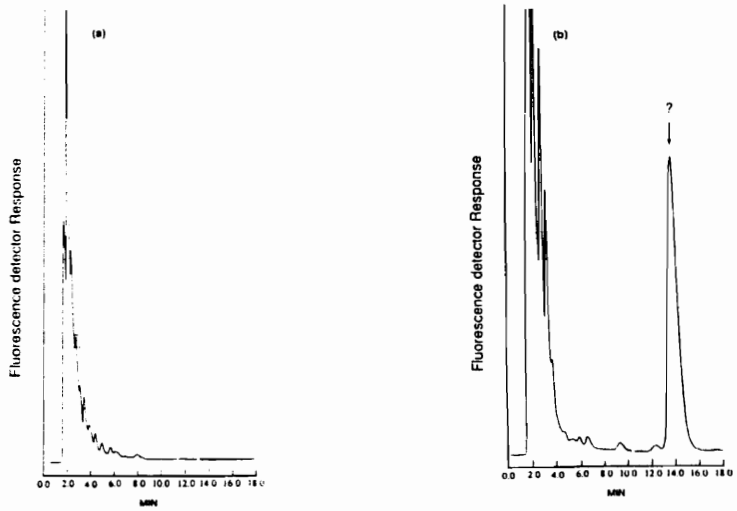

Figure 46. HPLC/fluorescence tracings of (a) control and (b) HPTP-treated baboon urine analyzed by modified mobile phase (pH 3).

Another major question we need to answer concerns the mass balance of the drug administered to baboons. As described earlier, unchanged HPTP was rarely observed in the urine samples. The recovery of HPTP from the Sep-pak is 70 to 75% which suggests that the low recovery is not due to a technical problem. The amounts of pyridinium metabolites in the urine samples are low. The fluorescence and UV tracings show no characterizable compounds. When coupled with the results of our in vivo mice studies, it is clear that these data are totally inadequate. Additional studies will have to be performed to help characterize better the mass balance issue.

Experimental

Chemicals. HPTP·HCl was synthesized in this laboratory. Tween 80, haloperidol free base (Sigma Chemicals Co., St. Louis, MO), hydroxypropyl-β-cyclodextrin (used as a vehicle, Janssen Biotech N. V., Olen, Belgium), and HPLC-grade solvents Fisher Scientific Co., Springfield, NJ) were obtained from commercial sources.

(1) General methods. Reaction were carried out under nitrogen atmosphere. Gas chromatography-electron ionization mass spectrometry (GC-EIMS), employed Hewlett Packard 5890 GC fitted with an HP-1 capillary column (24 m x 200 μm x 0.33 μm film thickness) which was coupled to a Hewlett Packard 5870 mass-selective detector. Data were acquired using an HP 5970 ChemStation. Ultraviolet (UV) spectra were taken on Beckman DU-50 spectrophotometer. ^{1}H NMR spectrum was measured on a Bruker WP 270 spectrometer and melting point was determined on a Thomas-Hoover capillary melting point apparatus.

(2) Synthesis of 4-(4-chlorophenyl)-1-[4-(4-fluorophenyl)-4-oxo-butyl]-1,2,3,6-tetrahydropyridine Hydrochloride (HPTP·HCl). A solution of haloperidol free base (24.4 g, 65 mmol) in 1300 mL of 6 N HCl was heated under reflux with vigorous stirring for 6 h. The crude product was recrystallized three times from water/ethanol (4/1). Each time, sample was analyzed by HPLC/fluorescence and UV to monitor the purity. Analysis: mp 182-183 °C (decomposed); ^{1}H NMR (DMSO-d_6) δ 7.4-8.1 (m, 8 H, ArH), 6.25 [s, 1 H, C(5)-H], 2.1-4.0 (complex m, 12 H, aliphatic proton signals); GC/MS [isothermal at 125 °C for 2 min followed by a ramp of 40 °C/min for 4 min (t_R = 7.2 min)] m/z 357 (M^+, 8%), 219 (20%), 206 (30%), 192 (100%), 165 (20%), 129 (30%), 123 (80%), 95 (65%), 75 (20%).

(3) Animal Studies. This animal study was conducted at Potchefstroom University, South Africa under Dr. Cornelis J. Van der Schyf. Ten male baboons were caught in the wild and used for these studies. Four baboons were used for controls which were injected with vehicle (Tween 80 or 0.35 M hydroxypropyl-β-cyclodextrin) only intramuscularly during the whole study. The other 6 baboons were treated with HPTP three times per week. Treatment was started on March 2, 1994 at the dose of 1.52 mg/Kg HPTP in 20 % Tween 80. The HPTP dose was gradually increased over 15 weeks to 7 mg/Kg in 0.35 M hydroxypropyl-β-cyclodextrin. After 6 injections of HPTP 7 mg/Kg or vehicle, the first set of urine samples were collected over a 24 hour period. The experimental samples were treated with concentrated HCl to adjust the pH to 3 and stored at 5 °C. Before lyophilization, the pH was adjusted to 8.5 with 0.5 M K_2HPO_4 and the resulting solution was centrifuged and filtered. The control samples were treated in the same way except that the pH was not

adjusted to 3 with HCl. The dose was increased to 8 mg/Kg from November 23, 1994. All samples were treated in the same way as the first set. After the samples were received, they were stored at -70 °C prior to analysis.

(4) Sample preparation. Lyophilized urine samples were reconstituted to the original volume using human control urine. A 400 μL-aliquot of the sample was treated with 2 mL of 0.5 M K_2HPO_4/ 20 mM $NaHCO_3$ (1/1 v/v) to adjust the pH to 8.5. The resulting solution then was loaded onto a Millipore Sep-pak (Vac 3 cc, C18 cartridge, Millipore-Waters, Bedford, MA). The Sep-paks process was the same as described in Chapter 4. The residue was dissolved in the HPLC mobile phase using 10 times the loaded sample volume.

In order to examine the possibility of the presence of CPP in the HPTP-treated baboon urine, samples were processed by a slightly modified method (the method which is used in Dr. Pond's group). The procedure is as follows: 100 mg lyophilized urine was weighed into an Eppendorf tube to which 0.75 mL 0.1% lactic acid in water (v/v) was added and the urine was dissolved. Then, 0.75 mL 0.1% lactic acid in CH_3CN was added, the solution was vortexed and sonicated for 6 min, and centrifuged at 12000 g for 20 min. The supernatant was decanted into test tubes containing 5 mL of 30 mM NH_4OAc and mixed. C18 Sep-pak cartridges were preconditioned by successive 5 mL loadings of methanol, water and 30 mM NH_4OAc. The entire sample was loaded onto the cartridge which was then washed with 5 mL NH_4OAc followed by 5 mL 50% methanol. The cartridge was then eluted with 3 mL 0.5% lactic acid/0.5% acetic acid in methanol (v/v). The eluant was evaporated to dryness under N_2 at 40 °C.

(5) HPLC analysis. HPLC analysis is the same as described in Chapter 4. The mobile phase used for the CPP assay consisted of acetonitrile/30 mM NH_4OAc (28/72 v/v) containing 0.2% of triethylamine, pH 3.0 adjusted with trifluoroacetic acid was also used for the analysis using same HPLC conditions.

6.3. Urine analysis of HP-treated patients.

This project was pursued in collaboration with Dr. Richard Riker at the Department of Critical Care Medicine, Maine Medical Center. The aim of this project was to evaluate the effects of high HP doses on movement disorders and whether or not such disorders can be related to the levels of pyridinium metabolites in the urine of these critically ill patients.

Results and Discussion

HPLC/fluorescence tracings of urine extracts obtained from HP-treated patients are shown in Figure 47. Other than $RHPP^+$ and HPP^+ peaks, no significant peak was observed. Although the $RHPP^+$ peak seems to dominate, it must be remembered that the detection response of $RHPP^+$ in this assay is approximately 4 times greater than that of HPP^+ (see Chapter 4). Therefore the ratio of $RHPP^+/HPP^+$ in this tracing is only 1/1. This ratio is similar to that observed in urine obtained from HPTP-treated baboons (Chapter 6.2.) and much higher than that found in urine obtained from HPTP or HP-treated C57BL/6 mice (chapter 6.1.). The HP dose, $RHPP^+/HPP^+$ ratio, % of the dose administered, accumulative dose, the amount of accumulative pyridinium metabolites excreted and accumulative % of the dose for these patients are summarized in Table 26.

In an effort to analyze these results, they were plotted in several ways. First, accumulative % of $RHPP^+$ and HPP^+ in the urine and total HP dose (mg) were plotted against duration of therapy (Fig. 48). As the total HP dose increases, the accumulative % of both pyridinium metabolites increases in a

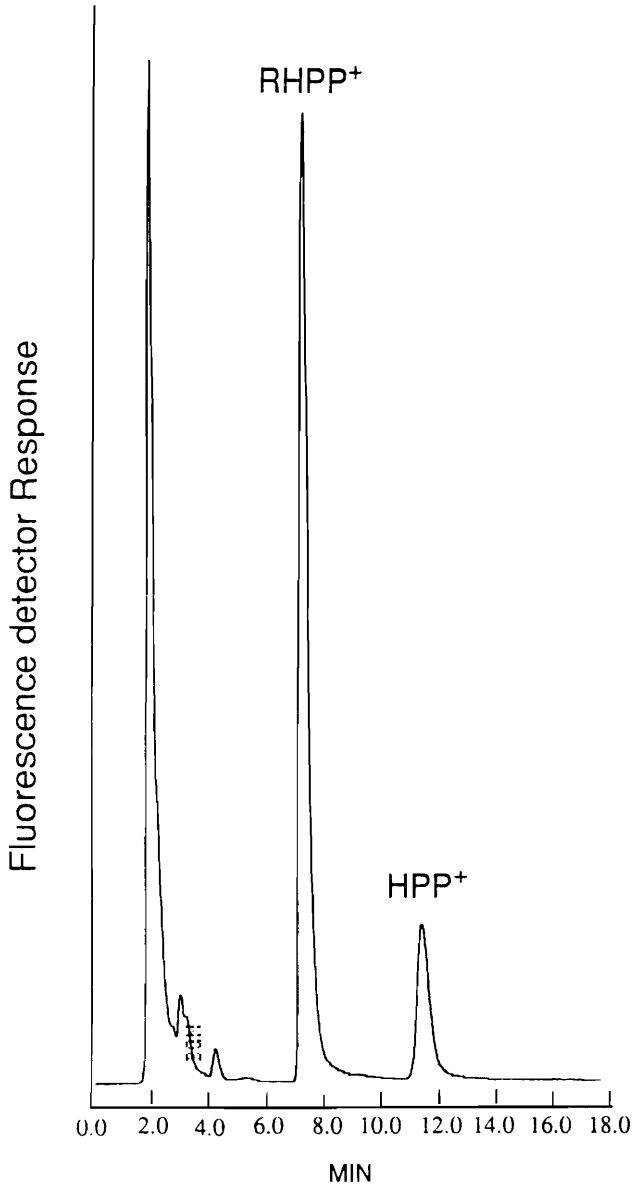

Figure 47. HPLC/fluorescence tracing of urine extracts obtained from an HP-treated patient.

similar way. This is especially apparent when the duration of therapy is longer (at least over 10 days); both curves clearly fit each other. The ratio of accumulative % RHPP+/% HPP+ excreted in urine also was plotted against

duration of therapy (Figure 49). In most patients the ratios increase with time like baboons (Chapter 6.2.) and eventually plateau. The results with some individuals (patient #9 in particular) are quite different. According to Dr. Riker's report, four patients developed self-limited tremors (TR) about 3 days after HP was discontinued. Six patients developed no tremor (NO). The tremors persisted an average of 9 days and completely resolved in all cases. The peak daily dose of HP was greater for TR (318 mg vs. 157 mg NO, $p = 0.05$), as was the average daily dose of HP (185 mg TR vs. 86 mg NO, $p = 0.03$). The cumulative HP dose was also greater for TR (3842 mg vs. 1181 mg NO, $p = 0.02$), as was the duration of HP therapy (21 days TR vs. 13 days NO, $p = 0.03$). The TR group also had greater peak doses (103 mg/day TR vs. 18 mg/day NR, $p = 0.01$) and greater mean doses of lorazepam (56 mg/day TR vs. 7 mg/day NO, $p < 0.01$). These patients also were younger (36 years TR vs. 64 years NO, $p = 0.005$). It was tentatively concluded that self-limited tremors following discontinuation of high-dose HP infusion are related to HP and benzodiazepine doses and age. It is unclear if this is a drug-related effect (delayed toxicity or withdrawal or altered metabolism) or if the higher doses are markers of illness severity. Additional study needs to be conducted. A through pharmacokinetic analysis of these results is being conducted by Dr. Riker.

TABLE 26

Summary table of the urine analysis of HP-treated patients.

Haloperidol was administered by continuous infusion and urine was collected over 24 hours, unless it is stated in the table.

Patient #1

Sample	Date	HP dose (mg)	R^+/H^+ [a] (μmol)	% of the dose [b]	Total dose (mg)	Accum. P^+ (μmol) [c]	Accum. % of the dose
01	6/30	120	3.34/3.23	1.05/1.01	120	3.34/3.23	1.05/1.01
02	7/01	96	3.66/1.69	1.43/0.66	216	7.00/4.92	1.22/0.86
03	7/02	60	4.30/2.48	2.69/1.55	276	11.3/7.40	1.54/1.01
04	7/03	3	2.38/1.63	29.8/20.4	279	13.68/9.03	1.84/1.22

[a] R^+: $RHPP^+$, H^+: HPP^+ [b] % of the dose: % of the dose administered [c] Accum.: Accumulative

Patient #2

Sample	Date	HP dose (mg)	R^+/H^+ (μmol)	% of the dose	Total dose (mg)	Accum. P^+ (μmol)	Accum. % of the dose
01	6/30	158	2.38/1.63	0.57/0.39	158	2.38/1.63	0.57/0.39
02	7/01	126	9.81/3.15	2.93/0.94	284	12.19/4.78	1.61/0.63
03	7/03	144	8.02/2.11	2.09/0.55	428	20.21/6.89	1.78/0.61
04	7/04	144	9.06/2.67	2.37/0.70	572	29.27/9.56	1.92/0.63
05	7/05	144	15.35/4.22	4.01/1.10	716	44.62/13.78	2.34/0.72
06	7/06	144	12.96/3.56	3.38/0.93	860	57.58/17.34	2.52/0.76
07	7/07	120	7.70/2.12	2.41/0.66	980	65.28/19.46	2.50/0.75
08	7/08	120	18.48/5.68	5.79/1.42	1100	83.76/25.14	2.86/0.86
09	7/09	120	12.90/3.51	4.04/1.10	1220	96.66/28.65	2.98/0.88
10	7/10	72	10.40/2.61	5.43/1.36	1292	107.06/31.26	3.12/0.91
11	7/11	72	10.49/4.19	5.48/2.19	1364	117.55/35.45	3.24/0.98
12	7/12	72	8.92/1.75	4.66/0.91	1436	126.47/37.2	3.31/0.97 **T**
13	7/13	72	9.02/1.75	4.71/0.91	1508	135.49/38.95	3.38/0.97 **T, F**
14	7/15	144	16.88/4.31	4.41/1.13	1652	152.37/43.26	3.47/0.98 **T, F**
15	7/16	40 (oral)	7.44/2.24	6.99/2.11	1692	159.81/45.50	3.55/1.01**T**

16	7/17	30 (oral)	6.72/3.78	8.42/4.74	1722	166.53/49.28	3.64/1.08 **T**
17	7/18	15 (oral)	6.42/1.36	16.09/3.41	1737	172.95/50.64	3.74/1.10 **T**
18	7/19	0	2.50/0.13		1737	175.45/50.77	3.80/1.10 **T**
19	7/20	0	2.18/ -		1737	177.63/50.77	3.85/1.10 **T**
20	7/21	0	3.26/ -		1737	180.89/50.77	3.92/1.10 **T**
21	7/22	0	2.63/ -		1737	183.52/50.77	3.97/1.10 **T**
22	7/23	0	2.09/ -		1737	185.61/50.77	4.02/1.10 **T**
23	7/24	0	1.18/ -		1737	186.79/50.77	4.04/1.10 **T**

-: Not detected

Patient experienced tremor (**T**) which we're not certain was pseudo-parkinsonism from HP or benzodiazepine withdrawal (these severely ill patients were sedated with HP, bezodiazepines, and narcotics during mechanical ventilation). Tremor resolved by 8/16. Also had tongue fasciculation without perioral tremor (**F**) which resolved much more quickly by 7/16.

Patient #3

Sample	Date	HP dose (mg)	R^+/H^+ (μmol)	% of the dose	Total dose (mg)	Accum. P^+ (μmol)	Accum. % of the dose
01	7/04	205	1.69/1.44	0.31/0.26	205	1.69/1.44	0.31/0.26
02	7/05	240	1.61/1.93	0.25/0.30	445	3.30/3.37	0.28/0.28
03	7/06	80 (oral)	2.08/1.57	0.98/0.74	525	5.38/4.94	0.39/0.35
05	7/07	65 (oral)	1.51/0.67	0.87/0.39	590	6.89/5.61	0.44/0.36
06	7/08	0	0.40/0.83		590	7.29/6.44	0.46/0.41
07	7/09	0	0.79/0.29		590	8.08/6.73	0.51/0.43
08	7/10	0	0.83/0.42		590	8.91/7.15	0.57/0.46
09	7/11	0	0.57/0.23		590	9.48/7.38	0.60/0.47 **T**
10	7/12	0	0.77/0.46		590	10.25/7.84	0.65/0.50 **T**

Patient #4

Sample	Date	HP dose (mg)	R^+/H^+ (μmol)	% of the dose	Total dose (mg)	Accum. P^+ (μmol)	Accum. % of the dose
01	7/22	48	2.10/1.99	1.65/1.56	48	2.10/1.99	1.65/1.56
02	7/23	48	2.26/2.89	1.77/2.26	96	4.36/4.88	1.71/1.91
03	7/24	48	2.81/2.51	2.20/1.97	144	7.17/7.39	1.87/1.93
04	7/25	31	1.00/0.98	1.21/1.19	175	8.17/8.37	1.76/1.80
05	7/26	24	4.53/3.64	7.10/5.70	199	12.70/12.01	2.40/2.27
06	7/27	4	2.21/0.97	20.77/9.12	203	14.91/12.98	2.76/2.40
07	7/28	5	1.87/0.73	14.06/5.49	208	16.78/13.71	3.03/2.48
08	7/29	10	1.45/0.58	5.45/2.18	218	18.23/14.29	3.14/2.46
09	7/30	15	1.35/0.56	3.38/1.40	233	19.58/14.85	3.16/2.40
10	7/31	25	1.05/0.60	1.58/0.90	258	20.63/15.45	3.01/2.25
11	8/01	15	0.90/0.61	2.26/1.53	273	21.53/16.06	2.97/2.21

No movement disorders following two weeks after HP discontinued.

Patient #5

Sample	Date	HP dose (mg)	R^+/H^+ (μmol)	% of the dose	Total dose (mg)	Accum. P^+ (μmol)	Accum. % of the dose
01	7/27	375	7.06/6.83	0.71/0.68	375	7.06/6.83	0.71/0.68
02	7/28	370	14.55/13.96	1.48/1.42	745	21.61/20.79	1.09/1.05
03	7/29	500	17.50/15.15	1.32/1.14	1245	39.11/35.94	1.18/1.09
04	7/30	390	23.86/19.55	2.30/1.88	1635	62.97/55.49	1.45/1.28
05	7/31	232	24.95/17.61	4.04/2.85	1867	87.92/73.10	1.77/1.47
06	8/01	120	20.82/13.19	6.52/4.13	1987	108.74/86.29	2.06/1.63
07	8/02	120	18.29/9.89	5.73/3.10	2107	127.03/96.18	2.27/1.72
08	8/03	45	11.85/8.25	9.90/6.89	2152	138.88/104.43	2.43/1.82
09	8/04	14	12.25/7.19	32.90/19.31	2166	151.13/111.62	2.62/1.94
10	8/05	2	10.06/4.84	189.1/91.0	2168	161.19/116.46	2.80/2.02
11	8/06	0	5.88/2.93		2168	167.07/119.39	2.90/2.07
12	8/07	0	4.35/1.45		2168	171.42/120.84	2.97/2.10 **T**
13	8/08	0	2.39/1.33		2168	173.81/122.17	3.01/2.12 **T**
14	8/09	0	1.46/0.96		2168	175.27/123.13	3.04/2.14 **T**
15	8/10	0	1.43/0.89		2168	176.70/124.02	3.06/2.15 **T**

16	8/11	0	1.28/ -		2168	177.98/124.02	3.09/2.15 **T**
17	8/12	0	0.94/ -		2168	178.92/124.02	3.10/2.15

Transient tremor (**T**) after drug tapered, resolved prior to discharge.

Patient #6

Sample	Date	HP dose (mg)	R^+/H^+ (μmol)	% of the dose	Total dose (mg)	Accum. P^+ (μmol)	Accum. % of the dose
01	8/01	55	0.19/0.17	0.13/0.12	55	0.19/0.17	0.13/0.12
02	8/02	72	0.57/0.39	0.30/0.20	127	0.76/0.56	0.23/0.17
03	8/03	72	0.77/0.50	0.40/0.26	199	1.53/1.06	0.29/0.20
04	8/04	56	1.30/0.86	0.87/0.58	255	2.83/1.92	0.42/0.28
05	8/05	48	0.84/0.47	0.66/0.37	303	3.67/2.39	0.46/0.30
06	8/06	48	0.47/0.29	0.37/0.23	351	4.14/2.68	0.44/0.29
07	8/07	48	0.49/0.28	0.38/0.22	399	4.63/2.96	0.44/0.28
08	8/08	64	0.40/0.29	0.24/0.17	463	5.03/3.25	0.41/0.26
09	8/09	77	0.41/0.31	0.20/0.15	540	5.44/3.56	0.38/0.25
10	8/10	60	0.50/0.38	0.31/0.24	600	5.94/3.94	0.37/0.25
11	8/11	25	0.63/ -	0.95/ -	625	6.57/3.94	0.40/0.24

12	8/12	15	0.44/0.15	1.10/0.38	640	7.01/4.09	0.41/0.24
13	8/13	35	0.23/0.18	0.25/0.19	675	7.24/4.27	0.40/0.24
14	8/14	5	0.15/ -	1.13/ -	680	7.39/4.27	0.41/0.24
15	8/15	0	0.19/ -		680	7.58/4.27	0.42/0.24
16	8/16	0	0.14/ -		680	7.72/4.27	0.43/0.24
17	8/17	0	0.19/-		680	7.91/4.27	0.44/0.24
18	8/18	0	-/-		680	7.91/4.27	0.44/0.24
19	8/19	0	-/-		680	7.91/4.27	0.44/0.24
20	8/20	0	0.31/-		680	8.22/4.27	0.45/0.24
21	8/21	0	0.21/-		680	8.43/4.27	0.47/0.24
22	8/22	0	0.18/-		680	8.61/4.27	0.48/0.24
23	8/23	0	0.29/-		680	8.90/4.27	0.49/0.24
24	8/24	0	-/-		680	8.90/4.27	0.49/0.24

No movement disorders.

Patient #7

Sample	Date	HP dose (mg)	R+/H+ (μmol)	% of the dose	Total dose (mg)	Accum. P+ (μmol)	Accum. % of the dose
01	8/19	120	0.41/-	0.13/-	120	0.41/-	0.13/-
02	8/20	109	0.89/1.11	0.31/0.38	229	1.30/1.11	0.21/0.18
03	8/21	16	0.83/0.65	1.95/1.53	245	2.13/1.76	0.33/0.27
04	8/22	0	0.99/-		245	3.12/1.76	0.48/0.27
05	8/23	0	0.51/-		245	3.63/1.76	0.56/0.27

No movement disorders.

Patient #8

Sample	Date	HP dose (mg)	R+/H+ (μmol)	% of the dose	Total dose (mg)	Accum. P+ (μmol)	Accum. % of the dose
01	8/25	80	0.83/1.50	0.39/0.71	80	0.83/1.50	0.39/0.71
02	8/26	84	0.75/0.93	0.34/0.42	164	1.58/2.43	0.36/0.56
03	8/27	117	1.04/1.06	0.33/0.34	281	2.62/3.49	0.35/0.47
04	8/28	125	0.97/0.87	0.29/0.26	406	3.59/4.36	0.33/0.40
05	8/29	125	0.76/0.59	0.23/0.18	531	4.35/4.95	0.31/0.35
06	8/30	138	1.14/0.50	0.31/0.14	669	5.49/5.45	0.31/0.31

07	8/31	32	1.28/0.68	1.50/0.80	701	6.77/6.13	0.36/0.33
08	9/1	14	0.93/0.21		715	7.70/6.34	0.40/0.33
09	9/2	0	0.77/0.25		715	8.47/6.59	0.45/0.35
10	9/3	0	0.84/-		715	9.31/6.59	0.49/0.35
11	9/4	0	0.91/-		715	10.22/6.59	0.54/0.35
12	9/5	0	0.59/-		715	10.81/6.59	0.57/0.35
13	9/6	0	0.33/-		715	11.14/6.59	0.59/0.35
14	9/7	0	0.31/-		715	11.45/6.59	0.60/0.35
15	9/8	0	0.25/-		715	11.70/6.59	0.62/0.35
16	9/9	0	0.18/-		715	11.88/6.59	0.62/0.35
17	9/10	0	0.35/-		715	12.23/6.59	0.64/0.35
18	9/11	0	0.16/-		715	12.39/6.59	0.65/0.35

No movement disorders.

Patient #9

Sample	Date	HP dose (mg)	R^+/H^+ (μmol)	% of the dose	Total dose (mg)	Accum. P^+ (μmol)	Accum. % of the dose
01	9/07	230	0.33/0.13	0.05/0.02	230	0.33/0.13	0.05/0.02
02	9/08	240	0.77/0.29	0.12/0.05	470	1.10/0.42	0.09/0.03
03	9/09	280	1.56/0.47	0.21/0.06	750	2.66/0.89	0.13/0.04
04	9/10	260	1.54/0.43	0.22/0.06	1010	4.20/1.32	0.16/0.05
05	9/11	250	2.76/0.64	0.42/0.10	1260	6.96/1.96	0.21/0.06
06	9/12	240	5.99/1.31	0.94/0.21	1500	12.95/3.27	0.32/0.08
07	9/13	245	6.35/1.55	0.97/0.24	1745	19.30/4.82	0.42/0.10
08	9/14	250	7.51/2.34	1.13/0.35	1995	26.81/7.16	0.51/0.13
09	9/15	240	2.13/0.85	0.33/0.13	2235	28.94/8.01	0.49/0.13
10	9/16	240	6.76/2.43	1.06/0.38	2475	35.70/10.44	0.54/0.16
11	9/17	240	2.52/0.81	0.39/0.13	2715	38.22/11.25	0.53/0.16
12	9/18	240	4.68/2.31	0.73/0.36	2955	42.90/13.56	0.55/0.17
13	9/19	240	6.74/1.08	1.06/0.17	3195	49.64/14.64	0.58/0.17
14	9/20	240	3.20/2.66	0.50/0.42	3435	52.84/17.30	0.58/0.19
15	9/21	207	6.50/5.74	1.18/1.04	3642	59.34/23.04	0.61/0.24

16	9/22	159	6.62/7.14	1.57/1.69	3801	65.96/30.18	0.65/0.30
17	9/23	144	4.61/3.77	1.20/0.98	3945	70.57/33.95	0.67/0.32
18	9/24	103	10.23/7.78	3.73/2.84	4048	80.80/41.73	0.75/0.39
19	9/25	96	9.98/7.16	3.91/2.80	4144	90.78/48.89	0.82/0.44
20	9/26	61	7.73/4.50	4.76/2.77	4205	98.51/53.59	0.88/0.48
21	9/27	2	5.76/2.95	108.3/55.46	4207	104.27/56.34	0.93/0.50
22	9/28	0	9.10/3.69		4207	113.37/60.03	1.01/0.54 **T**
23	9/29	0	1.45/0.32		4207	114.82/60.35	1.03/0.54 **T**
24	9/30	0	2.64/0.68		4207	117.46/61.03	1.05/0.55 **T**
25	10/1	0	1.62/0.38		4207	119.08/61.41	1.06/0.55 **T**
26	10/2	0	0.89/-		4207	119.97/61.41	1.07/0.55 **T**
27	10/3	0	0.55/-		4207	120.52/61.41	1.08/0.55 **T**
28	10/1	0	0.53/0.20		4207	121.05/61.41	1.08/0.55 **T**
29	10/2	0	0.40/-		4207	121.45/61.41	1.09/0.55 **T**
30	10/3	0	0.05/-		4207	121.50/61.41	1.09/0.55 **T**

Tremor resolved by 10/13.

Patient #10

Sample	Date	HP dose (mg)	R^+/H^+ (μmol)	% of the dose	Total dose (mg)	Accum. P^+ (μmol)	Accum. % of the dose
01	10/4	215	0.71/1.68	0.12/0.29	215	0.71/1.68	0.12/0.29
02	10/5	195	1.58/3.61	0.30/0.70	410	2.29/5.29	0.21/0.49
03	10/6	180	2.33/2.39	0.49/0.49	590	4.62/7.68	0.29/0.49
04	10/7	120	3.09/4.53	0.97/1.42	710	7.71/12.21	0.41/0.65
05	10/8	67	2.35/2.84	1.32/1.59	777	10.06/15.05	0.49/0.73
06	10/9	95	3.02/2.92	0.53/0.51	872	13.08/17.97	0.50/0.68
	and						
	10/10	120			992		
07	10/11	120	6.81/4.78	1.07/0.75	1112	19.89/22.75	0.61/0.69
	and						
	10/12	120			1232		
08	10/13	119	5.02/6.67	1.59/2.11	1351	24.91/29.42	0.69/0.82
09	10/14	95	1.70/1.45	0.67/0.57	1446	26.61/30.87	0.69/0.80
10	10/15	72	2.50/2.07	1.31/1.08	1518	29.11/32.94	0.72/0.82
11	10/16	48	2.39/1.64	1.87/1.28	1566	31.50/34.58	0.76/0.83

12	10/17	22	1.39/0.73	2.38/1.25	1588	32.89/35.31	0.78/0.84
13	10/18	0	1.66/-		1588	34.55/35.31	0.82/0.84
14	10/19	0	0.81/-		1588	35.36/35.31	0.84/0.84
15	10/20	0	0.46/-		1588	35.82/35.31	0.85/0.84

Patient #1

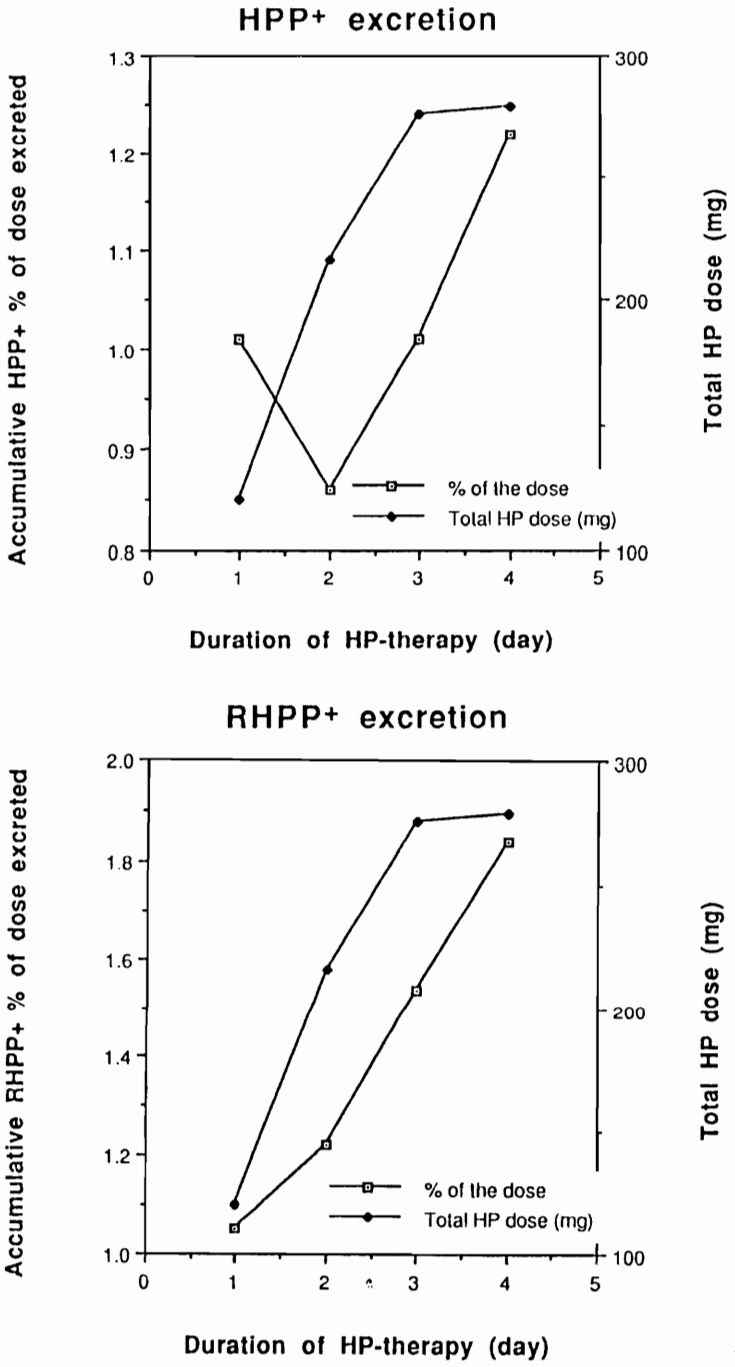

Figure 48. Plots of the accumulative % of RHPP+ and HPP+ in the urine and total HP dose (mg) versus duration of therapy (continue to the page 212).

Patient #2

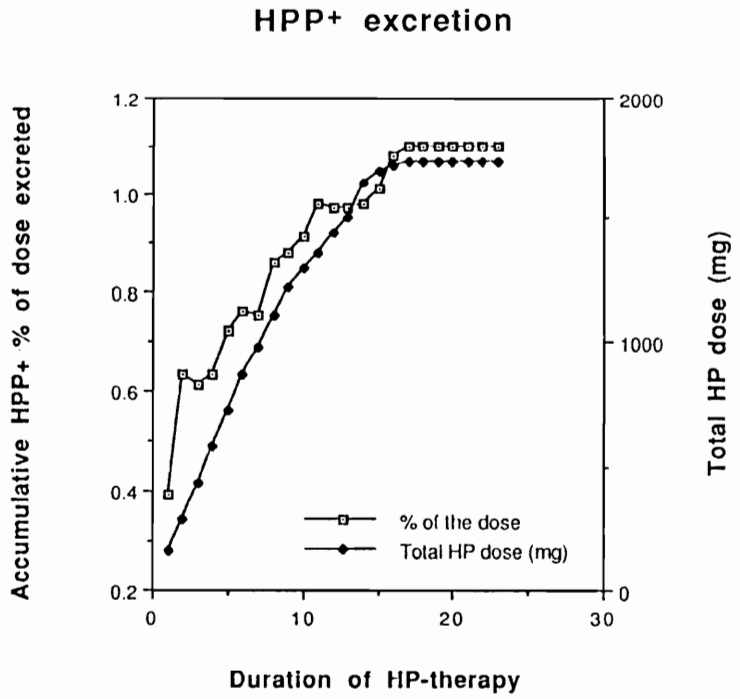
HPP+ excretion
Accumulative HPP+ % of dose excreted
1.2
1.0
0.8
0.6
0.4
0.2
2000
1000
0
Total HP dose (mg)
% of the dose
Total HP dose (mg)
0
10
20
30
Duration of HP-therapy

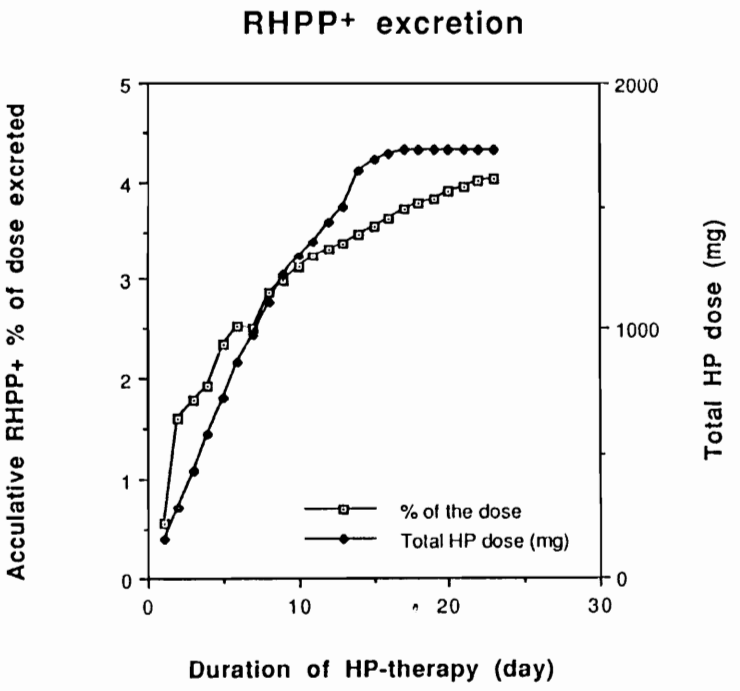
RHPP+ excretion
Acculative RHPP+ % of dose excreted
5
4
3
2
1
0
2000
1000
0
Total HP dose (mg)
% of the dose
Total HP dose (mg)
0
10
20
30
Duration of HP-therapy (day)

Patient #3

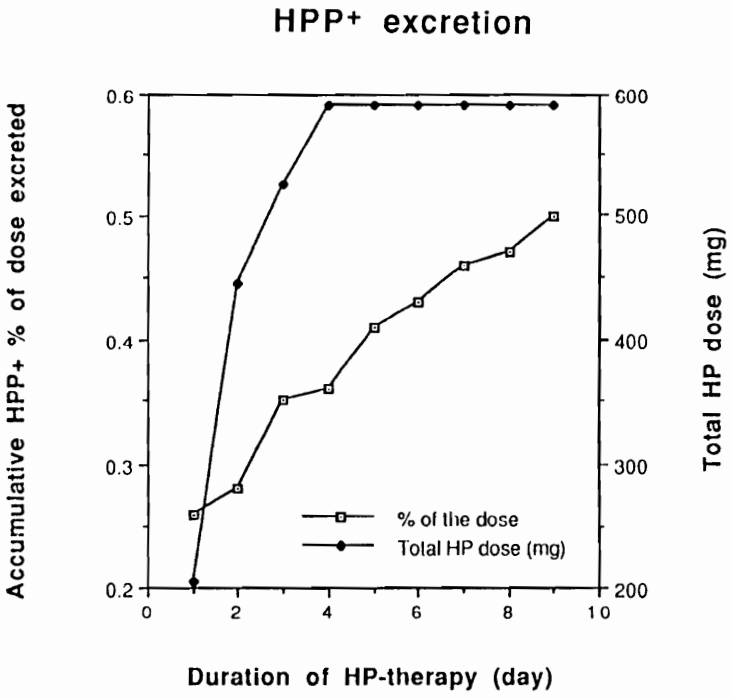
HPP+ excretion
Accumulative HPP+ % of dose excreted
Total HP dose (mg)
% of the dose
Total HP dose (mg)
Duration of HP-therapy (day)

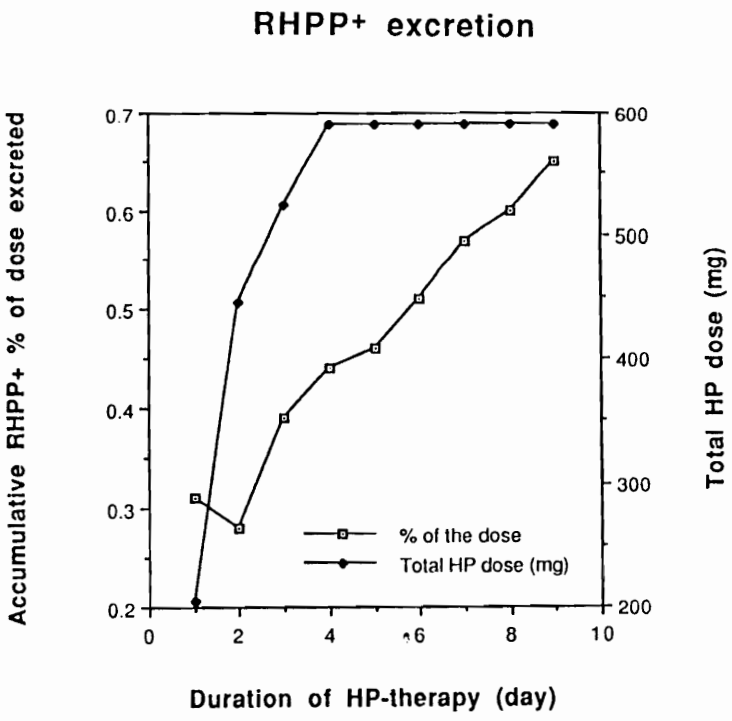
RHPP+ excretion
Accumulative RHPP+ % of dose excreted
Total HP dose (mg)
% of the dose
Total HP dose (mg)
Duration of HP-therapy (day)

Patient #4

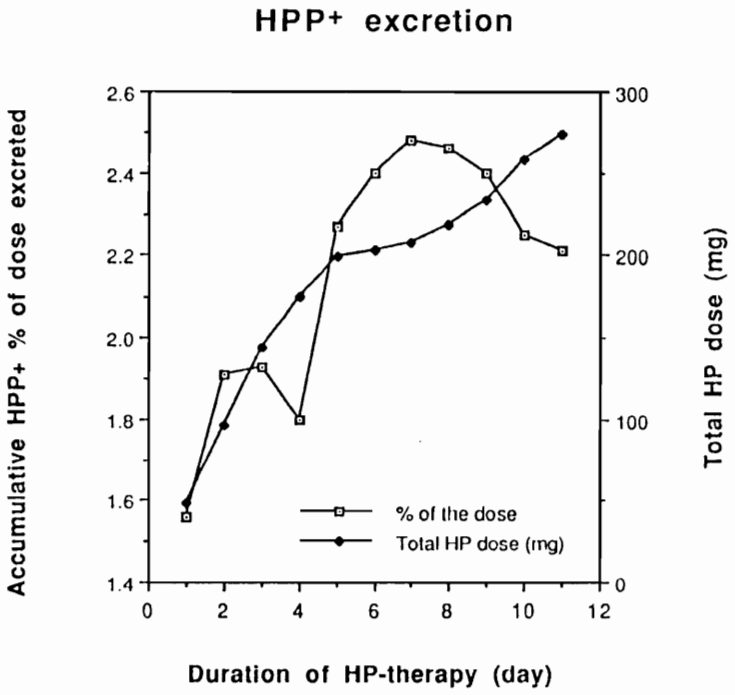
HPP+ excretion
Accumulative HPP+ % of dose excreted
Total HP dose (mg)
% of the dose
Total HP dose (mg)
Duration of HP-therapy (day)

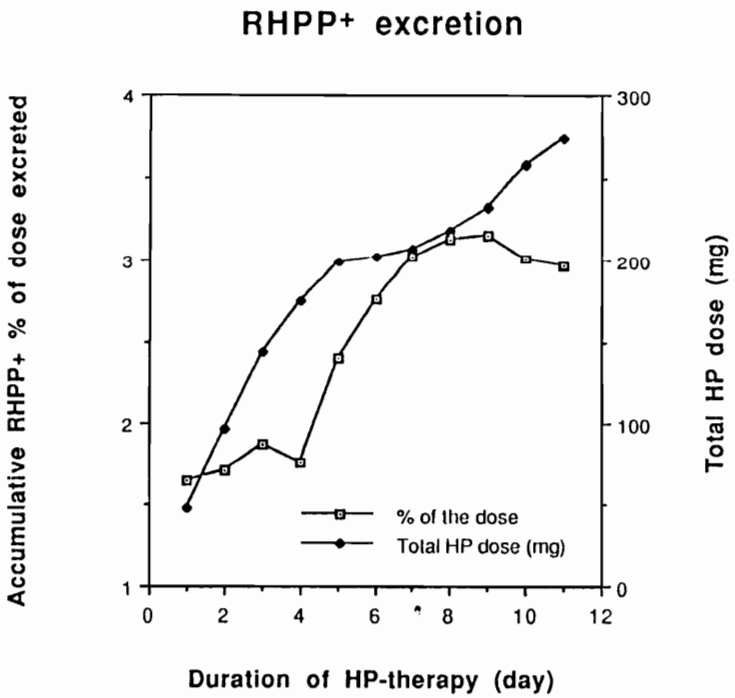
RHPP+ excretion
Accumulative RHPP+ % of dose excreted
Total HP dose (mg)
% of the dose
Total HP dose (mg)
Duration of HP-therapy (day)

Patient #5

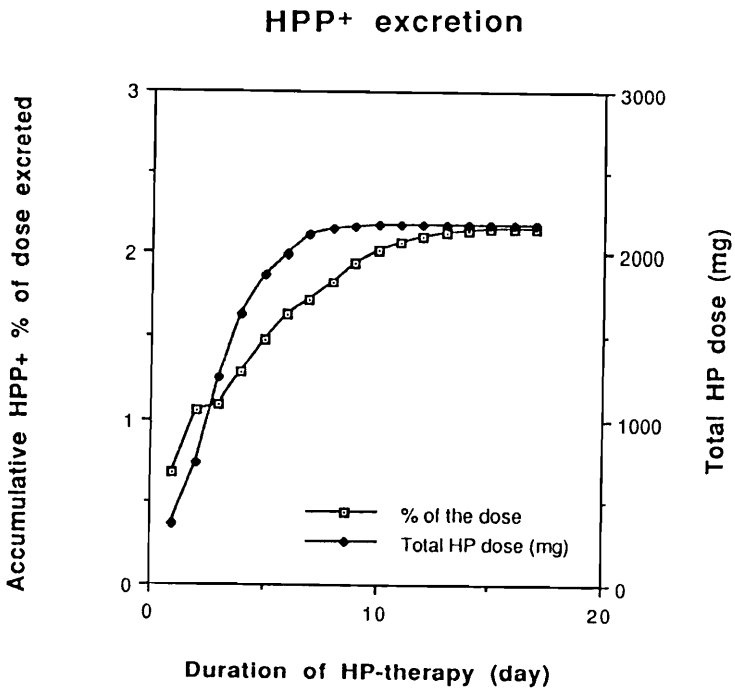
HPP+ excretion
Accumulative HPP+ % of dose excreted
Total HP dose (mg)
% of the dose
Total HP dose (mg)
Duration of HP-therapy (day)
0
1
2
3
0
1000
2000
3000
0
10
20

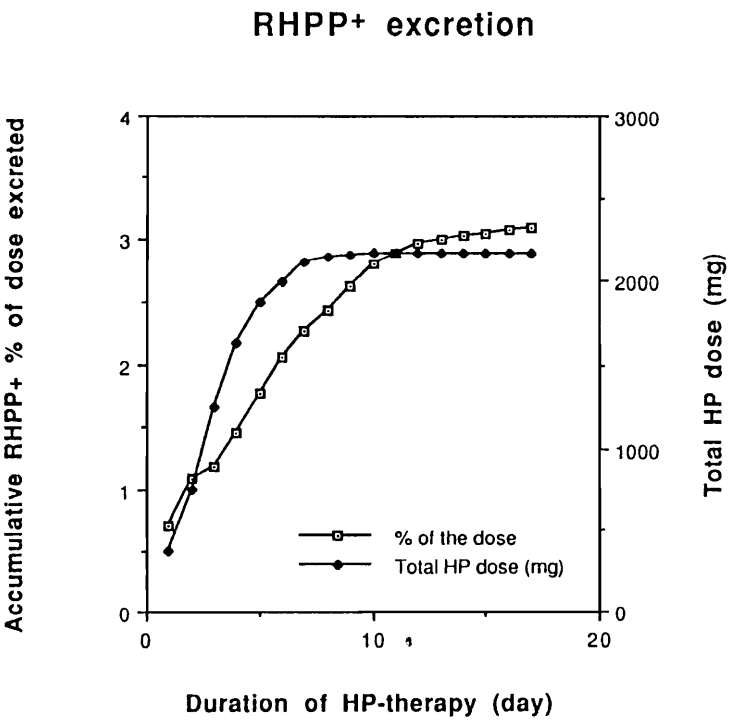
RHPP+ excretion
Accumulative RHPP+ % of dose excreted
Total HP dose (mg)
% of the dose
Total HP dose (mg)
Duration of HP-therapy (day)
0
1
2
3
4
0
1000
2000
3000
0
10
20

Patient #6

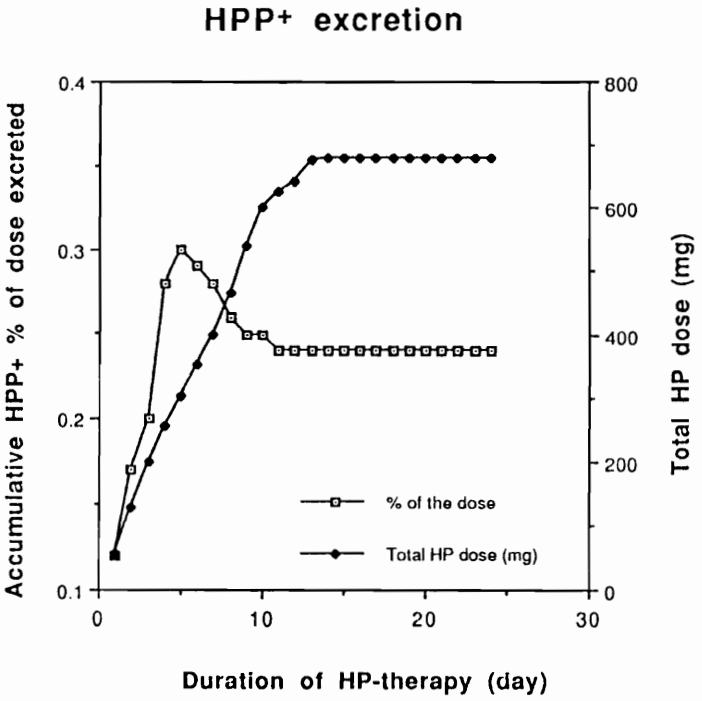
HPP+ excretion
Accumulative HPP+ % of dose excreted
Total HP dose (mg)
% of the dose
Total HP dose (mg)
Duration of HP-therapy (day)
0.4
0.3
0.2
0.1
800
600
400
200
0
0
10
20
30

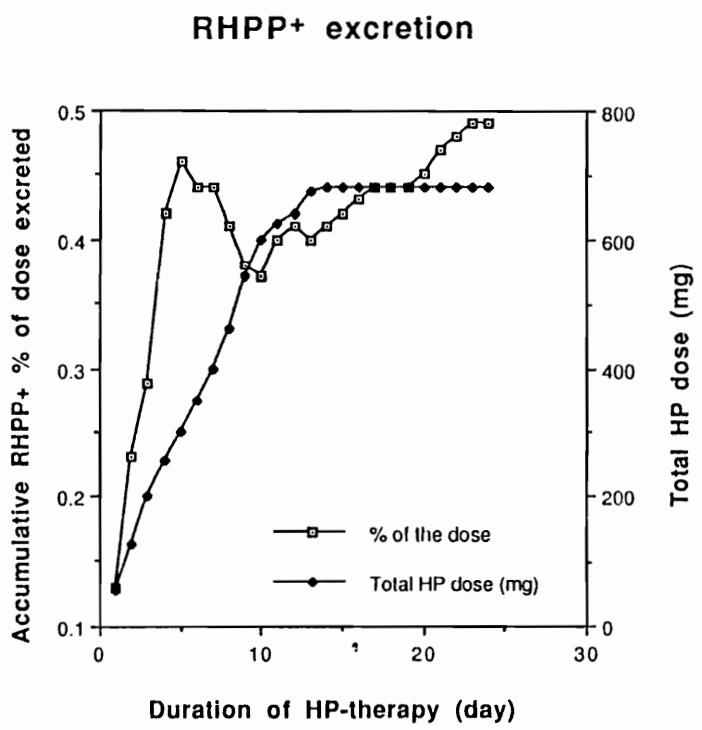
RHPP+ excretion
Accumulative RHPP+ % of dose excreted
Total HP dose (mg)
% of the dose
Total HP dose (mg)
Duration of HP-therapy (day)
0.5
0.4
0.3
0.2
0.1
800
600
400
200
0
0
10
20
30

Patient #7

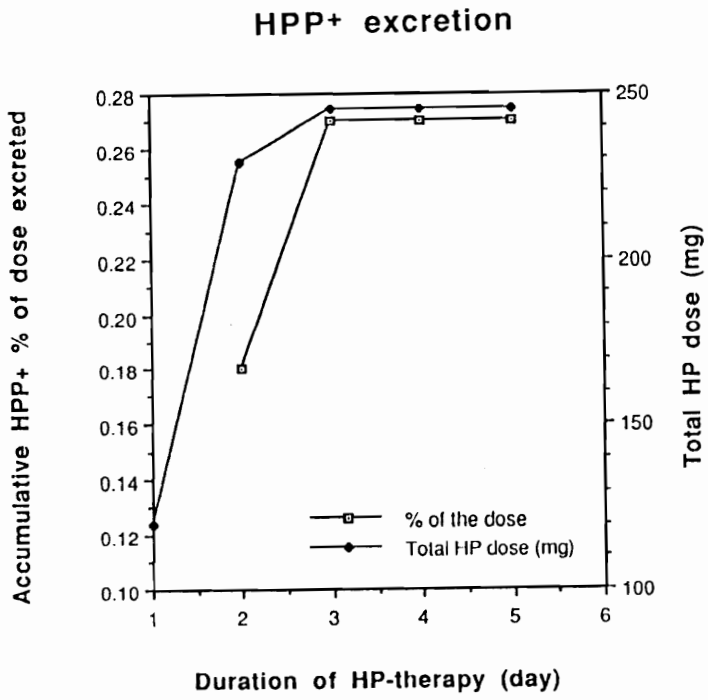
HPP+ excretion
Accumulative HPP+ % of dose excreted
0.28
0.26
0.24
0.22
0.20
0.18
0.16
0.14
0.12
0.10
250
200
150
100
Total HP dose (mg)
% of the dose
Total HP dose (mg)
1
2
3
4
5
6
Duration of HP-therapy (day)

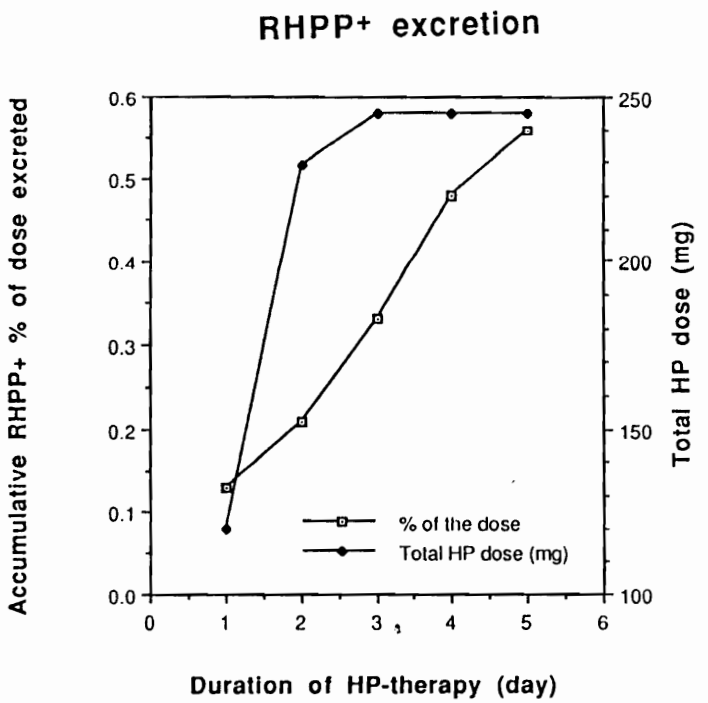
RHPP+ excretion
Accumulative RHPP+ % of dose excreted
0.6
0.5
0.4
0.3
0.2
0.1
0.0
250
200
150
100
Total HP dose (mg)
% of the dose
Total HP dose (mg)
0
1
2
3
4
5
6
Duration of HP-therapy (day)

Patient #8

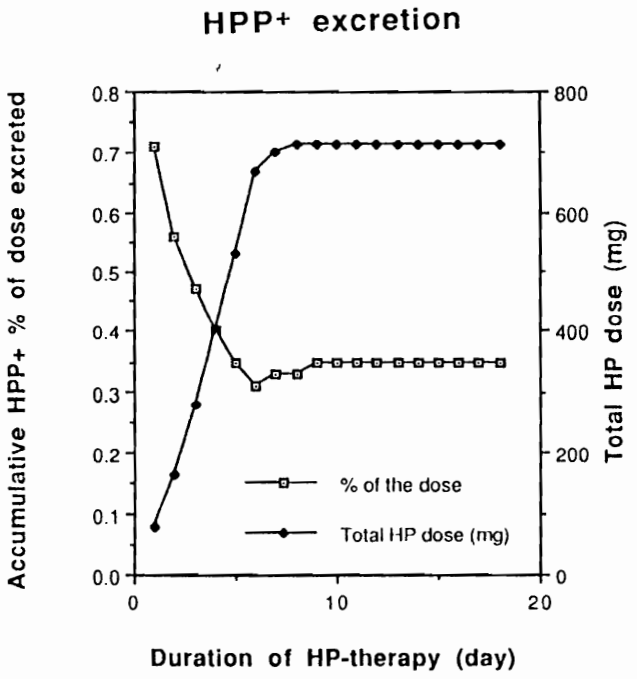
HPP+ excretion
Accumulative HPP+ % of dose excreted
Total HP dose (mg)
% of the dose
Total HP dose (mg)
Duration of HP-therapy (day)
0.0
0.1
0.2
0.3
0.4
0.5
0.6
0.7
0.8
0
200
400
600
800
0
10
20

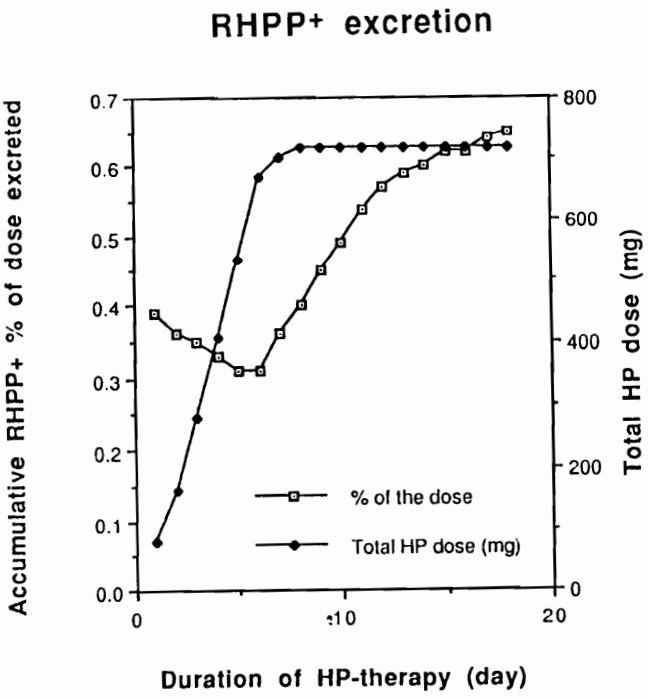
RHPP+ excretion
Accumulative RHPP+ % of dose excreted
Total HP dose (mg)
% of the dose
Total HP dose (mg)
Duration of HP-therapy (day)
0.0
0.1
0.2
0.3
0.4
0.5
0.6
0.7
0
200
400
600
800
0
10
20

Patient #9

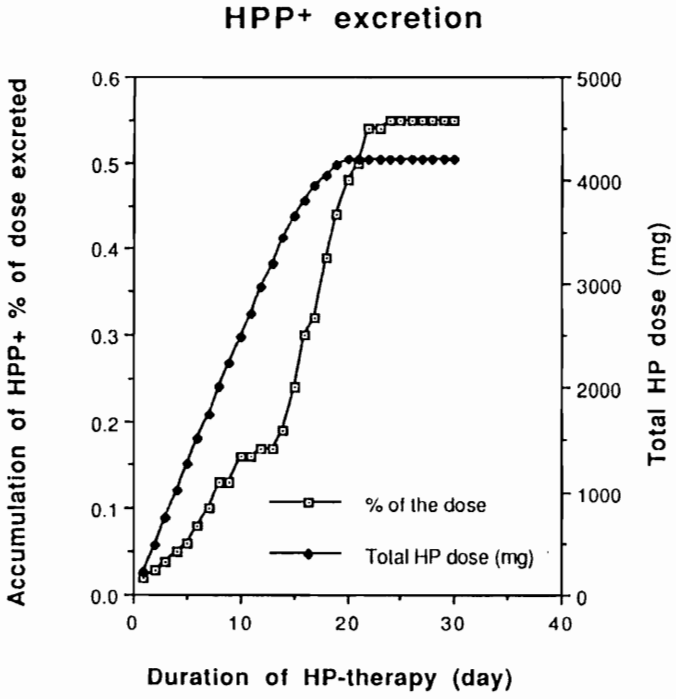
HPP+ excretion
Accumulation of HPP+ % of dose excreted
Total HP dose (mg)
% of the dose
Total HP dose (mg)
Duration of HP-therapy (day)
0.0
0.1
0.2
0.3
0.4
0.5
0.6
0
1000
2000
3000
4000
5000
0
10
20
30
40

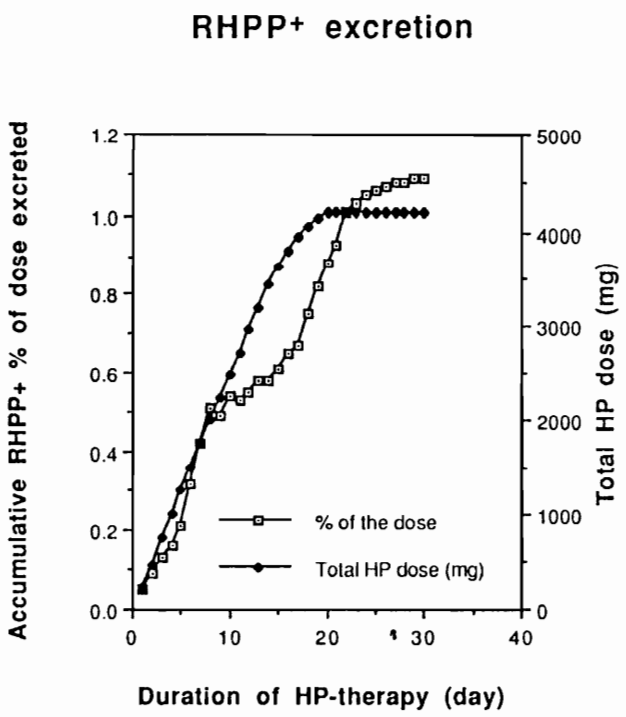
RHPP+ excretion
Accumulative RHPP+ % of dose excreted
Total HP dose (mg)
% of the dose
Total HP dose (mg)
Duration of HP-therapy (day)
0.0
0.2
0.4
0.6
0.8
1.0
1.2
0
1000
2000
3000
4000
5000
0
10
20
30
40

Patient #10

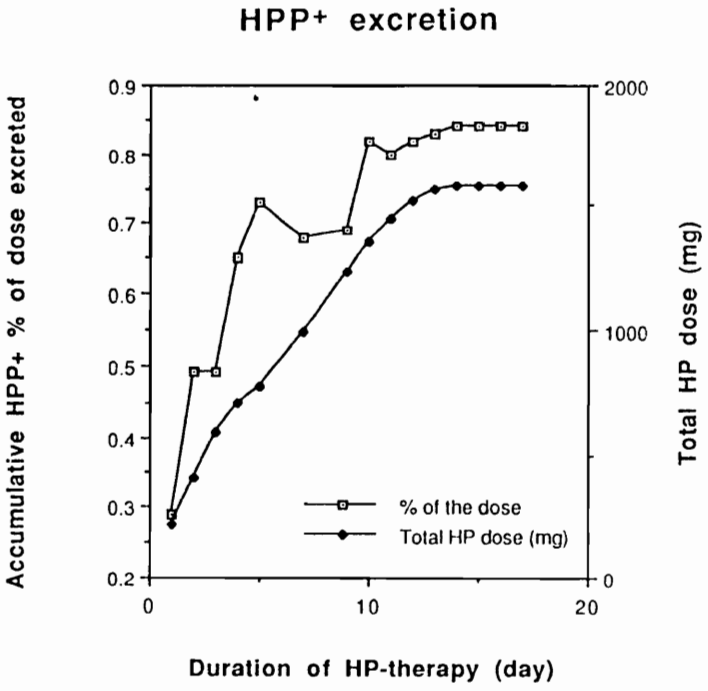
HPP+ excretion
Accumulative HPP+ % of dose excreted
Total HP dose (mg)
% of the dose
Total HP dose (mg)
Duration of HP-therapy (day)

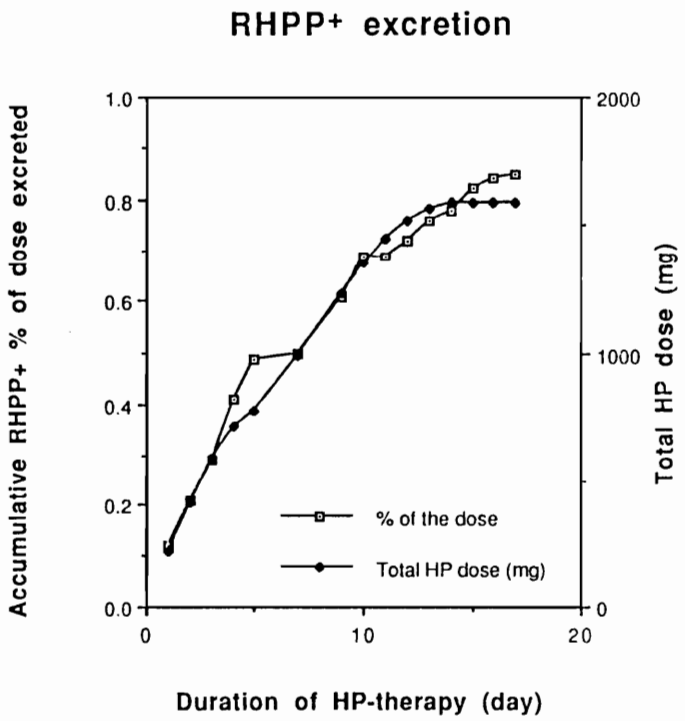
RHPP+ excretion
Accumulative RHPP+ % of dose excreted
Total HP dose (mg)
% of the dose
Total HP dose (mg)
Duration of HP-therapy (day)

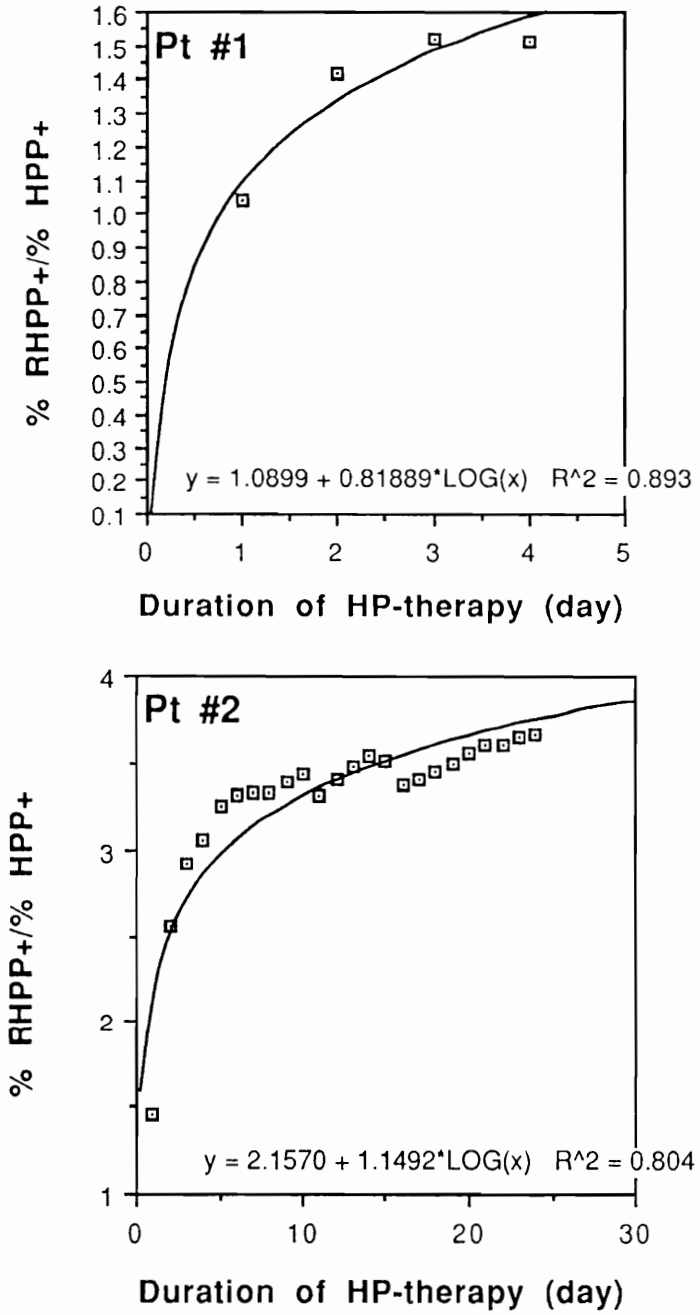

Figure 49. Plots of the accumulative % RHPP+/% HPP+ excreted in urine plotted against duration of therapy (continue to page 217).

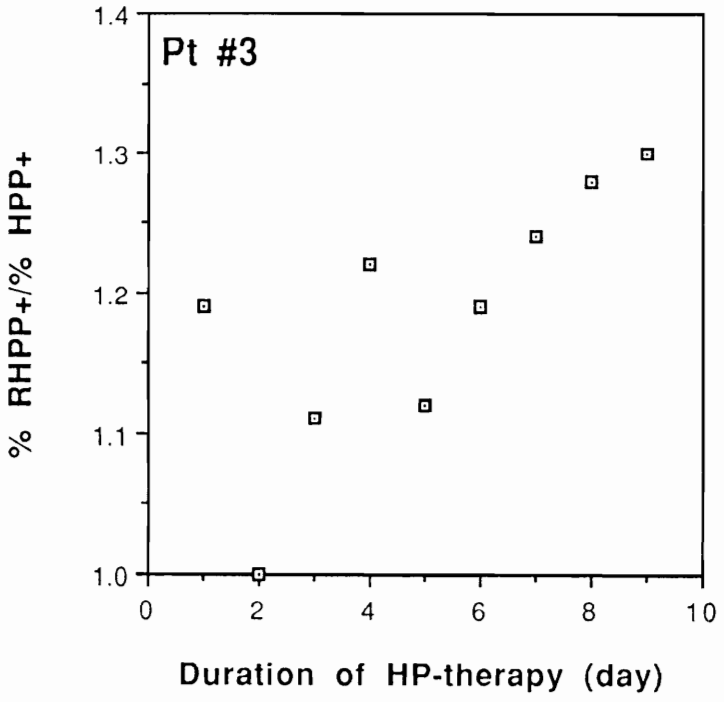
Pt #3
% RHPP+/% HPP+
1.4
1.3
1.2
1.1
1.0
0
2
4
6
8
10
Duration of HP-therapy (day)

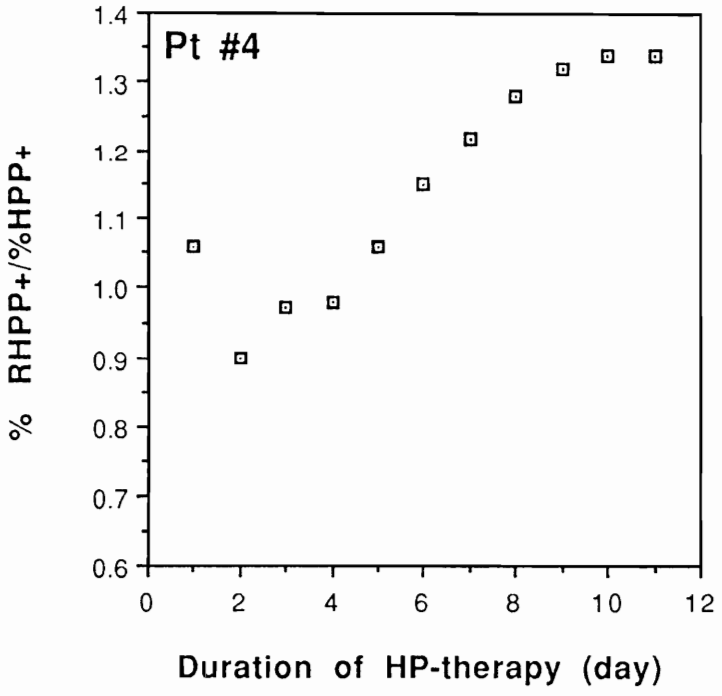
Pt #4
% RHPP+/%HPP+
1.4
1.3
1.2
1.1
1.0
0.9
0.8
0.7
0.6
0
2
4
6
8
10
12
Duration of HP-therapy (day)

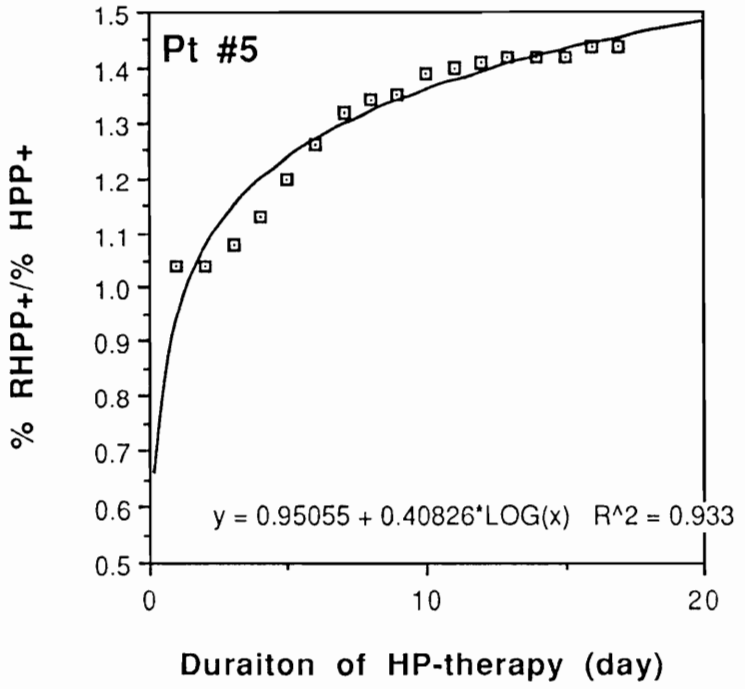
Pt #5
% RHPP+/% HPP+
y = 0.95055 + 0.40826*LOG(x) R^2 = 0.933
Duraiton of HP-therapy (day)

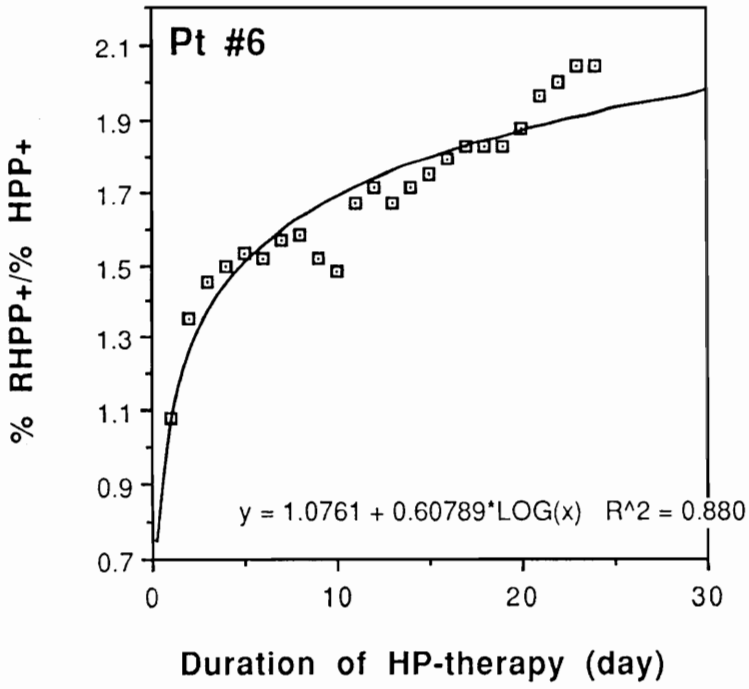
Pt #6
% RHPP+/% HPP+
y = 1.0761 + 0.60789*LOG(x) R^2 = 0.880
Duration of HP-therapy (day)

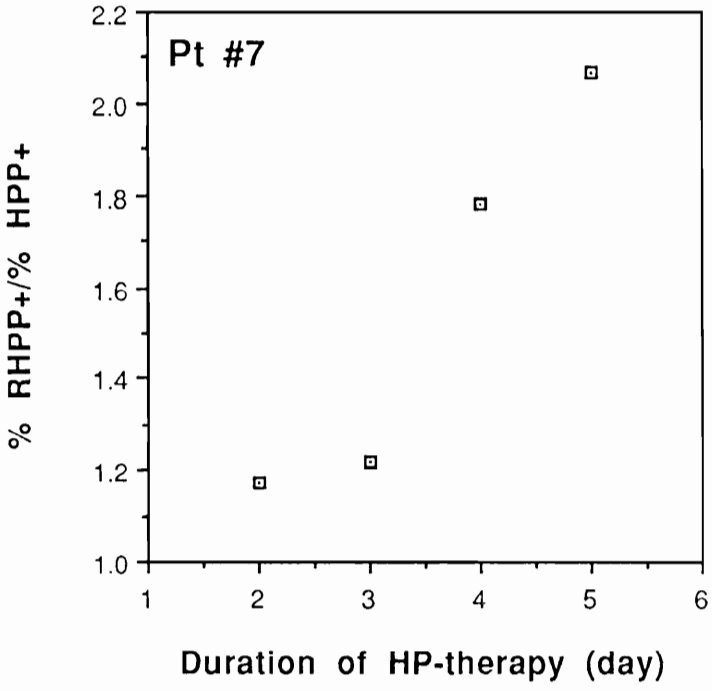
Pt #7
% RHPP+/% HPP+
2.2
2.0
1.8
1.6
1.4
1.2
1.0
1
2
3
4
5
6
Duration of HP-therapy (day)

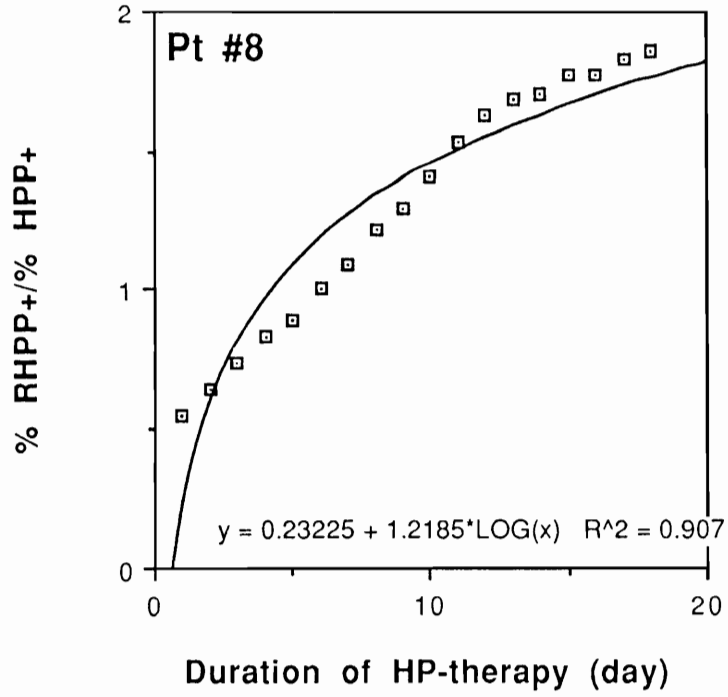
Pt #8
% RHPP+/% HPP+
2
1
0
y = 0.23225 + 1.2185*LOG(x) R^2 = 0.907
0
10
20
Duration of HP-therapy (day)

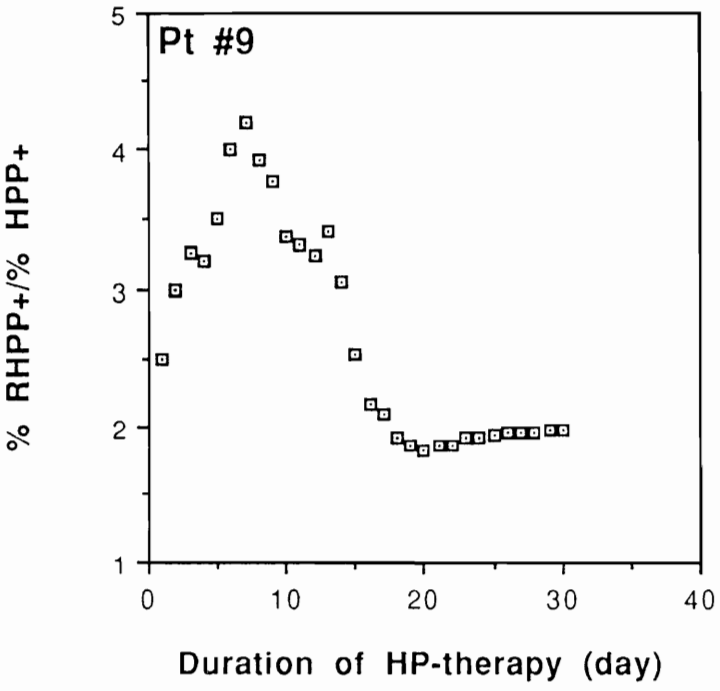
Pt #9
% RHPP+/% HPP+
5
4
3
2
1
0
10
20
30
40
Duration of HP-therapy (day)

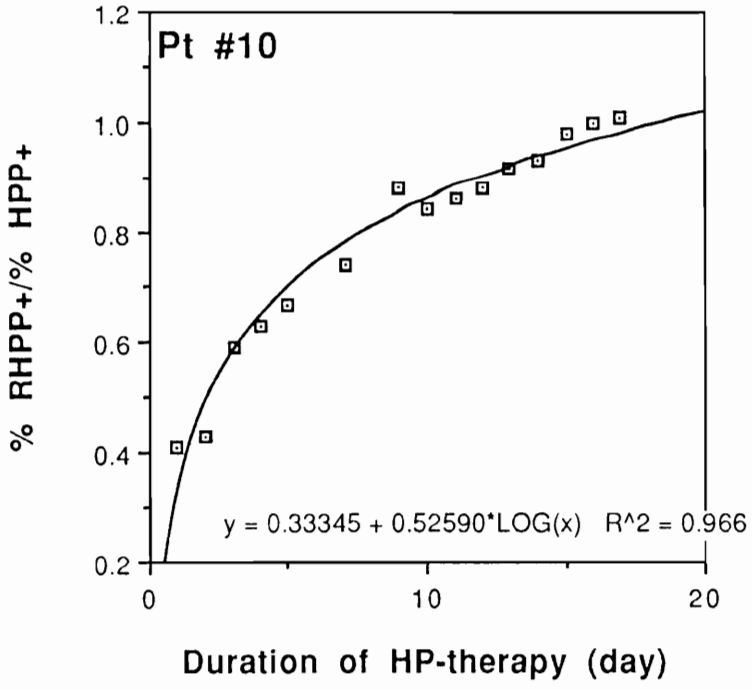
Pt #10
% RHPP+/% HPP+
1.2
1.0
0.8
0.6
0.4
0.2
0
10
20
y = 0.33345 + 0.52590*LOG(x) R^2 = 0.966
Duration of HP-therapy (day)

Experimental

(1) Protocol. The adult ICU patients with agitation refractory to intermittent parenteral benzodiazepines, narcotics, and HP were treated with continuous infusion of HP. The decision to begin or end this therapy and the doses were selected by the treating physician. Daily doses were tabulated and movement disorders were identified using the Abnormal Involuntary Movement Scale (AIMS) with daily assessment during and for 10 days following continuous HP use. The urine samples were collected synchronously with these infusions so that sample #1-01 was collected during the same time the patient 1 was receiving 120 mg (see Table 26).

(2) HPLC analysis. Since we received frozen urine samples (10 mL each), first samples were thawed and vortexed. A 400-μL aliquot of sample was loaded on Sep-pak cartridge. Sample processes and HPLC conditions are the same as described in Chapter 4.

Chapter 7

Studies on [^{3}H]HPTP Metabolism

In previous in vivo studies of HPTP metabolism, we could not account for the fate of approximately 90% of the parent compound. When HPP^+, one of the metabolites of interest to us, was administered, a maximum of only 20% was recovered in urine and feces. Since our analyses were limited to HPLC/fluorescence and UV detection following HPLC separation, we wanted to use tritium-labeled HPTP in both in vitro and in vivo studies to obtain further insight into the fate and the distribution of HPTP and its metabolites in the body using HPLC/UV-radio chromatography (HPLRC).

Results and Discussion

7.1. Synthesis of [^{3}H]HPTP

The original plan to synthesize [^{3}H]HPTP was via dehydration of commercially available [^{3}H]HP (**33** -> **34**, Scheme 7) by *p*-toluenesulfonic acid in toluene under refluxing conditions. This method worked in the trial experiments using unlabeled HP. However, in the experiment with [^{3}H]HP, all of the tritium was lost in the aqueous fraction during work up. It appeared that [^{3}H]HP was unstable under these conditions (stability of the material is discussed in a later section). Therefore, we needed to find an alternative method to synthesize [^{3}H]HPTP under milder conditions.

After several experiments, the final conditions developed employed treating [^{3}H]HP (14.6 nmol, 1.44 x 10^8 dpm) with 20 equivalents of boron trifluoride diethyl etherate ($BF_3 \cdot OEt_2$, 65 μL, 532 μmol) in dichloromethane

(CH_2Cl_2, 1 mL) for 3 days at room temperature. Unlabeled HP (10 mg, 26.6 μmol) was added to the reaction mixture in order for us to monitor the reaction easier by TLC and GC/MS (Fig. 50). After the work up, the crude product was purified with preparative alumina TLC. The tritium activity in both organic and aqueous fractions from work up was counted by scintillation counter (Beckman LS 3800) and we confirmed that all the tritium activity remained in the organic phase. The final product was stored in ethanol/0.1N HCl (9/1 v/v) solution.

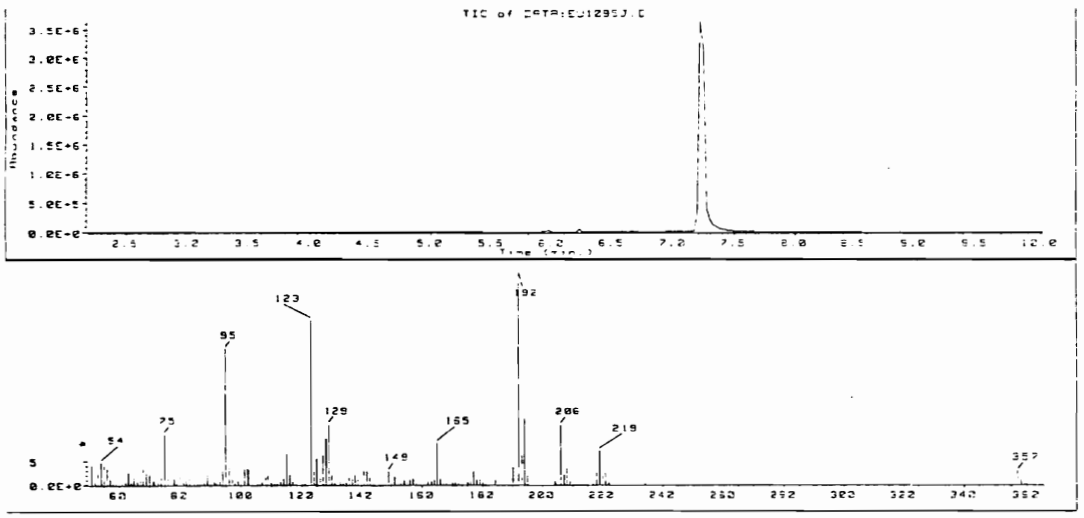

Figure 50. GC/MS spectrum of [^{3}H]HPTP.

The specific activity of the starting material and product were measured as follows: The [^{3}H]-activity of a 5 μL-aliquot of the reaction mixture ([^{3}H]HP in CH_2Cl_2, before the addition of $BF_3{\cdot}OEt_2$) was measured. At the same time, a 5-μL aliquot of the same solution was diluted (~1 in 500) and a UV spectrum was obtained. By knowing its ε value, the concentration of HP or HPTP in the sample was calculated ($A = \varepsilon cl$). Since we know the total volume of the sample, we can calculate both the total amount of the compound and [^{3}H]-activity. Actual [^{3}H] counting is obtained in cpm. However, the specific activity needs to be described as dpm/μmol. It should be remembered that the efficiency of the [^{3}H] counting by scintillation depends on the scintillation cocktail. Normally, if the instrument is working well, the efficiency of [^{3}H] counting should be around 40 %. However, our instrument Beckman LS 3800 had shown a much lower efficiency (5% using Packard Ultima-M, 10% using Fisher, ScintiVerse BD, 12% with ScintiVerse E). In order to estimate the specific activity in dpm/μmol, a known amount of tritiated water standard was added to the samples and the numbers were corrected each time with the aid of this internal standard. The specific activity of the starting material was 5.42×10^6 dpm/μmol and that of the final product [^{3}H]HPTP (after a preparative TLC purification) was 3.01×10^6 dpm/μmol. Therefore about half of the tritium was lost in the reaction. However, the % recovery of HPTP from the purification step by analytical TLC plates was essentially quantitative (determined by obtaining UV spectra for each step).

As mentioned earlier, [^{3}H]HP was unstable when heated in the presence of acid. We found out this [^{3}H]HP (purchased from DuPont) was synthesized by catalytic exchange with T_2O. The tritium was located at the carbon atom α to the carbonyl carbon (according to DuPont) and therefore it was rather labile.

We also encountered the instability problem with [^{3}H]HPTP. After 2 months [^{3}H] HPTP of storage in acidic ethanol solution, the purity of the [^{3}H]HPTP was monitored by HPLC/UV-radio chromatography. A 5 μL-aliquot of the stock solution was diluted in 2 mL of mobile phase to adjust the concentration to be 100 μM. This solution was analyzed. The UV trace showed only one peak corresponding to HPTP. However, 2 peaks were observed in the HPLRC trace (Fig. 51a). One was [^{3}H]HPTP (t_R 14.5 min). The other peak had an earlier retention time (t_R 2.7 min) which suggests that this unknown compound is more polar than HPTP. The ratio of [^{3}H]-activity in the unknown peak to the HPTP peak on the radio chromatography trace was 1/2 when the sample was analyzed 2 months after the compound was stored. The purity of starting material [^{3}H]HP was confirmed by TLC and HPLRC (Fig. 51b) before the reaction. Therefore this 2.7 min peak was not present in the starting material and was derived from [^{3}H]HPTP. This ratio increased to 1/1 after 2 additional months. [^{3}H]HPTP was purified by analytical basic alumina TLC plates (checked by HPLRC, Fig. 51c).

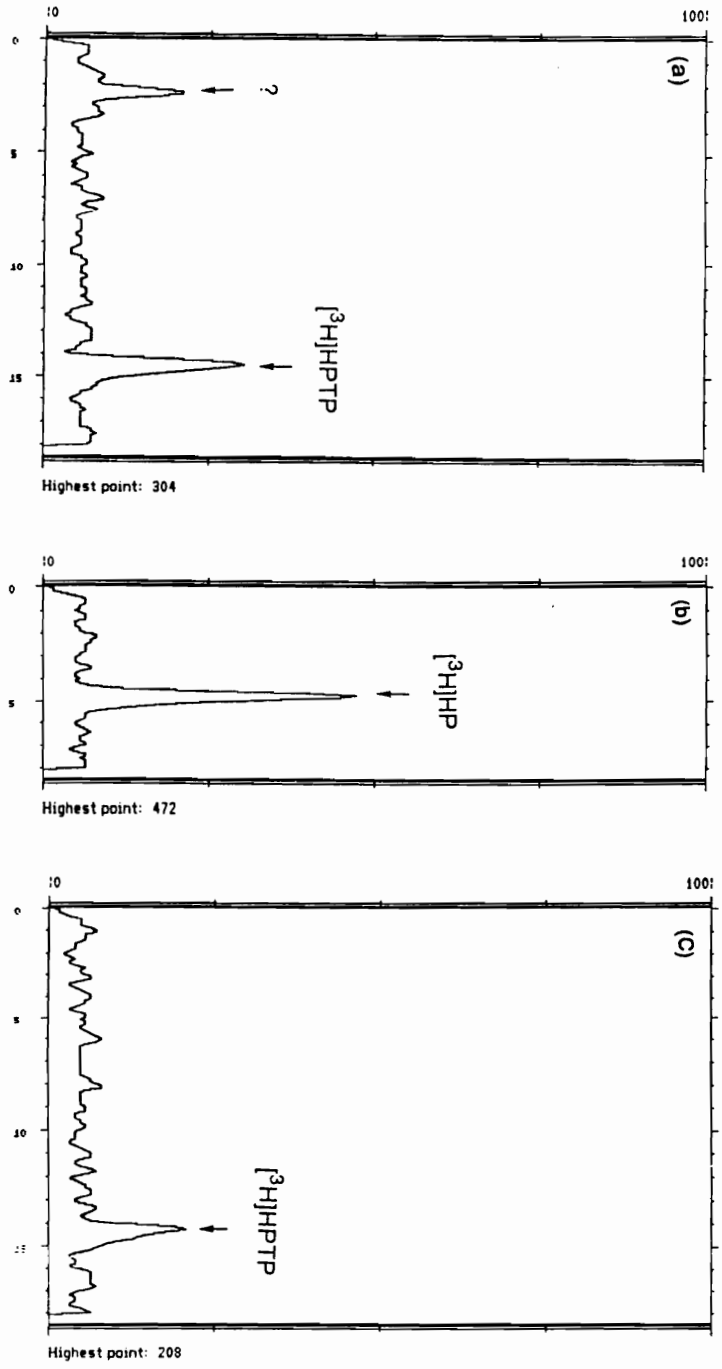

Figure 51. HPLRC tracings of (a) crude [^{3}H]HPTP, (b) starting material [^{3}H]HP and (c) [^{3}H]HPTP after TLC purification.

We attempted to check the stability of HPTP in acidic solution. Unlabeled HPTP was dissolved in 9/1 ethanol/0.1 HCl (the same solvent used with [^{3}H]HPTP) and was kept at room temperature for one week and analyzed by GC/MS. HPTP was the only peak observed in the sample. Therefore, it appears that HPTP is stable in acidic ethanol. The structure of this radioactive material remains unclear. In order to insure accurate data, the sample was purified by preparative TLC prior to biological experiments. The purification was conducted on a small scale to give only the amount needed each time just before the experiment.

7.2. In vitro studies

[^{3}H]HPTP was incubated with C57BL/6 mouse brain homogenates. Results from earlier experiments showed that HPTP and HP are converted to HPP^+ by mouse brain homogenates. HPTP was converted 10 times more efficiently than HP and therefore we have focused on HPTP metabolism in an effort to learn more about brain metabolism, especially to see if there is any other metabolite in the brain. We employed UV and radioactive flow detectors. Brain homogenates (1 mg/mL) were incubated with [^{3}H]HPTP for 0, 30 and 60 minutes. A 10 μL or 20 μL-aliquot of the 5 mM [^{3}H]HPTP solution was added to the incubation mixture (total volume 1 mL) for the final substrate concentration to be 50 μM and 100 μM, respectively. [^{3}H]-activity of 5 mM [^{3}H]HPTP was 7118 dpm/μL. Therefore, 50 μM substrate sample should have 71180 x 10 = 71180 dpm/mL incubation mixture. After the reaction was terminated by the addition of acetonitrile containing 2% acetic acid, the sample was centrifuged and the supernatant was used for [^{3}H]-activity measurement by scintillation counting

and HPLC/fluorescence analysis for quantitation of pyridinium metabolites and HPLC(UV)-radio chromatography (HPLRC) analysis.

Results and discussion

Typical HPLC/UV and HPLRC tracings of the incubation mixtures of [^{3}H]HPTP with mouse brain homogenates are shown in Figure 52 (a) and (b), respectively. Major UV peaks were HPP^+ (t_R 5.5 min) and unchanged HPTP (t_R 13.4 min). RHPTP (t_R 7.2 min) was observed as a minor peak (no quantitation was conducted due to the unknown degradation contaminant peak which somewhat overlaps with RHPTP peak). In HPLRC traces, we observed 2 peaks; the major peak was [^{3}H]HPTP (t_R 14.0 min). From the UV trace and the fact that t_R on the HPLRC is normally 0.4 to 0.7 minutes longer than HPLC/UV, we assumed the other peak (t_R 6.1 min) was HPP^+. By measuring [^{3}H] of the [^{3}H]HPTP by scintillation counting and by HPLRC, we assumed the efficiency of HPLRC was 22 % and [^{3}H]-activity of each peak in HPLRC traces was calculated as HPP^+ (dpm) and HPTP (dpm) and summarized in Table 27. Table 27 also summarizes the recovery of [^{3}H]-activity after the sample processing.

As mentioned earlier, theoretically a [^{3}H]HPTP (50 μM) incubation mixture should have [^{3}H]-activity of 71180 dpm/mL. Thus, a 1200-μL supernatant should contain 71180 x 600/1000 = 42708 dpm. The [^{3}H]-activity of a 100 μL-aliquot of the supernatant was measure and multiplied 1200/100 gave total [^{3}H]-activity in the whole supernatant. This value was compared to the theoretical value and the average % recovery was 88%.

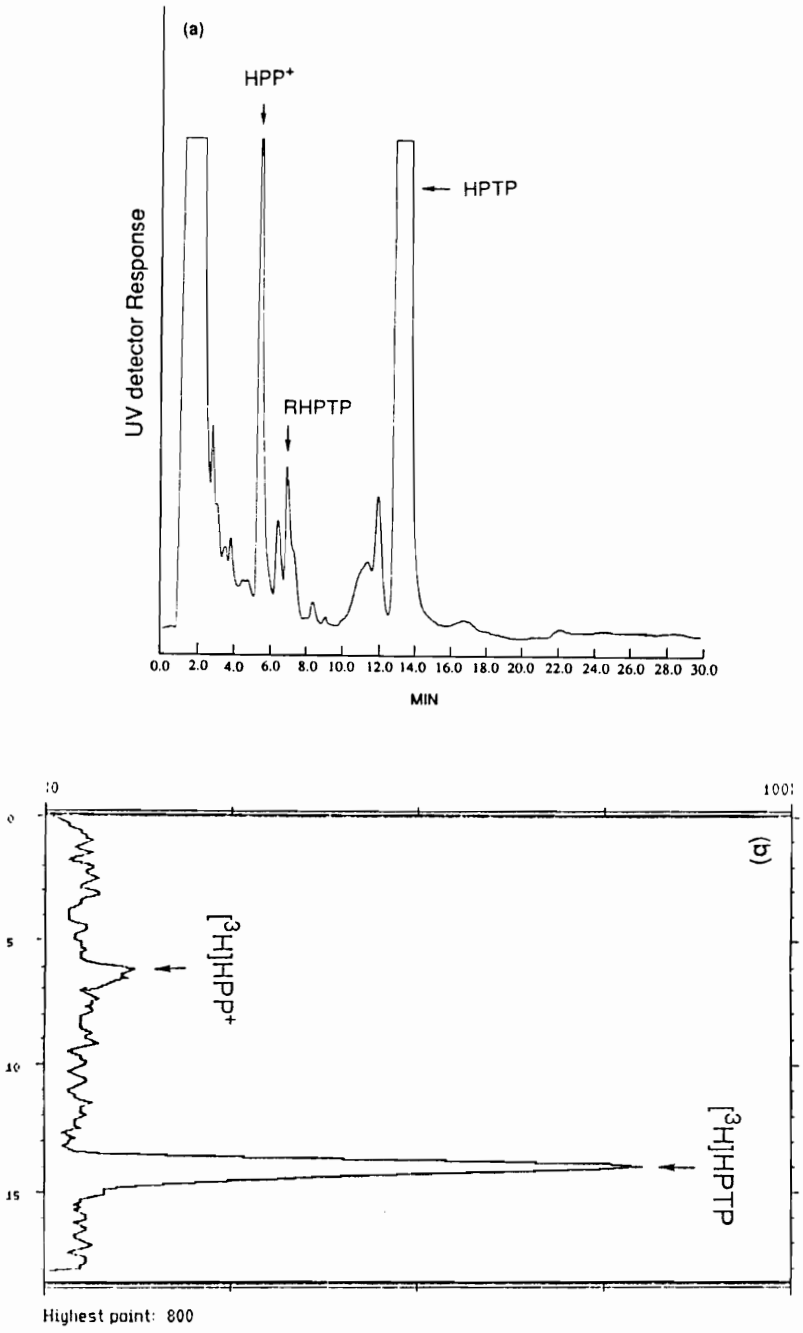

Figure 52. Typical HPLC tracings of [^{3}H]HPTP incubation mixtures with mouse brain homogenates. (a) HPLC/UV and (b) HPLRC.

TABLE 27

Summary of [^{3}H]-activity and distribution

Sample [conc.] incubation time	Theoretical [^{3}H]-activity in 1200 µL (dpm)	100 µL sup x 1200/100 (dpm)	^{3}H on column (dpm)	HPP+ (dpm)[a]	HPTP (dpm)[a]	H+ + HPTP (dpm)[a]
(1) 50 µM 60 min	42078	27204 (65 %)[b]	5790	N.D.[c]	6545 (113 %)	6545 (113 %)
(2) 100 µM 30 min	85416	87588 (103 %)	31841	4436 (14 %)[d]	27564 (87 %)	32000 (101 %)
(3) 100 µM 60 min	85416	87996 (103 %)	36360	4255 (12 %)	29200 (80 %)	33455 (92 %)
(3)' 100 µM 60 min	85416	91536 (107 %)	40734	5564 (14 %)	29200 (72 %)	34764 (86 %)
(4) 50 µM 0 min	42078	39120 (93 %)	15786	N.D.	22218 (>100)	22218 (>100)
(5) 50 µM 0 min, no BH[e]	42078	23652 (56 %)	11756	N.D.	11709 (100 %)	11709 (100 %)

[a]: The efficiency of radio chromatography was assumed to be 22% by ^{3}H counting of [^{3}H]HPTP and HPLRC injection. [b]: % recovery of [^{3}H]-activity considering theoretical [^{3}H]-activity in 1200 µL supernatant as 100%. [c]: Not detectable, signal was not significantly different from noise level. [d]: % recovery

of [^{3}H]-activity considering [^{3}H]-activity injected on HPLC column as 100%. e: Brain Homogenate.

As shown in Figure 52a, HPP^+ was clearly present. We were, however, unable to detect the HPP^+ peak in the HPLRC tracings of samples with 50 μM substrate concentration due to the high noise level in HPLRC tracings. The average % recovery of [^{3}H]HPTP was 104 % for 50 μM substrate and 80 % for 100 μM substrate, respectively.

Unchanged [^{3}H]HPTP concentration in the incubation mixture was measured by HPLC/UV using an external standard calibration curve (0~ 3.75 μM, 4 points). Table 28 summarizes the results.

TABLE 28

HPTP recovery in incubation samples

HPTP concentration in the incubation mixture was measured by HPLC(UV) using external standard calibration curve (o~ 3.75 μM, 4 points).

Sample	[HPTP] in incubation mixture	% recovery
(1) 50 μM, 60 min	35.2	70
(2) 100 μM, 30 min	67.1	67
(3) 100 μM, 60 min	63.3	63
(3)' 100 μM, 60 min	70.9	71
(4) 50 μM, 0 min	35.9	72
(5) 50 μM, 0 min, no BH	25.9	52

The average % recovery for 50 μM and 100 μM substrate were 64% and 67%, respectively. These values were lower than that we calculated based on the [^{3}H]-activity (shown in Table 27). The 50 μM sample with no brain homogenate (control) showed only 52% recovery. This question remains unanswered.

Also the amount of HPP$^+$ was measured by HPLC/fluorescence and [^{3}H]-activity was calculated with the efficiency of HPLRC as 22% (Table 3).

TABLE 29

HPP$^+$ formation (measured by HPLC/fluorescence) and [^{3}H]-activity

Sample	HPP$^+$ (nM)	% of conversion from HPTP	[^{3}H]-activity	% of the total ^{3}H
(1) 50 μM, 60 min	2155	4.3	N.D.	-
(2) 100 μM, 30 min	1776	1.8	4436	14
(3) 100 μM, 60 min	2561	2.6	4255	12
(3)' 100 μM, 60 min	3120	3.1	5564	24
(4) 50 μM, 0 min	194	0.3	N.D.	-
(5) 50 μM, 0 min, no BH	61	0.1	N.D.	-

The % conversion from HPTP to HPP$^+$ was 2 to 3% by HPLC/fluorescence measurements, consistent with previous measurements with unlabeled HPTP (see Chapter 6.3.). However, the % of the [^{3}H]-activity

derived from HPP^+ peak against total activity in the sample injected onto column was much higher (12 to 14%).

This inconsistency is most likely due to the error in HPLRC measurements. Although HPLRC traces have high backgrounds, the numbers in the table above were simply calculated as {integrated CPM/0.22 = DPM} using the efficiency 22% without background subtraction. Therefore the HPLRC results need to be considered as approximate only qualitative.

All results suggests that HPP^+ is the only significant metabolite in brain homogenates. Since the % conversion of [^{3}H]HPTP to [^{3}H]HPP^+ was not so high (2 to 4%) according to HPLC/fluorescence analysis, this outcome (not observing any peak other than [^{3}H]HPP^+ except [^{3}H]HPTP) was rather surprising.

7.2. In vivo studies

Previously, we have administered unlabeled HP, HPTP and HPP^+ to C57BL/6 (i.p.) and studied the metabolic fate of these compounds (see Chapter 6.1.). From urine, feces and tissue analyses, we learned that HPP^+ and $RHPP^+$ were formed after HP and HPTP administrations. However, the % conversions were very small (1 to 3% conversion to the pyridinium metabolites excreted into urine). Furthermore, unchanged HP and HPTP were not observed (HPLC/UV). When HPP^+ was administered, only 20% (15 % in urine, 5% in feces over 3 days) was excreted as HPP^+ and no further metabolism from HPP^+ was observed. Also, from the washout studies with HPP^+, HPP^+ was no longer excreted into urine in significant amounts after one week. Thus, we have not been able to account for the in vivo fate of more than 10% of the HP and HPTP

administered in these experiments. In order to investigate this problem, we wanted to attempt a new approach that would be more general. Therefore, we attempted in vivo experiments with [^{3}H]HPTP, the compound of special interest to us because of the baboon toxicity studies under way.

The [^{3}H]HPTP (i.p) in vivo experiments were conducted three times. In each experiment, we employed 50 mg HPTP/Kg or 3 x 10^6 dpm. The concentration and [^{3}H]-activity of the [^{3}H]HPTP injection solution were measured by UV and scintillation counting to insure that the exact amount of [^{3}H]HPTP was administered to the mouse. In the first experiment, we encountered the problem with the injection solution. For the in vivo experiment with unlabeled HPTP, 10% Tween-80/saline is used to dissolve compounds (1.5 mg HPTP·HCl/200 μL). However, since the [^{3}H]HPTP was first purified by TLC and the extract was dried under nitrogen, the residue was much harder to reconstitute into an aqueous solution than was crystalline HPTP. Therefore ethanol (80 μL) was used to wet the surface to help this solubility problem. Then 200 μL of saline was added. The mouse died 30 minutes after the administration, probably due to alcohol intoxication. No urine or feces samples were obtained. However, brain and liver were isolated and analyzed later. The injection solution was modified for the next two experiments. After drying [^{3}H]HPTP stock solution, Tween 80 was added to this sample vial. The amount of Tween 80 was calculated to be 20% of the total volume. This vial was vortexed well to make a good solution and then the calculated amount of saline was added and the resulting solution was sonicated for approximately 15 minutes. The doses in the second and the third experiments were 35 mg/Kg (2.5 μmol, 3 x 10^6 dpm) and 43 mg/Kg (3.3 μmol, 2.5 x 10^6 dpm), respectively.

These values suggested that the specific activity had somewhat changed with time. Although the reason for the loss was not found, since the specific activity and the amount of [^{3}H]HPTP in each injection solution was accurately measured, our data should be reliable. After the i.p. administration, the mouse was housed in a metabolic cage for 3 days and urine and feces were collected. After 3 days, the mouse was sacrificed by cervical dislocation and several organs were dissected and analyzed.

Results and Discussion

(1) Experiment 1. Thirty minutes after the i.p. administration of [^{3}H] HPTP 3.7 x 10^6 dpm (5.8 μmol), the mouse died. The organs were isolated and urine was obtained from the bladder by syringe and needle. A large amount of body fluid came out from abdominal cavity and some of the fluid was collected. Organs were homogenized and [^{3}H]-activity was counted (Table 30). As we expected, the compound did not distribute into organs in such a short time period. High radioactivity was observed in the abdominal fluid. This is most likely due to the acute dehydration caused by the ethanol.

TABLE 30

[^{3}H]-activity in the dissected tissues and body fluids

Sample	Supernatant		Precipitate		% of the total ^{3}H
	dpm	total dpm	dpm	total dpm	%
Brain	134	2425	102	882	0.09
Heart	78	608	94	99	0.02

Kidney	161	3945	196	398	0.12
Liver	91	6061	194	5112	0.31
Lung	108	691	83	247	0.03
Stomach	116	1624	126	223	0.05

	dpm	total dpm	%
Urine (bladder)	108	562	0.02
Abdominal fluid	530	?	?

The organs were homogenized with 4 volumes of 1.15% KCl aqueous. Since some organs were very hard to homogenize (hard membranes), we were not certain whether [^{3}H]-activity can be extracted into supernatant or not. Therefore both supernatant and precipitate (pellet) were used for the scintillation counting. It appeared that, except for the liver, the [^{3}H]-activity was extracted mostly into supernatant.

(2) Experiment 2. Total [^{3}H]-activity of 3.1 x 10^6 dpm and 2.5 μmoles of HPTP (35 mg/Kg) was administered. The results of the radioactivity counting are summarized in Table 31. The urine sample and the supernatant of the brain homogenate were analyzed by HPLC/fluorescence and HPLRC. The supernatant of the brain homogenate had [^{3}H]-activity and the presence of HPP^+ was confirmed by HPLC/fluorescence analysis. However, when the same supernatant was analyzed by HPLRC, no peak was observed. The urine analyses of experiments 2 and 3 are summarized in section (4).

TABLE 31

[^{3}H]-activity in dissected tissues and urine, feces

Sample	Supernatant		Precipitate		% of the total ^{3}H
	dpm	total dpm	dpm	total dpm	%
Brain	320	5824	212	1972	0.25
Heart	148	1154	81	318	0.05
Kidney	296	5594	94	613	0.20
Liver	250	16675	228	7692	0.78
Lung	282	1946	156	236	0.07
Spleen	266	638	102	117	0.02
Stomach	360	7272	118	923	0.26
Feces (24 hrs)	1765	17650	747	747	0.59
Feces (48 hrs)	3961	39610	1473	1473	1.32
Feces (72 hrs)	2025	20250	438	438	0.67

	dpm	total dpm	%
Urine (24 hrs)	29198	102193	3.29
Urine (48 hrs)	19986	143899	4.63
Urine (72 hrs)	2663	32488	1.04

Quench correction was done only for feces and urine samples.

These data show that after 3 days the total [^{3}H]-activity was 2.6% in feces and 9.0% in urine. Compared to experiment (1), the % of the total [^{3}H]-activity administered in tissues is somewhat higher. However, the numbers are still very small. Since the [^{3}H]-activity detected in these samples were so low, the carcass was homogenized and [^{3}H]-activity was counted. Surprisingly, the carcass contained 77% of the activity (2.4×10^6 dpm) administered. This homogenate was extracted under physiological (no pH adjustment), basic (pH 10) and acidic (pH 1) conditions with ether. We found that 17% of the radioactive material was extracted into the acidic fraction (0.4×10^6 dpm). This is the only extract that showed radioactivity. The acidic extracts were combined and concentrated under a nitrogen stream and reconstituted in the mobile phase for HPLRC analysis. Since this residue was oily (highly viscous), the reconstituted sample was filtered through a syringe filter (GHP acrodisc, 0.45 μm x 13 mm, Gelman Sciences, Ann Arbor, MI) before the injection. Although the sample had 4500 dpm on column (high enough to detect any eluting peak on HPLRC), no radioactive peak was detected. This may indicate that the radioactive material is decomposed and no longer associated with specific compounds that behave normally on a C18 column. The acidic extract was filtered through a basic Al_2O_3 column with ethyl acetate. None of 3 mL fractions showed significant [^{3}H]-activity. Thus, the results show that a major part (77%) of the [^{3}H]-activity stays in the carcass, some portion of activity can be extracted in organic phase. Unfortunately no useful information on the nature of the radioactive material could be obtained.

(3) Experiment 3. The above experiment was repeated. Total [^{3}H]-activity of 2.5 x 10^6 dpm, 3.3 μmoles of HPTP (43 mg/Kg) was administered. Urine samples were collected over 72 hours. [^{3}H]-Activity in the whole brain homogenate was higher than that observed in the second experiment (Table 32). For the urine sample, 3 days total [^{3}H]-activity was 22.5%. Although this is higher than that found in the second experiment, still about 80% was not excreted or extracted from organs.

TABLE 32

[^{3}H]-activity in brain homogenate and urine

Sample	dpm	total volume (μL)	total dpm	% of the total ^{3}H administered
Brain (homogenate)	2610	1600	41760	1.7
Urine (24 hrs)	37181	850	395050	15.8
Urine (48 hrs)	5520	1640	113160	4.5
Urine (72 hrs)	3244	1380	55960	2.2

(4) Urine analysis. Urine extracts were analyzed by HPLC/fluorescence and the amounts of $RHPP^+$ and HPP^+ were measured using external calibration curves (Table 33). The % conversion of HPTP to both pyridinium species were 0.1% and 2-3%, respectively. These numbers were in the same range as observed in unlabeled HPTP in vivo studies.

TABLE 33

Summary of pyridinium metabolites excreted into urine

	Experiment 2	Experiment 3
	RHPP+/HPP+	RHPP+/HPP+
24 hr urine		
nmoles	1.3/30.8	3.1/59.7
% of the dose	0.05/1.25	0.09/1.82
48 hr urine		
nmoles	2.3/44.2	0.35/9.3
% of the dose	0.09/1.80	0.01/0.28
72 hr urine		
nmoles	N/A*	0.13/3.6
% of the dose	N/A	0.004/0.11
3 days total	0.14/3.1 (2 days total)	0.1/2.2

*Not available. Sample was used for other analysis and not used for HPLC/fluorescence analysis.

HPLRC tracings of the urine extracts show two radioactive peaks (Fig. 53a). The retention times were 2.6 min and 6.3 min, respectively. These retention times would correspond approximately to 2 min and 5.6 min on the UV tracings. Although the HPLC/UV tracings look complicated due to the high biological background (Fig. 53b), a major peak eluted at 5.6 min which coeluted with synthetic HPP^+. Consistent with the pyridinium structure, treatment of the urine with $NaBH_4$ caused this peak to disappear, presumably due to conversion to the corresponding tetrahydropyridine derivative. This disappearance was

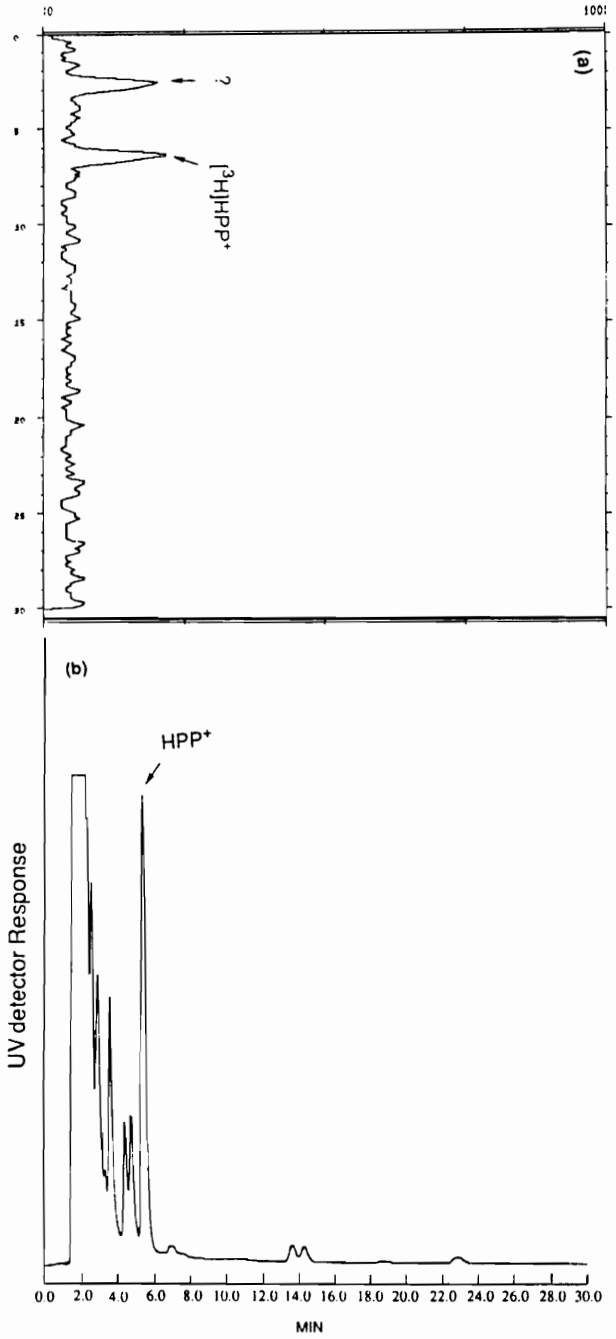

Figure 53. HPLC tracings of urine extracts obtained from [^{3}H]HPTP-treated mouse (a) HPLRC and (b) HPLC/UV tracing.

confirmed by HPLC/fluorescence analysis. As this peak disappeared, a new peak appeared at 7.2 min on the UV tracing (7.8 min on the HPLRC tracing) (Fig. 54a, b). This peak coeluted with synthetic RHPTP.

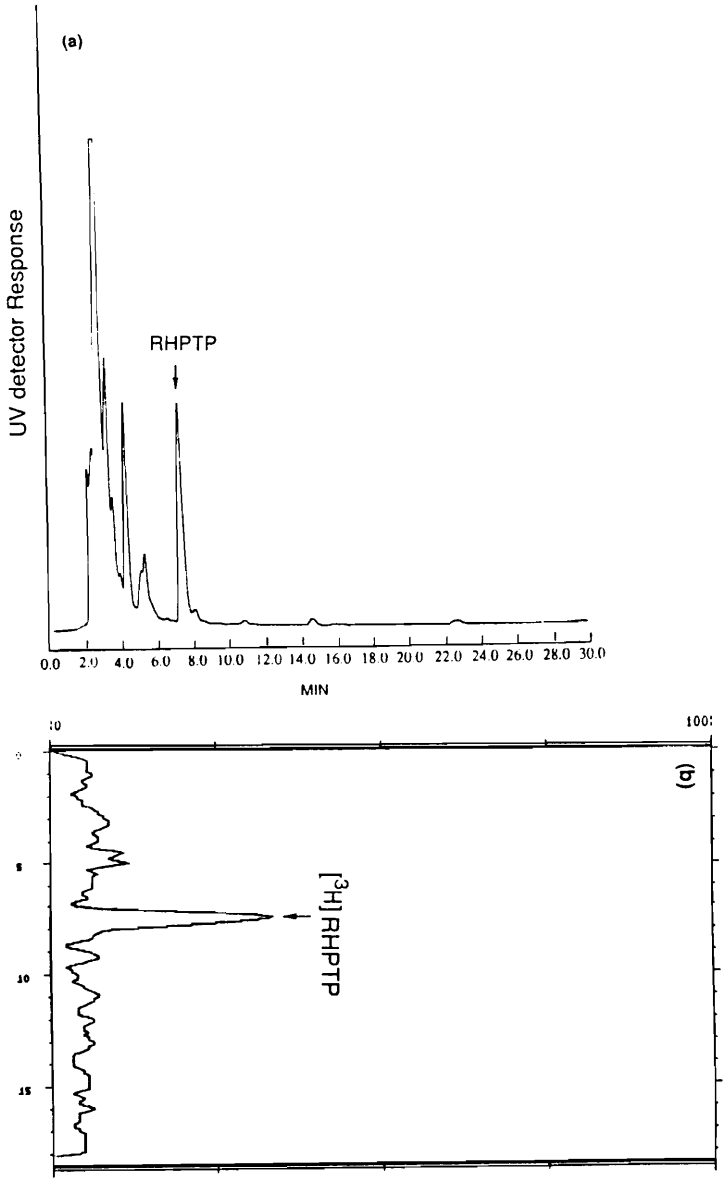

Figure 54. HPLC tracings of the urine extracts obtained from a [^{3}H]HPTP-treated C57BL/6 mouse after $NaBH_4$ treatment. (a) HPLC/UV and (b) HPLRC.

Synthetic HPP+ and [^{3}H]HPTP were also treated with $NaBH_4$ and HPP+ was reduce to RHPTP (by UV, Fig. 55) and [^{3}H]HPTP was reduced to [^{3}H]RHPTP (HPLRC, Fig. 56). Interestingly, the unknown peak in [^{3}H]HPTP stock solution (t_R 2.3 min on HPLRC) was also converted to RHPTP.

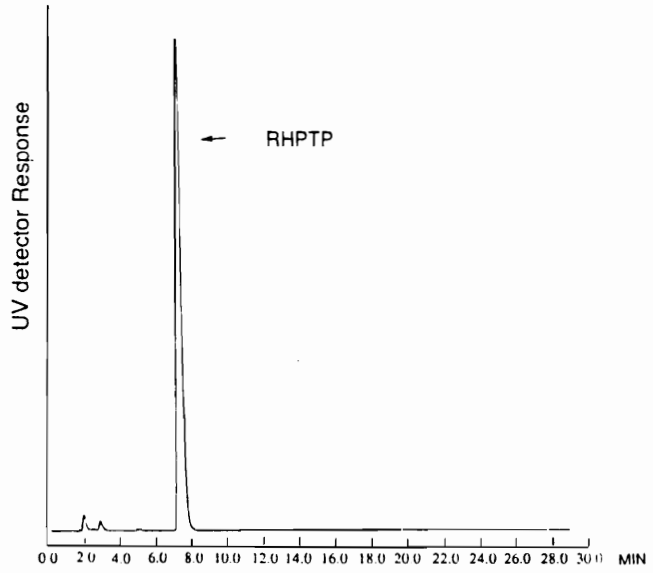

Figure 55. HPLC/UV tracing of synthetic HPP+ treated with $NaBH_4$.

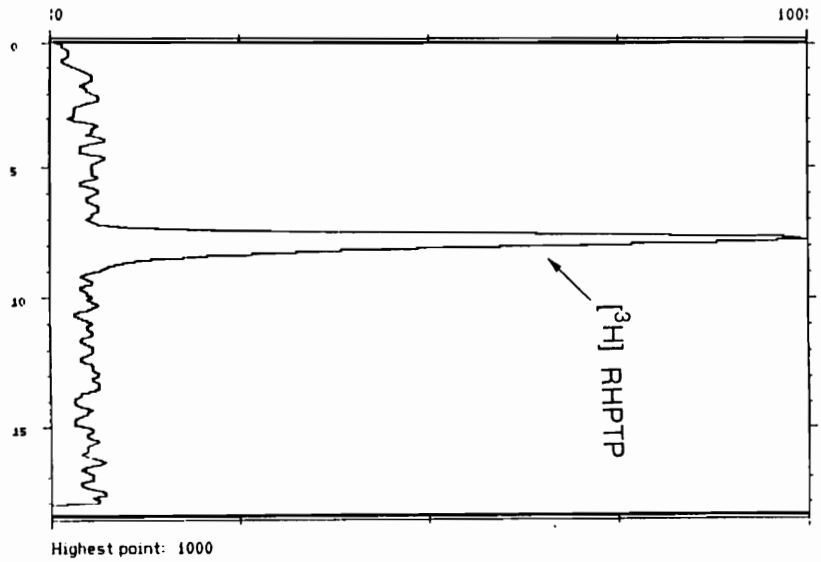

Figure 56. HPLRC tracing of [^{3}H]HPTP treated with $NaBH_4$.

Synthetic HPP^+ was spiked in urine sample (experiment 3, 48-h urine) and after confirming the coelution of this 5.6 min UV peak and HPP^+, the mixed sample was treated with $NaBH_4$ and analyzed by HPLC/UV-HPLRC. The same 48-hour urine sample was reduced without spiking with HPP^+. These two samples showed the same HPLC pattern (Fig. 57a, b).

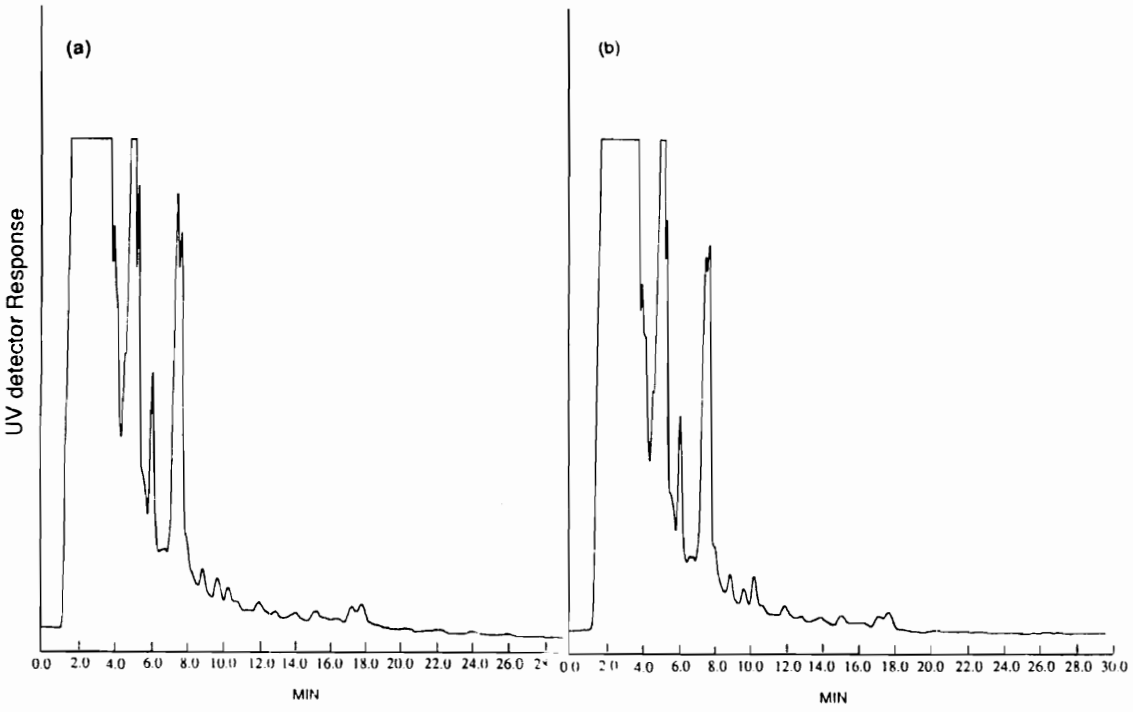

Figure 57. HPLC/UV tracings of [^{3}H]HPTP-treated mouse urine (a) spiked with HPP^+ and (b) not spiked with HPP^+, after $NaBH_4$ treatment.

The 24-hour urine sample (experiment 3) was extracted with ethyl acetate without processing through a Sep-pak (sample pH was approximately 7 and was not adjusted). The sample was analyzed by HPLC. HPLRC tracing (Fig. 58a) showed a third peak (t_R 4.1 min) in addition to the 2.7 min and 6.3 min peaks. This peak corresponds to the peak at 3.8 min on the UV trace (Fig. 58b) which coelutes with synthetic $RHPP^+$.

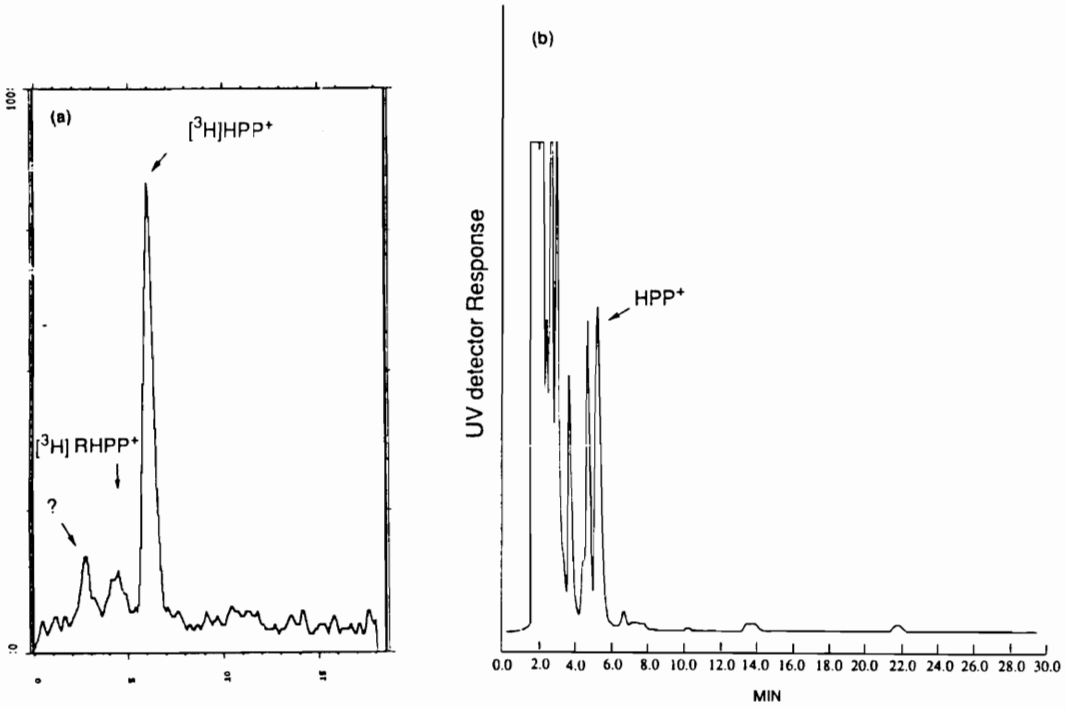

Figure 58. HPLC tracing of ethyl acetate extract (without Sep-pak purification) obtained from 24-h urine obtained of [^{3}H]HPTP-treated mouse. (a) HPLRC and (b) HPLC/UV tracing.

The other peak present in the HPLRC tracing (t_R 2.7 min) was not resolved in the HPLC/UV chromatogram due to the biological background. However, we attempted to identify this peak by modifying mobile phase. A possible assignment was 3-*p*-fluorobenzoylpropionic acid (PFBPA, **43**). This compound is a known metabolite of HP[95] and the retention time on the C18 column is expected to be early. The retention time of synthetic standard PFBPA on HPLC/UV was 2.1 min and could correspond to the 2.7 min peak on the HPLRC tracing. Therefore an ion-pair agent (tetrabutylammonium hydroxide) was added to the mobile phase (1 mM) and triethylamine was removed in order for the PFBPA to elute at a longer retention time and not to overlap with biological background. With this modified mobile phase (pH 4.8), the retention time of PFBPA moved from 2.1 min to 3.6 min. However, the retention time of HPP^+ moved from 5.6 min to 3.1 min and HPTP moved from 14.1 min to 4.3 min. As a result, the three compounds eluted close to each other . Since all 3 compounds were still resolved on HPLC/UV, the 24-hour urine sample was injected onto HPLC and 2 peaks were detected on HPLRC (Fig. 59). The retention time of these two peaks are 2.5 min and 3.8 min, respectively. The 3.8 min peak corresponds to HPP^+. If PFBPA were present, the retention time would be at 4.0 to 4.3 min. We tentatively concluded, therefore, that PFBPA was not in the urine sample. The other peak (2.5 min) is most likely as the same peak as the 2.7 min peak in the original pH 6.2 min mobile phase. However, no further investigation was attempted.

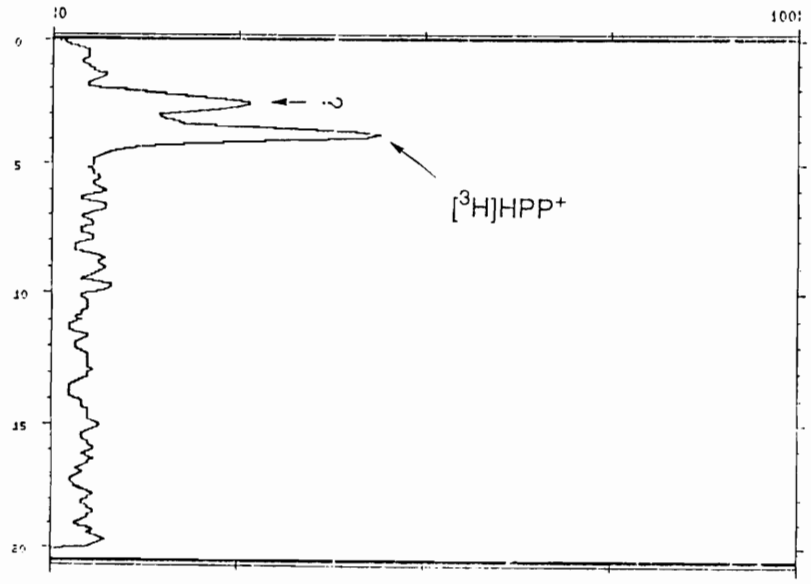

Figure 59. HPLRC tracing of [^{3}H]HPTP-treated mouse urine analyzed by with a pH 4.8 mobile phase.

Experimental

Chemicals. [^{3}H]HP (DuPont, Boston, MA), $BF_3 \cdot OEt_2$ (Aldrich Chemicals, Milwaukee, WI), Tween 80, $NADP^+$, glucose 6-phosphate and glucose 6-phosphate dehydrogenase (Sigma Chemical Co., St. Louis, MO), tritiated water (Packard Instrument Company, Inc. Downers Grove, IL) and HPLC-grade solvents (Fisher Scientific Co., Springfield, NJ) were obtained from commercial sources.

Synthesis of [^{3}H]HPTP

(1) General methods. The reaction was carried out under a nitrogen atmosphere. All glassware were flame-dried and dichloromethane was distilled from sodium benzophenone ketyl. Gas chromatography-electron ionization mass spectrometry (GC-EIMS) employed a Hewlett Packard 5890 GC fitted with

an HP-1 capillary column (24 m x 200 μm x 0.33 μm film thickness) which was coupled to a Hewlett Packard 5870 mass-selective detector. Data were acquired using an HP 5970 ChemStation. Normalized peak heights are reported as a percentage of the base peak. Ultraviolet (UV) spectra were taken on Beckman DU-50 spectrophotometer. Analytical thin-layer chromatography (TLC) was carried out on basic alumina (0.2 mm thickness, Selecto Scientific). Preparative TLC was performed on Alumina GF plates (20 x 20 x 250 μm, Analtech).

(2) [^{3}H] 4-(4-chlorophenyl)-1-[4[(4-fluorophenyl)-4-oxobutyl]-1,2,3,6-tetrahydropyridine. A solution of 160 μL of [^{3}H]HP (in ethanol/0.1 N HCl 9/1, 14.6 nmol, 1.44 x 10^8 dpm} was transferred to a round bottom flask and dried under N_2. After reconstituting the residue in 1 mL of CH_2Cl_2, unlabeled HP (10 mg, 26.6 μmol) was added to the solution. Before the addition of $BF_3{\cdot}OEt_2$, a 10 μL-aliquot of the solution (labeled and unlabeled HP in 1 mL of CH_2Cl_2) was taken out and [^{3}H]-activity was counted to measure the specific activity. $BF_3{\cdot}OEt_2$ (65 μL, 532 μmol, 20 equivalents) were added to the solution. After stirring at room temperature for 3 days, the reaction mixture was quenched with 500 μL of saturated $NaHCO_3$. The product was extracted with CH_2Cl_2 (1 mL x 6) and the combined extracts were dried over $MgSO_4$ and concentrated under N_2. In order to collect as much product as possible, the $MgSO_4$ was washed several times with CH_2Cl_2 until all [^{3}H]-activity was removed. The organic extracts were combined and dried under N_2. This dried product was redissolved in 550 μL of methanol and spotted on a preparative aluminum TLC (solvent: hexane/ethyl acetate 4/5). [^{3}H]HPTP band was scraped off from TLC and extracted with CH_2Cl_2 (50 mL x 4, stirred in a beaker

for 30 min each, no sonication to avoid small alumina particles). All CH_2Cl_2 extracts (200 mL) were combined and dried by rotary evaporator. The residue was redissolved in 600 μL of methanol and concentration and [^{3}H]-activity were measured to measure the specific activity of the final product. The solution was dried under nitrogen again and redissolved in 600 μL of ethanol/0.1 N HCl (9/1 v/v). This solution was stored as a stock solution in a refrigerator (in a 5 mL round bottom flask and covered with aluminum foil). The product was characterized by basic alumina TLC (solvent: hexane/ethyl acetate 4/5) and GC/MS [isothermal at 125 °C for 2 min followed by a ramp of 40 °C/min for 4 min (t_R = 7.2 min)] m/z 357 (M^+, 8), 219 (20), 206 (30), 192 (100), 165 (20), 129 (30), 123 (80), 95 (65), 75 (20). **(3) Purification of [^{3}H]HPTP (small scale).** Just before the experiment, the [^{3}H]HPTP stock solution was spotted on basic alumina TLC (15 μL per 22 mm x 65 mm TLC plate) and the plate was developed with hexane/ethyl acetate (4/5). The alumina containing HPTP band was scraped off and transferred into polypropylene Eppendorf tube. Ethanol was added to this tube and vortexed and centrifuged. This step was repeated 3 times to extract HPTP from alumina and all ethanol extracts were combined and dried under N_2 and reconstituted in the solvent system used for the experiments.

In vitro incubation studies

(1) Preparation of mouse brain homogenates. The procedure is the same as described in Chapter 5.3.

(2) Brain metabolism. The brain homogenate (1 mg protein/mL incubation) was incubated with [^{3}H]HPTP (50 μM or 100 μM) and 50 mM phosphate buffer, pH 7.4, in the presence of an NADPH-generating system

[$NADP^+$ (1 mM), glucose 6-phosphate (5 mM) and glucose 6-phosphate dehydrogenase (1 Unit/mL), $MgCl_2$ (3 mM)] at 37 °C for 0 to 60 minutes.

Stock [^{3}H]HPTP (12 μL in ethanol/0.1 N HCl 9/1) were dried under N_2 and reconstituted in 112 μL of methanol to adjust the concentration to be 5 mM. Aliquots (10 μL and 20 μL) of this solution were added to the incubation mixtures (total volume 1 mL) for the final substrate concentration to be 50 μM and 100 μM, respectively. Methanol (10 μL) was added to 50 μM of the substrate incubation mixture such that the % methanol would be consistently 2% in all incubation samples. Control incubations were conducted in the absence of protein or substrate.

The reaction was initiated by the addition of substrate and terminated by the addition of 600 μL ice-cold acetonitrile containing 2% acetic acid to 600 μL-aliquot of incubation mixture. The resulting mixtures were agitated vigorously on a vortexer and the resulting protein precipitate was removed by centrifugation (14000 rpm x 6 min). An aliquot (100-μL) of the supernatant was used to count [^{3}H]-activity. [^{3}H]-activity in the 5 mM solution was 7118 dpm/μL (after the quench correction). Therefore, theoretically [50 μM] tubes should have 3559 dpm in 100 μL supernatant and [100 μM] tubes should have 7118 dpm in 100 μL.

Also another 100-μL aliquot of the supernatant was used for HPLC/fluorescence analyses for the HPP^+ measurement and rest (1000 μL) was used for HPLC (UV)/Radio chromatography. This 1000 μL sample was dried under N_2 and reconstituted in the mobile phase (120 μL) and 10 μL was used for ^{3}H counting and rest was injected on HPLRC.

In vivo experiments

(1) Animal studies. [^{3}H]HPTP (35 to 45 mg/Kg) was administered intraperitoneally in 200 μL of saline containing 20% Tween 80 to retired breeder male C57BL/6 mice (Harlan-Splague Dawley, Dublin, VA) weighing approximately 30 g each. 80 μL of [^{3}H]HPTP stock solution was dried in a vial under nitrogen (concentration and radioactivity were measured by UV and scintillation counter before drying). The amount of Tween 80 added to the vial was calculated to be 20% of the total volume. This vial was vortexed well to make a suspension and then the calculated amount of saline was added and sonicated for approximately 15 min to make a clear solution. For urine collections, animals were housed in individual metabolic cages designed to separate urine and feces. Food and drinking water were supplied *ad libitum*. Urine samples were collected during the 72-hour period following the injection of drug. At the termination of the urine collections, animals were sacrificed by cervical dislocation and whole brains were isolated. The samples were stored at -70 °C prior to analysis.

(2) Sample preparation for [^{3}H]-activity counting. A 100 μL-aliquot of urine was mixed with 5 mL of ScintiVerse BD (Fisher scientific) and [^{3}H]-activity was measured by scintillation counter (Beckman). Feces samples were weighed and soaked in 1 mL methanol overnight and ground (manually) and centrifuged at 14000 rpm for 4 min. A 100 μL-aliquot of supernatant and precipitate were counted separately. Several organs were dissected 3 days after the injection and homogenized with 4 times volume of 1.15% KCl and centrifuged. Both supernatant (100 μL) and precipitate (weighed) were used for ^{3}H counting. Quench correction was done by adding 10 μL (25400 dpm) of

tritiated water (^3H-H_2O standard, 2.54 x 10^6 dpm/g), to the scintillation vials after those vials were counted without spiking this standard.

(3) HPLC analysis. The sample preparation is the same as described in Chapter 4. After the Sep-pak extraction, the eluents were evaporated to dryness under N_2 and the residue was dissolved in the HPLC mobile phase (see Chapter 4) in an amount that was adjusted depending on the radioactivity of the sample. For the HPLC/fluorescence studies, these samples were diluted up to 1 in 200 to give concentrations of analytes that would produce peak heights within the recording range of the integrator following injection of a 50-μL aliquot. The HPLC/fluorescence assay is the same as described in Chapter 4. For the HPLC/UV-radio chromatography studies, [^3H]-activity of a 10 μL-aliquot of sample was measured using Beckman LS 3800 liquid scintillation system and 80 to 100 μL of the sample was injected onto the column without dilution. This HPLC system consisted of Phenomenex C18 5 μm, 150 mm x 4.6 mm column, a Spectromonitor D variable wavelength detector (set at 254 nm), a Shimadzu C-R3A integrator, and a Altex 110A pump set at a flow rate of 1 mL/min. Tritium-labeled material was analyzed using a Radiomatic Flo-one\β model IC radioactive flow detector placed in-line after a Spectromonitor D variable wavelength detector. The Radiomatic detector's data acquisition, data storage, and reporting were controlled on an IBM-compatible computer with version 3e Radiomatic Flo-one\β software. The mobile phase used in HPLC/fluorescence analysis was mainly used for this system. Also, a slightly modified mobile phase (pH 4.8) was used much lesser extent on this system. The mobile phase was prepared as follows: To 400 mL of CH_3CN and 600 mL of 10 mM NH_4OAc were added 0.8 mL of glacial acetic

acid and the ion-pair agent tetrabutylammonium hydroxide (final concentration 1 mM). For the radiochemical detection, 1 part of mobile phase was mixed dynamically (post column) with 3 parts of Packard Ultima-M liquid scintillation cocktail and the window was set for ^3H. The schematic flow of HPLRC is shown in Figure 59.

(4) $NaBH_4$ reduction. Urine samples (Sep-pak processed and dissolved in mobile phase) were dried under N_2 and redissolved in 1 mL of methanol. Solid $NaBH_4$ (0.4 mg) was added to the methanol solutions and these mixtures were vortexed and then were allowed to stand at room temperature for 30 minutes. Then these solutions were dried under nitrogen and $NaBH_4$ was quenched with saturated $NaHCO_3$ and the reduced material (s) were extracted with CH_2Cl_2. These extracts were dried and reanalyzed using HPLC/fluorescence and HPLC(UV)-radio chromatography. Synthetic HPP^+ and [^3H]HPTP also were subjected to $NaBH_4$ reduction as same procedure as above.

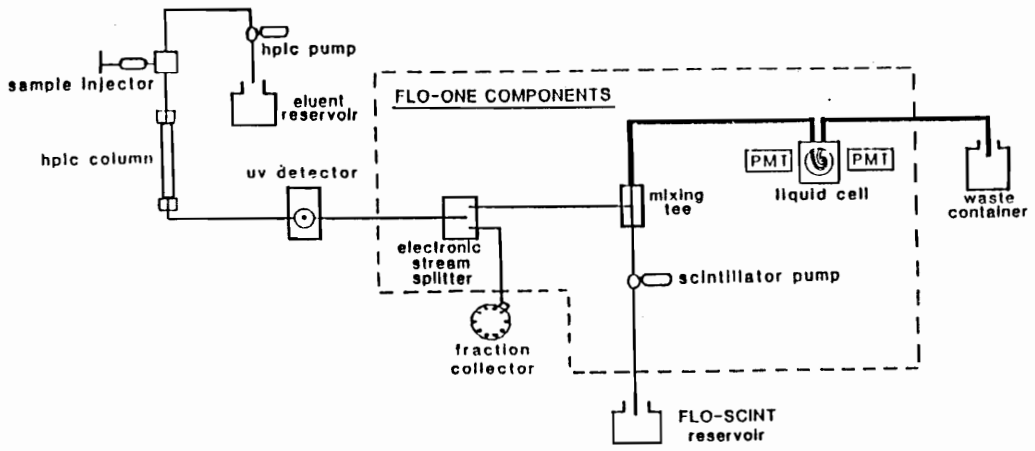

Figure 60. Schematic flow path of HPLRC.

Chapter 8

Conclusions

This thesis is concerned with the in vitro and in vivo biotransformation of the neuroleptic agent haloperidol (HP) and its tetrahydropyridine analog HPTP to potentially neurotoxic pyridinium metabolites that may contribute to the extrapyramidal side effects, particularly the sometimes irreversible tardive dyskinesias, that are associated with long term drug treatment. The genesis of this work is the neurodegenerative properties of the parkinsonian inducing MPTP, a tetrahydropyridine analog of HPTP that is bioactivated by monoamine oxidase B to a highly potent and highly selective pyridinium neurotoxin (MPP^+) that accumulates in the dopaminergic nigrostriatal neurons where it inhibits Complex 1 of the mitochondrial respiratory chain. Independent studies have shown that HP in humans and both HP and HPTP in rodents are metabolized to two pyridinium metabolites, HPP^+ derived from HP and $RHPP^+$ derived from reduced haloperidol (RHP), the major circulating metabolite of HP in humans. The literature reports, for the most part, have been qualitative in nature only. These compounds are of toxicological interest because, like MPP^+, they can be localized in the terminals of dopaminergic (and also serotonergic) neurons. HPP^+ also has been shown to be 10 times more potent in inhibiting mitochondrial respiration (Complex 1) than MPP^+. Evidence for the formation of these compounds in HP treated patients, and in particular their presence in the brains of these patients, would raise the possibility that they could mediate some of the extrapyramidal side effects, such as the irreversible tardive dyskinesias.

In order to evaluate the quantitative metabolic fate of HP and HPTP, a sensitive, robust and versatile bioanalytical procedure was required. To this effect, an HPLC assay employing a fluorescent detector has been established which can be used to estimate HPP^+ $RHPP^+$ in the pmole range on column. This assay has been employed to provide quantitative estimations of the formation of these metabolites in a variety of biologically important settings. Data supporting the MAO-A catalyzed oxidation of HPTP (but not HP) to HPP^+ are reported. Extensive liver microsomal studies employing both rat and human liver microsomal preparations have been conducted. A major finding in the human is the selective cytochrome P450 3A4 catalyzed oxidation of both HP and HPTP the HPP^+. Rodent liver cytochrome P450 also catalyzes this oxidation but the specific form or forms responsible for the biotransformation have not been identified. Attempts to identify other significant metabolic products by HPLC with both fluorescence and UV detection in these incubation mixtures were not successful. This seems strange since only a few percent of the total substrate can be accounted for as pyridinium metabolites. These studies have been extended to include the analysis of potential bioactivation pathways of HP and HPTP by rodent brain enzymes. Clear evidence for the formation of HPP^+ is presented both for HP and HPTP but again the exact enzymes involved remain to be fully identified. A variety of studies indicate that MAO-A, cytochrome P450 (i.e. NADPH dependent) and, perhaps, peroxidase activity may contribute to this conversion.

In vivo metabolic studies have been carried out in rodents, baboons, and humans. The results have provided detailed information on the quantities of HPP^+ and $RHPP^+$ in urine samples of humans treated with HP and baboons

and rodents treated with both HP and HPTP. A major finding is the dominance of $RHPP^+$ in the primate metabolic profiles compared to that of the rodent where HPP^+ is the major urinary pyridinium species. This outcome almost certainly is a consequence of the presence of ketone reductase activity in the human and subhuman primate that, apparently, is lacking in the C57BL/6 mouse species that were used in these studies. Surprisingly, the quantitative estimates of urinary HPP^+ and $RHPP^+$ excretion in rodents, baboons and humans showed that the % of the dose excreted as these pyridinium metabolites always was within the range of 1 to 5% irrespective of the species or the dose administered. A second major outcome of this work is the apparent absence of other major urinary metabolites. It must be emphasized that only the pyridinium metabolites are likely to be fluorescent. Even so, attempts to find other metabolites, including those reported in the literature, using HPLC with UV detection did not provide evidence for major urinary products derived from HP or HPTP. This is a significant limitation of this work since the mass balance is so poor. Less than 10% of the administered dose of the drugs have been accounted for. When attempts were made to determine if HPP^+ was processed further in vivo in the mouse, disappointing results again were obtained since less than 20% of the administered dose could be accounted for in urine, feces and major organs. The poor accounting for the injected HPP^+ was not due to analytical problems with the HPLC/fluorescence assay since excellent recoveries of HPP^+ from all matrices could be documented.

A final effort to obtain information on the mass balance of HPTP both in vitro and in vivo was undertaken with the aid of tritium labeled HPTP which was synthesized by treating commercially available [^{3}]HP-labeled with $BF_3{\cdot}Et_2O$ in

the presence of a dehydrating agent (to avoid exchange of the label which was located on the carbon atom α to the carbonyl group). The product could be obtained in pure form and was used to follow the metabolic fate of HPTP in rodent brain homogenates and following intraperitoneal injection. Unfortunately, little new information was realized in these studies. In the brain homogenates only parent compound and HPP^+ were found by HPLC with radiochemical detection and by HPLC with fluorescence detection. The findings from the in vivo study were rather remarkable in that only the pyridinium metabolites could be fully characterized. Estimations suggested that 4% of the HPTP was converted to the pyridinium metabolites. Only about 10% of the radioactivity was excreted in the urine. The remaining activity, however, was eventually identified in the carcass of the animals but no discrete metabolite could be associated with this activity.

Consequently, at least from the perspective of the results obtained in the work, the pyridinium metabolites represent are significant well characterized end products of HP and HPTP metabolism. Their presence in the brain of treated animals opens the possibility that they may cause neurotoxic effects that may be associated with the tardive dyskinesias observed in patients on chronic HP therapy. A better understanding of the fate of HP in terms of mass balance needs to be achieved before the significance of the pyridinium metabolites can be fully assessed.

Chapter 9

References

(1) Delay, J., Denikar, P., Harl, J. M. (1952) Utilisation en thérapeutique psychiatrique d'une phenothiazine d'action centrale élective. *Annales medico-psychologiques.* **110**, 112-117.

(2) Steck, H. (1954) Le syndrome extrapyramidal et diencéphalique au cours des traitements au Largactil et au Serpasil. *Annales medico-psychologiques.* **112**, 737-743.

(3) Marsden, C. D., Jenner, P. (1980) The pathophysiology of extrapyramidal side-effects of neuroleptic drugs. *Psychological Medicine* **10**, 55-72.

(4) Montastruc, J. L., Llau, M. E., Rascol, O., Senard, J. M. (1994) Drug-induced parkinsonism: a review. *Fundam. Clin. Pharmacol.* **8**, 293-306.

(5) Forno, L. S. (1982) Pathology of Parkinson's disease. In *Movement Disorders*, Neurology 2 (Marsden, C. D., Fahn, S., Eds.), pp. 25-40, Butterworths, London.

(6) Ehringer, H., Hornykiewicz, O. (1960) Verteilung von Noradrenalin und Dopamin (3-Hydroxytryamin) im Gehirn des Menschen und ihr Verhalten bei Erkrankungen des extrapyramidalen Systems. *Klin. Wochenschr.* **38**, 1236-1239.

(7) Bianchine, J. R. (1985) Drugs for Parkinson's disease, spasticity, and acute muscle spasm. In *Goodman and Gilman's the pharmacological basis of therapeutics* (Gilman, A. G., Goodman, L. S., Rall, T. W., Murad, F., Eds), pp. 473-490, Macmillan, New York.

(8) Jenner, P., and Marsden, C. D. (1993) MPTP-induced parkinsonism: a model of Parkinson's disease and its relevance to the disease process.

In *Parkinson's Disease and Movement Disorders* , (Jankovic, J., Tolosa, E., Eds.), pp. 55-75, Williams &Wilkins, London.

(9) Arblaster, C. A., Lakie, M., Mutch, W. J., Semple, M. A. (1993) Study of the early signs of drug-induced parkinsonism. *J. Neurol. Neurosurg. Psychiatry* **56**, 301-303.

(10) Johnson, W. G., Hodge, S. E., Duvoisin, R. (1990) Twin studies and the genetics of Parkinson's disease-a reappraisal. *Movement Disorder* **5**, 187-194.

(11) Ayd, F. J. (1961) A survey of drug induced extrapyramidal reactions. *J.A.M.A.* **175**, 1054-1060.

(12) Gimenez-Roldan, S., Mateo, D. (1991) Cinnarizine-induced parkinsonism. Susceptibility related to aging and essential tremor. *Clin. Neuropharmacol.* **14**, 156-164.

(13) Johnson, D. W. A. (1978) Prevalence and treatment of drug-induced extrapyramidal symptoms. *Br. J. Psychiatry* **132**, 27-30.

(14) Tarsy, D. (1983) Neuroleptic induced extrapyramidal reactions: classification, description and diagnosis. *Clin. Neuropharmacol.* **6** (suppl 1), s9-26.

(15) O'hara, P., Brugha, T. S., Lesage, A., and Wing, J. (1993) New findings on tardive dyskinesia in a community sample. *Psychological Medicine* **23**, 453-465.

(16) Gerlach, J., Casey, D. E. (1988) Tardive dyskinesia. *Acta psychiatr. scand.* **77**, 369-378.

(17) Richardson, M. A., Pass, R., Craig, T. J. (1986) The coexistence of parkinsonism-like symptoms and tardive dyskinesia. In *Biological*

psychiatry, 1985 (Shagass, C., Josiassen, R. C., Bridger, W. H., Weiss, K. J., Stoff, D., Simpson, G. M., Eds), pp. 1211-1213, Elsevier, New York, Amsterdam.

(18) Casey, D. E., Hansen, T. E. (1984) Spontaneous dyskinesia. In *Neuropsychiatric movement disorders* (Jeste, D. V., Wyatt, R. J., Eds.), pp. 68-95, America Psychiatric Press., Washington D.C.

(19) Casey, D. E. Tardive dyskinesia. (1987) In *Psychoparmacology: The third generation of progress* (Meltzer, H. Y., Ed.), pp. 1411-1419, Raven Press, New York.

(20) Kane, J. M., Woerner, M., Lieberman, J. (1985) Tardive dyskinesia: Prevalence, incidence, and risk factors. In *Dyskinesia-Research and Treatment (Psychopharmacology Suppl. 2)* (Casey, D. E., Chase, T., Christensen, A. V., Gerlach, J., Eds.), pp. 72-78, Springer-Verlag., Berlin.

(21) Marsden, C. D. (1985) Is tardive dyskinesia a unique disorder? In *Dyskinesia-Research and Treatment (Psychopharmacology Suppl. 2)* (Casey, D. E., Chase, T., Christensen, A. V., Gerlach, J., Eds.), pp. 64-71, Springer-Verlag., Berlin.

(22) Klawans, H. L., Goetz, C. G., Perlik, S. (1980) Tardive dyskinesia: Review and update. *Am. J. Psychiatry* **137**, 900-911.

(23) Baldessarini, R. J., Tarsy, D. (1980) Pathophysilogic basis of tardive dyskinesia. In *Long-Term Effects of Neuroleptics (Adv. Biochem. Psychopharmacol. Vol. 24)* (Cattabeni, F., Ed.), pp. 451-455, Raven Press, New York.

(24) Baldessarini, R. J. (1980) Dopamine and the pathophysiology of dyskinesias induced by antipsychotic drugs. *Ann. Rev. Neurosci.* **3**, 23-41.

(25) Coward, D. M. (1993) The pharmacology of clozapine-like, atypical antipsychotics. In Antipsychotic drugs and their side-effects (Barnes, T., Ed.), pp. 27-44, Academic Press, London.

(26) Farde, L., Nordström, A-L., Wiesel, F-A., Pauli, S., Halldin, C., Sedvall, G. (1992) Positron emission tomographic analysis of central D_1 and D_2 dopamine receptor occupancy in patients treated with classical neuroleptics and clozapine. Relation to extrapyramidal side effects. *Arch. Gen. Psychiatry* **49**, 538-544.

(27) Barnes, T. R. E., Edwards, J. G. (1993) The side-effects of antipsychotic drugs. I. CNS and Neuromuscular effects. In Antipsychotic drugs and their side-effects (Barnes, T., Ed.), pp. 213-247, Academic Press, London.

(28) Scatton, B., Javoy-Agid, F., Rouquier, L., Dubois, B., and Agid, Y. (1983) Reduction of cortical dopamine, noradrenaline, serotonin and their metabolites in Parkinson's disease. *Brain Res.* **275**, 321-328.

(29) Tohgi, H., Abe, T., Takahashi, S., Takahashi, J., and Hamato, H. (1993) Concentrations of serotonin and its related substances in the cerebrospinal fluid of Parkinsonian patients and their relations to the severity of symptoms. *Neuroscience Lett.* **150**, 71-74.

(30) Scheel-Krüger, J., Arnt, J. (1985) New aspect on the role of dopamine, acetylcholine, and GABA in the development of tardive dyskinesia. In *Dyskinesia-Research and Treatment (Psychopharmacology Suppl. 2)*

(Casey, D. E., Chase, T., Christensen, A. V., Gerlach, J., Eds.), pp. 46-57, Springer-Verlag., Berlin.

(31) Stahl, S. M., Davis, K. L., and Berger, P. A. (1982) Neuropharmacology of tardive dyskinesia, spontaneous dyskinesia and other dystonias. *J. Clin. Psychopharmacol.* **2**, 321-328.

(32) Berger, P. A., Rexroth, K. (1980) Tardive dyskinesia: Clinical, biological and pharmacological perspectives. *Schizophr. Bull.* **6**, 102-116.

(33) Langston, J. W., Ballard, P., Tetrud, J. W., and Irwin, I. (1983) Chronic Parkinsonism in humans due to a product of meperidine-analog synthesis. *Science* (Washington D. C.) **219**, 979-980.

(34) Markey, S. P., Schmuff, N. R. (1986) The pharmacology of Parkinsonian syndrome producing neurotoxin MPTP (1-methyl-4-phenyl-1,2,3,6-tetrahydropyridine) and structurally related compounds. *Med. Res. Rev.* **6**, 389-429.

(35) Davis, G. C., Williams, A. C. Markey, S. P., Ebert, M. H., Caine, E. D., Reichert, C. M. and Kopin, I. J. (1979) Chronic parkinsonism secondary to intravenous injections of meperidine analogues. *Psychiatry Res.* **1**, 249-254.

(36) Burns, R. S., Chiueh, C. C., Markey, S. P., Ebert, M. H., Jacobowitz, D. M., and Kopin, I. J. (1983) A primate model of Parkinsonism: Selective destruction of dopaminergic neurons in the pars compacta of the substantia nigra by N-methyl-4-phenyl-1,2,3,6-tetrahydropyridine. *Proc. Natl. Acad. Sci. U.S.A.* **80**, 4546-4550.

(37) Langston, J. W., Forno, L. S., Rebert, C. S. and Irwin, I. (1984) Selective nigral toxicity after systematic administration of 1-methyl-4-phenyl-

1,2,3,6-tetrahydropyridine (MPTP) in the squirrel monkey. *Brain Res.* **292**, 390-394.

(38) Hallman, H., Lange, J., Olson, L., Stromberg, I. and Jonsson, G. (1985) Neurochemical and histochemical characterization of neurotoxic effects of 1-methyl-4-phenyl-1,2,3,6-tetrahydropyridine on brain catecholamine neurons in the mouse. *J. Neurochem.* **44**, 117-127.

(39) Heikkila, R. E., Hess, A. and Duvoisin, R. C. (1984) Dopaminergic neurotoxicity of 1-methyl-4-phenyl-1,2,3,6-tetrahydropyridine in mice. *Science* (Washington D. C.) **224**, 1451-1453.

(40) Gupta, M., Felten, D. L. and Gash, D. M. (1984) MPTP alters central catecholamine neurons in addition to the nigrostriatal system. *Brain Res. Bull.* **13**, 737-742.

(41) Sundstrom, E., Stromberg, I., Tsutsumo, T., Olson, L. and Jonsson, G. (1987) Studies on the effect of 1-methyl-4-phenyl-1,2,3,6-tetrahydropyridine (MPTP) on central catecholamine neurons in the C57BL/6 mouse: Comparison with three other strains. *Brain Res.* **405**, 26-38.

(42) Chiba, K., Trevor, A. and Castagnoli, N., Jr. (1984) Metabolism of the neurotoxic tertiary amine, MPTP, by brain monoamine oxidase. *Biochem. Biophys. Res. Commun.* **120**, 574-578.

(43) Castagnoli, N., Jr., Chiba, K. and Trevor, A. J. (1985) Potential bioactivation pathways for the neurotoxin 1-methyl-4-phenyl-1,2,3,6-tetrahydropyridine (MPTP). *Life Sci.* **36**, 225-230.

(44) Langston, J. W., Irwin, I., Langston, E. B. and Forno, L. S. (1984) Pargyline prevents MPTP-induced Parkinsonism in primates. *Science* (Washington D. C.) **225**, 1480-1482.

(45) Heikkila, R. E., and Manzino, L. (1984) Behavioral properties of GBR 12,909, GBR 13,069, GBR 13,098: Specific inhibitors of dopamine uptake. *Eur. J. Pharmacol.* **103**, 241-248.

(46) Markey, S. P., Johannsessen, J. N., Chiueh, C. C., Burns, R. S. and Herkenham, M. A. (1984) Intraneuronal generation of a pyridinium metabolite may cause drug-induced Parkinsonism. *Nature* (London) **311**, 464-467.

(47) Javitch, J. A., D'amato, R. J., Strittmatter, S. M. and Snyder, S. H. (1985) Parkinsonism-inducing neurotoxin, N-methyl-4-phenyl-1,2,3,6-tetrahydropyridine: Uptake of the metabolite N-methyl-4-phenylpyridine by dopamine neurons explains selective toxicity. *Proc. Natl. Acad. Sci. U.S.A.* **82**, 2173-2177.

(48) Mayer, R. A., Kindt, M. V. and Heikkila, R. E. (1986) Prevention of the nigrostriatal toxicity of 1-methyl-4-phenyl-1.2.3.6-tetrahydropyridine by inhibitors of 3,4-dihydroxyphenylethylamine transport. *J. Neurochem.* **47**, 1073-1079.

(49) Ramsay, R. R., Salach, J. I. and Singer, T. P. (1986) Uptake of the neurotoxin 1-methyl-4-phenylpyridine (MPP^+) by mitochondria and its relation to the inhibition of the mitochondrial oxidation of NAD^+-linked substrates by MPP^+. *Biochem. Biophys. Res. Commun.* **134**, 743-748.

(50) Nicklas, W. J., Vyas, I. and Heikkila, R. E. (1985) Inhibition of NADH-linked oxidation in brain mitochondria by 1-methyl-4-phenylpyridinium, a

metabolite of the neurotoxin 1-methyl-4-phenyl-1,2,3,6-tetrahydropyridine. *Life Sci.* **36**, 2503-2508.

(51) Vyas, I., Heikkila, R. E. and Nicklas, W. J (1986) Studies on the neurotoxicity of 1-methyl-4-phenyl-1,2,3,6-tetrahydropyridine: Inhibition of NAD-linked substrate oxidation by its metabolite, 1-methyl-4-phenylpyridinium. *J. Neurochem.* **46**, 1501-1507.

(52) Chan, P. Ellanney, L. E., Irwin, I., Langston, J. W. and Dimonte, D. (1992) MPTP-induced ATP loss in mouse brain. *Ann. N. Y. Acad. Sci.* **648**, 306-308.

(53) Dimonte, D., Jewell, S. A., Ekstrom, G., Sandy, M. S. and Smith, M. T. (1986) 1-Methyl-4-phenyl-1,2,3,6-tetrahydropyridine (MPTP) and 1-methyl-4-phenylpyridine (MPP^+) cause rapid ATP depletion in isolated hepatocytes. *Biochem. Biophys. Res. Commun.* **137**,310-315.

(54) Rollema, H., Johnson, E. A., Booth, R. G., Caldera, P., Lampen, P., Youngster, S. K., Trevor, A., Naiman, N. and Castagnoli, N., Jr. (1990) In vivo intracerebral microdialysis studies in rats of MPP^+ analogs and related charged species. *J. Med. Chem.* **33**, 2221-2230.

(55) Collins, M. A., Neafsey, E. J., Matsubara, K., Cobuzzi, R. J. and Rollema, H. (1992) Indole-N-methylated beta-carbolinium ions as potential brain bioactivated neurotoxins. *Brain Res.* **570**, 1-2.

(56) Youngster, S. K., Nicklas, W. J. and Heikkila, R. E. (1989) Structure-activity study of the mechanism of 1-methyl-4-phenyl-1,2,3,6-tetrahydropyridine (MPTP) induced neurotoxicity. II. Evaluation of the biological activity of the pyridinium metabolites formed from the

monoamine oxidase-catalyzed oxidation of MPTP analogs. *J. Pharmacol. Exp. Ther.* **249**, 828-835.

(57) Saporito, M. S., Heikkila, R. E., Youngster, S. K., Nicklas, W. J. and Geller, H. B. (1992) Dopaminergic neurotoxicity of 1-methyl-4-phenylpyridinium analogs in cultured neurons: Relationship to the dopamine uptake system and inhibition of mitochondrial respiration. *J. Pharmacol. Exp. Ther.* **260**, 1400-1409.

(58) Mytilineou, C., Choen, G. and Heikkila, R. E. (1985) 1-Methyl-4-phenylpyridine (MPP^+) is toxic to mesencephalic dopamine neurons in culture. *Neurosci. Lett.* **57**, 1951-1953.

(59) Heikkila, R. E., Sonsalla, P. K. (1992) The MPTP, treated mouse as a model of parkinsonism: how good is it? Neurochem. Int. 20, Suppl. s299-s303.

(60) Rose, J. and Castagnoli, N., Jr. (1983) The metabolism of tertiary amines. *Med. Res. Rev.* **3**, 73-88.

(61) Oritz de Montellano, P. R. (1986) Oxygen activation and transfer. In *Cytochrome P450,: Structure, mechanism, and biochemistry* (Oriz de Montellano, P. R. Ed.), pp. 217-271. Plenum, New York.

(62) Singer, T. P., Ramsay, R. R., Sonsalla, P. K., Nicklas, W. J. and Heikkila, R. E. (1993) Biochemical mechanism underlying MPTP-induced and idiopathic parkinsonism-new vistas. In *Advances in Neurology, Parkinson's disease from basic research to treatment.* pp. 300-305. Raven Press, New York.

(63) Tipton, K. F. and Singer, T. P. (1993) Advances in our understanding of the mechanism of the neurotoxicity of MPTP and related compounds. *J. Neurochem.* **61**, 1191-1206.

(64) Wu, E., Shinka, T., Caldera-Munoz, P., Yoshizumi, H., Trevor, A. and Castagnoli, N., Jr. (1988) Metabolic studies on the nigrostriatal toxin MPTP and its MAO B generated dihydropyridinium metabolite $MPDP^+$. *Chem. Res. Toxicol.* **1**, 186-194.

(65) Ottoboni, S., Carlson, T. J., Trager, W. F., Castagnoli, K. and Castagnoli, N., Jr. (1990) Studies on the cytochrome P-450 catalyzed ring α-carbon oxidation of the nigrostriatal toxin 1-methyl-4-phenyl-1,2,3,6-tetrahydropyridine (MPTP). *Chem. Res. Toxicol.* **3**, 423-427.

(66) Krishna, D. R., Klotz, U. (1994) Extrahepatic metabolism of drugs in humans. *Clin. Pharmacokinet.* **26**, 144-160.

(67) Guengerich, F. P. (1987) Cytochrome P-450 enzymes and drug metabolism. In *Progress in Drug Metabolism*, Vol. 10, Chap. 1 (Bridges, J. W., Chasseaud, L. F., Gibson, G. G., Eds.), pp. 1-54. Taylor & Francis, London.

(68) Guengerich, F. P. (1989) Characterization of human microsomal cytochrome P-450 enzymes. *Ann. Rev. Pharmacol. Toxicol.* **29**, 241-264.

(69) Nelson, D. R., Kamataki, T., Waxman, D. J., Guengerich, F. P., Estabrook, R. W., Feyereisen, R., Gonzales, F. J., Coon, M. J., Gunsalus, I. C., Gotoh, O., Okuda, K., Nebert, D. W. (1993) The P450 superfamily: Update on new sequences, gene mapping, accession numbers, early trivial names of enzymes, and nomenclature. *DNA Cell Biol.* **12**, 1-51.

(70) Gonzales, F. J. (1992) Human cytochromes P450: problems and prospects. *Trends Pharmacol. Sci.* **13**, 346-352.

(71) Guengerich, F. P. (1994) Catalytic selectivity of human cytochrome P450 enzymes: relevance to drug metabolism and toxicity. *Toxicol. Lett.* **70**, 133-138.

(72) Wrighton, S. A., Stevens, J. C. (1992) The human hepatic cytochromes P450 involved in drug metabolism. *Crit. Rev. Toxicol.* **22**, 1-21.

(73) Warner, M., Strömstedt, M., Wyss, A., Gustafsson, J-Å. (1993) Regulation of cytochrome P450 in the central nervous system. *J. Steroid Biochem. Molec. Biol.* **47**, 191-194.

(74) Guengerich, F. P. (1990) Mechanism-based inactivation of human liver microsomal cytochrome P-450IIIA4 by gestodene. *Chem. Res. Toxicol.* **3**, 363-371.

(75) Halpert, J. R., Guengerich, F. P., Bend, J. R., Correia, M. A. (1994) Contemporary issues in toxicology. Selective inhibitors of cytochrome P450. *Toxicol. Appl. Pharmacol.* **125**, 163-175.

(76) Guengerich, F. P. (1994) Analysis and characterization of enzymes. In *Principles and Methods of Toxicology*, Chap. 35 (Hayes, W. Ed.), pp. 1259-1313. Raven Press, Ltd. New York.

(77) Strolin Benedetti, M., Dostert, P. and Tipton, K. F. (1988) Contributions of monoamine oxidase to the metabolism of xenobiotics. *Progr. Drug Metab.* **11**, 149-174.

(78) Strolin Benedetti, M. and Dostert, P. (1994) Contribution of amine oxidases to the metabolism of xenobiotics. *Drug Metab. Rev.* **26**, 507-535.

(79) Glover, V., Sandler, M., Owen, F. (1977) Dopamine is a monoamine oxidase B substrate. *Nature* **265**, 80-81.

(80) Houslay, M. D. and Tipton, K. F. (1976) Multiple forms of monoamine oxidase: Fact and artefact. *Life Sci.* **19**, 467-478.

(81) White, H. L. and Glassman, A. T. (1977) Multiple binding sites of human brain and liver monoamine oxidase: Substrate specificities, selective inhibitions, and attempts to separate enzyme forms. *J. Neurochem.* **29**, 987-997.

(82) Donnelly, C. H., Murphy, D. L. (1977) Substrate- and inhibitor-related characteristics of human platelet monoamine oxidase. *Biochem. Pharmacol.* **26**, 853-858.

(83) Gómez, N., Balsa, D. and Unzeta, M. (1988) A comparative study of some kinetic and molecular properties of microsomal and mitochondrial monoamine oxidase. *Biochem. Pharmacol.* **37**, 3407-3413.

(84) Unzeta, M., Castro, J., Gomez, N. and Tipton, K. F. (1983) Comparisons between the monoamine oxidase activities associated with mitochondria and microsomes in rat liver. *Br. J. Pharmacol.* **80**, 622P.

(85) Young, W. F., Laws, E. R., Sharbrough, F. W., Weinshilboum, R. M. (1986) Human monoamine oxidase: Lack of brain and platelet correlation. *Ach. Gen. Psychiatry* **43**, 604-609.

(86) Hall, D. W. R., Bridget, W., Logan, W. and Parsons, G. H. (1969) Further studies on the inhibition of monoamine oxidase by M & B 9302 (clorgyline): I Substrate specificity in various mammalian species. *Biochem. Pharmacol.* **18**, 1447-1454.

(87) Youdim, M. B. H. and Finberg, J. P. M. (1991) New directions in monoamine oxidase A and B: Selective inhibitors and substrates. *Biochem. Pharmacol.* **41**, 155-162.

(88) Salach, J. I. and Weyler, W. (1987) Preparation of the flavin-containing aromatic amine oxidases of human placenta and beef liver. *Methods Enzmol.* **142**, 627-637.

(89) Baldessarini, R. J. (1991) Drugs and the treatment of psychiatric disorders. In *The Pharmacological Basis of Therapeutics* (Gilman, A., Gilman, A., Goodman, L. S., Eds.), pp. 383-435, Pregamon Press, New York.

(90) Froemming, J. S., Francic Lam, Y. W., Jann, M. W. and Davis, C. M. (1989) Pharmacokinetics of Haloperidol. *Clin. Pharmacokinet.* **17**, 396-423.

(91) Reynolds, G. P. (1992) Development in the drug treatment of schizophrenia. *Trends Pharmacol. Sci.* **13**, 116-121.

(92) Oboyle, K. M., Gavin, K. T. and Harrison, N. (1993) Chronic antagonist treatment does not alter the mode of interaction of dopamine with rat striatal dopamine receptors. *J. Recep. Res.* **13**, 1-4.

(93) Glazer, W. M., Moore, D. C., Schooler, N. R., Brenner, L. M. and Morgenstern, H. (1984) Tardive Dyskinesia. *Arch. Gen. Psychiatry* **42**, 623-627.

(94) Fang, J., Gorrod, J. W. (1991) Dehydration is the first step in the bioactivation of haloperidol to its pyridinium metabolite. *Toxicol. Lett.* **59**, 117-123.

(95) Forsman, A., Fölsch, G., Larsson, M. and Ohman, R. (1977) On the metabolism of haloperidol in man. *Curr. Ther. Res.* **21**, 606-617.

(96) Miyazaki, H., Matsunaga, Y., Nambu, K., Ohe, Y., Yoshida, K., Hashimoto, M. (1986) Disposition and metabolism of [^{14}C]-haloperidol in rats. *Arzheim.-Forsch./Drug Res.* **36**, 443-452.

(97) Matsunaga, Y., Nambu, K., Ohe, Y., Miyazaki, H., Hashimoto, M. (1986) Excretion and metabolism of intramuscularly administered [^{14}C]-haloperidol decanoate in rats. *Arzheim.-Forsch./Drug Res.* **36**, 453-456.

(98) Soudijn, W., Van Wijngaarden, I. and Allewijn, F. (1967) Distribution, excretion and metabolism of neuroleptics of the butyrophenone type. Part I. Excretion and metabolism of haloperidol and nine related butyrophenone-derivatives in the wistar rat. *Eur. J. Pharmacol.* **1**, 47-57.

(99) Forsman, A., Larsson, M. (1978) Metabolism of haloperidol. *Curr. Ther. Res.* **24**, 567-569.

(100) Pape, B. E. (1981) Isolation and identification of a metabolite of haloperidol. *J. Anal. Toxicol.* **5**, 113-117.

(101) Inaba, T., Kovacs, J. (1989) Haloperidol reductase in human and guinea pig livers. *Drug Metab. Dispos.* **17**, 330-333.

(102) Inaba, T., Kalow, W., Someya, T., Takahashi, S., Cheung, S. W., Tang, S. W. (1989) Haloperidol reduction can be assayed in human red blood cells. *Can. J. Physiol. Pharmacol.* **67**, 1468-1469.

(103) Korpi, E. R., Wyatt, R. J. (1984) Reduced haloperidol: Effects on striatal dopamine metabolism and conversion to haloperidol in the rat. *Psychopharmacology* **83**, 34-37.

(104) Korpi, E. R., Costakos, D. T., Wyatt, R. J. (1985) Interconversions of haloperidol and reduced haloperidol in guinea pig and rat liver microsomes. *Biochem. Pharmacol.* **34**, 2923-2927.

(105) Eyles, D. W., Whiteford, H. A., Stedman, T. J., Pond, S. M. (1992) Determination of haloperidol and reduced haloperidol in the plasma and blood of patients on depot haloperidol. *Psychopharmacology* **106**, 268-274.

(106) Eyles, D. W., Pond, S. M. (1992) Stereospecific reduction of haloperidol in human tissues. *Biochem. Pharmacol.* **44**, 867-871.

(107) Jann, M. W., Francis Lam, Y. W. and Chang, W. H. (1990) Reversible metabolism of haloperidol and reduced haloperidol in Chinese schizophrenic patients. *Psychopharmacology* **101**, 107-111.

(108) Korpi, E. R., Costakos, D. T., Wyatt, R. J. (1985) Rapid formation of reduced haloperidol in guinea pigs following haloperidol administration. *Acta. Pharmacol. et Toxicol.* **56**, 94-98.

(109) Llerena, A., Alm. C., Dahl, M. L., Ekqvist, B., Bertilsson, L. (1992) Haloperidol disposition is dependent on debrisoquine hydroxylation phenotype. *Ther. Drug Monit.* **14**, 92-97.

(110) Llerena, A., Dahl, M. L., Ekqvist, B., Bertilsson, L. (1992) Haloperidol disposition is dependent on the debrisoquine hydroxylation phenotype: Increased plasma levels of the reduced metabolite in poor metabolizers. *Ther. Drug Monit.* **14**, 261-264.

(111) Tyndale, R. F., Kalow, W., Inaba, T. (1991) Oxidation of reduced haloperidol to haloperidol: involvement of human P450IID6

(sparteine/debrisoquine monooxygenase). *Br. J. Clin. Pharmacol.* **31**, 655-660.

(112) Benitez, J., Ladero, J. M., Jimenez-Jimenez, F. J., Martinez, C., Puerto, A. M., Valdivielso, M. J., Llerena, A., Cobaleda, J., Munoz, J. J. (1990) Oxidative polymorphism of debrisoquine in Parkinson's disease. *J. Neurol. Neurosurg. Psychiatry* **53**, 289-292.

(113) Young, D., Midha, K. K., Fossler, M. J., Hawes, E. M., Hubbard, J. W., McKay, G., Koqrchinski, E. D. (1993) Effect of quinidine on the interconversion kinetics between haloperidol and reduced haloperidol in humans: implications for the involvement of cytochrome P450IID6. *Eur. J. Clin. Pharmacol.* **44**, 433-438.

(114) Oida, T., Terauchi, Y., Yoshida, K. Kagemoto, A., Sekine, Y. (1989) Use of antisera in the isolation of human specific conjugates of haloperidol. *Xenobiotica* **19**, 781-793.

(115) Someya, T., Shibasaki, M., Noguchi, T., Takahashi, S., Inaba, T. (1992) Haloperidol metabolism in psychiatric patients: Importance of glucuronidation and carbonyl reduction. *J. Clin. Psychopharmacol.* **12**, 169-174.

(116) Ilett, K. F., Mackie, A. E., Jellett, L. B., Marsden, B. W., Somers, K. and Hughes, I. E. (1978) Pharmacokinetics of ^{14}C-haloperidol in man. *Clin. Exp. Pharmacol.* **5**, 267-268.

(117) Subramanyam, B., Rollema, H., Woolf, T., Castagnoli, N., Jr. (1990) Identification of a potentially neurotoxic pyridinium metabolite of haloperidol in rats. *Biochem. Biophys. Res. Commun.* **166**, 238-244.

(118) Subramanyam, B., Pond, S. M., Eyles, D. W., Whiteford, H. A., Fouda, H. G., Castagnoli, N., Jr. (1991) Identification of a potentially neurotoxic pyridinium metabolite in the urine of schizophrenic patients treated with haloperidol. *Biochem. Biophys. Res. Commun.* **181**, 573-578.

(119) Rollema, H., Skolnik, M., d'Engelbronner, J., Igarashi, K., Usuki, E. and Castagnoli, N., Jr. (1994) MPP^+-like neurotoxicity of a pyridinium metabolite derived from haloperidol: In vivo microdialysis and in vitro mitochondrial studies. *J. Pharmacol. Exp. Ther.* **268**, 380-387.

(120) Rollema, H., Subramanyam, B., Skolnik, M., d'Engelbronner, J. and Castagnoli, N., Jr. (1991) MPP^+-like neurotoxicity of HPP^+, a pyridinium metabolite of haloperidol: A microdialysis study. In *Monitoring molecules in neuroscience* (Rollema, H., Westerink, B. H., C., Drijfhout, W. J. Eds.), pp. 367-369. University center for pharmacy, Groningen, The Netherlands.

(121) Bloomquist, J., King, E., Wright, A., Mytilineou, C., Kimura, K., Castagnoli, K. and Castagnoli, N., Jr. (1994) 1-Methyl-4-phenylpyridinium-like neurotoxicity of a pyridinium metabolite derived from haloperidol: Cell culture and neurotransmitter uptake studies. *J. Pharmacol. Exp. Ther.* 270, 822-830.

(122) Fang, J., Yu, P. H. (1995) Effect of haloperidol and its metabolites on dopamine and noradrenaline uptake in rat brain slices. *Psychopharmacology* **121**, 379-384.

(123) Fang, J., Yu, P. H. (1995) Comparison of cytotoxicity of a quaternary pyridinium metabolite of haloperidol (HP^+) with neurotoxin N-methyl-4-

phenylpyridinium (MPP^+) towards cultured dopaminergic neuroblastoma cells. *Psychopharmacology* **121**, 373-378.

(124) Subramanyam, B., Woolf, T., Castagnoli, N., Jr. (1991) Studies on the in vitro conversion of haloperidol to a potentially neurotoxic pyridinium metabolite. *Chem. Res. Toxicol.* **4**, 123-128.

(125) Rollema, H., Fries, D. S., de Vries, J. B., Mastebroek, D. and Horn, A. S. (1985) HPLC-assay with electrochemical detection for the neurotoxin MPTP, its metabolite MPP^+ and MPTP-analogues in biological samples after purification over sephadex G10. *Life Sci.* **37**, 1633-1640.

(126) Naoi, M., Takahashi, T. and Nagatsu, T. (1987) A fluorometric determination of N-Methyl-4-phenylpyridinium ion, using high-performance liquid chromatography. *Anal. Biochem.* **162**, 540-545.

(127) Kuttab, S., Kalgutkar, A. and Castagnoli, N., Jr. (1994) Mechanistic studies on the monoamine oxidase B catalyzed oxidation of 1,4-disubstituted tetrahydropyridines. *Chem. Res. Toxicol.* **7**, 740-744.

(128) Dimonte, D. A., Schipper, H. M., Hetts, S., Langston, J. W. (1995) Iron-mediated bioactivation of 1-methyl-4-phenyl-1,2,3,6-tetrahydropyridine (MPTP) in glial cultures. *Glia* **15**, 203-206.

(129) Igarashi, K. and Castagnoli, N., Jr. (1992) Determination of the pyridinium metabolite derived from haloperidol in brain tissue, plasma and urine by high-performance liquid chromatography with fluorescence detection. *J. Chromatogr.* **579**, 277-283.

(130) Eyles, D. W., McLennan, H. R., Jones, A., McGrath, J. J., Stedman, T. J. and Pond, S. M. (1994) Quantitative analysis of two pyridinium

metabolites of haloperidol in patients with schizophrenia. *Clin. Pharmacol. Ther.* **56**, 512-520.

(131) Fang, J., Gorrod, J. W. (1993) High-performance liquid chromatographic method for the detection and quantitation of haloperidol and seven of its metabolites in microsomal preparations. *J. Chromatogr.* **614**, 267-273.

(132) Gorrod, J. W., Fang, J. (1993) On the metabolism of haloperidol. *Xenobiotica* **23**, 495-508.

(133) Fang, J., Yu, P. H., Gorrod, J. W., Boulton, A. A. (1995) Inhibition of monoamine oxidases by haloperidol and its metabolites: pharmacological implications for the chemotherapy of schizophrenia. *Psychopharmacology*, **118**, 206-212.

(134) Janssen, P. A. J., Van de Westeringh, C., Jageneau, A. H. M., Demoen, P. J. A., Hermans, B. K. F., Van der Eycken, G. H. P., Schellekens, K. H. L., Van der Eycken, C. A. M., Niemegeers, C. J. E. (1959) Chemistry and pharmacology of CNS depressants related to 4-(4-hydroxy-4-phenylpiperidino)butyrophenone: Part I-synthesis and screening data in mice. *J. Med. Pharm. Chem.* **1**, 281-297.

(135) Kalgutkar, S. A. (1993) Dissertation : Synthesis and biological evaluation of novel MPTP analogs as potential monoamine oxidase B inhibitors.

(136) Bradford, M. M. (1976) A rapid and sensitive method for the quantitation of microgram quantities of protein utilizing the principle of protein-dye binding. *Anal. Biochem.* **72**, 248-254.

(137) Igarashi, K., Kasuya, F., Fukui, M., Abe, T., Castagnoli, N., Jr. (1995) Simultaneous determination of haloperidol and its neurotoxic metabolite in plasma and brain tissue from schizophrenic patients treated with

haloperidol using HPLC and solid-phase extraction. *Jpn. Forensic Toxicol.* **13**, 31-38.

(138) Dutton, D. R. and Parkinson, A. (1989) Reduction of 7-alkoxyresorufins by NADPH-cytochrome P450 reductase and its differential effects on their O-dealkylation by rat liver microsomal cytochrome P450. *Arch. Biochem. Biophys.* **268**, 617-629.

(139) Pearce, R., Greenway, D. and Parkinson, A. (1992) Species differences and interindividual variation in liver microsomal cytochrome P450 2A enzymes: Effects on coumarin, dicumarol, and testosterone oxidation. *Arch. Biochem. Biophys.* **298**, 211-225.

(140) Brian, W. R., Srivastava, P. K., Umbenhauer, D. R., Lloyd, R. S. and Guengerich, F. P. (1989) Expression of a human liver cytochrome P-450 protein with tolbutamide hydroxylase activity in *Saccharomyces cerevisiae. Biochemistry* **28**, 4993-4999.

(141) Srivastava, P. K., Yun, C. H., Beaune, P. H., Ged, C. and Guengerich, F. P. (1991) Separation of human liver microsomal tolbutamide hydroxylase and (S)-mephenytoin 4'-hydroxylase cytochrome P-450 enzymes. *Mol. Pharmacol.* **40**, 69-79.

(142) Kronbach, T. (1991) Bufuralol, dextromethorphan, and debrisoquine as prototype substrates for human P450IID6. *Methods Enzymol.* **206**, 509-517.

(143) Peter, R., Bocker, R., Beaune, P. H., Iwasaki, M., Guengerich, F. P. and Yang, C. S. (1990) Hydroxylation of chlorzoxazone as a specific probe for human liver cytochrome P-450IIE1. *Chem. Res. Toxicol.* **3**, 566-573.

(144) Sonderfan, A. J., Arlotto, M. P., Dutton, D. R., McMillen, S. K. and Parkinson, A. (1987) Regulation of testosterone hydroxylation by rat liver microsomal cytochrome P-450. *Arch. Biochem. Biophys.* **255**, 27-41.

(145) Halvorson, M., Greenway, D., Eberhart, D., Fitzgerald, K. and Parkinson, A. (1990) Reconstitution of testosterone oxidation by purified rat cytochrome P450p (IIIA1). *Arch. Biochem. Biophys.* **277**, 166-180.

(146) Romano, M. C., Straub, K. M., Yodis, L. A. P., Eckardt, R. D. and Newton, J. F. (1988) Determination of microsomal lauric acid hydroxylase activity by HPLC with flow-through radiochemical quantitation. *Anal. Biochem.* **170**, 83-93.

(147) In addition to the data reported in reference 134 on P450 2A and 3A, we have observed, but not yet published, similar cross reactivity with several other antibodies raised against rat P450s.

(148) Van der Schyf, C. J., Castagnoli, K., Usuki, E., Fouda, H. G., Rimoldi, J. and Castagnoli, N., Jr. (1994) Metabolic studies on haloperidol and its tetrahydropyridine analog in C57BL/6 mice. *Chem. Res. Toxicol.* **7**, 281-285.

(149) Eberhart, D. C., Gemzik, B., Halvorson, M. R. and Parkinson, A. (1991) Species differences in the toxicity and cytochrome P450IIIA-dependent metabolism of digitoxin. *Mol. Pharmacol.* **40**, 859-867.

(150) Lemoine, A., Gautier, J. C., Azoulay, D., Loffe, L., Belloc, C., Guengerich, F. P., Maurel, P., Beaune, P. and Leroux, J. P. (1993) Major pathway of imipramine metabolism is catalyzed by cytochromes P-450 1A2 and P-450 3A4 in human liver. *Mol. Pharmacol.* **43**, 827-832.

(151) Bell, K. and Portoghese, P. (1973) Stereochemical studies on medicinal agents. 14. Relative stereochemistries and analgetic potencies of diastereomeric 3-allyl and 3-propyl derivatives of 1-methyl-4-phenyl-4-propionoxypiperidine. *J. Med. Chem.* **16**, 203-205.

(152) Igarashi, K., Kasuya, F., Fukui, M., Usuki, E. and Castagnoli, N., Jr. (1995) Studies on the metabolism of haloperidol (HP): The role of CYP3A in the production of the neurotoxic pyridinium metabolite HPP^+ found in rat brain following i.p. administration of HP. *Life Sci.* **57**, 2439-2446.

(153) Baldwin, S. J., Bloomer, J. C., Smith, G. J., Ayrton, A. D., Clarke, S. E. and Chenery, R. J. (1995) Ketoconazole and sulphaphenazole as the respective selective inhibitors of P450 3A and 2C9. *Xenobiotica* **25**, 261-270.

(154) Schwab, G. E., Raucy, J. L., Johnson, E. F. (1988) Modulation of rabbit and human hepatic cytochrome P-450-catalyzed steroid hydroxylation by α-naphthoflavone. *J. Pharmacol. Exp. Ther.* **33**, 493-499.

(155) Fabre, G., Julian B., Saint-Aubert, B., Joyeux, H., Berger, Y. (1993) Evidence for CYP3A-mediated N-deethylation of amiodarone in human liver microsomal fractions. *Drug Metab. Dispos.* **21**, 978-985.

(156) Yun, C.-H., Okerholm, R. A. and Guengerich, F. P. (1993) Oxidation of the antihistaminic drug terfenadine in human liver microsomes. *Drug Metab. Dispos.* **21**, 403-409.

(157) Coutts, R. T., Su, P. and Baker, G. B. (1994) Involvement of CYP2D6, CYP3A4, and other cytochrome P-450 isozymes in N-dealkylation reactions. *J. Pharmacol. Toxicol. Methods* **31**, 177-186.

(158) Omura, T., and Sato, R. (1964) The carbon monoxide-binding pigment of liver microsomes. *J. Biol. Chem.* **239**, 2370-2378.

(159) Parkinson, A., Gemzik, B. (1991) Production and purification of antibodies against rat liver P-450 enzymes. *Methods Enzymol.* **206,** 233-245.

(160) Anandatheerthavarada, H. K., Shankar, S. K. and Ravindranath, V. (1990) Rat brain cytochromes P-450: catalytic, immunochemical properties and inducibility of multiple forms. *Brain Res.* **536**, 339-343.

(161) Jayyosi, Z., Cooper, K. O. and Thomas, P. E. (1992) Braian cytochrome P450 and testosterone metabolism by rat brain subcellular fractions: presence of cytochrome P450 3A immunoreactive protein rat brain mitochondria. *Arch. Biochem. Biophys.* **298**, 265-270.

(162) Ravindranath, V., Boyd, M. R. (1995) Xenobiotic metabolism in a brain. *Drug Metab. Rev.* **27**, 41-448.

(163) White, R. E. and Coon, M. J. (1980) Oxygen activation by cytochrome P-450. *Ann. Rev. Biochem.* **49**, 315-356.

(164) Zanger, U. M., Vilbois, F., Hardwick, J. P., Meyer, U. A. (1988) Absence of hepatic cytochrome P450bufl causes genetically deficient debrisoquine oxidation in man. *Biochemistry* **27**, 5447-5454.

(165) Hammock, B. D., Beale, A. M., Work, T., Gee, S. H., Gunther, R., Higgins, R., J., Shinka, T. Castagnoli, N. Jr. (1989) A sheep model for MPTP induced parkinson-like symptoms. *Life Sci.* **45**, 1601-1608.

(166) Usuki, E., Pearce, R., Parkinson, A. and Castagnoli, N., Jr. (1996) Studies on the conversion of haloperidol and its tetrahydropyridine dehydration

product to potentially neurotoxic pyridinium metabolites by human liver microsomes. *Chem. Res. Toxicol.* **9**, 800-806.

(167) Corcos, L. (1992) Phenobarbital and dexamethasone induce expression of cytochrome P-450 genes from subfamilies IIB, IIC, and IIIA in mouse liver. *Drug Metab. Dispos.* **20**, 797-801.

(168) Simmons, D. L., McQuiddy, P. and Kasper, C. B. (1987) Induction of the hepatic mixed-function oxidase system by synthetic glucocorticoids. *J. Biol. Chem.* **262**, 326-332.

VITA

Etsuko Usuki was born on August 23, 1964, in Kobe, Japan. She received her Bachelor of Science degree in Pharmaceutical Sciences from Kobegakuin University, Kobe, Japan, in 1987. She worked at Takeda Chemical Industries, Ltd., in Osaka, Japan. In the spring of 1992, she started graduate program in the Department of Chemistry at Virginia Polytechnic Institute and State University under the direction of Professor Neal Castagnoli, Jr. Her research was sponsored by the Harvey W. Peters Research Center for Parkinson's Disease and Disorders of the Central Nervous System and NIH. She received the Doctor of Philosophy degree in Chemistry from Virginia Polytechnic Institute and State University in the Summer of 1996.

Etsuko Usuki